APPROVAL SHEET

Title of Dissertation: *"*High Mobility Group Box 1 (HMGB1) enhances immune suppression by regulating Myeloid-Derived Suppressor Cell (MDSC) differentiation, function, and survival."

Name of Candidate: Katherine Parker
Doctor of Philosophy, 2015

Dissertation and Abstract Approved: _____
Suzanne Ostrand-Rosenberg
Professor of Biological Sciences
Robert and Jane Meyerhoff
Professors of Biochemistry

Date Approved: _____

ABSTRACT

Title of Document:	HIGH MOBILITY GROUP BOX 1 (HMGB1) ENHANCES IMMUNE SUPPRESSION BY REGULATING MYELOID-DERIVED SUPPRESSOR CELL (MDSC) DIFFERENTIATION, FUNCTION, AND SURVIVAL
	Katherine Helene Parker, Ph.D., 2015
Directed By:	Dr. Suzanne Ostrand-Rosenberg, Professor, Biological Sciences, Robert and Jane Meyerhoff, Professors of Biochemistry, Department of Biological Sciences

Chronic inflammation is associated with malignant transformation and tumor progression. The immune system also plays a role in tumor progression, with tumor immune escape recognized as a hallmark of cancer. During tumor immune escape, tumor cells produce inflammatory molecules that promote the accumulation and function of myeloid-derived suppressor cells (MDSC). Therefore, inflammation promotes tumor progression through the induction of MDSC, which inhibits the development of anti-tumor immunity. Since the damage associated molecular pattern molecule (DAMP) and alarmin high mobility group box protein 1 (HMGB1) are pro-inflammatory and are binding partners, inducers, and/or chaperones for many of the pro-inflammatory molecules that drive MDSC, we examined HMGB1 as a potential regulator of MDSC. Using murine tumor systems, this dissertation demonstrates that HMGB1 is ubiquitously present in the tumor microenvironment, that HMGB1 can activate MDSC via the NF-κB

signal transduction pathway, and that HMGB1 regulates MDSC quantity, quality, and survival. HMGB1 drives MDSC development from bone marrow progenitor cells and promotes MDSC accumulation in the tumor, spleen, and blood of tumor-bearing mice. Additionally, HMGB1 helps MDSC suppress antigen-driven activation of $CD4^+$ and $CD8^+$ T cells, increases MDSC production of the type 2 cytokine IL-10, enhances crosstalk between MDSC and macrophages, and facilitates MDSC's ability to down-regulate expression of the homing receptor L-selectin on naive T cells. It is well appreciated that HMGB1 facilitates tumor cell survival by inducing autophagy. Therefore, we sought to determine if HMGB1 regulates MDSC survival through the induction of autophagy. Inhibition of autophagy or HMGB1 increased the quantity of apoptotic MDSC, demonstrating that autophagy and HMGB1 prolong the survival of tumor-induced MDSC. Circulating tumor-induced MDSC have a default autophagic phenotype, while tumor-infiltrating MDSC are more autophagic. This heightened autophagic state is consistent with the notion that inflammatory conditions within the microenvironment of solid tumors contributes to tumor progression by enhancing immune suppressive MDSC. Taken together, these results demonstrate that the inflammatory molecule HMGB1 contributes to tumor progression by driving the development, function, and viability of MDSC. Therefore, the immunosuppressive activities of HMGB1 must be considered when designing cancer immunotherapies.

HIGH MOBILITY GROUP BOX 1 (HMGB1) ENHANCES IMMUNE SUPPRESSION BY REGULATING MYELOID-DERIVED SUPPRESSOR CELL (MDSC) DIFFERENTIATION, FUNCTION, AND SURVIVAL

By

Katherine Helene Parker

Dissertation submitted to the Faculty of the Graduate School of the
University of Maryland, Baltimore County, in partial fulfillment
of the requirements for the degree of
Doctor of Philosophy
2015

Acknowledgements

I would like to begin by thanking my family and friends. My parents have always been supportive of me while I was continuing my education. Even when working 14 hour days to complete tedious experiments, my parents would offer assistance in any way they could, whether it was watching my dog or offering me a warm meal when I got home. I can't tell them how much I appreciate all that they have done for me.

To my fiancé, Chris. I don't know how, but somehow I tricked you into sticking with me for the past three years. We started dating when I was studying for my prelim and now we are planning our wedding as I am preparing to defend. If anything, I think you are a glutton for punishment. I can't put into words how much I appreciate your support. You are always there for me when I am stressed, tired from a 14 hour day, or excited because I finally got an experiment to work. It might sound cheesy but you really are my rock and I am thrilled to start this next part of our lives together.

To my siblings, Keith and Andrew. While we don't always see eye to eye, our sibling rivalry has certainly given me the drive to always strive to be better. As we grow older and advance in our careers and lives, I value our friendship more and more.

To all of my friends, I want to thank you for keeping me sane. When I was swamped with work, you talked me into hanging out and relaxing when I needed it the most.

To my committee members all of you have been extremely helpful over the past five years. You've provided me with guidance, thoughtful questions, and insight, and for that I thank you.

To Julie Wolf. One year in the AMB program taught me more than four years of undergrad. You taught me all the basics about doing research from designing primers and gel purifying DNA to how to keep a proper notebook, the latter of which is an invaluable skill that has made me a far better researcher. But, I think the most valuable lessons I learned from you weren't about science at all. By having the pleasure of teaching with you for the past four years, I've gotten to know you outside of the lab. From you I learned that sometimes we need to laugh at our mistakes, we all need hobbies, and that youth is not age dependent – it's merely a state of mind. If there is one thing that I hope I can carry with me from you it's that you are only as old as you feel. I truly hope that years from now I am still brewing beer, baking amazing cakes from scratch, bike riding, and still having time to pick up new hobbies.

To my co-workers. Ginny, you are an amazing person and the glue that keeps our lab together. When I first joined the lab, I remembered you as the friendly face that would always help me locate whatever reagent I needed. I look forward to hearing about your vacations for years to come. Pratima, you were the first person to train me in mouse work and you taught me to be fearless. Over the years of working

with you, I have learned so much. You are a great researcher and I hope that one day I can design experiments with your precision.

Dan and Lucas. You two are really like brothers to me. Lucas you were my first student I trained and you were by far the best. Seeing how much you have grown from an AMB student to a PhD candidate makes me extremely proud. I know that you will accomplish great things in your life. And Dan, to be honest you were a huge factor in why I joined the lab. You have always been extremely friendly and quite entertaining, not to mention you are one of the smartest people I know – even if you choose to focus your brain power on a dozen different hobbies. I know some people consider us to be lab spouses as a result of our bickering, but I think that's just a testament to our friendship. You are the first person I go to bounce ideas off of. I am truly going to miss having someone with your intelligence at the bench beside me. The both of you have made my time here at UMBC really enjoyable and I'll be sad to go into a new lab and not see you guys every day.

To my mentor, Sue. You've been an unmatched example of dedication and professionalism. You know how to break through obstacles to get things done, and I have learned so much from watching you tackle difficult challenges with intelligence, patience and perseverance. Even though you are incredibly busy, you have never denied me help. You've also helped me become a much better writer. I have an enormous amount of respect for you and I hope that one day I can phrase complicated facts as eloquently as you. Your guidance and wisdom has brought me to a new place in my career, and for that I am forever grateful.

Table of Contents

List of Tables

Chapter 2. High Mobility Group Box Protein 1 enhances immune suppression by facilitating the differentiation and suppressive activity of myeloid-derived suppressor cells

List of Figures

Chapter 1. Introduction

Chapter 2: High Mobility Group Box Protein 1 enhances immune suppression by facilitating the differentiation and suppressive activity of myeloid-derived suppressor cells

Chapter 1: Introduction

A. Opening remarks

In this dissertation I will discuss the research I have conducted and give an explanation of my results, but will first start with an introduction to immunology. The introduction will describe the immune system, how cancer arises, and how the body can fight cancer, as well as barriers to anti-tumor immunity and lastly, discuss forms of cancer treatment. This background information will supply the reader with sufficient knowledge of the immune system to understand the experiments described in this dissertation.

B. Innate and adaptive immunity

The immune system is divided into innate and adaptive immune responses. An innate immune response occurs rapidly, in a matter of hours, in reaction to exposure from an infectious particle, bacteria, and allergens, while an adaptive immune response can take days. The innate immune response consists largely of phagocytes and soluble anti-microbial compounds that recognize common molecular surface markers and facilitate clearance of the foreign particle (1).

The soluble molecules of the innate immune response include complement, lysozyme, and interferons (IFN). Complement is made of a group of proteins found in an inactive state in serum. During an immune response complement proteins are converted into their active form, allowing them to damage the membrane of pathogens. Lysozyme is a hydrolytic enzyme with the ability to cleave peptidoglycan components of bacterial cell walls. Interferons are a group of proteins released by virus infected cells that stimulate a heightened immune responsive state. A key feature of the innate immune

system is the utilization of pattern recognition receptors, such as Toll-Like Receptors (TLRs), to initiate a response in the form of these soluble molecules. Pattern recognition receptors can bind a plethora of pathogens, which allows for a quick response by the innate immune system (1).

The adaptive immune system, in contrast to the innate immune system, displays a high level of specificity in response to antigens. Only when an antigen has been identified by its specific receptor, not a general pattern recognition receptor is the adaptive immune system activated. The term antigen describes a substrate that is capable of inducing an immune response. The adaptive immune response has four unique characteristics; antigen specificity, diversity, immunogenic memory, and self-nonself recognition. Specificity refers to the immune system's ability to distinguish between two proteins that differ by as little as one amino acid. The immune system is highly diverse in that it generates billions of recognition molecules (T cell receptors (TCRs) and antibodies), all of which are uniquely compatible with a specific antigen. Another critical component of the adaptive immune system is its ability to generate immunologic memory. Immunologic memory is generated after an initial response to an antigen. Upon a second encounter with the same antigen a heightened immune response is activated, which can allow extended immunity against that specific antigen. Lastly, the ability of the immune system to identify self- versus non-self is vital. Inappropriate immune response to self-antigens causes harmful autoimmune diseases that can be life threatening (1).

C. How cancer occurs

Cancer is the second most common cause of death in the United States. For 2014 it was estimated that 585,720 Americans died of cancer, roughly at a rate of 1,600 per

day, with around 1,665,540 new cases diagnosed that same year (2). Therefore, understanding how cancer occurs and how we can treat it has been the focal point of a vast amount of research over the past hundred years.

The transformation of a normal cell into a cancer cell is the result of a multi-step mutation process. Mutation can occur via environmental, viral, or genetic means. Environmental exposure to asbestos, ultraviolet light, DNA alkylating agents, tobacco smoke, and poor diet have all been linked to increased risks for cancer. Viral DNA from SV40, human papilloma, hepatitis B and C, human immunodeficiency, Epstein-Barr, and polyoma viruses have been shown to integrate randomly into host chromosomal DNA, thereby causing cancer. Lastly, genetic abnormalities in genes that regulate cell proliferation or cellular death such as, myc, K-ras, p53, and Bcl-2 are highly associated with tumorigenesis.

D. The immune response to cancer

Transformed cells that are not eradicated and become cancerous can be eliminated by the immune system through antigen-specific responses, and non-antigen-specific responses. Antigen-specific responses are induced by cytotoxic T lymphocytes (CTLs) recognizing tumor antigens expressed on major histocompatibility complex I (MHC) of tumors. Non-antigen-specific responses are mediated by natural killer cells (NK cells) and macrophages, and do not depend on MHC expression. Fc receptors on NK cells and macrophages can bind to antibody coated tumor cells resulting in antibody-dependent cellular cytotoxicity (ADCC). Another mode of anti-tumor activity facilitated by macrophages is mediated through the expression of lytic enzymes, reactive oxygen species (ROS), nitrogen intermediates, and the production of tumor necrosis factor alpha

(TNF-α). While the immune system expresses multiple modes for recognizing and eliminating transformed cells, the body cannot effectively eliminate all tumors, therefore some tumors escape the immune system.

It has been demonstrated that tumors go through a process called immunoediting which embodies three phases (**1**) elimination, (**2**) equilibrium, and (**3**) escape (3) (**Figure 1**). This process of immunoediting describes how tumors are able avoid elimination by the immune system (3).

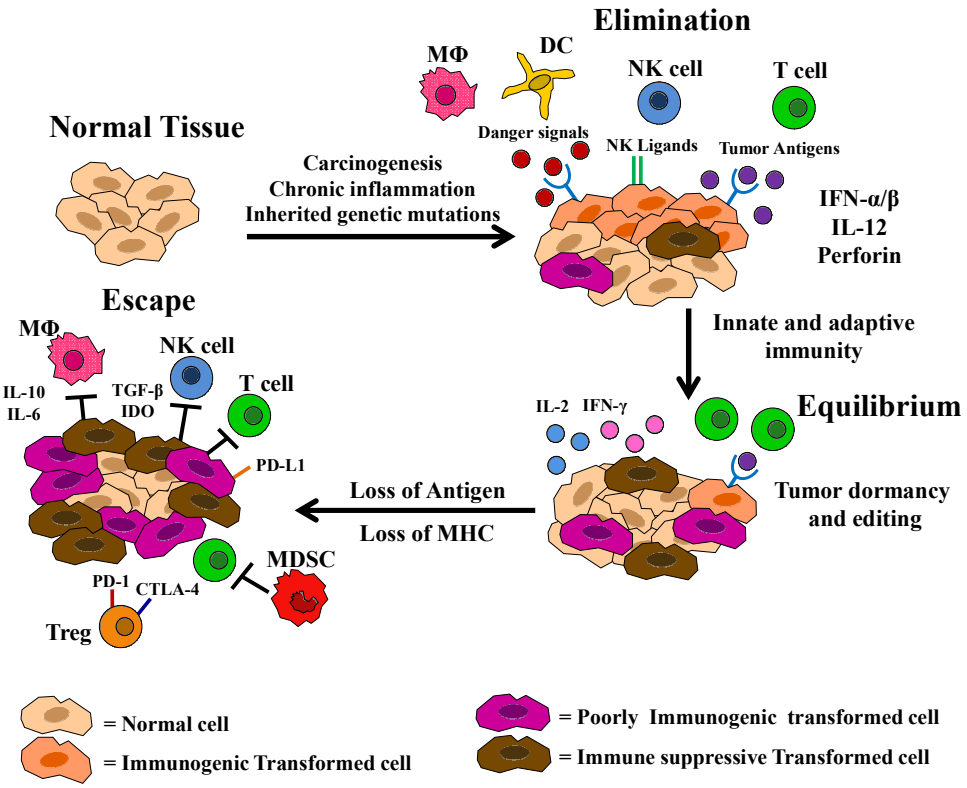

Figure 1: Tumors can be eliminated by or escape the immune system. Normal tissue becomes transformed through various random mutations that can alter cell cycle. Mutations can occur as result of exposure to carcinogens, inherited genetic defects, or chronic inflammation resulting in transformed cells that divide at an uncontrolled rate. These transformed cells release danger signals and express tumor antigens that designate themselves as tumor cells. This designation allows tumor cells to be targeted for elimination by dendritic cells (DC), macrophages, NK cells and T cells, through the aid of adaptive and innate immunity. However, since transformed cells are a result of random mutations every once in a while tumor cells become immune evasive and go in a phase of editing and dormancy. Due to constant immune selection pressure genetically unstable tumor cells can emerge out of the equilibrium phase. These immune evasive and immune suppressive tumor cells are no longer recognized, as a result of loss of antigen and MHC, and are able to induce immune suppression. Immune suppression takes the form of releasing tumor promoting cytokines transforming growth factor beta (TGF-β), indoleamine 2,3-dioxygenase (IDO), as well as promoting immune suppressive cells such as, myeloid-derived suppressor cells (MDSC) and regulatory T cells (Tregs) which hold the ability to suppress T cell activation.

D1. Elimination

During the process of elimination the innate and adaptive immune systems work in synergy to identify and destroy a developing tumor. The process of elimination is initiated when the innate immune system detects tumor development and responds by activating an adaptive immune response. The innate response can be sparked by danger signals such as damage associated molecular pattern molecules (DAMPs), for example high mobility group box 1 (HMGB1). DAMPs such as HMGB1 are released from dying tumor cells or from surrounding tissue that is damaged during tumor growth (4). Binding of a DAMP to its reciprocal receptor on an innate immune cell causes the release of pro-inflammatory cytokines that enables the development of an anti-tumor adaptive response (5). Detection of tumor development can be achieved through recognition of tumor cell expressed stress ligands such as MICA/B. These stress ligands induce the release of pro-inflammatory cytokines which promote the development of a tumor-specific adaptive immune response (5). Activation of the adaptive immune system plays a critical part in the process of elimination as effector $CD4^+$ and $CD8^+$ T cells have the power to eliminate tumor cells.

D2. Equilibrium

Occasionally the adaptive immune system can prevent tumor cell growth, while unintentionally at the same time sculpting the immunogenicity of the tumor, this phase is called equilibrium (3). During this equilibrium phase tumor cells can lie dormant for decades before resuming growth as either metastases or recurrent primary tumors (6). Confirmation that tumor cells lie dormant for prolonged periods of time came from experiments showing that immunocompetent mice given low doses of the carcinogen 3'-methylcholanthrene possessed dormant cancer cells however, over an extended period of

time the mice did not develop tumors (7). Only when the immune system of these mice was compromised, through treatment with monoclonal antibodies targeting T cells and IFN-γ, was rapid tumor outgrowth observed. Further analysis into this process revealed that adaptive immunity in the form of $CD4^+$ and $CD8^+$ T cells, as well as IL-12 and IFN-γ, were responsible for maintaining tumor cells in the equilibrium phase. Therefore, the immune system can keep tumor cells at bay and dormant however, if the immune system is weakened, these dormant tumor cells will capitalize and proliferate at rapid rates. It is thought that these dormant tumor cells are under selective pressure which selects for the most immune evasive mutations allowing the tumor to be successful in evading elimination (3).

D3. Escape

The process of tumor escape is accomplished by the tumor acquiring the ability to evade immune recognition and/or destruction, and emerge as a progressively growing tumor. Tumor cells evade the immune system through decreased antigen recognition, due to the loss of tumor antigen expression and decreased expression of MHC I, which reduces the ability of the tumor cell to present antigens for recognition. Additionally, tumor cells can also lose the ability to process antigens, which concurrently results in reduced expression of tumor antigens (8). Overall, the loss of antigen presentation exhibited by tumor cells is thought to arise from the inherent genetic instability of tumors in combination with the process of immunoselection (9, 10). Immunoselection describes a process in which tumor cells mutate constantly until a poorly immunogenic variant that can escape the immune system is generated. The escape process can also be mediated by the establishment of an immunosuppressive state within the tumor microenvironment

(TME) (11). This immunosuppressive state is promoted by tumor cell produced vascular endothelia growth factor (VEGF), IDO, TGF-β, and the recruitment of immunosuppressive cells that inhibit anti-tumor immune responses (12). Interestingly, the DAMP HMGB1, which can initiate an anti-tumor immune response, also functions to promote tumor growth and immune suppression after a tumor has been established (13, 14).

E. Anti-tumor immunity barriers

The ability of tumor cells to evade elimination results from the loss of antigen presentation, tumor-derived factors corrupting immune cells, manipulation of immune checkpoint molecules, and promotion of immune suppressive cells (**Figure 2**). The following sections will describe these mechanisms utilized by tumor cells to evade elimination.

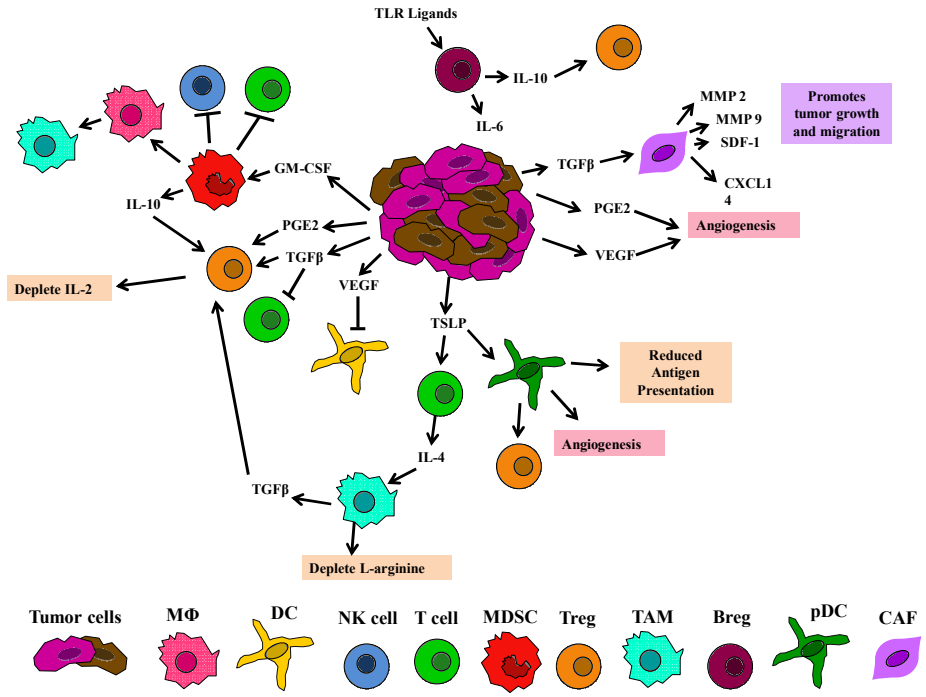

Figure 2: Barriers to anti-tumor immunity. Within the TME tumors produces immune suppressive molecules including TGFβ, PGE_2, VEGF, TSLP, and GM-CSF all of which can promote the induction of various immune suppressive cells. These immune suppressive cells include tumor-associated macrophage (TAMs), cancer-associated fibroblast (CAFs), Tregs, regulatory B cell (Bregs), plasmacytoid dendritic cell (pDC), and MDSC. Each of these immune suppressive cells are able to promote tumor growth by driving angiogenesis, migration, or by inhibiting immune reactive cells such as T cells, NK cells, DC, and macrophages.

E1. Loss of antigen presentation

Frequently tumors have impaired antigen presentation as a result of downregulation of antigen processing machinery (15). Tumor cells also exhibit mutations in β-2 microglobuin, an essential component of MHC I molecules, as well as reduced transcription of MHC I which reduces recognition by effector CTLs (16). By reducing antigen presentation tumors can effectively evade the immune system.

E2. Tumor-derived factors corrupt immune cells

Various cytokines produced by tumor cells have potent immunosuppressive qualities, including the promotion of immunosuppressive cells. Tumor-derived thymic stromal lymphoprotein (TSLP) induces mature dendritic cells to express OX40-L, which promotes the generation of Th2 cells, that in turn accelerates breast cancer development through the release of IL-4 and IL-13 (17). Accelerated tumorigenesis is attributed to IL-4 and IL-13 preventing the apoptosis of tumor cells as well as stimulating tumor-associated macrophages to produce epidermal growth factor, which in turn promotes tumor cell proliferation (18).

Prostaglandin E2 (PGE_2) is another pro-tumor cytokine in the TME that is also immunosuppressive, in that it promotes tumor growth by inhibiting tumor cell apoptosis and promoting neoangiogenesis (19, 20). PGE_2 is a potent inflammatory mediator that is generated by COX_2 (cyclooxygenase-2) conversion of arachidonic acid to PGG2 (prostaglandin G2), and further modified by PGE synthase to PEG_2. PGE_2 encourages tumor growth by promoting angiogenesis, stimulating tumor cell proliferation, and protecting against apoptosis (21). Many human and mouse tumors as well as tumor-infiltrating cells produce COX_2 and PGE_2 (22). In mouse models PGE_2 promotes differentiation of immune suppressive MDSC, at the expense of DC (23, 24).

VEGF is produced by most tumors and plays a vital role in neovascularization of tumors. Elevated levels of VEGF are associated with poor prognosis and impaired DC differentiation (25, 26). In a mouse tumor model VEGF neutralizing antibodies allowed for improved DC differentiation, leading to increased levels of mature DC (27, 28). Therefore, VEGF promotes tumor growth by weakening anti-tumor immunity through the inhibition of DC differentiation.

About 30% of human cancer cell lines spontaneously release granulocyte macrophage colony-stimulating factor (GM-CSF) (29). Tumors that release GM-CSF promote accumulation of immature myeloid cells, which is associated with impaired T cell activation (29-31).

TGF-β is another tumor derived factor described as a pleiotropic immunosuppressive cytokine that inhibits T cell activation, proliferation, and differentiation (32). The immunosppressive capacity of TGF-β on T cells is accredited to the cytokine's ability to repress the expression of perforin, granzyme A, granzyme B, Fas L, and IFN-γ, all of which mediate functionality of CTLs (33). TGF-β also promotes the induction of Tregs, which are immune suppressive T cells that inhibit anti-tumor immune responses (34, 35).

While tumor-derived factors manipulate the environment into one that can support tumor growth, this environment also promotes the induction of immune suppressive cells. These immune suppressive cells such as Tregs and MDSC are induced by factors such as TGF-β, and can also generate immune suppressive molecules such as IL-10 produced by both Tregs and MDSC, and PGE_2 produced by Tregs (23, 36). IL-10 functions as an anti-inflammatory cytokine that prevents excessive inflammation and autoimmune pathologies however, in the TME immune suppressive cells exploit the anti-inflammatory properties of IL-10 (37). Both Tregs and MDSC produce IL-10 which contributes to their immunosuppressive phenotype. The immunosuppressive function of IL-10 results from its ability to impair DC function, and protect tumor cells from CTLs by downregulating TAP1 and TAP2 (38, 39). TAP1 and TAP2 are critical components of antigen processing machinery. Therefore, the TME generates a self-sustaining environment that promotes its

growth through self-generated factors, and by inducing immune suppressive cells that can also generate tumor promoting factors, as well as display immune inhibitory factors.

E3. Manipulation of immune checkpoints

When mounting an immune response against a tumor, tumor-specific antigens must be accessible to antigen presenting cells (APCs), so that APCs can activate effector T cells through ligation of the antigen-MHC complex to the TCR expressed on the T cell. The process of antigen presentation also requires co-stimulation, without co-stimulation T cells go into a nonresponsive state called anergy. Several molecules on T cells are able to function as co-stimulators including CD2, CD28, CD40, 4-1BB, OX40, ICOS, and LFA-1. However, CD28 signaling through CD80 or CD86 is the most robust enhancer of TCR signaling (40). In an effort to maintain homeostasis after immune clearance, co-inhibitory molecules function as immune checkpoints dampening the immune response (41). However, inappropriate regulation of these immune checkpoints interferes with the purpose of these molecules ensuring that an appropriate immune repose occurs for the proper length of time. Tumors have manipulated the function of these immune checkpoints, and express them as means to weaken the anti-tumor immune response.

One of the most studied immune checkpoint molecules is cytotoxic T lymphocyte antigen-4 (CTLA-4). CTLA-4 inhibits T cell activation by downregulating IL-2 production, by binding co-stimulatory molecule (CD80) with a higher affinity compared to its activator ligand CD28 (42). Inhibition of CTLA-4 and CD80 interaction enhances anti-tumor immune responses (43). CTLA-4 is also able to down regulate CD80 and CD86 on APC, through an adhesion dependent mechanism (44). Additionally CTLA-4 can physically remove ligands from APC by transendocytosis, causing lysosomal

degradation of the endocytosed molecule (45). Another immune checkpoint molecule is called programmed death-1 (PD-1), which binds PD-L1 or PD-L2, and reduces T cell activation (46). Inhibition of PD-L1 increased T cell-mediated tumor rejection as a result of reduced T cell apoptosis (47, 48). Tumor cells utilize these immune checkpoint molecules and exploit their immunosuppressive function in an effort to sustain their progression, thus highlighting another means that tumor cells can manipulate the immune system. The targeting of immune checkpoints as immunotherapies has seen great success in recent years, further information about clinical applications for these therapies can be found in the immunotherapeutics section of chapter 1.

E4. Induction of immunosuppressive cells

In the process of tumors establishing a tumor-supportive microenvironment the tumor promotes the induction of immune suppressive cells such as Tregs, TAMs, CAFs, pDC, Bregs, and MDSC. Each of these populations of regulatory cells exhibit unique features that allows them to inhibit anti-tumor immunity.

E4-1. Tregs

Tregs express CD4 and CD25 (IL-2R) on their surface and transcription factor, Foxp3 internally. Tregs are important regulators of self-tolerance that exist naturally in the thymus (49). Under normal conditions Tregs play a role in maintaining homeostasis of innate lymphocytes, and regulating expansion and activation of T and B cells (50). Inflammatory mediators commonly found in the TME, such as IL-10, TGF-β and PGE_2 promote the accumulation of Tregs (51). Interestingly, Tregs also produce IL-10 and TGF-β, which are potent immune suppressive molecules (52, 53). The ability of Tregs to suppress effector T cell activation is in part attributed to their high expression of CD25, which depletes IL-2 from the surrounding area (54). Immune checkpoint molecule

CTLA-4 is constitutively express on the surface of Tregs, and aids in their ability to suppress conventional T cells (55). Additionally, Tregs express CD39 which hydrolyzes extracellular adenosine triphosphate (ATP) to adenosine diphosphate (ADP) or adenosine monophosphate (AMP), and CD73, which further degrades AMP to adenosine (56, 57). Adenosine is a potent immune suppressive molecule that inhibits DC and activated T cells, by elevating cyclic AMP (58). Tregs can also induce death of effector T cells, NK cells, and DC by expressing granzyme B (59), perforin (60) or galectin-1 (61).

E4-2. TAMs

Macrophages are abundant in the TME of solid tumors. As the TME evolves and inflammatory mediators are produced, the environment shifts from a Th1 T helper-like inflammatory response, to a Th2 type response that induces the differentiation of TAMs. Factors within the microenvironment that drive polarization of macrophages include IL-4, produced by $CD4^+$T cells or tumors cells (62, 63), tumor produced GM-CSF (64), and colony stimulating factor 1 (CSF1) (65). The majority of TAMs in murine tumor models originate from the bone marrow-derived $Ly6C^+$ monocytes, while minor contributions come from extramedullary hematopoiesis in the spleen (66, 67). Within the TME TAMs can inhibit anti-tumor immunity through the expression of immune checkpoint molecules, production of immune suppressive molecules, and induction of other immunosuppressive cells. TAMs can trigger death of T cells through expression of PD-L1 and CD80, which bind to PD-1 and CTLA-4 (68-70). Arginase production by TAMs depletes L-arginine from the environment, which reduces T cell activation, by inhibiting TCRζ chain expression (71-74). TAMs can also reduce effector T cell function through their production of IL-10 and TGF-β (75, 76), both of which induce the suppressive function of Tregs by upregulating Foxp3 (77).

E4-3. CAFs

CAFs are the most abundant cell type found in the tumor stroma of various cancers including prostate, breast, and pancreatic carcinoma (78). In the TME fibroblasts become activated and turn into CAFs upon expression of activation markers. These activation markers include α- smooth muscle actin (α-SMA), fibroblast specific protein (FSP), platelet-derived growth factor receptor-β (PDGF-Rβ), and fibroblast activation protein (FAP) (79). The activation of CAFs is achieved by tumor-derived factors including TGF-β1 (80), PDGFα and PDGFβ (81, 82), basic fibroblast growth factor (bFGF) (83), and IL-6 (84). CAFs promote tumor development in numerous ways including the secretion of stromal cell-derived factor-1 (SDF-1), which promotes invasiveness of pancreatic cancer cells (85). Secretion of the chemokine CXCL14 by CAFs increases growth and migration of fibroblasts in pancreatic cancer, which in turn promotes angiogenesis and macrophage infiltration (86). CAFs also contribute to metastasis through the production of matrix metallopeptidases 2 and 9 (MMP-2 and MMP-9), which promote epithelial-mesenchymal transition (EMT) of tumor cells, mediated by the downregulation of E-cadherin (84). Lastly, CAFs can regulate tumor metabolism by providing energy rich metabolites. Tumor cells that are undergoing rapid cell division are constantly depleting their energy sources. Through a process called myo-fibroblast differentiation, which occurs when CAFs are in contact with epithelial cancer cells, CAFs produce lactate and pyruvate, thereby providing cancer cells with metabolites they can use to survive (87).

E4-4. pDCs

Human pDC are characterized based on their expression of CD303 (88). Under normal conditions pDC function to fight viral encounters through the secretion of IFN-α

(89). pDC also regulate the maturation of activated B cells into plasma cells by mediating cytokine and surface signaling (90, 91). Within the tumor pDC have tumor-promoting functions attributed in part to their reduced production of IFN-α, which promotes $CD4^+$ T cells to differentiate into IL-10 producing Tregs (92). Reduced production of IFN-α is also associated with weakened functions of CTLs and DC, as they each require type I IFNs for effective cross-presentation of tumor antigens (93, 94). Lastly, pDC release pro-angiogenic cytokines that promote tumor angiogenesis (95, 96).

E4-5. Bregs

An immune suppressive subset of B cells have been identified and classified as Bregs. The induction of Bregs as opposed to mature B cells requires the activation of CD40 (97). Ligation of CD40 with its ligand CD154 on T cells normally stimulates B cells to produce antibodies (98) however, prolonged stimulation with CD154 has inhibitory effects on the secretion of antibodies (99). Breg induction also requires the engagement of TLRs, specifically TLR 2 and 4. Agonists for TLR2 and 4 promote IL-10 and IL-6 production from Bregs, which is increased following engagement with CD40 (100). Stimulation of B cells with a TLR9 ligand increases the production of IL-10 from B cells (100).

While it has been determined how Bregs are induced, the origin of Bregs is still under debate. It has been suggested that Bregs arise from follicular (FO) B cells and gain suppressive function following stimulation with TLRs and engagement of CD40 (101). However, it has also been proposed that Bregs arise from transitional 2-marginal zone precursor (T2-MZP) B cells, which are an immature state of B cells and function as quick responders to environmental triggers (102). Through this model it is suggested that T2-MZP B cells form an immune response to a pathogen and are activated via TLRs,

resulting in the production of IL-10. As an inflammatory response ensues autoreactive T cells accumulate and provide B cells with epitopes for CD40, BCR, and CD80, which enhance and stabilize IL-10 production (103). The stabilization of IL-10 in turn promotes the induction of Tregs, which aid in driving an immune suppressive environment (104). Evidence that Bregs are directly involved in tumor-induced immune suppression has been generated from a tumor model utilizing mice that are deficient in B cells. Mice lacking B cells had an increased antitumor response by CTLs that was attributed to reduced levels of IL-10 produced by B cells (105).

E4-6. MDSC

MDSC are a heterogeneous population of immature myeloid cells that accumulate in individuals with chronic inflammation and cancer. The phenotype and function of MDSC can vary with cancer progression, since tumor cells evolve and change through immunoediting (106). MDSC are classified based on suppressive function and the surface markers CD14, CD15, CD33, and CD11b in humans while CD11b and Gr1 are expressed on the surface of murine MDSC (107-109). Gr1 includes two isoforms Ly6C and Ly6G. The differential expression Ly6C and Ly6G differentiates monocytic and granulocytic MDSC. Monocytic MDSC are $Gr1^{mid}CD11b^{+}Ly6C^{+}Ly6G^{low/-}$ while granulocytic MDSC are $Gr1^{hi/mid}CD11b^{+}$ $Ly6C^{-}Ly6G^{+}$(110).

The suppressive capacity of MDSC is mediated by immune suppressive factors such as arginase (Arg1), ROS, inducible nitric oxide synthase (iNOs), as well as high IL-10 production. MDSC suppress adaptive and innate anti-tumor immunity by blocking the activation of $CD4^{+}$ and $CD8^{+}$ T lymphocytes, and producing high levels of IL-10, which reduces the production of IL-12 from macrophages through crosstalk interactions (108, 111, 112). Further discussion of other suppressive mechanisms utilized by MDSC

including depletion of amino acids, expression of PD-L1, induction of Tregs, and inhibition of NK cell-mediated cytotoxicity can be found in appendix 5.

MDSC can directly inhibit T cells via the production of ROS, nitric oxide (NO) and peroxynitrite (113-115). One of the most potent forms of suppression mediated by MDSC comes from the reactive oxidant peroxynitrate, which nitrates the TCR and MHC I molecules, making the TCR incapable of recognizing peptides bound to MHC (113, 114, 116). Without TCR recognition of MHC there is a decrease in the activation of $CD4^+$ T cells by APCs, and a decrease in cytotoxic $CD8^+$ T cell specificity. High levels of ROS inhibit myeloid cell differentiation and sustain MDSC in their immature state (117). Intracellular ROS is regulated by NADPH oxidase (NOX2). NOX2 consists of $p47^{phox}$ and $gp91^{phox}$ which are in turn regulated by STAT3 (118).

MDSC suppressive functions are subject to regulation by signaling molecules. For instance, VEGF production by MDSC is regulated by STAT3 (117). VEGF can reduce T cell activation, inhibit DC development, and increase $Gr1^+$ cells (119)(119)(119)(119)(119)(119)(118)(118) . Peroxynitrite is also activated through STAT3 signaling, and arises from interaction of NO and superoxide (120). NO induces T cell apoptosis and blocks STAT5 and JAK3 signaling in T cells, which in turn inhibits T cell responsed to IL-2 (121-124). NO can also suppress T cell activation by destabilizing IL-2 mRNA and blocking phosphorylation of the signal transduction molecules JAK1, JAK3, STAT5, ERK, and Akt (125). IL-2 synthesis and activation of these signaling molecules, which are downstream of the IL-2R, are vital for T cell proliferation (126). T cell proliferation can also be inhibited by MDSC produced Arg1. Arg1 deprives T cells of L-arginine, and results in the down regulation of TCR-associated ζ chain (127, 128).

TCR-associated ζ chain is critical for T cell activation since it signals the activation of cyclin D3 and cyclin-dependent kinase 4 which initiates cell proliferation (129).

Not only do MDSC directly and in-directly inhibit T cell activation, they also impair T cell trafficking. Tumors producing high levels of GM-CSF have limited infiltration of $CD8^+$ T cells, and exhibit increased infiltration of mononuclear MDSC, which express chemokine receptor CCR2 (130). CCL2 (the ligand for CCR2) is present in the TME and acts as a chemoattractant for mononuclear MDSC (131). When mononuclear MDSC were depleted from GM-CSF secreting tumors there was an influx in $CD8^+$ T cells suggesting that mononuclear MDSC inhibit the infiltration of T cells (130). T cell trafficking to lymph nodes and tumor sites is dependent on T cell expression of L-selectin (CD62L). MDSC decrease the expression of CD62L on $CD4^+$ and $CD8^+$ naïve T cells in tumor-bearing and aged mice. MDSC reduce CD62L expression through the translocation of ADAM17 (disintegrin and metalloproteinase 17) from their cytosol to their plasma membrane. ADAM17 expressed on the cell surface cleaves CD62L on T cells (132). It is clear that MDSC are equipped with an arsenal of mechanisms to inhibit anti-tumor immunity. Several of the suppressive mechanisms utilized by MDSC are highlighted in **Figure 3**. A more detailed discussion of MDSC history, function, regulation, as well as therapeutic strategies targeting MDSC can be found in appendix 5 containing the MDSC review "Myeloid-derived suppressor cells: critical cells driving immune suppression in the tumor microenvironment".

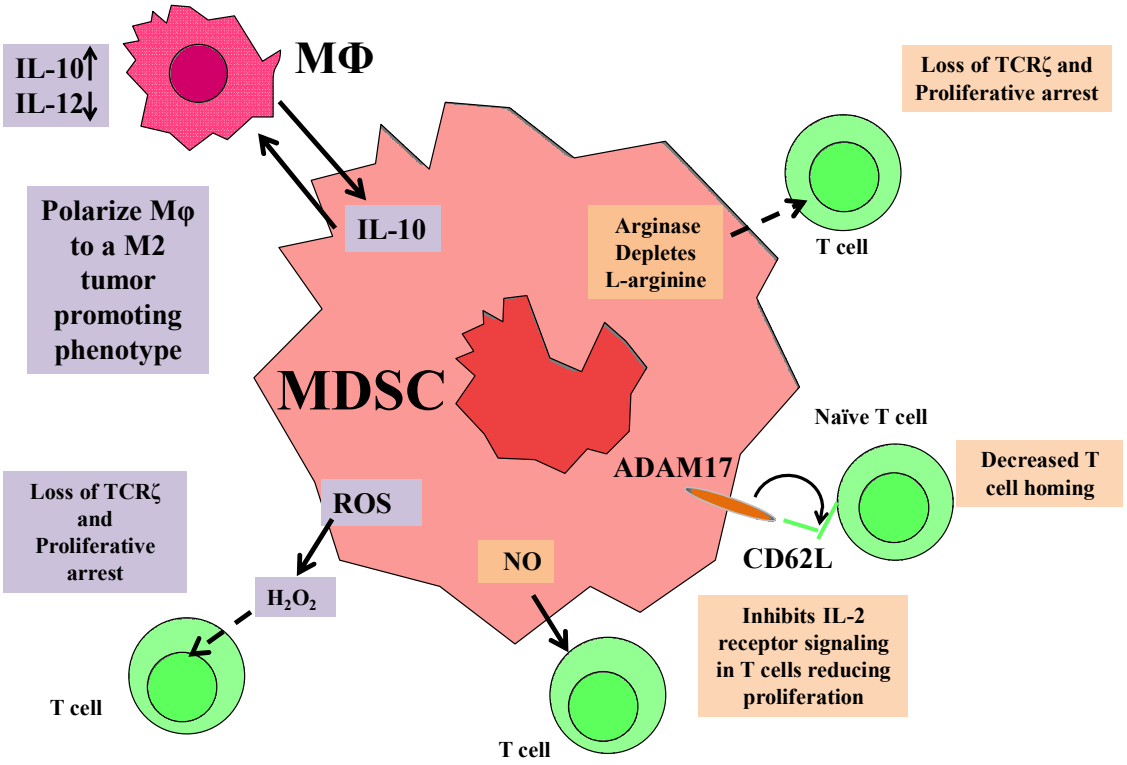

Figure 3: Suppressive mechanisms utilized by MDSC. MDSC crosstalk with macrophages through the high production of IL-10 which down regulates macrophage production of IL-12 and polarizes macrophages to a tumor promoting type 2 phenotype. MDSC cause down regulation of TCRζ signaling in T cells through the production of ROS, NO and arginase. MDSC also reduce T cell homing through the expression of ADAM17 which cleaves CD62L off of T cells.

F. Traditional cancer treatment

The most common cancer treatment methods utilized today fall under the category of traditional or conventional treatment. Conventional treatment includes surgical removal of the tumor combined with chemotherapy and radiation to eliminate the cancer cells. Radiation and chemotherapy are often given in combination with surgery, either before or after surgery. Radiation uses extremely powerful X-rays to damage the DNA of cancer cells resulting in their death, or inability to replicate. Chemotherapeutic treatments include alkalyating agents that prevent cell division, antimetabolites that

replace cell nutrients with inactive substances, hormonal treatments that suppress hormones tumors were using to grow, and alkaloids which block cell division by disrupting the internal structure of the cell (133).

In general chemotherapies non-specifically target rapidly dividing cells however, targeted therapies aim to solely inhibit tumor development by blocking biochemical pathways or proteins tumor cells require for survival (134). These targeted treatments include anti-angiogenic drugs, which block the development of new blood vessels thereby inhibiting the necessary blood supply which sustains tumor growth (135). Another form of targeted therapy consists of small-molecules targeted against kinases. For example, imatinib, a BCR-ABL kinase inhibitor, is effective at reducing tumor proliferation and enhancing apoptosis of tumor cells (136).While chemotherapeutics are undoubtedly useful at killing tumor cells and technology has increased precision for the delivery of radiation, these treatments have proven to be not enough to effectively fight cancer. Over a hundred years ago Paul Ehrlich proposed the idea that cancer occurs spontaneously in the body, and that the immune system is able to recognize and destroy it (137). Today numerous immunotherapeutic approaches are finding success in clinical trials.

G. Immunotherapeutics

Immunotherapy aims to harvest the power of the immune system to generate a more effective anti-tumor immune response. Types of immunotherapies include treatment with interferons, interleukins, and stimulation of co-stimulatory signals. Treatment with large quantities of interferons was successful in generating an antitumor response, by increasing CTL activity and inhibiting of tumor cell division however, their use is

complicated by toxic side effects (138). Clinical trials combining IL-2 and IFN-α showed complete tumor regression in 7 patients, and partial regression in 18 patients out of 91 (139). However, the dosing and administration of interferons and cytokines has proven to be particularly tricky as they often times these molecules can act antagonistically with severe consequences (140). The activation of co-stimulatory molecules is required for T cells to mount a successful immune response. Recently, experiments utilizing the soluble form of the co-stimulatory molecule CD80 have demonstrated great success in vitro. In these experiments soluble CD80 facilitated T cell activation by co-stimulating through CD28, and by binding to PD-L1 and inhibiting PD-L1 /PD-1 induced apoptosis of T cells (141).

G1. Checkpoint inhibitors

Checkpoint inhibitors provide a significant barrier in anti-tumor immunity. In recent years the neutralization of checkpoint inhibitors has found great success. In mouse tumor models inhibition of CTLA-4 reduced tumor growth, which was a result of increased activation of T cells (43, 142-144). Inhibition of CTLA-4, through a CTLA-4 inhibitory antibody gave rise to reduced Treg levels in mice as a consequence of ADCC mediated by cells expression Fcγ receptor (145-147). Clinical use of a CTLA-4 inhibitory antibody, called ipilimumab, delivered durable survival advantages in metastatic melanoma patients whom previously failed existing traditional therapies (148-150). The success of ipilimumab clinical trials led to FDA approval in 2011 for its use in treating metastatic melanoma, and it is currently being considered for use in patients with non-small cell lung carcinoma, small cell lung carcinoma, bladder cancer, and prostate cancer.

Blockade of the PD-1/PD-L1 pathway has also found success in recent years with neutralizing PD-1 antibodies nivolumab (Bristol-Myers Squibb) and pembrolizumab (Merck) displaying durable survival benefits in treating melanoma patients (151, 152). Additionally, clinical trials blocking PD-L1 were effective in treating patients with other solid tumors such as melanoma, colorectal cancer, renal cell cancer, non-small cell lung cancer, ovarian cancer and metastatic bladder cancer (153-155). While there has been landmark success with immune checkpoint inhibitors the clinical trials utilizing these molecules are currently focused on smoking-related lung cancers, and melanomas. Both of these cancers are predicted to be highly immunogenic due to a high mutation rate. Melanoma and lung cancers are most commonly carcinogen-induced and result in a higher mutation rate (156). Increased mutation rate generates a large amount of unique neoantigens that can be recognized on tumor cells making these tumor cells highly immunogenic (157).

G2. Adoptive cell transfer

Another type of immunotherapy is adoptive cell transfer. Expansion of tumor infiltrating lymphocytes (TIL), generation of T cells with genetically engineered TCRs, and transfer of NK cells and DC have produced survival benefits in recent years.

Current clinical results from TIL infusions found that in 93 patients with metastatic melanoma 72% had a response, while 36% achieved survival greater than three years (158). The most effective responses with TIL infusions occurs when patients are subjected to lymphodepletion prior to infusion, and when the TIL infusion contains $CD4^+$ and $CD8^+$ T cells (159, 160). While this approach has produced successful results, as evidenced by the transferred cells had functional activity in vivo, and could traffic to

tumor sites leading to tumor regression (160), the process of generating sufficient quantities of cells for infusions is a daunting task. Alternative approaches that do not require huge expansion of cells, but still mount an effect immune response have been developed. These alternative approaches include the generation of TCRs that recognize tumor-associated antigens, which can be engrafted on T cells (161, 162). Clinical use of T cells with tumor-associated specific antigen TCRs reduces tumor burden in metastatic melanoma, and in ovarian cancer patients (161, 163, 164).

Genetic modification of T cells has been further advanced by the creation of chimeric-antigen receptors (CAR). CARs are constructed so that a monoclonal antibody is coupled to intracellular T cell-activating signaling domains. The use of CARs allows for cytolytic T cell function without MHC-peptide complexes. The efficacy of CARs has been demonstrated in treating B cell malignancies (165-167), with 90% of patients reaching complete remission (168). In solid tumor models such as ovarian, renal, and neuroblastoma CARs are less effective in controlling tumor growth rates (164, 169-173).

NK cells are also suitable for adoptive transfer as they can mount an effective anti-tumor immune response. NK cells mediate lysis of tumor cells through mismatches with killer cell Ig-like receptors (KIRs) and MHC I molecules on target cells. The process of KIR mediated lysis by NK cells allows patients to receive NK cells from a haploidentical family member. NK cells can also initiate lysis of tumor cells through expression of FcγR, which mediates ADCC. In addition, death receptors expressed by NK cells can induce tumor cell death via caspase pathways (174). The greatest amount of success achieved with adoptive NK cell therapy has been observed in patients with hematological malignancies who received alloreactive haploidentical NK cells (175,

176). In human transplants NK cell transfer was effective at eliminating leukemia relapse, as well as graft rejection (175). In a clinical trial on acute myeloid leukemia patients, 5 out of 19 went into complete hematologic remission after NK cell transfer (176).

DC based therapies have also been used as DC can be generated or expanded in vitro and then exposed to tumor-associated antigens allowing them to function as activated APCs. Introduction of tumor-associated antigen can be achieved by pulsing with synthetic peptides, exposure to tumor lysates, or by transfection (177). Clinical studies using DC-based therapies have shown that a small portion of patients exhibit promising results (178-180). In pediatric patients with solid tumors, 1 out of 10 exhibited a significant reduction in multiple metastatic sites (180). A clinical trial on adults with metastatic melanoma found objective responses in 3 out of 16 patients (178), while metastatic renal cell carcinoma patients displayed low tumor-related mortality rates with only 3 out of 10 dying after an average follow up time of 19.9 months (179).

H. High Mobility Group Box 1 a pro-inflammatory alarmin

The focus of my research has been investigating a molecule called high mobility group box 1 (HMGB1). This section of the introduction will describe HMGB1's structure, its intracellular and extracellular functions as well as its role in regulating cancer, and involvement in other clinical syndromes and diseases.

HMGB1 is an extremely abundant protein with normal levels hovering above one million molecules per cell (181). The sequence of HMGB1 is highly conserved with over 98% sequence homology between humans and rodents (182-184). Under basal conditions HMGB1 is found inside the nucleus of a cell, while under stressed conditions HMGB1 can be found in the cytosol and secreted by immune cells. Extracellular HMGB1 has

many pro-inflammatory properties, owing to the molecule's classification as a DAMP. The pro-inflammatory properties of HMGB1 have been implicated in various inflammatory conditions including cancer, arthritis, and sepsis (185-187).

H1. Structure of HMGB1 and distinct functions of the domains in HMGB1

HMGB1 is a 215 AA protein that contains two functional domains called the A and B boxes, followed by an acidic tail. Structurally the boxes of HMGB1 consist of three alpha-helices that are arranged in an L-shaped conformation (188). Within these two sections of the molecule there are various pro and anti-inflammatory activities, which result from binding to receptors including TLR4 and receptor for advanced glycation endproducts (RAGE) (**Figure 4**).

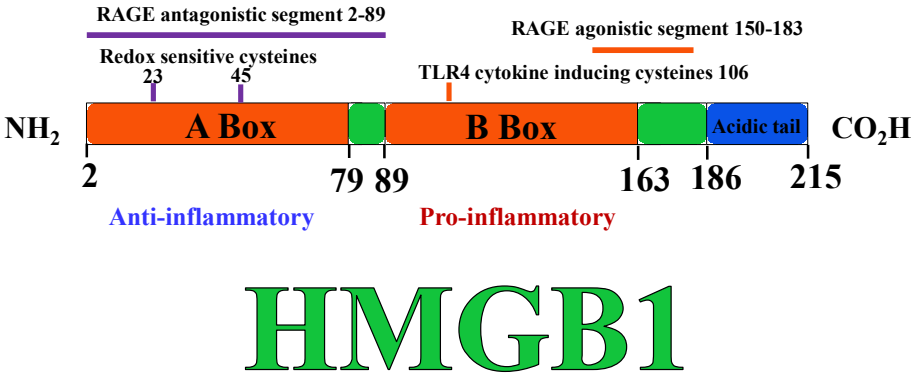

Figure 4: Structure of HMGB1 HMGB1 is composed of 215 amino acids and has a molecular weight of 25kDa. There are two DNA binding domains, the A and the B boxes followed by a negatively charged C-terminal tail, the green regions represent connecting segments between each domain. The A box has anti-inflammatory properties, while the B box has pro-inflammatory properties.

A part of the B box and acidic tail (150-183) has RAGE agonistic activity, which was confirmed by the use of a neutralizing B box antibody, which inhibited the ability of HMGB1 to induce recruitment of mesoangioblasts (189). Recent studies have identified amino acid cysteine 106 as the specific location of HMGB1 that is required for HMGB1

binding to TLR4 in macrophages. This position is located in the B box of HMGB1 and is associated with pro-inflammatory cytokine release in macrophages (190).

It is interesting that while the B box of HMGB1 is generally considered pro-inflammatory, it also induces the phenotypic maturation of DC, causing an increase in the markers CD83, CD54, CD80, CD40, CD58, and MHC II (191). Upon stimulating DC with B box, an increase in type 1 cytokines IL-12, IL-6, IL-1α, IL-8, TNF-α, and RANTES occurs (191). The peptide segment of HMGB1 corresponding to amino acids 106-123 was found to be the driving factor in the up-regulation of CD83 and IL-6 production, which was dependent on the p38 MAPK pathway (191). Therefore, this segment in the B box stimulates a pro-inflammatory cytokine response from macrophages and also induces maturation of DC.

The A box of HMGB1 is associated with the anti-inflammatory activity of the molecule and it is generally kept inactive, due to the existence of a disulfide bridge between cysteines 23 and 45. The ability of the A box to act as a competitor for the B box results from a section with RAGE antagonistic activity. This section of the protein binds to RAGE, but fails to stimulate signaling and is therefore seen as a competitor for HMGB1-RAGE inflammatory signaling (192). Yang et al. have also shown that the A box of HMGB1 prevents the HMGB1-mediated release of IL-1β and TNF-α from macrophage-like RAW cells (192). In vivo studies have demonstrated that if mice are given the A box of HMGB1 intraperitoneally within 24 hours after a toxic dose of LPS, then septic shock is reversed (192). These findings further support the notion that the A box of HMGB1 is anti-inflammatory, and acts as a competitor for the pro-inflammatory activity of the B box.

H2. Pro-tumor functions of HMGB1; HMGB1 promotes metabolism, invasion, angiogenesis, autophagy, and inhibits anti-tumor immunity

Tumor cells characteristically exhibit high expression levels of HMGB1, and a rise in HMGB1 expression in tumor cells correlates with increases in tumor growth, invasion, angiogenesis, and metastasis (4, 187). Tumor cells and infiltrating leukocytes are able to secrete HMGB1, when subjected to stress stimuli such as hypoxia and inflammatory molecules both of which are commonly found in the TME (193). The pro-tumor effects of HMGB1 have been attributed to the molecule's promotion of metabolism, invasion, angiogenesis, and its ability to inhibit anti-tumor immunity (14, 194, 195).

Tumor cells consume high amounts of energy as a result of continuous division, evasion of death by autophagy, and the production of inflammatory molecules. The ability of tumor cells to alter and accelerate their metabolism is termed the Warburg effect, and is one of the most common phenotypes found in tumors (196). Recombinant and endogenous HMGB1 increases ATP production and cell proliferation in pancreatic tumor cells (194). Generation of ATP affords tumor cells an increased capacity for invasion and metastasis. HMGB1's ability to promote increased metabolic energy in tumor cells results from signaling through RAGE. Expression of HMGB1 in the extracellular environment promotes increased expression of RAGE in the mitochondria, which in turn promotes ATP production (194). Mice that are RAGE deficient display reduced tumorigenesis in the skin, pancreas and intestine, which is associated with inhibition of ATP production and stifles tumor growth (197-199). Therefore, the ability of HMGB1 to alter tumor cell metabolism is linked to its interaction with RAGE.

HMGB1 promotion of tumor cell invasion is also linked to its interaction with RAGE. Suppressing the interaction of RAGE and HMGB1 in vitro inhibits cancer cell growth, invasion, and migration (200). Blockage of HMGB1 binding to RAGE prevents tumor growth in a mouse lung cancer model (201). The interaction between HMGB1 and RAGE can also promote tumor angiogenesis. The knockdown of RAGE or neutralization of HMGB1 impedes tumor angiogenesis and metastasis (195, 202). The ability of HMGB1 to promote tumor growth is attributed to stimulating increased release of TNF-α, IL-1β, and IL-6 from macrophages, which induces neovascularization (203, 204). Within the TME there is increased release of HMGB1 and amplified expression of RAGE, which is associated with hypoxic regions (205, 206). Therefore not only does HMGB1 interacting with RAGE promote tumor growth, but the TME in turn promotes increased HMGB1 and RAGE expression.

The TME is a hostile environment that contains multiple pro-inflammatory mediators that generate a stressed environment (207). Many tumor cells utilize autophagy to survive under stressed conditions (208). Autophagy provides a survival advantage to stressed cells, as it enables cells to maintain metabolic activity by engulfing cytoplasmic components that are degraded in autolysosomes (209). Degradation of cytoplasmic components through starvation-induced autophagy regenerates amino acids, that are utilized in the trichloroacetic acid cycle to produce energy the cell needs to survive, thereby allowing them to avoid death (210). The process of autophagy involves the formation of autophagosomes, mediated by a series of membrane rearrangements involving autophagy-related proteins (Atg) (211) (**Figure 5**).

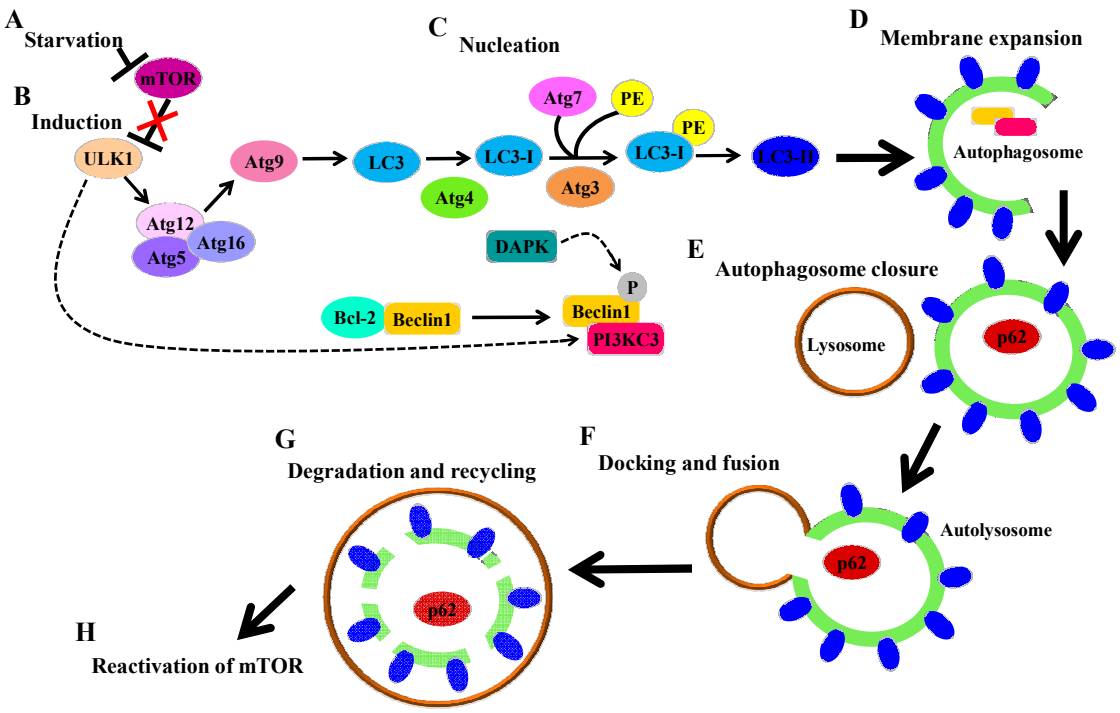

Figure 5: Schematic overview of autophagy. (**A**) Starvation results in down regulation of mechanistic target of Rapamycin (mTOR), causing mTOR to release its inhibition on ULK1. (**B**) ULK1 in turn induces vacuole formation by activating phosphoinositide 3-kinase class 3 (PI3KC3), Beclin1 (Atg6), and the Atg12, 5, and 16 complex. This complex then interacts with Atg9 to mediate the induction of an autophagosome. Activation of PI3KC3 promotes the dissociation of Bcl-2 from Belcin1. Death-associated protein kinase (DAPK) can also phosphorylate Beclin1, causing the dissociation of Bcl-2. (**C**) The process of nucleation requires association of Beclin1 and PI3KC3 as well as modification of LC3 via an ubiquitin-like conjugation pathway. The ubiquitin-like pathway involves Atg4, which encodes a cysteine protease that cleaves LC3 to form LC3-I. LC3-I then undergoes C terminal lipid modification through conjugation with phosphatidylethanolamine (PE) to form LC3-II with the assistance of Atg7 and Atg3. LC3-II is then incorporated into the lumen of an autophagosome. (**D**) LC3-II and Beclin1 assist in membrane expansion by recruiting lipid molecules that expand the membrane. (**E**) With closure of the autophagosome cellular cargo, as well as adaptor proteins including p62, are contained in the autophagosome. p62 contains a LC3 interacting region and allows the autophagosome to target designated cargo. (**F**) Maturation of an autolysosome is accomplished by the docking and fusing of a lysosome to an autophagosome. (**G**) Autolysosomes allow the breakdown of autophagosomal contents that are recycled to temporarily sustain survival. (**H**) mTOR signaling is inhibited with initial starvation however, with prolonged starvation and the degradation of autophagosomal products, mTOR activity is restored and autolysosomes develop into lysosomes.

HMGB1 regulates autophagy by binding to Beclin1 and promoting the phosphorylation of Bcl-2 by extracellular signal-regulated kinase (ERK), resulting in dissociation of Bcl-2 from Beclin1 (212). Further evidence for HMGB1 as a regulator of autophagy has been achieved, through shRNA knockdown and mutation of HMGB1 in tumor cell lines (212). Knockdown of HMGB1 sustains the interaction of Beclin1 with Bcl-2, while mutation of HMGB1 at cysteines 23 and 45 impede HMGB1 association with Beclin1. Cysteines 23 and 45 form a disulfide bridge. Therefore, these mutation studies suggest that the disulfide bridge between cystines 23 and 45 of HMGB1 is needed to bind Beclin1 and induce autophagy (212). Mutation of HMGB1 at another critical cysteine, 106, resulted in the release of HMGB1 into the cytosol, resulting in increased dissociation of Bcl-2 from Beclin1 (212). This mutant form of HMGB1 (C106) has been described as "oxidized HMGB1" found most commonly in the cytosol. To further prove that cytosolic HMGB1 is responsible for regulating autophagy Tang et al utilized an HMGB1 inhibitor, ethyl pyruvate, which blocks HMGB1 release into the cytosol. Tang et al observed a reduction in LC3 positive autophagosome formation with the addition of ethyl pyruvate, suggesting that inhibition of HMGB1 reduces autophagic flux (212, 213). Therefore, the release of HMGB1 into the cytosol, and the existence of a disulfide bridge between cysteines 23 and 45 enable HMGB1 to serve as an inducer of autophagy.

Several studies have examined the functions of reduced vs. oxidized HMGB1, and interestingly, oxidative stress is known to induce autophagy (214). A major source of oxidative stress is ROS, of which MDSC generate ample amounts (118). ROS can be regulated by SOD (super oxide dismutase), glutathione, or catalase (215). Knockdown of

SOD1 in fibroblasts by siRNA, increased LC3-II formation (216), supporting the idea that increased oxidative stress results in increased autophagic flux. To substantiate the association between HMGB1 and ROS, Tang et al utilized a ROS inhibitor, NAC (N-acetylcysteine), that reduced translocation of HMGB1 to the cytosol, confirming that oxidative stress promotes HMGB1 release into the cytosol (216). Furthermore, stimulation of fibroblasts and cancer cells with oxidative source H_2O_2 induced LC3-II formation that was inhibited by knockdown of HMGB1 (216). Therefore, ROS induces HMGB1 release which in turn induces autophagy.

In an effort to decipher the signaling pathway involved in HMGB1 regulated autophagy, RAGE was knocked down in tumor cells, and autophagy induced by chemotherapeutic agents. Kang et al discovered that the knockdown of RAGE resulted in a limited increase in LC3-II and enhanced degradation of p62, suggesting a reduction in autophagy (217). The RAGE knockdown cells also exhibited slower tumor growth and increased apoptosis in vivo (217). Interestingly, knockdown of HMGB1 in tumor cells made them more sensitive to chemotherapy and increased their rate of apoptosis, resulting in less LC3-II accumulation (217). Therefore, knocking down HMGB1 or RAGE in tumor cells makes cells less autophagic, suggesting that HMGB1 utilizes RAGE to promote autophagy.

HMGB1 can also promote tumor growth by negatively regulating anti-tumor immune cells, or positively regulating immune suppressive cells. HMGB1 promotes the apoptosis of macrophage-derived DC (218), thereby reducing the quantity of APC available to mount an effective anti-tumor immune response. The accumulation of TAMs, which provide growth factors supporting tumor angiogenesis, is also linked to

HMGB1 in that macrophage accumulation results from HMGB1 promoted the expression of lymphotoxinα1β2 on tumor infiltrating T cells (219). Enhanced production of IL-10 from immune suppressive Tregs is also promoted by HMGB1 (220). And, recently I established that HMGB1 drives immune suppressive MDSC differentiation, accumulation, and suppressive function (14), thus establishing HMGB1 as a potent inhibitor of anti-tumor immunity. These studies are described in chapter 2. The functions of HMGB1 can be described as bi-polar in that while it has numerous means of promoting tumor progression, it can also inhibit tumor progression.

H3. Anti-tumor functions of HMGB: HMGB1 interacts with tumor suppressor gene Rb, increases genome stability, promotes autophagy, promotes maturation of APCs

Anti-tumor aspects of HMGB1 are attributed to HMGB1 interacting with tumor suppressor genes, increasing genome stability, promoting autophagy, and promoting maturation of APC. HMGB1 directly interacts with tumor suppressor protein Rb, which is dysfunctional in many cancers (221). Binding of HMGB1 to Rb causes G1 arrest and induction of apoptosis in tumor cells (221). HMGB1 contributes to genome stability by mediating DNA damage repair (222). Additionally, genome stability is increased by HMGB1 regulating telomere length, through its binding to topoisomerase IIα. HMGB1 promotes the activity and expression of topoisomerase IIα, an enzyme that regulates topologic state of DNA during transcription and is implicated in chromosome replication, segregation, and recombination (223). Telomeres are caps on chromosomes consisting of tandem TTAGGG repeats (224). With each cell division the length of a telomere is shortened due to incomplete replication of the 3' end of the chromosome. In an effort to prevent genomic abnormalities when telomeres reach a critically short length, this

induces senescence and apoptosis of the cell (225). Recent meta-analysis revealed that shortened telomeres are associated with cancer occurrence (226).

While the induction of autophagy is not desirable in established tumors, it is desirable during initial tumor development as it can have anti-tumor functions. Defective autophagy genes (Beclin1, Atg5, UVRAG, and Bif-1) have been implicated in increased genome instability, oxidative stress, inflammation, and mitochondrial injury, all of which promote tumorigenesis (227-230). Since HMGB1 is a critical regulator of autophagy (212, 231), it is possible that HMGB1 mediated autophagy promotes genome stability and reduces inflammation by degrading defective cellular components. Recently, I established that autophagy-induced by HMGB1 facilitates immune suppression by promoting the survival of tumor-induced MDSC. These studies are described in chapter 3.

Finally, HMGB1 promotes the maturation of DC, increasing their release of TNF-α, IL-1α, IL-6, IL-8, and IL-12, while also increasing expression of CD40, CD54, CD58, CD80, and CD83 (232, 233). Administration of recombinant HMGB1 in combination with chemo-radiation delayed tumor growth in a murine tumor model. The ability of HMGB1 to reduce tumor growth is attributed to HMGB1 signaling through TLR4 on DC, causing an increase in antigen presentation (234). Apetoh et al also showed that breast cancer patients with dysfunctional TLR4s relapse at a faster rate after chemotherapy as opposed to patients with a functional TLR4, suggesting that TLR4 stimulation is necessary for a prolonged antitumor impact (234). Taken together these data suggest that HMGB1 has multiple functions that have anti-tumor implications.

H4. HMGB1 involvement in clinical syndromes and diseases

Elevated levels of HMGB1 have been linked to various pro-inflammatory immune reactions including sepsis, tissue repair, infection, and arthritis. In mouse models of severe sepsis, HMGB1 levels are extremely elevated in the serum, while the inhibition of HMGB1 through immunization with a neutralizing antibody, is able to prevent lethality from sepsis (185). The administration of recombinant HMGB1 is lethal as it causes dysfunction in epithelial-cell barrier, which promotes septic shock, however HMGB1 does not cause septic shock itself (235). It has been suggested that HMGB1 promotes the recruitment of inflammatory cells for tissue repair, as burned animals exhibit increased expression of HMGB1 mRNA (236). Cells infected with Chlamydia spp or flavivirus exhibit elevated release of HMGB1 that is associated with resistance to apoptotic death, which may or may not be from HMGB1 promoting autophagy (237, 238). High levels of HMGB1 are also observed in inflamed joints of patients with rheumatoid arthritis (186). Therefore, HMGB1 is associated with numerous inflammatory immune responses.

H5. Intracellular function of HMGB1, and how it is released from the nucleus through modifications including acetylation, methylation, phosphorylation, and oxidation

HMGB1 shuttles between the nucleus and the cytoplasm, but is normally found in the nucleus where it will bind to the minor groove of DNA without sequence specificity. The binding of HMGB1 to DNA causes a structural change in DNA, in the form of a bend, which facilitates interaction between transcription factors such as p53 and NF-κB (4). The localization of HMGB1 in the nucleus results from HMGB1 containing two nuclear localization signal sequences, one residing in the A box, and the other directly before the acidic tail (239). Release of HMGB1 from the nucleus can be achieved

through passive release from a cell upon necrosis, or active release as a result of various modifications such as acetylation, phosphorylation, and methylation. The oxidation status of HMGB1 also plays a critical role in the location and function of HMGB1 (240).

The release of HMGB1 by activated macrophages and DC is controlled by acetylation (241). In these activated immune cells it is thought that activation promotes the inhibition of deacetylases that are typically abundant in the nucleus (242). With the inhibition of deacetylases there is an increase in acetylation, which occurs on a number of lysine residues of which several reside near the nuclear-localization signals of HMGB1. With an acetylated nuclear-localization signal HMGB1 cannot properly interact with the nuclear-importer protein complex, thus inhibiting HMGB1's retention in the nucleus (241). Acetylated cytosolic HMGB1 will migrate into cytoplasmic secretory vesicles that will eventually be released from the cell (241). Phosphorylation of HMGB1's nuclear localization signals by protein kinase C also regulates the shuttling of HMGB1 between the nucleus and the cytoplasm (243, 244). Similar to acetylation, phosphorylation inhibits HMGB1 from binding nuclear cargo protein, which results in HMGB1's accumulation in secretory vesicles that will eventually be released into the extracellular space. Mono-methylated HMGB1 has been found in the cytoplasm of neutrophils. The site of methylation is lysine-42 which causes conformational changes in the A box of HMGB1, disrupting HMGB1's ability to bind DNA and there by inhibiting its retention in the nucleus (245). Therefore, modification of HMGB1's nuclear localization signals, or its ability to bind DNA result in its release from the nucleus.

Within the past few years the oxidation status of HMGB1 has been highly investigated as the pro-inflammatory activity of HMGB1 is dependent on the redox status

of cysteines 23,45, and 106 (**Figure 4**). Cysteines 23 and 45 can form an intra-molecular disulfide bond, while 106 is unpaired (246). The existence of a disulfide bridge between cysteines 23 and 45 results in a fold within the A box of the molecule, which impedes the A box of HMGB1 having any signaling capacity (247). This disulfide bridge might explain why the predominantly observed functions of HMGB1 are seen as pro-inflammatory, since the A box is kept inactive most of the time by this bond. The existence of a disulfide bridge between cysteines 23 and 45, as well as a thiol on cysteine 106 are necessary for the pro-inflammatory properties of HMGB1 (240, 246). The pro-inflammatory activity of HMGB1 is inhibited when all three cysteines are irreversible oxidized to sulphonates, or when all three are reduced to thiols (246). Interestingly all thiol HMGB1 maintains chemoattractant activity, only terminally oxidized HMGB1 with all three cysteines as sulfonates, lacks any activity (240). Terminally oxidized HMGB1 is released from necrotic cells (248). It has been suggested that the ability of HMGB1 to self-regulate it's activity based on oxidative status is a mechanism used by the immune system to dampen DAMPs (249). In this regard DAMPs stimulate an immune response that causes oxidative stress. Oxidative stress in turn promotes resolution of inflammation by inactivating DAMPs.

H6. Extracellular function of HMGB1 as a pro-inflammatory cytokine that can signal through numerous receptors

Cytokines are defined as proteins that are released from activated immunocytes that mediate an array of metabolic and immunological responses in other immune cells (250). In the extracellular environment HMGB1 can act as a pro-inflammatory cytokine (251). When in the extracellular environment HMGB1 can bind to a multitude of

receptors including RAGE, TLR2, TLR4, TLR9 (252), CD24 (4, 253), TIM3 (254), IL-1R (255) and CXCR4 (256) (**Figure 6**).

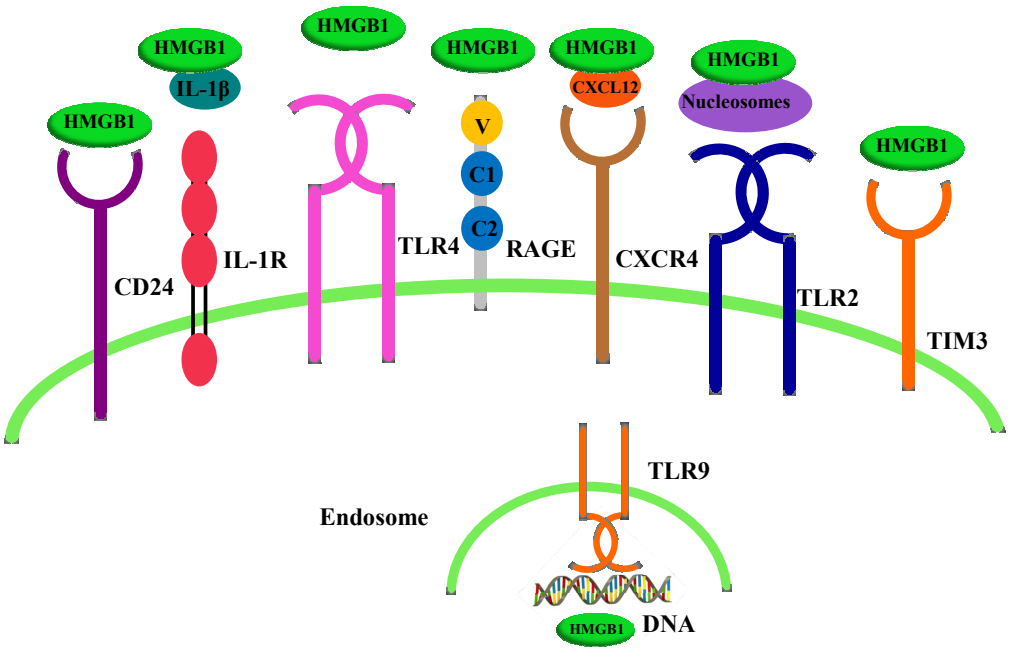

Figure 6: HMGB1 can bind to a multitude of receptors. HMGB1 can bind CD24, TIM3, RAGE, and TLR4 independently. When HMGB1 is bound to IL-1β it may signal through IL-1R. HMGB1 coupled to CXCL12 will signal through CXCR4, while when coupled to a nucleosome HMGB1 will signal through TLR2. Internally HMGB1 can signal through TLR9 when bound to DNA.

HMGB1 through RAGE has pro-inflammatory effects that drive tumor progression; while blockade of RAGE and HMGB1 binding suppresses tumor growth (13). HMGB1 interaction with TLR4 supports hemorrhagic shock and systemic inflammation (257), while in ischemia TLR4-dependent ROS production induces the release of HMGB1 from hepatocytes (258). Therefore, HMGB1 signaling through TLR4 stimulates an inflammatory immune response. While HMGB1 signals independently

through TLR4 and RAGE it can be coupled with other molecules and signal through other receptors including TLR2 and TLR9.

HMGB1 bound to nucleosomes signals through TLR2 inducing macrophages and DC to release IL-1β, IL-6, IL-10 and TNF-α (259). TLR9 is expressed internally and HMGB1 signals through TLR9 when it is bound to DNA. HMGB1 signaling through TLR9 induces IFN-α production from pDCs or IL-6, IL-12 and TNF-α from bone marrow derived DC (252, 260). In the presence of IL-1β, HMGB1 can form a complex with this interleukin and signal through IL-1R, resulting in heightened production of TNF-α (255). HMGB1 can also form a complex with the chemokine CXCL12. The HMGB1 and CXCL12 complex then act through CXCR4 to stimulate the recruitment of inflammatory mononuclear cells to damaged tissue (256). Therefore, in various inflammatory settings HMGB1 is able to function as an activator of the immune system by inducing cytokine release as well as the recruitment of immune cells.

While signaling initiated by HMGB1 can activate an immune response, it can also dampen it. DC in the TME expressing TIM3 can interact with HMGB1. This interaction of TIM3 and HMGB1 interferes with the efficacy of DNA vaccines by diminishing the immunogenicity of nucleic acids released by dying tumor cells, as a result of reduced transport of nucleic acids to endosomal vesicles (254). Another immune dampening property of HMGB1 is present in its interaction with CD24. In a liver injury model that induces sterile inflammation the binding of HMGB1 to CD24 reduces the pro-inflammatory activity of HMGB1, by inhibiting its ability to activate NF-κB (261). Therefore, depending on the setting in which HMGB1 is released, and if it is coupled to any other molecules HMGB1 can mediate activation of the immune system into a pro-

inflammatory response, or dampen it into a tolerogenic response. The ability of HMGB1 to possess these opposing effects could be a result of the molecule unique structure, and it containing several redox sensitive cysteines that are capable of altering its structure.

I. Goal of dissertation research

The focus of my dissertation research has been on understanding tumor-induced immune suppression. Within the TME are a plethora of immune suppressive cells including MDSC that are induced by inflammation (262). Up-regulation of a bi-functional cytokine HMGB1 with predominantly pro-inflammatory properties is associated with malignant phenotypes in numerous cancers (263). Therefore, with the association between inflammation inducing immune suppression, and HMGB1 as a driver of inflammation, the hypothesis that HMGB1 functions as an upstream regulator of inflammation and promotes immune suppression was generated. Chapter 2 explores the effect HMGB1 has on MDSC, and establishes HMGB1 as an enhancer of tumor-induced immune suppression through the promotion of MDSC differentiation, accumulation, and suppressive activity. Chapter 3 investigates how HMGB1 regulates MDSC-induced immune suppression, and describes a new mechanism for how HMGB1 promotes tumor progression, by maintaining MDSC survival through the induction of autophagy. Taken together, these studies identify HMGB1 as a potent driver of tumor-induced immune suppression.

J. Citations

1. Kindt, T., R. Goldby, B. Osborne, and J. Kuby. 2007. *Immunology*. W. H. Freeman and Company, W. H. Freeman and Company, New York, NY.
2. Society, A. C. 2015. American Cancer Society, *Cancer Facts & Figures 2015*.
3. Schreiber, R. D., L. J. Old, and M. J. Smyth. 2011. Cancer immunoediting: integrating immunity's roles in cancer suppression and promotion. *Science* 331: 1565-1570.
4. Sims, G. P., D. C. Rowe, S. T. Rietdijk, R. Herbst, and A. J. Coyle. 2010. HMGB1 and RAGE in inflammation and cancer. *Annu Rev Immunol* 28: 367-388.
5. Guerra, N., Y. X. Tan, N. T. Joncker, A. Choy, F. Gallardo, N. Xiong, S. Knoblaugh, D. Cado, N. M. Greenberg, N. R. Greenberg, and D. H. Raulet. 2008. NKG2D-deficient mice are defective in tumor surveillance in models of spontaneous malignancy. *Immunity* 28: 571-580.
6. Aguirre-Ghiso, J. A. 2007. Models, mechanisms and clinical evidence for cancer dormancy. *Nat Rev Cancer* 7: 834-846.
7. Koebel, C. M., W. Vermi, J. B. Swann, N. Zerafa, S. J. Rodig, L. J. Old, M. J. Smyth, and R. D. Schreiber. 2007. Adaptive immunity maintains occult cancer in an equilibrium state. *Nature* 450: 903-907.
8. Johnsen, A. K., D. J. Templeton, M. Sy, and C. V. Harding. 1999. Deficiency of transporter for antigen presentation (TAP) in tumor cells allows evasion of immune surveillance and increases tumorigenesis. *J Immunol* 163: 4224-4231.

9. Dunn, G. P., A. T. Bruce, H. Ikeda, L. J. Old, and R. D. Schreiber. 2002. Cancer immunoediting: from immunosurveillance to tumor escape. *Nat Immunol* 3: 991-998.

10. Khong, H. T., and N. P. Restifo. 2002. Natural selection of tumor variants in the generation of "tumor escape" phenotypes. *Nat Immunol* 3: 999-1005.

11. Quail, D. F., and J. A. Joyce. 2013. Microenvironmental regulation of tumor progression and metastasis. *Nat Med* 19: 1423-1437.

12. Vesely, M. D., M. H. Kershaw, R. D. Schreiber, and M. J. Smyth. 2011. Natural innate and adaptive immunity to cancer. *Annu Rev Immunol* 29: 235-271.

13. Taguchi, A., D. C. Blood, G. del Toro, A. Canet, D. C. Lee, W. Qu, N. Tanji, Y. Lu, E. Lalla, C. Fu, M. A. Hofmann, T. Kislinger, M. Ingram, A. Lu, H. Tanaka, O. Hori, S. Ogawa, D. M. Stern, and A. M. Schmidt. 2000. Blockade of RAGE-amphoterin signalling suppresses tumour growth and metastases. *Nature* 405: 354-360.

14. Parker, K. H., P. Sinha, L. A. Horn, V. K. Clements, H. Yang, J. Li, K. J. Tracey, and S. Ostrand-Rosenberg. 2014. HMGB1 enhances immune suppression by facilitating the differentiation and suppressive activity of myeloid-derived suppressor cells. *Cancer Res* 74: 5723-5733.

15. Marincola, F. M., E. M. Jaffee, D. J. Hicklin, and S. Ferrone. 2000. Escape of human solid tumors from T-cell recognition: molecular mechanisms and functional significance. *Adv Immunol* 74: 181-273.

16. Rivoltini, L., M. Carrabba, V. Huber, C. Castelli, L. Novellino, P. Dalerba, R. Mortarini, G. Arancia, A. Anichini, S. Fais, and G. Parmiani. 2002. Immunity to

cancer: attack and escape in T lymphocyte-tumor cell interaction. *Immunol Rev* 188: 97-113.

17. Aspord, C., A. Pedroza-Gonzalez, M. Gallegos, S. Tindle, E. C. Burton, D. Su, F. Marches, J. Banchereau, and A. K. Palucka. 2007. Breast cancer instructs dendritic cells to prime interleukin 13-secreting CD4+ T cells that facilitate tumor development. *J Exp Med* 204: 1037-1047.

18. De Monte, L., M. Reni, E. Tassi, D. Clavenna, I. Papa, H. Recalde, M. Braga, V. Di Carlo, C. Doglioni, and M. P. Protti. 2011. Intratumor T helper type 2 cell infiltrate correlates with cancer-associated fibroblast thymic stromal lymphopoietin production and reduced survival in pancreatic cancer. *J Exp Med* 208: 469-478.

19. Sheng, H., J. Shao, J. D. Morrow, R. D. Beauchamp, and R. N. DuBois. 1998. Modulation of apoptosis and Bcl-2 expression by prostaglandin E2 in human colon cancer cells. *Cancer Res* 58: 362-366.

20. Masferrer, J. L., K. M. Leahy, A. T. Koki, B. S. Zweifel, S. L. Settle, B. M. Woerner, D. A. Edwards, A. G. Flickinger, R. J. Moore, and K. Seibert. 2000. Antiangiogenic and antitumor activities of cyclooxygenase-2 inhibitors. *Cancer Res* 60: 1306-1311.

21. Wang, D., and R. N. DuBois. 2008. Pro-inflammatory prostaglandins and progression of colorectal cancer. *Cancer Lett* 267: 197-203.

22. Greenhough, A., H. J. Smartt, A. E. Moore, H. R. Roberts, A. C. Williams, C. Paraskeva, and A. Kaidi. 2009. The COX-2/PGE2 pathway: key roles in the

hallmarks of cancer and adaptation to the tumour microenvironment. *Carcinogenesis* 30: 377-386.

23. Sinha, P., V. K. Clements, A. M. Fulton, and S. Ostrand-Rosenberg. 2007. Prostaglandin E2 promotes tumor progression by inducing myeloid-derived suppressor cells. *Cancer Res* 67: 4507-4513.

24. Eruslanov, E., I. Daurkin, J. Ortiz, J. Vieweg, and S. Kusmartsev. 2010. Pivotal Advance: Tumor-mediated induction of myeloid-derived suppressor cells and M2-polarized macrophages by altering intracellular PGE_2 catabolism in myeloid cells. *J Leukoc Biol* 88: 839-848.

25. Toi, M., S. Kondo, H. Suzuki, Y. Yamamoto, K. Inada, T. Imazawa, T. Taniguchi, and T. Tominaga. 1996. Quantitative analysis of vascular endothelial growth factor in primary breast cancer. *Cancer* 77: 1101-1106.

26. Gabrilovich, D. I., H. L. Chen, K. R. Girgis, H. T. Cunningham, G. M. Meny, S. Nadaf, D. Kavanaugh, and D. P. Carbone. 1996. Production of vascular endothelial growth factor by human tumors inhibits the functional maturation of dendritic cells. *Nat Med* 2: 1096-1103.

27. Gabrilovich, D. I., T. Ishida, S. Nadaf, J. E. Ohm, and D. P. Carbone. 1999. Antibodies to vascular endothelial growth factor enhance the efficacy of cancer immunotherapy by improving endogenous dendritic cell function. *Clin Cancer Res* 5: 2963-2970.

28. Ishida, T., T. Oyama, D. P. Carbone, and D. I. Gabrilovich. 1998. Defective function of Langerhans cells in tumor-bearing animals is the result of defective maturation from hemopoietic progenitors. *J Immunol* 161: 4842-4851.

29. Bronte, V., D. B. Chappell, E. Apolloni, A. Cabrelle, M. Wang, P. Hwu, and N. P. Restifo. 1999. Unopposed production of granulocyte-macrophage colony-stimulating factor by tumors inhibits CD8+ T cell responses by dysregulating antigen-presenting cell maturation. *J Immunol* 162: 5728-5737.

30. Serafini, P., R. Carbley, K. A. Noonan, G. Tan, V. Bronte, and I. Borrello. 2004. High-dose granulocyte-macrophage colony-stimulating factor-producing vaccines impair the immune response through the recruitment of myeloid suppressor cells. *Cancer Res* 64: 6337-6343.

31. Fu, Y. X., G. Watson, J. J. Jimenez, Y. Wang, and D. M. Lopez. 1990. Expansion of immunoregulatory macrophages by granulocyte-macrophage colony-stimulating factor derived from a murine mammary tumor. *Cancer Res* 50: 227-234.

32. Li, M. O., Y. Y. Wan, S. Sanjabi, A. K. Robertson, and R. A. Flavell. 2006. Transforming growth factor-beta regulation of immune responses. *Annu Rev Immunol* 24: 99-146.

33. Thomas, D. A., and J. Massagué. 2005. TGF-beta directly targets cytotoxic T cell functions during tumor evasion of immune surveillance. *Cancer Cell* 8: 369-380.

34. Fu, S., N. Zhang, A. C. Yopp, D. Chen, M. Mao, H. Zhang, Y. Ding, and J. S. Bromberg. 2004. TGF-beta induces Foxp3 + T-regulatory cells from CD4 + CD25 - precursors. *Am J Transplant* 4: 1614-1627.

35. Yamagiwa, S., J. D. Gray, S. Hashimoto, and D. A. Horwitz. 2001. A role for TGF-beta in the generation and expansion of CD4+CD25+ regulatory T cells from human peripheral blood. *J Immunol* 166: 7282-7289.

36. Sinha, P., V. K. Clements, S. K. Bunt, S. M. Albelda, and S. Ostrand-Rosenberg. 2007. Cross-talk between myeloid-derived suppressor cells and macrophages subverts tumor immunity toward a type 2 response. *J Immunol* 179: 977-983.

37. Saraiva, M., and A. O'Garra. 2010. The regulation of IL-10 production by immune cells. *Nat Rev Immunol* 10: 170-181.

38. Gerlini, G., A. Tun-Kyi, C. Dudli, G. Burg, N. Pimpinelli, and F. O. Nestle. 2004. Metastatic melanoma secreted IL-10 down-regulates CD1 molecules on dendritic cells in metastatic tumor lesions. *Am J Pathol* 165: 1853-1863.

39. Kurte, M., M. López, A. Aguirre, A. Escobar, J. C. Aguillón, J. Charo, C. G. Larsen, R. Kiessling, and F. Salazar-Onfray. 2004. A synthetic peptide homologous to functional domain of human IL-10 down-regulates expression of MHC class I and Transporter associated with Antigen Processing 1/2 in human melanoma cells. *J Immunol* 173: 1731-1737.

40. Smith-Garvin, J. E., G. A. Koretzky, and M. S. Jordan. 2009. T cell activation. *Annu Rev Immunol* 27: 591-619.

41. Chen, L. 2004. Co-inhibitory molecules of the B7-CD28 family in the control of T-cell immunity. *Nat Rev Immunol* 4: 336-347.

42. Sotomayor, E. M., I. Borrello, E. Tubb, J. P. Allison, and H. I. Levitsky. 1999. In vivo blockade of CTLA-4 enhances the priming of responsive T cells but fails to prevent the induction of tumor antigen-specific tolerance. *Proc Natl Acad Sci U S A* 96: 11476-11481.

43. Leach, D. R., M. F. Krummel, and J. P. Allison. 1996. Enhancement of antitumor immunity by CTLA-4 blockade. *Science* 271: 1734-1736.

44. Oderup, C., L. Cederbom, A. Makowska, C. M. Cilio, and F. Ivars. 2006. Cytotoxic T lymphocyte antigen-4-dependent down-modulation of costimulatory molecules on dendritic cells in CD4+ CD25+ regulatory T-cell-mediated suppression. *Immunology* 118: 240-249.

45. Qureshi, O. S., Y. Zheng, K. Nakamura, K. Attridge, C. Manzotti, E. M. Schmidt, J. Baker, L. E. Jeffery, S. Kaur, Z. Briggs, T. Z. Hou, C. E. Futter, G. Anderson, L. S. Walker, and D. M. Sansom. 2011. Trans-endocytosis of CD80 and CD86: a molecular basis for the cell-extrinsic function of CTLA-4. *Science* 332: 600-603.

46. Freeman, G. J., A. J. Long, Y. Iwai, K. Bourque, T. Chernova, H. Nishimura, L. J. Fitz, N. Malenkovich, T. Okazaki, M. C. Byrne, H. F. Horton, L. Fouser, L. Carter, V. Ling, M. R. Bowman, B. M. Carreno, M. Collins, C. R. Wood, and T. Honjo. 2000. Engagement of the PD-1 immunoinhibitory receptor by a novel B7 family member leads to negative regulation of lymphocyte activation. *J Exp Med* 192: 1027-1034.

47. Dong, H., S. E. Strome, D. R. Salomao, H. Tamura, F. Hirano, D. B. Flies, P. C. Roche, J. Lu, G. Zhu, K. Tamada, V. A. Lennon, E. Celis, and L. Chen. 2002. Tumor-associated B7-H1 promotes T-cell apoptosis: a potential mechanism of immune evasion. *Nat Med* 8: 793-800.

48. Iwai, Y., M. Ishida, Y. Tanaka, T. Okazaki, T. Honjo, and N. Minato. 2002. Involvement of PD-L1 on tumor cells in the escape from host immune system and tumor immunotherapy by PD-L1 blockade. *Proc Natl Acad Sci U S A* 99: 12293-12297.

49. Sakaguchi, S., N. Sakaguchi, J. Shimizu, S. Yamazaki, T. Sakihama, M. Itoh, Y. Kuniyasu, T. Nomura, M. Toda, and T. Takahashi. 2001. Immunologic tolerance maintained by CD25+ CD4+ regulatory T cells: their common role in controlling autoimmunity, tumor immunity, and transplantation tolerance. *Immunol Rev* 182: 18-32.

50. Josefowicz, S. Z., L. F. Lu, and A. Y. Rudensky. 2012. Regulatory T cells: mechanisms of differentiation and function. *Annu Rev Immunol* 30: 531-564.

51. Yamaguchi, T., and S. Sakaguchi. 2006. Regulatory T cells in immune surveillance and treatment of cancer. *Semin Cancer Biol* 16: 115-123.

52. Sakaguchi, S. 2004. Naturally arising CD4+ regulatory t cells for immunologic self-tolerance and negative control of immune responses. *Annu Rev Immunol* 22: 531-562.

53. Piccirillo, C. A., J. J. Letterio, A. M. Thornton, R. S. McHugh, M. Mamura, H. Mizuhara, and E. M. Shevach. 2002. CD4(+)CD25(+) regulatory T cells can mediate suppressor function in the absence of transforming growth factor beta1 production and responsiveness. *J Exp Med* 196: 237-246.

54. Vignali, D. A., L. W. Collison, and C. J. Workman. 2008. How regulatory T cells work. *Nat Rev Immunol* 8: 523-532.

55. Takahashi, T., T. Tagami, S. Yamazaki, T. Uede, J. Shimizu, N. Sakaguchi, T. W. Mak, and S. Sakaguchi. 2000. Immunologic self-tolerance maintained by CD25(+)CD4(+) regulatory T cells constitutively expressing cytotoxic T lymphocyte-associated antigen 4. *J Exp Med* 192: 303-310.

56. Borsellino, G., M. Kleinewietfeld, D. Di Mitri, A. Sternjak, A. Diamantini, R. Giometto, S. Höpner, D. Centonze, G. Bernardi, M. L. Dell'Acqua, P. M. Rossini, L. Battistini, O. Rötzschke, and K. Falk. 2007. Expression of ectonucleotidase CD39 by Foxp3+ Treg cells: hydrolysis of extracellular ATP and immune suppression. *Blood* 110: 1225-1232.

57. Kobie, J. J., P. R. Shah, L. Yang, J. A. Rebhahn, D. J. Fowell, and T. R. Mosmann. 2006. T regulatory and primed uncommitted CD4 T cells express CD73, which suppresses effector CD4 T cells by converting 5'-adenosine monophosphate to adenosine. *J Immunol* 177: 6780-6786.

58. Ernst, P. B., J. C. Garrison, and L. F. Thompson. 2010. Much ado about adenosine: adenosine synthesis and function in regulatory T cell biology. *J Immunol* 185: 1993-1998.

59. Gondek, D. C., L. F. Lu, S. A. Quezada, S. Sakaguchi, and R. J. Noelle. 2005. Cutting edge: contact-mediated suppression by CD4+CD25+ regulatory cells involves a granzyme B-dependent, perforin-independent mechanism. *J Immunol* 174: 1783-1786.

60. Cao, X., S. F. Cai, T. A. Fehniger, J. Song, L. I. Collins, D. R. Piwnica-Worms, and T. J. Ley. 2007. Granzyme B and perforin are important for regulatory T cell-mediated suppression of tumor clearance. *Immunity* 27: 635-646.

61. Garín, M. I., C. C. Chu, D. Golshayan, E. Cernuda-Morollón, R. Wait, and R. I. Lechler. 2007. Galectin-1: a key effector of regulation mediated by CD4+CD25+ T cells. *Blood* 109: 2058-2065.

62. Coussens, L. M., L. Zitvogel, and A. K. Palucka. 2013. Neutralizing tumor-promoting chronic inflammation: a magic bullet? *Science* 339: 286-291.

63. Gocheva, V., H. W. Wang, B. B. Gadea, T. Shree, K. E. Hunter, A. L. Garfall, T. Berman, and J. A. Joyce. 2010. IL-4 induces cathepsin protease activity in tumor-associated macrophages to promote cancer growth and invasion. *Genes Dev* 24: 241-255.

64. Su, S., Q. Liu, J. Chen, F. Chen, C. He, D. Huang, W. Wu, L. Lin, W. Huang, J. Zhang, X. Cui, F. Zheng, H. Li, H. Yao, F. Su, and E. Song. 2014. A positive feedback loop between mesenchymal-like cancer cells and macrophages is essential to breast cancer metastasis. *Cancer Cell* 25: 605-620.

65. Lin, E. Y., V. Gouon-Evans, A. V. Nguyen, and J. W. Pollard. 2002. The macrophage growth factor CSF-1 in mammary gland development and tumor progression. *J Mammary Gland Biol Neoplasia* 7: 147-162.

66. Shand, F. H., S. Ueha, M. Otsuji, S. S. Koid, S. Shichino, T. Tsukui, M. Kosugi-Kanaya, J. Abe, M. Tomura, J. Ziogas, and K. Matsushima. 2014. Tracking of intertissue migration reveals the origins of tumor-infiltrating monocytes. *Proc Natl Acad Sci U S A* 111: 7771-7776.

67. Movahedi, K., D. Laoui, C. Gysemans, M. Baeten, G. Stangé, J. Van den Bossche, M. Mack, D. Pipeleers, P. In't Veld, P. De Baetselier, and J. A. Van Ginderachter. 2010. Different tumor microenvironments contain functionally distinct subsets of macrophages derived from Ly6C(high) monocytes. *Cancer Res* 70: 5728-5739.

68. Noman, M. Z., G. Desantis, B. Janji, M. Hasmim, S. Karray, P. Dessen, V. Bronte, and S. Chouaib. 2014. PD-L1 is a novel direct target of HIF-1α, and its blockade under hypoxia enhanced MDSC-mediated T cell activation. *J Exp Med* 211: 781-790.

69. Ding, L., P. S. Linsley, L. Y. Huang, R. N. Germain, and E. M. Shevach. 1993. IL-10 inhibits macrophage costimulatory activity by selectively inhibiting the up-regulation of B7 expression. *J Immunol* 151: 1224-1234.

70. Kennedy, B. C., C. R. Showers, D. E. Anderson, L. Anderson, P. Canoll, J. N. Bruce, and R. C. Anderson. 2013. Tumor-associated macrophages in glioma: friend or foe? *J Oncol* 2013: 486912.

71. Doedens, A. L., C. Stockmann, M. P. Rubinstein, D. Liao, N. Zhang, D. G. DeNardo, L. M. Coussens, M. Karin, A. W. Goldrath, and R. S. Johnson. 2010. Macrophage expression of hypoxia-inducible factor-1 alpha suppresses T-cell function and promotes tumor progression. *Cancer Res* 70: 7465-7475.

72. Sharda, D. R., S. Yu, M. Ray, M. L. Squadrito, M. De Palma, T. A. Wynn, S. M. Morris, and P. A. Hankey. 2011. Regulation of macrophage arginase expression and tumor growth by the Ron receptor tyrosine kinase. *J Immunol* 187: 2181-2192.

73. Rodriguez, P. C., A. H. Zea, J. DeSalvo, K. S. Culotta, J. Zabaleta, D. G. Quiceno, J. B. Ochoa, and A. C. Ochoa. 2003. L-arginine consumption by macrophages modulates the expression of CD3 zeta chain in T lymphocytes. *J Immunol* 171: 1232-1239.

74. Rodriguez, P. C., D. G. Quiceno, J. Zabaleta, B. Ortiz, A. H. Zea, M. B. Piazuelo, A. Delgado, P. Correa, J. Brayer, E. M. Sotomayor, S. Antonia, J. B. Ochoa, and A. C. Ochoa. 2004. Arginase I production in the tumor microenvironment by mature myeloid cells inhibits T-cell receptor expression and antigen-specific T-cell responses. *Cancer Res* 64: 5839-5849.

75. Oh, S. A., and M. O. Li. 2013. TGF-β: guardian of T cell function. *J Immunol* 191: 3973-3979.

76. Ng, T. H., G. J. Britton, E. V. Hill, J. Verhagen, B. R. Burton, and D. C. Wraith. 2013. Regulation of adaptive immunity; the role of interleukin-10. *Front Immunol* 4: 129.

77. Adeegbe, D. O., and H. Nishikawa. 2013. Natural and induced T regulatory cells in cancer. *Front Immunol* 4: 190.

78. Pietras, K., and A. Ostman. 2010. Hallmarks of cancer: interactions with the tumor stroma. *Exp Cell Res* 316: 1324-1331.

79. Kalluri, R., and M. Zeisberg. 2006. Fibroblasts in cancer. *Nat Rev Cancer* 6: 392-401.

80. Löhr, M., C. Schmidt, J. Ringel, M. Kluth, P. Müller, H. Nizze, and R. Jesnowski. 2001. Transforming growth factor-beta1 induces desmoplasia in an experimental model of human pancreatic carcinoma. *Cancer Res* 61: 550-555.

81. Bronzert, D. A., P. Pantazis, H. N. Antoniades, A. Kasid, N. Davidson, R. B. Dickson, and M. E. Lippman. 1987. Synthesis and secretion of platelet-derived growth factor by human breast cancer cell lines. *Proc Natl Acad Sci U S A* 84: 5763-5767.

82. Shao, Z. M., M. Nguyen, and S. H. Barsky. 2000. Human breast carcinoma desmoplasia is PDGF initiated. *Oncogene* 19: 4337-4345.

83. Strutz, F., M. Zeisberg, B. Hemmerlein, B. Sattler, K. Hummel, V. Becker, and G. A. Müller. 2000. Basic fibroblast growth factor expression is increased in human renal fibrogenesis and may mediate autocrine fibroblast proliferation. *Kidney Int* 57: 1521-1538.

84. Giannoni, E., F. Bianchini, L. Masieri, S. Serni, E. Torre, L. Calorini, and P. Chiarugi. 2010. Reciprocal activation of prostate cancer cells and cancer-associated fibroblasts stimulates epithelial-mesenchymal transition and cancer stemness. *Cancer Res* 70: 6945-6956.

85. Matsuo, Y., N. Ochi, H. Sawai, A. Yasuda, H. Takahashi, H. Funahashi, H. Takeyama, Z. Tong, and S. Guha. 2009. CXCL8/IL-8 and CXCL12/SDF-1alpha co-operatively promote invasiveness and angiogenesis in pancreatic cancer. *Int J Cancer* 124: 853-861.

86. Augsten, M., C. Hägglöf, E. Olsson, C. Stolz, P. Tsagozis, T. Levchenko, M. J. Frederick, A. Borg, P. Micke, L. Egevad, and A. Ostman. 2009. CXCL14 is an autocrine growth factor for fibroblasts and acts as a multi-modal stimulator of prostate tumor growth. *Proc Natl Acad Sci U S A* 106: 3414-3419.

87. Pavlides, S., D. Whitaker-Menezes, R. Castello-Cros, N. Flomenberg, A. K. Witkiewicz, P. G. Frank, M. C. Casimiro, C. Wang, P. Fortina, S. Addya, R. G. Pestell, U. E. Martinez-Outschoorn, F. Sotgia, and M. P. Lisanti. 2009. The reverse Warburg effect: aerobic glycolysis in cancer associated fibroblasts and the tumor stroma. *Cell Cycle* 8: 3984-4001.

88. Palucka, K., and J. Banchereau. 2012. Cancer immunotherapy via dendritic cells. *Nat Rev Cancer* 12: 265-277.

89. Siegal, F. P., N. Kadowaki, M. Shodell, P. A. Fitzgerald-Bocarsly, K. Shah, S. Ho, S. Antonenko, and Y. J. Liu. 1999. The nature of the principal type 1 interferon-producing cells in human blood. *Science* 284: 1835-1837.

90. Jego, G., A. K. Palucka, J. P. Blanck, C. Chalouni, V. Pascual, and J. Banchereau. 2003. Plasmacytoid dendritic cells induce plasma cell differentiation through type I interferon and interleukin 6. *Immunity* 19: 225-234.

91. Shaw, J., Y. H. Wang, T. Ito, K. Arima, and Y. J. Liu. 2010. Plasmacytoid dendritic cells regulate B-cell growth and differentiation via CD70. *Blood* 115: 3051-3057.

92. Cao, W., L. Bover, M. Cho, X. Wen, S. Hanabuchi, M. Bao, D. B. Rosen, Y. H. Wang, J. L. Shaw, Q. Du, C. Li, N. Arai, Z. Yao, L. L. Lanier, and Y. J. Liu. 2009. Regulation of TLR7/9 responses in plasmacytoid dendritic cells by BST2 and ILT7 receptor interaction. *J Exp Med* 206: 1603-1614.

93. Diamond, M. S., M. Kinder, H. Matsushita, M. Mashayekhi, G. P. Dunn, J. M. Archambault, H. Lee, C. D. Arthur, J. M. White, U. Kalinke, K. M. Murphy, and R. D. Schreiber. 2011. Type I interferon is selectively required by dendritic cells for immune rejection of tumors. *J Exp Med* 208: 1989-2003.

94. Fuertes, M. B., A. K. Kacha, J. Kline, S. R. Woo, D. M. Kranz, K. M. Murphy, and T. F. Gajewski. 2011. Host type I IFN signals are required for antitumor CD8+ T cell responses through CD8{alpha}+ dendritic cells. *J Exp Med* 208: 2005-2016.

95. Coukos, G., F. Benencia, R. J. Buckanovich, and J. R. Conejo-Garcia. 2005. The role of dendritic cell precursors in tumour vasculogenesis. *Br J Cancer* 92: 1182-1187.

96. Curiel, T. J., P. Cheng, P. Mottram, X. Alvarez, L. Moons, M. Evdemon-Hogan, S. Wei, L. Zou, I. Kryczek, G. Hoyle, A. Lackner, P. Carmeliet, and W. Zou. 2004. Dendritic cell subsets differentially regulate angiogenesis in human ovarian cancer. *Cancer Res* 64: 5535-5538.

97. Kehry, M. R. 1996. CD40-mediated signaling in B cells. Balancing cell survival, growth, and death. *J Immunol* 156: 2345-2348.

98. Banchereau, J., F. Bazan, D. Blanchard, F. Brière, J. P. Galizzi, C. van Kooten, Y. J. Liu, F. Rousset, and S. Saeland. 1994. The CD40 antigen and its ligand. *Annu Rev Immunol* 12: 881-922.

99. Miyashita, T., M. J. McIlraith, A. C. Grammer, Y. Miura, J. F. Attrep, Y. Shimaoka, and P. E. Lipsky. 1997. Bidirectional regulation of human B cell responses by CD40-CD40 ligand interactions. *J Immunol* 158: 4620-4633.

100. Barr, T. A., S. Brown, G. Ryan, J. Zhao, and D. Gray. 2007. TLR-mediated stimulation of APC: Distinct cytokine responses of B cells and dendritic cells. *Eur J Immunol* 37: 3040-3053.

101. Lampropoulou, V., K. Hoehlig, T. Roch, P. Neves, E. Calderón Gómez, C. H. Sweenie, Y. Hao, A. A. Freitas, U. Steinhoff, S. M. Anderton, and S. Fillatreau. 2008. TLR-activated B cells suppress T cell-mediated autoimmunity. *J Immunol* 180: 4763-4773.

102. Su, T. T., B. Guo, B. Wei, J. Braun, and D. J. Rawlings. 2004. Signaling in transitional type 2 B cells is critical for peripheral B-cell development. *Immunol Rev* 197: 161-178.

103. Mauri, C., and A. Bosma. 2012. Immune regulatory function of B cells. *Annu Rev Immunol* 30: 221-241.

104. Carter, N. A., R. Vasconcellos, E. C. Rosser, C. Tulone, A. Muñoz-Suano, M. Kamanaka, M. R. Ehrenstein, R. A. Flavell, and C. Mauri. 2011. Mice lacking endogenous IL-10-producing regulatory B cells develop exacerbated disease and present with an increased frequency of Th1/Th17 but a decrease in regulatory T cells. *J Immunol* 186: 5569-5579.

105. Inoue, S., W. W. Leitner, B. Golding, and D. Scott. 2006. Inhibitory effects of B cells on antitumor immunity. *Cancer Res* 66: 7741-7747.

106. Dunn, G. P., A. T. Bruce, H. Ikeda, L. J. Old, and R. D. Schreiber. 2002. Cancer immunoediting: from immunosurveillance to tumor escape. *Nat Immunol* 3: 991-998.

107. Gabrilovich, D. I., M. P. Velders, E. M. Sotomayor, and W. M. Kast. 2001. Mechanism of immune dysfunction in cancer mediated by immature Gr-1+ myeloid cells. *J Immunol* 166: 5398-5406.

108. Bronte, V., E. Apolloni, A. Cabrelle, R. Ronca, P. Serafini, P. Zamboni, N. P. Restifo, and P. Zanovello. 2000. Identification of a CD11b(+)/Gr-1(+)/CD31(+) myeloid progenitor capable of activating or suppressing CD8(+) T cells. *Blood* 96: 3838-3846.

109. Almand, B., J. I. Clark, E. Nikitina, J. van Beynen, N. R. English, S. C. Knight, D. P. Carbone, and D. I. Gabrilovich. 2001. Increased production of immature myeloid cells in cancer patients: a mechanism of immunosuppression in cancer. *J Immunol* 166: 678-689.

110. Parker, K. H., D. W. Beury, and S. Ostrand-Rosenberg. 2015. Myeloid-Derived Suppressor Cells: Critical Cells Driving Immune Suppression in the Tumor Microenvironment. *Adv Cancer Res* 128: 95-139.

111. Serafini, P., C. De Santo, I. Marigo, S. Cingarlini, L. Dolcetti, G. Gallina, P. Zanovello, and V. Bronte. 2004. Derangement of immune responses by myeloid suppressor cells. *Cancer Immunol Immunother* 53: 64-72.

112. Sinha, P., V. K. Clements, S. Miller, and S. Ostrand-Rosenberg. 2005. Tumor immunity: a balancing act between T cell activation, macrophage activation and tumor-induced immune suppression. *Cancer Immunol Immunother* 54: 1137-1142.

113. Lu, T., R. Ramakrishnan, S. Altiok, J. I. Youn, P. Cheng, E. Celis, V. Pisarev, S. Sherman, M. B. Sporn, and D. Gabrilovich. 2011. Tumor-infiltrating myeloid cells induce tumor cell resistance to cytotoxic T cells in mice. *The Journal of clinical investigation* 121: 4015-4029.

114. Lu, T., and D. I. Gabrilovich. 2012. Molecular pathways: tumor-infiltrating myeloid cells and reactive oxygen species in regulation of tumor microenvironment. *Clinical cancer research : an official journal of the American Association for Cancer Research* 18: 4877-4882.

115. Serafini, P. 2013. Myeloid derived suppressor cells in physiological and pathological conditions: the good, the bad, and the ugly. *Immunologic research* 57: 172-184.

116. Nagaraj, S., K. Gupta, V. Pisarev, L. Kinarsky, S. Sherman, L. Kang, D. L. Herber, J. Schneck, and D. I. Gabrilovich. 2007. Altered recognition of antigen is a mechanism of CD8+ T cell tolerance in cancer. *Nat Med* 13: 828-835.

117. Kujawski, M., M. Kortylewski, H. Lee, A. Herrmann, H. Kay, and H. Yu. 2008. Stat3 mediates myeloid cell-dependent tumor angiogenesis in mice. *J Clin Invest* 118: 3367-3377.

118. Corzo, C. A., M. J. Cotter, P. Cheng, F. Cheng, S. Kusmartsev, E. Sotomayor, T. Padhya, T. V. McCaffrey, J. C. McCaffrey, and D. I. Gabrilovich. 2009. Mechanism regulating reactive oxygen species in tumor-induced myeloid-derived suppressor cells. *J Immunol* 182: 5693-5701.

119. Gabrilovich, D., T. Ishida, T. Oyama, S. Ran, V. Kravtsov, S. Nadaf, and D. P. Carbone. 1998. Vascular endothelial growth factor inhibits the development of dendritic cells and dramatically affects the differentiation of multiple hematopoietic lineages in vivo. *Blood* 92: 4150-4166.

120. Raber, P. L., P. Thevenot, R. Sierra, D. Wyczechowska, D. Halle, M. E. Ramirez, A. C. Ochoa, M. Fletcher, C. Velasco, A. Wilk, K. Reiss, and P. C. Rodriguez. 2014. Subpopulations of myeloid-derived suppressor cells impair T cell responses through independent nitric oxide-related pathways. *International journal of cancer. Journal international du cancer* 134: 2853-2864.

121. Cheng, P., C. A. Corzo, N. Luetteke, B. Yu, S. Nagaraj, M. M. Bui, M. Ortiz, W. Nacken, C. Sorg, T. Vogl, J. Roth, and D. I. Gabrilovich. 2008. Inhibition of dendritic cell differentiation and accumulation of myeloid-derived suppressor cells in cancer is regulated by S100A9 protein. *J Exp Med* 205: 2235-2249.

122. Bronte, V., P. Serafini, A. Mazzoni, D. M. Segal, and P. Zanovello. 2003. L-arginine metabolism in myeloid cells controls T-lymphocyte functions. *Trends Immunol* 24: 302-306.

123. Bingisser, R. M., P. A. Tilbrook, P. G. Holt, and U. R. Kees. 1998. Macrophage-derived nitric oxide regulates T cell activation via reversible disruption of the Jak3/STAT5 signaling pathway. *J Immunol* 160: 5729-5734.

124. Rivoltini, L., M. Carrabba, V. Huber, C. Castelli, L. Novellino, P. Dalerba, R. Mortarini, G. Arancia, A. Anichini, S. Fais, and G. Parmiani. 2002. Immunity to cancer: attack and escape in T lymphocyte-tumor cell interaction. *Immunol Rev* 188: 97-113.

125. Mazzoni, A., V. Bronte, A. Visintin, J. H. Spitzer, E. Apolloni, P. Serafini, P. Zanovello, and D. M. Segal. 2002. Myeloid suppressor lines inhibit T cell responses by an NO-dependent mechanism. *J Immunol* 168: 689-695.

126. Bronte, V., and P. Zanovello. 2005. Regulation of immune responses by L-arginine metabolism. *Nat Rev Immunol* 5: 641-654.

127. Ezernitchi, A. V., I. Vaknin, L. Cohen-Daniel, O. Levy, E. Manaster, A. Halabi, E. Pikarsky, L. Shapira, and M. Baniyash. 2006. TCR zeta down-regulation under chronic inflammation is mediated by myeloid suppressor cells differentially distributed between various lymphatic organs. *J Immunol* 177: 4763-4772.

128. Rodriguez, P. C., A. H. Zea, K. S. Culotta, J. Zabaleta, J. B. Ochoa, and A. C. Ochoa. 2002. Regulation of T cell receptor CD3zeta chain expression by L-arginine. *J Biol Chem* 277: 21123-21129.

129. Rodriguez, P. C., D. G. Quiceno, and A. C. Ochoa. 2007. L-arginine availability regulates T-lymphocyte cell-cycle progression. *Blood* 109: 1568-1573.

130. Lesokhin, A. M., T. M. Hohl, S. Kitano, C. Cortez, D. Hirschhorn-Cymerman, F. Avogadri, G. A. Rizzuto, J. J. Lazarus, E. G. Pamer, A. N. Houghton, T. Merghoub, and J. D. Wolchok. 2012. Monocytic CCR2(+) myeloid-derived suppressor cells promote immune escape by limiting activated CD8 T-cell infiltration into the tumor microenvironment. *Cancer Res* 72: 876-886.

131. Huang, B., Z. Lei, J. Zhao, W. Gong, J. Liu, Z. Chen, Y. Liu, D. Li, Y. Yuan, G. M. Zhang, and Z. H. Feng. 2007. CCL2/CCR2 pathway mediates recruitment of myeloid suppressor cells to cancers. *Cancer Lett* 252: 86-92.

132. Hanson, E. M., V. K. Clements, P. Sinha, D. Ilkovitch, and S. Ostrand-Rosenberg. 2009. Myeloid-derived suppressor cells down-regulate L-selectin expression on CD4+ and CD8+ T cells. *J Immunol* 183: 937-944.

133. Tannock, I. F. 1998. Conventional cancer therapy: promise broken or promise delayed? *Lancet* 351 Suppl 2: SII9-16.

134. Vanneman, M., and G. Dranoff. 2012. Combining immunotherapy and targeted therapies in cancer treatment. *Nat Rev Cancer* 12: 237-251.

135. Jain, R. K. 2005. Normalization of tumor vasculature: an emerging concept in antiangiogenic therapy. *Science* 307: 58-62.

136. Druker, B. J. 2003. David A. Karnofsky Award lecture. Imatinib as a paradigm of targeted therapies. *J Clin Oncol* 21: 239s-245s.

137. Ehrlich, P. 1952. The collected papers of Paul Ehrlich. F. Himmelweit, ed. London: Pergamon Press, London.

138. Kirkwood, J. M., and M. S. Ernstoff. 1984. Interferons in the treatment of human cancer. *J Clin Oncol* 2: 336-352.

139. Rosenberg, S. A., M. T. Lotze, J. C. Yang, W. M. Linehan, C. Seipp, S. Calabro, S. E. Karp, R. M. Sherry, S. Steinberg, and D. E. White. 1989. Combination therapy with interleukin-2 and alpha-interferon for the treatment of patients with advanced cancer. *J Clin Oncol* 7: 1863-1874.

140. Quesada, J. R., M. Talpaz, A. Rios, R. Kurzrock, and J. U. Gutterman. 1986. Clinical toxicity of interferons in cancer patients: a review. *J Clin Oncol* 4: 234-243.

141. Haile, S. T., S. P. Dalal, V. Clements, K. Tamada, and S. Ostrand-Rosenberg. 2013. Soluble CD80 restores T cell activation and overcomes tumor cell programmed death ligand 1-mediated immune suppression. *J Immunol* 191: 2829-2836.

142. Walunas, T. L., D. J. Lenschow, C. Y. Bakker, P. S. Linsley, G. J. Freeman, J. M. Green, C. B. Thompson, and J. A. Bluestone. 1994. CTLA-4 can function as a negative regulator of T cell activation. *Immunity* 1: 405-413.

143. van Elsas, A., A. A. Hurwitz, and J. P. Allison. 1999. Combination immunotherapy of B16 melanoma using anti-cytotoxic T lymphocyte-associated antigen 4 (CTLA-4) and granulocyte/macrophage colony-stimulating factor (GM-

CSF)-producing vaccines induces rejection of subcutaneous and metastatic tumors accompanied by autoimmune depigmentation. *J Exp Med* 190: 355-366.

144. Hurwitz, A. A., B. A. Foster, E. D. Kwon, T. Truong, E. M. Choi, N. M. Greenberg, M. B. Burg, and J. P. Allison. 2000. Combination immunotherapy of primary prostate cancer in a transgenic mouse model using CTLA-4 blockade. *Cancer Res* 60: 2444-2448.

145. Laurent, S., P. Queirolo, S. Boero, S. Salvi, P. Piccioli, S. Boccardo, S. Minghelli, A. Morabito, V. Fontana, G. Pietra, P. Carrega, N. Ferrari, F. Tosetti, L. J. Chang, M. C. Mingari, G. Ferlazzo, A. Poggi, and M. P. Pistillo. 2013. The engagement of CTLA-4 on primary melanoma cell lines induces antibody-dependent cellular cytotoxicity and TNF-α production. *J Transl Med* 11: 108.

146. Simpson, T. R., F. Li, W. Montalvo-Ortiz, M. A. Sepulveda, K. Bergerhoff, F. Arce, C. Roddie, J. Y. Henry, H. Yagita, J. D. Wolchok, K. S. Peggs, J. V. Ravetch, J. P. Allison, and S. A. Quezada. 2013. Fc-dependent depletion of tumor-infiltrating regulatory T cells co-defines the efficacy of anti-CTLA-4 therapy against melanoma. *J Exp Med* 210: 1695-1710.

147. Wang, C., K. B. Thudium, M. Han, X. T. Wang, H. Huang, D. Feingersh, C. Garcia, Y. Wu, M. Kuhne, M. Srinivasan, S. Singh, S. Wong, N. Garner, H. Leblanc, R. T. Bunch, D. Blanset, M. J. Selby, and A. J. Korman. 2014. In vitro characterization of the anti-PD-1 antibody nivolumab, BMS-936558, and in vivo toxicology in non-human primates. *Cancer Immunol Res* 2: 846-856.

148. Hodi, F. S., S. J. O'Day, D. F. McDermott, R. W. Weber, J. A. Sosman, J. B. Haanen, R. Gonzalez, C. Robert, D. Schadendorf, J. C. Hassel, W. Akerley, A. J.

van den Eertwegh, J. Lutzky, P. Lorigan, J. M. Vaubel, G. P. Linette, D. Hogg, C. H. Ottensmeier, C. Lebbé, C. Peschel, I. Quirt, J. I. Clark, J. D. Wolchok, J. S. Weber, J. Tian, M. J. Yellin, G. M. Nichol, A. Hoos, and W. J. Urba. 2010. Improved survival with ipilimumab in patients with metastatic melanoma. *N Engl J Med* 363: 711-723.

149. Wolchok, J. D., B. Neyns, G. Linette, S. Negrier, J. Lutzky, L. Thomas, W. Waterfield, D. Schadendorf, M. Smylie, T. Guthrie, J. J. Grob, J. Chesney, K. Chin, K. Chen, A. Hoos, S. J. O'Day, and C. Lebbé. 2010. Ipilimumab monotherapy in patients with pretreated advanced melanoma: a randomised, double-blind, multicentre, phase 2, dose-ranging study. *Lancet Oncol* 11: 155-164.

150. Phan, G. Q., J. C. Yang, R. M. Sherry, P. Hwu, S. L. Topalian, D. J. Schwartzentruber, N. P. Restifo, L. R. Haworth, C. A. Seipp, L. J. Freezer, K. E. Morton, S. A. Mavroukakis, P. H. Duray, S. M. Steinberg, J. P. Allison, T. A. Davis, and S. A. Rosenberg. 2003. Cancer regression and autoimmunity induced by cytotoxic T lymphocyte-associated antigen 4 blockade in patients with metastatic melanoma. *Proc Natl Acad Sci U S A* 100: 8372-8377.

151. Topalian, S. L., M. Sznol, D. F. McDermott, H. M. Kluger, R. D. Carvajal, W. H. Sharfman, J. R. Brahmer, D. P. Lawrence, M. B. Atkins, J. D. Powderly, P. D. Leming, E. J. Lipson, I. Puzanov, D. C. Smith, J. M. Taube, J. M. Wigginton, G. D. Kollia, A. Gupta, D. M. Pardoll, J. A. Sosman, and F. S. Hodi. 2014. Survival, durable tumor remission, and long-term safety in patients with advanced melanoma receiving nivolumab. *J Clin Oncol* 32: 1020-1030.

152. Hamid, O., C. Robert, A. Daud, F. S. Hodi, W. J. Hwu, R. Kefford, J. D. Wolchok, P. Hersey, R. W. Joseph, J. S. Weber, R. Dronca, T. C. Gangadhar, A. Patnaik, H. Zarour, A. M. Joshua, K. Gergich, J. Elassaiss-Schaap, A. Algazi, C. Mateus, P. Boasberg, P. C. Tumeh, B. Chmielowski, S. W. Ebbinghaus, X. N. Li, S. P. Kang, and A. Ribas. 2013. Safety and tumor responses with lambrolizumab (anti-PD-1) in melanoma. *N Engl J Med* 369: 134-144.

153. Brahmer, J. R., S. S. Tykodi, L. Q. Chow, W. J. Hwu, S. L. Topalian, P. Hwu, C. G. Drake, L. H. Camacho, J. Kauh, K. Odunsi, H. C. Pitot, O. Hamid, S. Bhatia, R. Martins, K. Eaton, S. Chen, T. M. Salay, S. Alaparthy, J. F. Grosso, A. J. Korman, S. M. Parker, S. Agrawal, S. M. Goldberg, D. M. Pardoll, A. Gupta, and J. M. Wigginton. 2012. Safety and activity of anti-PD-L1 antibody in patients with advanced cancer. *N Engl J Med* 366: 2455-2465.

154. Brahmer, J. R., C. G. Drake, I. Wollner, J. D. Powderly, J. Picus, W. H. Sharfman, E. Stankevich, A. Pons, T. M. Salay, T. L. McMiller, M. M. Gilson, C. Wang, M. Selby, J. M. Taube, R. Anders, L. Chen, A. J. Korman, D. M. Pardoll, I. Lowy, and S. L. Topalian. 2010. Phase I study of single-agent anti-programmed death-1 (MDX-1106) in refractory solid tumors: safety, clinical activity, pharmacodynamics, and immunologic correlates. *J Clin Oncol* 28: 3167-3175.

155. Powles, T., J. P. Eder, G. D. Fine, F. S. Braiteh, Y. Loriot, C. Cruz, J. Bellmunt, H. A. Burris, D. P. Petrylak, S. L. Teng, X. Shen, Z. Boyd, P. S. Hegde, D. S. Chen, and N. J. Vogelzang. 2014. MPDL3280A (anti-PD-L1) treatment leads to clinical activity in metastatic bladder cancer. *Nature* 515: 558-562.

156. Pleasance, E. D., R. K. Cheetham, P. J. Stephens, D. J. McBride, S. J. Humphray, C. D. Greenman, I. Varela, M. L. Lin, G. R. Ordóñez, G. R. Bignell, K. Ye, J. Alipaz, M. J. Bauer, D. Beare, A. Butler, R. J. Carter, L. Chen, A. J. Cox, S. Edkins, P. I. Kokko-Gonzales, N. A. Gormley, R. J. Grocock, C. D. Haudenschild, M. M. Hims, T. James, M. Jia, Z. Kingsbury, C. Leroy, J. Marshall, A. Menzies, L. J. Mudie, Z. Ning, T. Royce, O. B. Schulz-Trieglaff, A. Spiridou, L. A. Stebbings, L. Szajkowski, J. Teague, D. Williamson, L. Chin, M. T. Ross, P. J. Campbell, D. R. Bentley, P. A. Futreal, and M. R. Stratton. 2010. A comprehensive catalogue of somatic mutations from a human cancer genome. *Nature* 463: 191-196.

157. Matsushita, H., M. D. Vesely, D. C. Koboldt, C. G. Rickert, R. Uppaluri, V. J. Magrini, C. D. Arthur, J. M. White, Y. S. Chen, L. K. Shea, J. Hundal, M. C. Wendl, R. Demeter, T. Wylie, J. P. Allison, M. J. Smyth, L. J. Old, E. R. Mardis, and R. D. Schreiber. 2012. Cancer exome analysis reveals a T-cell-dependent mechanism of cancer immunoediting. *Nature* 482: 400-404.

158. Rosenberg, S. A., J. C. Yang, R. M. Sherry, U. S. Kammula, M. S. Hughes, G. Q. Phan, D. E. Citrin, N. P. Restifo, P. F. Robbins, J. R. Wunderlich, K. E. Morton, C. M. Laurencot, S. M. Steinberg, D. E. White, and M. E. Dudley. 2011. Durable complete responses in heavily pretreated patients with metastatic melanoma using T-cell transfer immunotherapy. *Clin Cancer Res* 17: 4550-4557.

159. Yee, C., J. A. Thompson, D. Byrd, S. R. Riddell, P. Roche, E. Celis, and P. D. Greenberg. 2002. Adoptive T cell therapy using antigen-specific CD8+ T cell clones for the treatment of patients with metastatic melanoma: in vivo persistence,

migration, and antitumor effect of transferred T cells. *Proc Natl Acad Sci U S A* 99: 16168-16173.

160. Dudley, M. E., J. R. Wunderlich, P. F. Robbins, J. C. Yang, P. Hwu, D. J. Schwartzentruber, S. L. Topalian, R. Sherry, N. P. Restifo, A. M. Hubicki, M. R. Robinson, M. Raffeld, P. Duray, C. A. Seipp, L. Rogers-Freezer, K. E. Morton, S. A. Mavroukakis, D. E. White, and S. A. Rosenberg. 2002. Cancer regression and autoimmunity in patients after clonal repopulation with antitumor lymphocytes. *Science* 298: 850-854.

161. Morgan, R. A., M. E. Dudley, J. R. Wunderlich, M. S. Hughes, J. C. Yang, R. M. Sherry, R. E. Royal, S. L. Topalian, U. S. Kammula, N. P. Restifo, Z. Zheng, A. Nahvi, C. R. de Vries, L. J. Rogers-Freezer, S. A. Mavroukakis, and S. A. Rosenberg. 2006. Cancer regression in patients after transfer of genetically engineered lymphocytes. *Science* 314: 126-129.

162. Morgan, R. A., M. E. Dudley, Y. Y. Yu, Z. Zheng, P. F. Robbins, M. R. Theoret, J. R. Wunderlich, M. S. Hughes, N. P. Restifo, and S. A. Rosenberg. 2003. High efficiency TCR gene transfer into primary human lymphocytes affords avid recognition of melanoma tumor antigen glycoprotein 100 and does not alter the recognition of autologous melanoma antigens. *J Immunol* 171: 3287-3295.

163. Johnson, L. A., R. A. Morgan, M. E. Dudley, L. Cassard, J. C. Yang, M. S. Hughes, U. S. Kammula, R. E. Royal, R. M. Sherry, J. R. Wunderlich, C. C. Lee, N. P. Restifo, S. L. Schwarz, A. P. Cogdill, R. J. Bishop, H. Kim, C. C. Brewer, S. F. Rudy, C. VanWaes, J. L. Davis, A. Mathur, R. T. Ripley, D. A. Nathan, C. M. Laurencot, and S. A. Rosenberg. 2009. Gene therapy with human and mouse

T-cell receptors mediates cancer regression and targets normal tissues expressing cognate antigen. *Blood* 114: 535-546.

164. Kershaw, M. H., J. A. Westwood, L. L. Parker, G. Wang, Z. Eshhar, S. A. Mavroukakis, D. E. White, J. R. Wunderlich, S. Canevari, L. Rogers-Freezer, C. C. Chen, J. C. Yang, S. A. Rosenberg, and P. Hwu. 2006. A phase I study on adoptive immunotherapy using gene-modified T cells for ovarian cancer. *Clin Cancer Res* 12: 6106-6115.

165. Kochenderfer, J. N., and S. A. Rosenberg. 2013. Treating B-cell cancer with T cells expressing anti-CD19 chimeric antigen receptors. *Nat Rev Clin Oncol* 10: 267-276.

166. Kebriaei, P., H. Huls, B. Jena, M. Munsell, R. Jackson, D. A. Lee, P. B. Hackett, G. Rondon, E. Shpall, R. E. Champlin, and L. J. Cooper. 2012. Infusing CD19-directed T cells to augment disease control in patients undergoing autologous hematopoietic stem-cell transplantation for advanced B-lymphoid malignancies. *Hum Gene Ther* 23: 444-450.

167. Kochenderfer, J. N., M. E. Dudley, S. A. Feldman, W. H. Wilson, D. E. Spaner, I. Maric, M. Stetler-Stevenson, G. Q. Phan, M. S. Hughes, R. M. Sherry, J. C. Yang, U. S. Kammula, L. Devillier, R. Carpenter, D. A. Nathan, R. A. Morgan, C. Laurencot, and S. A. Rosenberg. 2012. B-cell depletion and remissions of malignancy along with cytokine-associated toxicity in a clinical trial of anti-CD19 chimeric-antigen-receptor-transduced T cells. *Blood* 119: 2709-2720.

168. Maude, S. L., N. Frey, P. A. Shaw, R. Aplenc, D. M. Barrett, N. J. Bunin, A. Chew, V. E. Gonzalez, Z. Zheng, S. F. Lacey, Y. D. Mahnke, J. J. Melenhorst, S.

R. Rheingold, A. Shen, D. T. Teachey, B. L. Levine, C. H. June, D. L. Porter, and S. A. Grupp. 2014. Chimeric antigen receptor T cells for sustained remissions in leukemia. *N Engl J Med* 371: 1507-1517.

169. Kandalaft, L. E., D. J. Powell, and G. Coukos. 2012. A phase I clinical trial of adoptive transfer of folate receptor-alpha redirected autologous T cells for recurrent ovarian cancer. *J Transl Med* 10: 157.

170. Lamers, C. H., S. Sleijfer, S. van Steenbergen, P. van Elzakker, B. van Krimpen, C. Groot, A. Vulto, M. den Bakker, E. Oosterwijk, R. Debets, and J. W. Gratama. 2013. Treatment of metastatic renal cell carcinoma with CAIX CAR-engineered T cells: clinical evaluation and management of on-target toxicity. *Mol Ther* 21: 904-912.

171. Lamers, C. H., S. Sleijfer, A. G. Vulto, W. H. Kruit, M. Kliffen, R. Debets, J. W. Gratama, G. Stoter, and E. Oosterwijk. 2006. Treatment of metastatic renal cell carcinoma with autologous T-lymphocytes genetically retargeted against carbonic anhydrase IX: first clinical experience. *J Clin Oncol* 24: e20-22.

172. Pule, M. A., B. Savoldo, G. D. Myers, C. Rossig, H. V. Russell, G. Dotti, M. H. Huls, E. Liu, A. P. Gee, Z. Mei, E. Yvon, H. L. Weiss, H. Liu, C. M. Rooney, H. E. Heslop, and M. K. Brenner. 2008. Virus-specific T cells engineered to coexpress tumor-specific receptors: persistence and antitumor activity in individuals with neuroblastoma. *Nat Med* 14: 1264-1270.

173. Louis, C. U., B. Savoldo, G. Dotti, M. Pule, E. Yvon, G. D. Myers, C. Rossig, H. V. Russell, O. Diouf, E. Liu, H. Liu, M. F. Wu, A. P. Gee, Z. Mei, C. M. Rooney, H. E. Heslop, and M. K. Brenner. 2011. Antitumor activity and long-term fate of

chimeric antigen receptor-positive T cells in patients with neuroblastoma. *Blood* 118: 6050-6056.

174. Vivier, E., E. Tomasello, M. Baratin, T. Walzer, and S. Ugolini. 2008. Functions of natural killer cells. *Nat Immunol* 9: 503-510.

175. Ruggeri, L., M. Capanni, E. Urbani, K. Perruccio, W. D. Shlomchik, A. Tosti, S. Posati, D. Rogaia, F. Frassoni, F. Aversa, M. F. Martelli, and A. Velardi. 2002. Effectiveness of donor natural killer cell alloreactivity in mismatched hematopoietic transplants. *Science* 295: 2097-2100.

176. Miller, J. S., Y. Soignier, A. Panoskaltsis-Mortari, S. A. McNearney, G. H. Yun, S. K. Fautsch, D. McKenna, C. Le, T. E. Defor, L. J. Burns, P. J. Orchard, B. R. Blazar, J. E. Wagner, A. Slungaard, D. J. Weisdorf, I. J. Okazaki, and P. B. McGlave. 2005. Successful adoptive transfer and in vivo expansion of human haploidentical NK cells in patients with cancer. *Blood* 105: 3051-3057.

177. Palucka, K., and J. Banchereau. 2013. Dendritic-cell-based therapeutic cancer vaccines. *Immunity* 39: 38-48.

178. Nestle, F. O., S. Alijagic, M. Gilliet, Y. Sun, S. Grabbe, R. Dummer, G. Burg, and D. Schadendorf. 1998. Vaccination of melanoma patients with peptide- or tumor lysate-pulsed dendritic cells. *Nat Med* 4: 328-332.

179. Su, Z., J. Dannull, A. Heiser, D. Yancey, S. Pruitt, J. Madden, D. Coleman, D. Niedzwiecki, E. Gilboa, and J. Vieweg. 2003. Immunological and clinical responses in metastatic renal cancer patients vaccinated with tumor RNA-transfected dendritic cells. *Cancer Res* 63: 2127-2133.

180. Geiger, J. D., R. J. Hutchinson, L. F. Hohenkirk, E. A. McKenna, G. A. Yanik, J. E. Levine, A. E. Chang, T. M. Braun, and J. J. Mulé. 2001. Vaccination of pediatric solid tumor patients with tumor lysate-pulsed dendritic cells can expand specific T cells and mediate tumor regression. *Cancer Res* 61: 8513-8519.

181. Müller, S., L. Ronfani, and M. E. Bianchi. 2004. Regulated expression and subcellular localization of HMGB1, a chromatin protein with a cytokine function. *J Intern Med* 255: 332-343.

182. Walker, J. M., K. Gooderham, J. R. Hastings, E. Mayes, and E. W. Johns. 1980. The primary structures of non-histone chromosomal proteins HMG 1 and 2. *FEBS Lett* 122: 264-270.

183. Paonessa, G., R. Frank, and R. Cortese. 1987. Nucleotide sequence of rat liver HMG1 cDNA. *Nucleic Acids Res* 15: 9077.

184. Yotov, W. V., and R. St-Arnaud. 1992. Nucleotide sequence of a mouse cDNA encoding the nonhistone chromosomal high mobility group protein-1 (HMG1). *Nucleic Acids Res* 20: 3516.

185. Yang, H., M. Ochani, J. Li, X. Qiang, M. Tanovic, H. E. Harris, S. M. Susarla, L. Ulloa, H. Wang, R. DiRaimo, C. J. Czura, J. Roth, H. S. Warren, M. P. Fink, M. J. Fenton, U. Andersson, and K. J. Tracey. 2004. Reversing established sepsis with antagonists of endogenous high-mobility group box 1. *Proc Natl Acad Sci U S A* 101: 296-301.

186. Andersson, U., and H. Erlandsson-Harris. 2004. HMGB1 is a potent trigger of arthritis. *J Intern Med* 255: 344-350.

187. Tang, D., R. Kang, H. J. Zeh, and M. T. Lotze. 2010. High-mobility group box 1 and cancer. *Biochim Biophys Acta* 1799: 131-140.

188. Read, C. M., P. D. Cary, C. Crane-Robinson, P. C. Driscoll, and D. G. Norman. 1993. Solution structure of a DNA-binding domain from HMG1. *Nucleic Acids Res* 21: 3427-3436.

189. Palumbo, R., M. Sampaolesi, F. De Marchis, R. Tonlorenzi, S. Colombetti, A. Mondino, G. Cossu, and M. E. Bianchi. 2004. Extracellular HMGB1, a signal of tissue damage, induces mesoangioblast migration and proliferation. *J Cell Biol* 164: 441-449.

190. Yang, H., H. S. Hreggvidsdottir, K. Palmblad, H. Wang, M. Ochani, J. Li, B. Lu, S. Chavan, M. Rosas-Ballina, Y. Al-Abed, S. Akira, A. Bierhaus, H. Erlandsson-Harris, U. Andersson, and K. J. Tracey. 2010. A critical cysteine is required for HMGB1 binding to Toll-like receptor 4 and activation of macrophage cytokine release. *Proc Natl Acad Sci U S A* 107: 11942-11947.

191. Messmer, D., H. Yang, G. Telusma, F. Knoll, J. Li, B. Messmer, K. J. Tracey, and N. Chiorazzi. 2004. High mobility group box protein 1: an endogenous signal for dendritic cell maturation and Th1 polarization. *J Immunol* 173: 307-313.

192. Yang, H., M. Ochani, J. Li, X. Qiang, M. Tanovic, H. E. Harris, S. M. Susarla, L. Ulloa, H. Wang, R. DiRaimo, C. J. Czura, J. Roth, H. S. Warren, M. P. Fink, M. J. Fenton, U. Andersson, and K. J. Tracey. 2004. Reversing established sepsis with antagonists of endogenous high-mobility group box 1. *Proc Natl Acad Sci U S A* 101: 296-301.

193. Jube, S., Z. S. Rivera, M. E. Bianchi, A. Powers, E. Wang, I. Pagano, H. I. Pass, G. Gaudino, M. Carbone, and H. Yang. 2012. Cancer Cell Secretion of the DAMP Protein HMGB1 Supports Progression in Malignant Mesothelioma. *Cancer Res* 72: 3290-3301.

194. Vernon, P. J., T. J. Loux, N. E. Schapiro, R. Kang, R. Muthuswamy, P. Kalinski, D. Tang, M. T. Lotze, and H. J. Zeh. 2013. The receptor for advanced glycation end products promotes pancreatic carcinogenesis and accumulation of myeloid-derived suppressor cells. *J Immunol* 190: 1372-1379.

195. van Beijnum, J. R., P. Nowak-Sliwinska, E. van den Boezem, P. Hautvast, W. A. Buurman, and A. W. Griffioen. 2013. Tumor angiogenesis is enforced by autocrine regulation of high-mobility group box 1. *Oncogene* 32: 363-374.

196. Koppenol, W. H., P. L. Bounds, and C. V. Dang. 2011. Otto Warburg's contributions to current concepts of cancer metabolism. *Nat Rev Cancer* 11: 325-337.

197. Gebhardt, C., A. Riehl, M. Durchdewald, J. Németh, G. Fürstenberger, K. Müller-Decker, A. Enk, B. Arnold, A. Bierhaus, P. P. Nawroth, J. Hess, and P. Angel. 2008. RAGE signaling sustains inflammation and promotes tumor development. *J Exp Med* 205: 275-285.

198. Kang, R., T. Loux, D. Tang, N. E. Schapiro, P. Vernon, K. M. Livesey, A. Krasinskas, M. T. Lotze, and H. J. Zeh. 2012. The expression of the receptor for advanced glycation endproducts (RAGE) is permissive for early pancreatic neoplasia. *Proc Natl Acad Sci U S A* 109: 7031-7036.

199. Heijmans, J., N. V. Büller, E. Hoff, A. A. Dihal, T. van der Poll, M. A. van Zoelen, A. Bierhaus, I. Biemond, J. C. Hardwick, D. W. Hommes, V. Muncan, and G. R. van den Brink. 2013. Rage signalling promotes intestinal tumourigenesis. *Oncogene* 32: 1202-1206.

200. Huttunen, H. J., C. Fages, J. Kuja-Panula, A. J. Ridley, and H. Rauvala. 2002. Receptor for advanced glycation end products-binding COOH-terminal motif of amphoterin inhibits invasive migration and metastasis. *Cancer Res* 62: 4805-4811.

201. Taguchi, A., D. C. Blood, G. del Toro, A. Canet, D. C. Lee, W. Qu, N. Tanji, Y. Lu, E. Lalla, C. Fu, M. A. Hofmann, T. Kislinger, M. Ingram, A. Lu, H. Tanaka, O. Hori, S. Ogawa, D. M. Stern, and A. M. Schmidt. 2000. Blockade of RAGE-amphoterin signalling suppresses tumour growth and metastases. *Nature* 405: 354-360.

202. Sasahira, T., T. Kirita, U. K. Bhawal, M. Ikeda, A. Nagasawa, K. Yamamoto, and H. Kuniyasu. 2007. The expression of receptor for advanced glycation end products is associated with angiogenesis in human oral squamous cell carcinoma. *Virchows Arch* 450: 287-295.

203. Bianchi, M. E., and A. A. Manfredi. 2007. High-mobility group box 1 (HMGB1) protein at the crossroads between innate and adaptive immunity. *Immunol Rev* 220: 35-46.

204. Schlueter, C., H. Weber, B. Meyer, P. Rogalla, K. Röser, S. Hauke, and J. Bullerdiek. 2005. Angiogenetic signaling through hypoxia: HMGB1: an angiogenetic switch molecule. *Am J Pathol* 166: 1259-1263.

205. Yan, W., Y. Chang, X. Liang, J. S. Cardinal, H. Huang, S. H. Thorne, S. P. Monga, D. A. Geller, M. T. Lotze, and A. Tsung. 2012. High-mobility group box 1 activates caspase-1 and promotes hepatocellular carcinoma invasiveness and metastases. *Hepatology* 55: 1863-1875.

206. Tafani, M., L. Schito, L. Pellegrini, L. Villanova, G. Marfe, T. Anwar, R. Rosa, M. Indelicato, M. Fini, B. Pucci, and M. A. Russo. 2011. Hypoxia-increased RAGE and P2X7R expression regulates tumor cell invasion through phosphorylation of Erk1/2 and Akt and nuclear translocation of NF-{kappa}B. *Carcinogenesis* 32: 1167-1175.

207. Balkwill, F., and A. Mantovani. 2001. Inflammation and cancer: back to Virchow? *Lancet* 357: 539-545.

208. White, E. 2012. Deconvoluting the context-dependent role for autophagy in cancer. *Nat Rev Cancer* 12: 401-410.

209. Yang, X., D. D. Yu, F. Yan, Y. Y. Jing, Z. P. Han, K. Sun, L. Liang, J. Hou, and L. X. Wei. 2015. The role of autophagy induced by tumor microenvironment in different cells and stages of cancer. *Cell Biosci* 5: 14.

210. Lum, J. J., D. E. Bauer, M. Kong, M. H. Harris, C. Li, T. Lindsten, and C. B. Thompson. 2005. Growth factor regulation of autophagy and cell survival in the absence of apoptosis. *Cell* 120: 237-248.

211. Tang, D., R. Kang, C. B. Coyne, H. J. Zeh, and M. T. Lotze. 2012. PAMPs and DAMPs: signal 0s that spur autophagy and immunity. *Immunol Rev* 249: 158-175.

212. Tang, D., R. Kang, K. M. Livesey, C. W. Cheh, A. Farkas, P. Loughran, G. Hoppe, M. E. Bianchi, K. J. Tracey, H. J. Zeh, and M. T. Lotze. 2010. Endogenous HMGB1 regulates autophagy. *J Cell Biol* 190: 881-892.

213. Ulloa, L., M. Ochani, H. Yang, M. Tanovic, D. Halperin, R. Yang, C. J. Czura, M. P. Fink, and K. J. Tracey. 2002. Ethyl pyruvate prevents lethality in mice with established lethal sepsis and systemic inflammation. *Proc Natl Acad Sci U S A* 99: 12351-12356.

214. Scherz-Shouval, R., and Z. Elazar. 2011. Regulation of autophagy by ROS: physiology and pathology. *Trends Biochem Sci* 36: 30-38.

215. Scherz-Shouval, R., and Z. Elazar. 2007. ROS, mitochondria and the regulation of autophagy. *Trends Cell Biol* 17: 422-427.

216. Tang, D., R. Kang, K. M. Livesey, H. J. Zeh, and M. T. Lotze. 2011. High mobility group box 1 (HMGB1) activates an autophagic response to oxidative stress. *Antioxid Redox Signal* 15: 2185-2195.

217. Kang, R., D. Tang, N. E. Schapiro, K. M. Livesey, A. Farkas, P. Loughran, A. Bierhaus, M. T. Lotze, and H. J. Zeh. 2010. The receptor for advanced glycation end products (RAGE) sustains autophagy and limits apoptosis, promoting pancreatic tumor cell survival. *Cell Death Differ* 17: 666-676.

218. Kusume, A., T. Sasahira, Y. Luo, M. Isobe, N. Nakagawa, N. Tatsumoto, K. Fujii, H. Ohmori, and H. Kuniyasu. 2009. Suppression of dendritic cells by HMGB1 is associated with lymph node metastasis of human colon cancer. *Pathobiology* 76: 155-162.

219. He, Y., J. Zha, Y. Wang, W. Liu, X. Yang, and P. Yu. 2013. Tissue damage-associated "danger signals" influence T-cell responses that promote the progression of preneoplasia to cancer. *Cancer Res* 73: 629-639.

220. Liu, Z., L. D. Falo, and Z. You. 2011. Knockdown of HMGB1 in tumor cells attenuates their ability to induce regulatory T cells and uncovers naturally acquired CD8 T cell-dependent antitumor immunity. *J Immunol* 187: 118-125.

221. Jiao, Y., H. C. Wang, and S. J. Fan. 2007. Growth suppression and radiosensitivity increase by HMGB1 in breast cancer. *Acta Pharmacol Sin* 28: 1957-1967.

222. Lange, S. S., and K. M. Vasquez. 2009. HMGB1: the jack-of-all-trades protein is a master DNA repair mechanic. *Mol Carcinog* 48: 571-580.

223. Stros, M., E. Polanská, S. Struncová, and S. Pospísilová. 2009. HMGB1 and HMGB2 proteins up-regulate cellular expression of human topoisomerase IIalpha. *Nucleic Acids Res* 37: 2070-2086.

224. Palm, W., and T. de Lange. 2008. How shelterin protects mammalian telomeres. *Annu Rev Genet* 42: 301-334.

225. Baird, D. M. 2008. Mechanisms of telomeric instability. *Cytogenet Genome Res* 122: 308-314.

226. Wentzensen, I. M., L. Mirabello, R. M. Pfeiffer, and S. A. Savage. 2011. The association of telomere length and cancer: a meta-analysis. *Cancer Epidemiol Biomarkers Prev* 20: 1238-1250.

227. Zhao, Z., S. Oh, D. Li, D. Ni, S. D. Pirooz, J. H. Lee, S. Yang, J. Y. Lee, I. Ghozalli, V. Costanzo, J. M. Stark, and C. Liang. 2012. A dual role for UVRAG

in maintaining chromosomal stability independent of autophagy. *Dev Cell* 22: 1001-1016.

228. Degenhardt, K., R. Mathew, B. Beaudoin, K. Bray, D. Anderson, G. Chen, C. Mukherjee, Y. Shi, C. Gélinas, Y. Fan, D. A. Nelson, S. Jin, and E. White. 2006. Autophagy promotes tumor cell survival and restricts necrosis, inflammation, and tumorigenesis. *Cancer Cell* 10: 51-64.

229. Mathew, R., S. Kongara, B. Beaudoin, C. M. Karp, K. Bray, K. Degenhardt, G. Chen, S. Jin, and E. White. 2007. Autophagy suppresses tumor progression by limiting chromosomal instability. *Genes Dev* 21: 1367-1381.

230. Takahashi, Y., T. Hori, T. K. Cooper, J. Liao, N. Desai, J. M. Serfass, M. M. Young, S. Park, Y. Izu, and H. G. Wang. 2013. Bif-1 haploinsufficiency promotes chromosomal instability and accelerates Myc-driven lymphomagenesis via suppression of mitophagy. *Blood* 121: 1622-1632.

231. Tang, D., R. Kang, K. M. Livesey, G. Kroemer, T. R. Billiar, B. Van Houten, H. J. Zeh, and M. T. Lotze. 2011. High-mobility group box 1 is essential for mitochondrial quality control. *Cell Metab* 13: 701-711.

232. Messmer, D., H. Yang, G. Telusma, F. Knoll, J. Li, B. Messmer, K. J. Tracey, and N. Chiorazzi. 2004. High mobility group box protein 1: an endogenous signal for dendritic cell maturation and Th1 polarization. *J Immunol* 173: 307-313.

233. Rovere-Querini, P., A. Capobianco, P. Scaffidi, B. Valentinis, F. Catalanotti, M. Giazzon, I. E. Dumitriu, S. Müller, M. Iannacone, C. Traversari, M. E. Bianchi, and A. A. Manfredi. 2004. HMGB1 is an endogenous immune adjuvant released by necrotic cells. *EMBO Rep* 5: 825-830.

234. Apetoh, L., F. Ghiringhelli, A. Tesniere, A. Criollo, C. Ortiz, R. Lidereau, C. Mariette, N. Chaput, J. P. Mira, S. Delaloge, F. André, T. Tursz, G. Kroemer, and L. Zitvogel. 2007. The interaction between HMGB1 and TLR4 dictates the outcome of anticancer chemotherapy and radiotherapy. *Immunol Rev* 220: 47-59.

235. Sappington, P. L., R. Yang, H. Yang, K. J. Tracey, R. L. Delude, and M. P. Fink. 2002. HMGB1 B box increases the permeability of Caco-2 enterocytic monolayers and impairs intestinal barrier function in mice. *Gastroenterology* 123: 790-802.

236. Fang, W. H., Y. M. Yao, Z. G. Shi, Y. Yu, Y. Wu, L. R. Lu, and Z. Y. Sheng. 2002. The significance of changes in high mobility group-1 protein mRNA expression in rats after thermal injury. *Shock* 17: 329-333.

237. Jungas, T., P. Verbeke, T. Darville, and D. M. Ojcius. 2004. Cell death, BAX activation, and HMGB1 release during infection with Chlamydia. *Microbes Infect* 6: 1145-1155.

238. Chu, J. J., and M. L. Ng. 2003. The mechanism of cell death during West Nile virus infection is dependent on initial infectious dose. *J Gen Virol* 84: 3305-3314.

239. Thomas, J. O., and A. A. Travers. 2001. HMG1 and 2, and related 'architectural' DNA-binding proteins. *Trends Biochem Sci* 26: 167-174.

240. Venereau, E., M. Casalgrandi, M. Schiraldi, D. J. Antoine, A. Cattaneo, F. De Marchis, J. Liu, A. Antonelli, A. Preti, L. Raeli, S. S. Shams, H. Yang, L. Varani, U. Andersson, K. J. Tracey, A. Bachi, M. Uguccioni, and M. E. Bianchi. 2012. Mutually exclusive redox forms of HMGB1 promote cell recruitment or proinflammatory cytokine release. *J Exp Med* 209: 1519-1528.

241. Bonaldi, T., F. Talamo, P. Scaffidi, D. Ferrera, A. Porto, A. Bachi, A. Rubartelli, A. Agresti, and M. E. Bianchi. 2003. Monocytic cells hyperacetylate chromatin protein HMGB1 to redirect it towards secretion. *EMBO J* 22: 5551-5560.

242. Zhang, X. D., S. K. Gillespie, J. M. Borrow, and P. Hersey. 2004. The histone deacetylase inhibitor suberic bishydroxamate regulates the expression of multiple apoptotic mediators and induces mitochondria-dependent apoptosis of melanoma cells. *Mol Cancer Ther* 3: 425-435.

243. Youn, J. H., and J. S. Shin. 2006. Nucleocytoplasmic shuttling of HMGB1 is regulated by phosphorylation that redirects it toward secretion. *J Immunol* 177: 7889-7897.

244. Oh, Y. J., J. H. Youn, Y. Ji, S. E. Lee, K. J. Lim, J. E. Choi, and J. S. Shin. 2009. HMGB1 is phosphorylated by classical protein kinase C and is secreted by a calcium-dependent mechanism. *J Immunol* 182: 5800-5809.

245. Ito, I., J. Fukazawa, and M. Yoshida. 2007. Post-translational methylation of high mobility group box 1 (HMGB1) causes its cytoplasmic localization in neutrophils. *J Biol Chem* 282: 16336-16344.

246. Yang, H., P. Lundbäck, L. Ottosson, H. Erlandsson-Harris, E. Venereau, M. E. Bianchi, Y. Al-Abed, U. Andersson, K. J. Tracey, and D. J. Antoine. 2012. Redox modification of cysteine residues regulates the cytokine activity of high mobility group box-1 (HMGB1). *Mol Med* 18: 250-259.

247. Sahu, D., P. Debnath, Y. Takayama, and J. Iwahara. 2008. Redox properties of the A-domain of the HMGB1 protein. *FEBS Lett* 582: 3973-3978.

248. Urbonaviciute, V., S. Meister, B. G. Fürnrohr, B. Frey, E. Gückel, G. Schett, M. Herrmann, and R. E. Voll. 2009. Oxidation of the alarmin high-mobility group box 1 protein (HMGB1) during apoptosis. *Autoimmunity* 42: 305-307.

249. Lotze, M. T., H. J. Zeh, A. Rubartelli, L. J. Sparvero, A. A. Amoscato, N. R. Washburn, M. E. Devera, X. Liang, M. Tör, and T. Billiar. 2007. The grateful dead: damage-associated molecular pattern molecules and reduction/oxidation regulate immunity. *Immunol Rev* 220: 60-81.

250. Nathan, C. F. 1987. Secretory products of macrophages. *J Clin Invest* 79: 319-326.

251. Wang, H., H. Yang, and K. J. Tracey. 2004. Extracellular role of HMGB1 in inflammation and sepsis. *J Intern Med* 255: 320-331.

252. Tian, J., A. M. Avalos, S. Y. Mao, B. Chen, K. Senthil, H. Wu, P. Parroche, S. Drabic, D. Golenbock, C. Sirois, J. Hua, L. L. An, L. Audoly, G. La Rosa, A. Bierhaus, P. Naworth, A. Marshak-Rothstein, M. K. Crow, K. A. Fitzgerald, E. Latz, P. A. Kiener, and A. J. Coyle. 2007. Toll-like receptor 9-dependent activation by DNA-containing immune complexes is mediated by HMGB1 and RAGE. *Nat Immunol* 8: 487-496.

253. Hori, O., J. Brett, T. Slattery, R. Cao, J. Zhang, J. X. Chen, M. Nagashima, E. R. Lundh, S. Vijay, and D. Nitecki. 1995. The receptor for advanced glycation end products (RAGE) is a cellular binding site for amphoterin. Mediation of neurite outgrowth and co-expression of rage and amphoterin in the developing nervous system. *J Biol Chem* 270: 25752-25761.

254. Chiba, S., M. Baghdadi, H. Akiba, H. Yoshiyama, I. Kinoshita, H. Dosaka-Akita, Y. Fujioka, Y. Ohba, J. V. Gorman, J. D. Colgan, M. Hirashima, T. Uede, A. Takaoka, H. Yagita, and M. Jinushi. 2012. Tumor-infiltrating DCs suppress nucleic acid-mediated innate immune responses through interactions between the receptor TIM-3 and the alarmin HMGB1. *Nat Immunol* 13: 832-842.

255. Sha, Y., J. Zmijewski, Z. Xu, and E. Abraham. 2008. HMGB1 develops enhanced proinflammatory activity by binding to cytokines. *J Immunol* 180: 2531-2537.

256. Schiraldi, M., A. Raucci, L. M. Muñoz, E. Livoti, B. Celona, E. Venereau, T. Apuzzo, F. De Marchis, M. Pedotti, A. Bachi, M. Thelen, L. Varani, M. Mellado, A. Proudfoot, M. E. Bianchi, and M. Uguccioni. 2012. HMGB1 promotes recruitment of inflammatory cells to damaged tissues by forming a complex with CXCL12 and signaling via CXCR4. *J Exp Med* 209: 551-563.

257. Kaczorowski, D. J., A. Nakao, R. Vallabhaneni, K. P. Mollen, R. Sugimoto, J. Kohmoto, B. S. Zuckerbraun, K. R. McCurry, and T. R. Billiar. 2009. Mechanisms of Toll-like receptor 4 (TLR4)-mediated inflammation after cold ischemia/reperfusion in the heart. *Transplantation* 87: 1455-1463.

258. Tsung, A., J. R. Klune, X. Zhang, G. Jeyabalan, Z. Cao, X. Peng, D. B. Stolz, D. A. Geller, M. R. Rosengart, and T. R. Billiar. 2007. HMGB1 release induced by liver ischemia involves Toll-like receptor 4 dependent reactive oxygen species production and calcium-mediated signaling. *J Exp Med* 204: 2913-2923.

259. Urbonaviciute, V., B. G. Fürnrohr, S. Meister, L. Munoz, P. Heyder, F. De Marchis, M. E. Bianchi, C. Kirschning, H. Wagner, A. A. Manfredi, J. R. Kalden, G. Schett, P. Rovere-Querini, M. Herrmann, and R. E. Voll. 2008. Induction of

inflammatory and immune responses by HMGB1-nucleosome complexes: implications for the pathogenesis of SLE. *J Exp Med* 205: 3007-3018.

260. Ivanov, S., A. M. Dragoi, X. Wang, C. Dallacosta, J. Louten, G. Musco, G. Sitia, G. S. Yap, Y. Wan, C. A. Biron, M. E. Bianchi, H. Wang, and W. M. Chu. 2007. A novel role for HMGB1 in TLR9-mediated inflammatory responses to CpG-DNA. *Blood* 110: 1970-1981.

261. Chen, G. Y., J. Tang, P. Zheng, and Y. Liu. 2009. CD24 and Siglec-10 selectively repress tissue damage-induced immune responses. *Science* 323: 1722-1725.

262. Ostrand-Rosenberg, S. 2008. Immune surveillance: a balance between protumor and antitumor immunity. *Curr Opin Genet Dev* 18: 11-18.

263. Nestl, A., O. D. Von Stein, K. Zatloukal, W. G. Thies, P. Herrlich, M. Hofmann, and J. P. Sleeman. 2001. Gene expression patterns associated with the metastatic phenotype in rodent and human tumors. *Cancer Res* 61: 1569-1577.

Chapter 2: High Mobility Group Box Protein 1 enhances immune suppression by facilitating the differentiation and suppressive activity of myeloid-derived suppressor cells

Footnotes

1. This chapter was published in Cancer Research. The published version is in Appendix I.

Abstract

Chronic inflammation frequently precedes malignant transformation and is associated with tumor progression. This association is not only correlative, but inflammation also contributes to tumor growth. Likewise, the immune system plays a role in tumor progression with tumor immune escape now recognized as a hallmark of cancer. Myeloid-derived suppressor cells (MDSC) are elevated in most individuals with cancer where their accumulation and suppressive activity are driven by inflammation. These findings led to the concept that one of the mechanisms by which inflammation promotes tumor progression is the induction of MDSC that inhibit the development of anti-tumor immunity. Since the Damage Associated Molecule Pattern molecule (DAMP) and alarmin High Mobility Group Box Protein I (HMGB1) is pro-inflammatory and is a binding partner, inducer, and/or chaperone for many of the pro-inflammatory molecules that drive MDSC, we examined HMGB1 as a potential regulator of MDSC. Using murine tumor systems, we show that HMGB1 is ubiquitously present in the tumor microenvironment, activates the NF-κB signal transduction pathway in MDSC, and regulates MDSC quantity and quality. HMGB1 drives MDSC development from bone marrow progenitor cells, contributes to the ability of MDSC to suppress antigen-driven activation of $CD4^+$ and $CD8^+$ T cells, increases MDSC production of the type 2 cytokine

IL-10, enhances crosstalk between MDSC and macrophages, and facilitates the ability of MDSC to down-regulate expression of the homing receptor L-selectin on naive T cells. These results suggest that the inflammatory molecule HMGB1 contributes to the development of MDSC in individuals with cancer.

Introduction

Anti-tumor immunity and immunotherapies that activate innate and/or adaptive immunity have potential for the prevention and/or treatment of primary and metastatic cancers. However, immunotherapies are frequently ineffective because cancer patients contain immunosuppressive cells. Myeloid-derived suppressor cells (MDSC) (1) are present in virtually all patients with solid tumors and are major contributors to immune suppression. They facilitate tumor progression through multiple immune mechanisms including the inhibition of T and NK cell activation (2), polarization of immunity towards a tumor-promoting type 2 phenotype through their production of IL-10 (3), and by perturbing the trafficking of naïve T cells by down-regulating L-selectin (4). MDSC also use non-immune mechanisms to enhance tumor growth. They produce VEGF and matrix metalloproteases that promote tumor vascularization (5) as well as invasion and metastasis (6).

Chronic inflammation has long been associated with tumor onset and progression (7). The role of chronic inflammation was originally attributed to its ability to foster genetic mutations, enhance tumor cell proliferation and survival, and promote metastases. Chronic inflammation also facilitates malignancy by inducing the accumulation and increasing the potency of MDSC, which prevent adaptive and innate immunity from delaying tumor progression (8). Multiple redundant pro-inflammatory molecules drive

MDSC. Since the Damage Associated Molecular Pattern molecule (DAMP) and alarmin High Mobility Group Box Protein I (HMGB1) is pro-inflammatory and is a binding partner, inducer, and/or chaperone for many of the pro-inflammatory molecules that drive MDSC (9), we have studied HMGB1 as a potential regulator of MDSC. HMGB1 was originally identified as a DNA binding protein in the nucleus. It performs multiple functions within the nucleus including changing the conformation of DNA to allow for the binding of regulatory proteins, facilitating the integration of transposons into DNA, and stabilizing nucleosome formation (10). Its role as a secreted protein and an immune modulator has only been recognized within the past 15 years (11).

We now report that in addition to many other cells, MDSC release HMGB1 and that HMGB1 activates MDSC through NF-κB and facilitates several immune suppressive mechanisms used by MDSC to inhibit anti-tumor immunity. HMGB1 drives the differentiation of MDSC from bone marrow progenitor cells, enhances crosstalk between MDSC and macrophages by increasing MDSC production of IL-10, and reduces the expression of L-selectin on circulating T cells. Collectively, these results suggest that HMGB1 contributes to immune suppression by inducing and activating MDSC.

Materials and Methods

Mice. BALB/c, C57BL/6, BALB/c IL-10$^{-/-}$, BALB/c TLR4$^{-/-}$, BALB/c DO11.10 (TCR-transgenic for the αβ-TCR specific for OVA peptide 323-339 restricted by I-A^{d}) and BALB/c clone 4 TCR-transgenic (αβ-TCR specific for influenza hemagglutinin 518-526 restricted by H-2K^{d}) mice were from The Jackson Laboratory (Bar Harbor, ME) and/or bred in the UMBC animal facility. Mice <6 months of age were used for all experiments. All animal procedures were approved by the UMBC IACUC.

Reagents and antibodies. Heparin sodium salt (grade IA) and ethyl pyruvate were from Sigma-Aldrich. Glycyrrhizin (ammonium salt) was from Calbiochem. Recombinant mouse IL-6 and GM-CSF were from Biolegend. Recombinant mouse IFN-γ, HMGB1, and TNFα were from R&D Systems, while recombinant LPS was from Difco. mAbs Gr1-APC-Cy7, Gr1-APC (RB6-8C5), CD45-PE (30-F11), CD8-FITC (53-6.7), CD4-PE (L3T4/GK1.5), CD3-PE-Cy7 (145-2C11), CD11b-PE (M1/70), CD11c-FITC (HL3), CD45R-B220-PE (RA3-6B2), CD62L-APC (MEL:14), c-kit-PE (CD117; ACK45), iNOS, arginase, rat IgG2b isotype, and annexin V were from BD Biosciences. CD11b-PacB (M1/70), F4/80-PE (BM8), F4/80-PacB (BM8), rat IgG1a-APC (RTK2758), and CD16/32 (93) were from BioLegend. CD45-TxR (MCD4517) was from Invitrogen. Anti-mouse ADAM17 mAb was from Abcam (ab2051). Secondary for ADAM17 antibody (goat-anti-rabbit; 554020) was from BD Biosciences. Anti-CD3 was from Dako (clone F7.2.38). Recombinant A Box (12, 13) and 2G7 (14) were produced as described.

Tumor inoculations, tumor measurements, 2G7, and A box treatment. C57BL/6 mice were inoculated s.c. in the flank with $5x10^5$ MC38 colon carcinoma cells, $1x10^6$ B78H1 melanoma cells, or $1x10^6$ AT3 mammary carcinoma cells (15). BALB/c mice were inoculated in the abdominal mammary fat pad with $7x10^3$ 4T1 mammary carcinoma cells or s.c. with 1 x 10^6 CT26 colon carcinoma cells. With the exception of AT3, which was obtained from Dr. S. Abrams (Roswell Park Cancer Center) ~5 years ago, all tumor cell lines have been in the authors' laboratory for >15 years. Cell lines are routinely checked for mycoplasma and early freeze-downs are preferentially used. Mice were administered

intraperitoneally with recombinant A box (300µg/100 µl/mouse), vehicle (PBS), 2G7 mAb (5µg/200µl/mouse), or control IgG2b antibody (MOPC 195; 5µg/200µl/mouse; Sigma Aldrich) 3x/week starting when tumors were first palpable (day 7-9 post inoculation). Tumors were measured in two perpendicular diameters every 2-3 days. Tumor volume = πr^2 where r = (diameter 1 + diameter 2)/4. Immunohistochemistry for tumor-infiltrating T cells was performed by CD3 staining of O.C.T. embedded tumors.

Tumor, MDSC, and macrophage supernatants; MEF cell lysates. 4T1, CT26, B78H1, MC38, and AT3 tumor cells were cultured at $5x10^6$ cells/ml in 6 well plates in serum-free HL-1 medium at 37ºC ,5% CO_2. MDSC and thioglycolate-elicited macrophages were similarly cultured except some wells contained 100ng/ml LPS. Supernatants were harvested after 18 hours and concentrated 10x using 10kDa Centricon filters (Millipore). Excised tumors were minced into small pieces using scissors, and placed in 10ml of serum-free HL-1 media containing 0.8µg/ml DNase. Tumor chunks were then dissociated into single cell suspensions using a GentleMACS Dissociator equipped with a GentleMACS C tube and program m_tumor 01.01 (Milltenyi Biotec). Dissociated material, including medium, was then plated in 10cm dishes and incubated at 37ºC , 5% CO_2 for 18 hours, after which the supernatants were collected and concentrated to 2ml using 10kDa Centricon filters. Wild type and HMGB1-knocked out MEF cells (16) were lysed in 300µl of M-Per buffer Mammalian Protein Extraction Reagent (Thermo Scientific) using a GentleMACS fitted with an M tube and program protein 01.01. Lysates were centrifuged at 10ºC and 650g for 5 minutes, and the supernatants removed and centrifuged at 10ºC and 160g for 15 min. Protein concentration of the supernatants

was determined at 280 absorbance.

Blood MDSC. Mice were bled from the submandibular vein into 1ml of PBS containing 0.008% heparin. RBC were removed by Gey's treatment (17). The remaining white blood cells were stained for Gr1 and CD11b and analyzed by flow cytometry. White blood cells that were >90% $Gr1^{+}CD11b^{+}$ were used in experiments.

MDSC- macrophage co-cultures. Peritoneal macrophage (>80%$CD11b^{+}F4/80^{+}$ cells) and MDSC co-cultures were performed as described (3). Briefly, cells were plated at $7.5x10^{5}$ MDSC and $7.5x10^{5}$ macrophages/well in 500ul of DMEM with 5% FBS, 100 ng/ml LPS, and 20 U/ml IFN-γ in 24 well plates. Co-cultures were incubated at 37°C, 5% CO_2 for 16-18 hrs. Supernatants were stored at -80°C until analyzed by ELISA.

C***ytokine detection.*** IL-10, IL-6, IL-12, and IL-1β were measured by ELISA according to the manufacturer's protocol (R&D Systems). Plates were read at 450 nm using a Bio-Tek synergy microplate reader. Data are the mean ± SD of triplicate wells.

MDSC generation from bone marrow cells. MDSC were generated (18) with the following adaptations: Bone marrow was flushed aseptically from femurs with RPMI medium using a syringe fitted with a 27g needle. RBC were lysed with Gey's solution. Resulting cells were cultured at 37°C, 5% CO_2 at 4.2 x 10^{5} cells/2ml in 6 well plates containing RPMI medium supplemented with 10% FCS, 40 ng/ml IL-6 and 40 ng/ml GM-CSF. After four days of culture, percent decrease in $Gr1^{mid}CD11b^{+}$ cells was determined ($Gr1^{mid}CD11b^{+}$ cells = 100% [(number of vehicle-treated cells – number of

inhibitor treated cells)/(number of vehicle-treated cells)]. Absolute number of cells = (total number of cells) x % of a given cell type as determined by flow cytometry.

T cell activation assays. T cell activation assays were performed as described (17). Briefly, splenocytes and irradiated (2500 Rad) 4T1-induced MDSC or bone marrow generated MDSC were co-cultured in 96 well plates at 10^5 cells/200µl/well of HL-1 media containing 1% penicillin, 1% streptomycin, 1% Glutamax, and 5 x 10^{-5} M β-mercaptoethanol. 14uM $OVA_{323-339}$ peptide or 28 µM $HA_{518-526}$ peptide was included for DO11.10 and clone 4 cells, respectively. Wells were pulsed with 1µCi of [^{3}H] thymidine/well on day 3, and 18 hours later the cells were harvested. Data are expressed as cpm ± SD of triplicate cultures. Hydrogen peroxide levels were measured as described (19).

HMGB1 western blots and ELISA. 50 µl of equivalent quantities of concentrated supernatants of cultured tumor cells, in vivo grown tumors, MDSC, macrophages, or 60ug of MEF cell lysates were mixed with 10 µl or the appropriate amount of 6x sample buffer and electrophoresed on 12% SDS-PAGE gels in SDS running buffer (BioRad) at 150 volts for 1 hour, and transferred overnight in transfer buffer (BioRad) at 30 volts to PVDF membranes (GE Healthcare). Membranes were blocked with 5% milk in TBST. HMGB1 was detected with anti-HMGB1 antibody (Epitomics) (5ng/ml in 10ml of 2.5% milk/TBST) followed by goat-anti-rabbit-HRP (Millipore) (40ng/ml in 10ml of 2.5% milk/TBST). Protein was visualized using an HRP detection kit (Denville Scientific, Inc). HMGB1 levels were measured by ELISA according to the manufacturer's directions (IBL

International, Hamburg, Germany).

Flow cytometry. Cells were labeled and analyzed by flow cytometry for cell surface molecules as described (17). For bone marrow experiments, cells were first stained using the LIVE/DEAD fixable yellow dead cell stain kit (Invitrogen) per the manufacture's protocol, followed by staining for cell surface markers withantibodies diluted in PBS/ 2% FCS (HyClone). For NF-κB staining of MDSC, $3x10^6$-$5x10^6$ leukocytes/ml RPMI were incubated with/without 50 ng/ml HMGB1 for 15 minutes at 37°C, fixed and permeabilized and then stained with rabbit mAb phospho-NF-κB p65 (Ser536; clone 93H1) and goat-anti-rabbit $(Fab')_2$-AlexaFluor 647 (Cell Signaling, Inc.) according to the manufacturer's protocol, followed by staining for Gr1 and CD11b. Peritoneal macrophages ($5x10^6$/5 ml DMEM) were similarly stained, except they were rested for 2 hrs at 37°C before stimulation with 20ng/ml TNFα or 100ug/ml LPS, and subsequently incubated with Fc block (CD16/32) for 15 min., followed by staining with NF-κB, CD11b, and F4/80 mAbs. For ADAM17 staining, $3x10^6$-$5x10^6$ leukocytes were incubated with or without HMGB1 (50 ng/ml) or ethyl pyruvate (10mM) for zero, two, and four hours and stained with mAb to ADAM17. For tumor-infiltrating MDSC, solid tumors were prepared as they were for tumor supernatants, except collagenase (300 U/ml) was included in the dissociation medium, and the resulting cells were centrifuged through ficoll to remove dead cells. Samples were run on a Cyan ADP flow cytometer and analyzed using Summit Software (Beckman/Coulter).

Statistical methods. Statistical analysis of tumor growth rate was conducted utilizing the compare Growth Curves function of the Statmod software package

(http://bioinf.wehi.edu.au/software/compareCurves). Student's *t* test was used to determine statistical significance between two sets of data. Single-factor ANOVA was used to determine statistical significance between groups of data.

Results

HMGB1 is ubiquitously present in the tumor microenvironment and activates MDSC via the NF-κB pathway. If HMGB1 is associated with the induction of MDSC, then HMGB1 will be present in the tumor microenvironment. To test this hypothesis BALB/c-derived 4T1 mammary carcinoma and CT26 colon carcinoma cells, and C57BL/6-derived B78H1 melanoma, MC38 colon carcinoma, and PyMT-MMTV-derived AT3 mammary carcinoma cells were cultured in serum free-media, and the supernatants assessed by western blot for HMGB1. Whole cell lysates of wild type MEF cells and their HMGB1-knocked out counterparts served as positive and negative controls, respectively. All tumors constitutively secreted HMGB1 (**Fig. 1*A***). Secretion of HMGB1 was confirmed and quantified by ELISA (**Supplementary Table 1**).

Since MDSC are driven by inflammation and themselves produce pro-inflammatory mediators (8, 20), we tested MDSC for secretion of HMGB1. MDSC generated in 4T1 tumor-bearing BALB/c mice were harvested from the blood, stained for Gr1 and CD11b, and assessed for their ability to suppress T cell activation (**Fig. 1*B***). Greater than 90% of the blood leukocytes were $CD11b^{+}Gr1^{+}$ and they were suppressive. We then tested MDSC for their ability to secrete HMGB1 by culturing them overnight and assaying the supernatant for HMGB1 by western blot and ELISA (**Fig. 1*C***, **Supplementary Table 1**). Macrophages are established producers of HMGB1 (11) and

LPS is reported to increase their secretion of HMGB1 (21). To determine if LPS similarly affects MDSC, MDSC were cultured with and without LPS. Both LPS-treated and untreated MDSC produced more HMGB1 than equivalent numbers of LPS-treated macrophages, demonstrating that MDSC constitutively secrete HMGB1.

To determine if HMGB1 is present in vivo within the tumor microenvironment, 4T1, CT26, B78H1, MC38, and AT3 tumors of BALB/c and C57BL/6 tumor-bearing mice were measured, and then excised and weighed. Explanted tumors were then dissociated into single cell suspensions without disrupting cell integrity, and incubated in serum-free medium. The resulting supernatants were assessed by western blot and ELISA for HMGB1 (**Fig. 1*C* right-hand 5 lanes**, **Supplementary Table 1**). All excised tumors released HMGB1; however, the quantity of HMGB1 released did not directly correlate with tumor burden. Since different types of tumors contain different quantities of HMGB1-producing cells and necrotic cells (i.e. tumor cells, macrophages, MDSC, etc.), it is not unexpected that HMGB1 levels are not proportional to tumor mass.

HMGB1 binds to multiple receptors including two receptors that are expressed by MDSC: TLR4 (22) and Receptor for Advanced Glycation Endproducts (RAGE) (23). Signaling through both of these receptors converges on the NF-κB signal transduction pathway. To determine if HMGB1 activates MDSC, leukocytes from the blood of tumor-free BALB/c mice were cultured with or without HMGB1, subsequently stained for phosphorylated NF-κB (pNF-κB), and the $Gr1^{+}CD11b^{+}$ cells gated and analyzed for pNF-κB (**Fig. 1*D***). HMGB1-treatment caused phosphorylation of NF-κB.

To confirm the specificity of the pNF-κB staining, macrophages from either $TLR4^{+/+}$ or $TLR4^{-/-}$ mice were treated with either LPS or TNFα. If the pNF-κB mAb is

specific, then TNFα will activate NF-κB in both $TLR4^{+/+}$ and $TLR4^{-/-}$ cells since it acts via the TNFα receptor. In contrast, NF-κB will only be activated by LPS in $TLR4^{+/+}$ cells, since LPS activates NF-κB via TLR4. TNFα activated NF-κB in both $TLR4^{+/+}$ and $TLR4^{-/-}$ cells, while LPS activated NF-κB in $TLR4^{+/+}$, but not $TLR4^{-/-}$ cells, confirming the specificity of the pNF-κB mAb (**Supplementary Fig. S1**).

These data indicate that HMGB1 is ubiquitously present in vivo in the tumor microenvironment, multiple cell populations within the tumor microenvironment produce HMGB1, MDSC contribute to the production of HMGB1, and HMGB1 activates the NF-κB signal transduction pathway in MDSC.

HMGB1 drives the differentiation of MDSC from bone marrow progenitor cells.

Since the differentiation, accumulation, and function of MDSC are driven by inflammation (8, 20, 24, 25), HMGB1 may regulate MDSC by either controlling their accumulation and/or affecting their functional activities. To assess if HMGB1 affects MDSC differentiation, bone marrow cells from the femurs of healthy BALB/c mice were cultured under conditions that drive the differentiation of MDSC (18). The HMGB1 inhibitors ethyl pyruvate and glycyrrhizin were included in some cultures. Ethyl pyruvate prevents extracellular secretion of HMGB1 from activated monocytes and macrophages by blocking NF-κB signaling (26). Glycyrrhizin prevents the binding of extracellular HMGB1 by attaching to two distinct regions of HMGB1 (27). At the end of the four day culture period, the presence of HMGB1 was confirmed by western blot (**Fig. 2*A***) and quantified by ELISA (**Supplementary Table 1**), and the absolute number of $Gr1^{mid}CD11b^{+}$ cells was determined by cell counting and flow cytometry (**Fig. 2*B***). At

the start of culture, $5.5x10^4$ cells were $Gr1^{mid}CD11b^+$. At the end of the culture period the vehicle control-treated cultures contained $1.6x10^5$ $Gr1^{mid}CD11b^+$ cells indicating that MDSC had expanded by almost 3 fold. Both HMGB1 inhibitors significantly reduced the absolute number of MDSC (**Fig. 2*C*, Supplementary Table 2**). The highest dose of glycyrrhizin reduced the number of $Gr1^{mid}CD11b^+$ cells by 82%, while ethyl pyruvate reduced the number by 80%. $Gr1^+CD11b^+$ MDSC induced under these conditions were just as suppressive as tumor-induced MDSC isolated from mice with 4T1 tumors (**Fig. 2D**). Glycyrrhizin and ethyl pyruvate also decreased the generation of DC ($CD11c^+$ cells, 43% and 67%, respectively) and macrophages ($F4/80^+CD11b^+$ cells, 66% and 68%, respectively), consistent with published reports showing that HMGB1 also drives the maturation of these cells (28). In contrast, B cells ($B220^+$ cells) and T cells ($CD3^+$ cells) were either not affected or only minimally decreased.

To determine if inhibition of HMGB1 reduces MDSC accumulation by inhibiting the proliferation of MDSC progenitor cells or by causing apoptosis of differentiated MDSC, bone marrow cells and matured MDSC were vehicle or ethyl pyruvate-treated and the levels of c-kit^+ (CD117) progenitor cells and Annexin V^+ PI^+apoptotic cells were determined by flow cytometry (**Fig. 2E, Supplementary Fig. S2A**). Ethyl pyruvate reduced the level of progenitor cells but did not induce apoptosis as compared to vehicle treatment. These data indicate that HMGB1 facilitates the expansion of myeloid cells, including MDSC, from bone marrow progenitor cells.

HMGB1 contributes to the ability of MDSC to suppress antigen-driven T cell activation. MDSC use multiple mechanisms to suppress anti-tumor immunity. Suppression of

antigen-driven T cell activation was one of the first mechanisms identified (29, 30). To determine if HMGB1 impacts MDSC suppression of T cell activation, MDSC from 4T1 tumor-bearing BALB/c mice were tested for their ability to prevent the proliferation of transgenic $CD4^+$ (DO11.10) or $CD8^+$ (Clone 4) T cells activated with cognate peptides (**Fig. 3*A***). Increasing concentrations of the HMGB1 inhibitor ethyl pyruvate restored T cell activation in the presence of MDSC. Since ethyl pyruvate prevents signaling through NF-κB and T cell activation requires NF-κB signaling (31), transgenic T cells were treated with ethyl pyruvate to ascertain that these doses were not affecting T cell proliferation (**Fig. 3*B***). Ethyl pyruvate did not increase T cell activation in the absence of MDSC, demonstrating that the increase in T cell activation seen in fig. 3A is an effect of ethyl pyruvate on MDSC and not an effect on T cells.

To determine how ethyl pyruvate inhibits MDSC, control and ethyl pyruvate-treated MDSC were assayed by flow cytometry for their content of molecules that mediate T cell suppression (arginase, iNOS, and H_2O_2), and for its impact on MDSC viability. Ethyl pyruvate did not decrease arginase or iNOS levels or alter MDSC apoptosis levels (**Supplementary Fig. S2B, S2C**), but modestly reduced H_2O_2 levels (**Supplementary Fig. S2D**) as compared to vehicle-treated cells. In previous studies, another NF-κB inhibitor, Withaferin A, also reduced the suppressive potency of MDSC (19). These results suggest that HMGB1 contributes to MDSC-mediated T cell suppression by increasing their expression of H_2O_2.

HMGB1 increases MDSC production of IL-10 and MDSC-macrophage crosstalk

One of the mechanisms MDSC use to inhibit anti-tumor immunity is their production of

IL-10. MDSC-produced IL-10 reduces macrophage production of IL-12, thereby skewing macrophages towards a type 2 tumor-promoting phenotype (3). Crosstalk between MDSC and macrophages increases MDSC production of IL-10, thereby contributing to MDSC suppression. MDSC-produced IL-10 also drives the differentiation and accumulation of T regulatory cells (32), further increasing immune suppression. To determine if HMGB1 drives MDSC production of IL-10 or MDSC-macrophage crosstalk with respect to IL-10, MDSC and macrophages were co-cultured with or without ethyl pyruvate and glycyrrhizin and IL-10 production was measured (**Fig. 4*A***). Both ethyl pyruvate and glycyrrhizin dose-dependently reduced the production of IL-10 by MDSC and by mixtures of MDSC plus macrophages. To ascertain that MDSC, rather than macrophages, are the producers of IL-10, macrophages and MDSC from IL-10-deficient BALB/c mice were used in conjunction with MDSC or macrophages, respectively, from wild type BALB/c mice (**Fig. 4*B***). Only marginal levels of IL-10 were detected in cultures containing IL-$10^{-/-}$ MDSC with wild type macrophages, demonstrating that MDSC are the cells producing the IL-10. The reduction of IL-10 is not due to reduced MDSC viability since ethyl pyruvate-treated MDSC cultured under the crosstalk conditions (with 5% serum) are more viable than vehicle-treated MDSC (**Supplementary Fig. S2C**). These findings indicate that HMGB1 regulates MDSC production of IL-10 and macrophage-induced increases in MDSC production of IL-10.

MDSC also promote a type 2 immune response by down-regulating macrophage production of IL-12 (3) and IL-6 (unpublished). To determine if HMGB1 mediates either of these effects, MDSC and macrophages were co-cultured with or without ethyl pyruvate and glycyrrhizin and IL-12 and IL-6 were quantified by ELISA (**Fig. 5**). Ethyl

pyruvate and glycyrrhizin reduced macrophage production of IL-12 and IL-6, and did not restore production of these cytokines in MDSC-macrophage co-cultures. IL-1β, a pro-inflammatory cytokine that is produced by MDSC and also drives the suppressive potency of MDSC (33, 34), was also assessed. Ethyl pyruvate and glycyrrhizin decreased MDSC production of IL-1β; however, HMGB1 inhibition restored IL-1β levels in co-cultures of MDSC and macrophages. These results indicate that HMGB1 regulates MDSC production of IL-1β during MDSC-macrophage crosstalk; however it is not involved in MDSC-mediated down-regulation of macrophage-produced IL-12 or IL-6.

Neutralization of HMGB1 delays tumor growth and reduces MDSC in tumor-bearing mice.

HMGB1 includes two functional domains: the pro-inflammatory B Box and the anti-inflammatory A Box. The B Box is a RAGE agonist, while the A Box is a RAGE antagonist (13). Although the A Box is a competitor for the B Box, the B Box of HMGB1 is dominant in vivo (27). However, if administered in vivo as a recombinant protein, A Box neutralizes endogenous HMGB1 (14). To determine if A Box impacts tumor progression, BALB/c and C57BL/6 mice bearing 4T1 or MC38 tumor, respectively, were treated with A Box or vehicle control starting when the tumors were first palpable (approximate day 7-9 after tumor cell inoculation) (**Fig. 6*A***). In both strains, A Box delayed tumor progression, supporting the concept that HMGB1 facilitates tumor growth. 4T1 tumor cells were also knocked-down by shRNA for HMGB1 (4T1/575 cells) and their tumorigenicity compared to that of 4T1 cells transfected with an irrelevant shRNA (4T1/irrelevant) (**Supplementary Fig. S3*A***). The effect of HMGB1 on

spontaneous metastatic disease was assessed by treating 4T1 tumor-bearing mice with glycyrrhizin and ethyl pyruvate and assessing the number of metastatic cells by clonogenic assay (35) (**Supplementary Fig. S3*B***). 4T1/575 tumor-bearing mice survived significantly longer than mice with 4T1/irrelevant cells supporting previously published work (36). Tumor-bearing mice treated with the inhibitors trended towards fewer metastatic cells; however, the values were not statistically significantly different. These results further confirm that HMGB1 enhances tumor progression.

To determine if HMGB1 drives MDSC accumulation in vivo, tumor-bearing mice were treated with a neutralizing HMGB1 mAb (2G7), and tumor-infiltrating MDSC and MDSC from the blood and spleen were compared to MDSC in vehicle-treated tumor-bearing mice. C57BL/6 mice were inoculated with the MC38 tumor on day 1 and 2G7 treatment was started on day 10-13. Mice were sacrificed at a late stage of disease when their primary tumors were approximately the same diameter, and total MDSC, monocytic MDSC, and granulocytic MDSC levels in the blood, spleen, and infiltrating the tumors were determined by flow cytometry (**Fig. 6B**). Total, monocytic, and granulocytic MDSC were reduced in the spleens, blood, and tumors of 2G7-treated mice with the exception of tumor-infiltrating granulocytic MDSC. These decreases were not a secondary effect of reduced tumor size since, at the time of analysis, the 2G7-treated and control-treated mice had similar-sized primary tumors. MDSC were similarly reduced in the blood of A Box-treated tumor-bearing mice. These results indicate that in vivo, neutralization of HMGB1 reduces the accumulation of MDSC in tumor-bearing mice.

Tumors from the HMGB1 mAb-treated (2G7) and isotype control-treated mice of **Fig. 6** were assessed by immunohistochemistry for the presence of $CD3^+$ T cells

(**Supplementary Fig. 4**). Both types of tumors contained few T cells; however, there was a trend towards more $CD3^+$ cells in the tumors of 2G7-treated mice.

HMGB1 down-regulates T cell expression of L-selectin.

MDSC also impair T cell immunity by perturbing the homing of naive T cells to lymph nodes where they could become activated. To enter lymph nodes T cells must first be tethered via L-selectin (CD62L) to the walls of high endothelial venules (HEV) so they can extravasate from the bloodstream. Our previous in vitro studies showed that MDSC reduce T cell levels of L-selectin through their constitutive expression of ADAM17 (a disintegrin and metalloproteinase domain 17), an enzyme that cleaves the ectodomain of L-selectin (4). Subsequent in vivo vital imaging studies showed that T cells with reduced expression of L-selectin do not enter HEVs (J. Muhich, S. Ostrand-Rosenberg, S. Abrams, and S. Evans, unpublished). To determine if HMGB1 impacts MDSC-mediated down-regulation of T cell-expressed L-selectin, A Box and control-treated mice were sacrificed 29 days after tumor inoculation and circulating $CD45^+CD3^+CD4^+$ and $CD45^+$ $CD3^+CD8^+$ T cells were analyzed for L-selectin by flow cytometry (**Fig. 7*A***). Circulating $CD4^+$ and $CD8^+$ T cells from tumor-free mice were controls for normal L-selectin expression. L-selectin was reduced in $CD4^+$ and $CD8^+$ T cells of tumor-bearing vehicle-treated mice, while A box-treatment partially restored L-selectin expression (**Fig. 7*B***). To confirm that HMGB1 acts on MDSC to reduce L-selectin, $Gr1^+CD11b^+$ cells from tumor-free and tumor-bearing mice were treated for zero, two, or four hours with HMGB1 or ethyl pyruvate, respectively. The cells were then stained with mAbs to Gr1, CD11b, and ADAM17, and the gated $Gr1^+CD11b^+$ cells were analyzed for plasma

membrane expression of ADAM17 (**Fig. 7*C***). HMGB1-treated $Gr1^+CD11b^+$ cells from tumor-free mice expressed more ADAM17, while ethyl pyruvate-treated MDSC from tumor-bearing mice had less ADAM17, as compared to vehicle-treated cells. These observations indicate that plasma membrane ADAM17 turns-over on MDSC and that HMGB1 contributes to the down-regulation of L-selectin on T cells by sustaining MDSC expression of ADAM17.

Discussion

The DAMP and alarmin HMGB1 is released by many tumor cells, is elevated in the serum of many cancer patients (37), and is recognized as an enhancer of tumor progression by its direct action on tumor cells (9, 10, 28). The studies reported here identify MDSC, along with tumor cells and macrophages, as producers of HMGB1. The observed decrease in MDSC of tumor-bearing mice following treatment with HMGB1 inhibitors, combined with the in vitro mechanistic studies demonstrate that HMGB1 (i) promotes the differentiation of MDSC from bone marrow progenitor cells; (ii) increases MDSC-macrophage crosstalk and MDSC production of IL-10; and (iii) increases MDSC-mediated down-regulation of L-selectin on naive T cells. These findings support the conclusion that HMGB1 contributes to the elevation and suppressive potency of MDSC in tumor-bearing mice, and identify a new pro-inflammatory mediator that regulates MDSC.

HMGB1 is likely to activate and drive MDSC because it induces, chaperones, and/or enhances the activity of several pro-inflammatory molecules that regulate MDSC. For example, IL-1β drives MDSC accumulation and T cell suppressive activity (33, 38)

and is induced by HMGB1 (14). Complexes of HMGB1 and IL-1β have increased pro-inflammatory activity relative to either molecule alone (39). HMGB1 also enhances the pro-inflammatory activity of IL-6 (40), TNFα (14), and prostaglandin E2 (41), three other pro-inflammatory mediators that drive MDSC (24, 34, 42, 43). Although neutralization of HMGB1 significantly down-regulates MDSC suppressive activity, it does not globally neutralize MDSC, most likely because the multiple pro-inflammatory mediators that drive MDSC are redundant and can also be regulated by molecules other than HMGB1.

HMGB1 is known to facilitate tumor progression by co-opting other immune cells and by directly affecting tumor cell growth (9, 10, 28) . It increases the accumulation of T regulatory cells and diverts type 1 T helper cells to a pro-tumor type 2 phenotype (36, 44). HMGB1 also acts directly on tumor cells to enhance tumor progression by binding to tumor cell-expressed RAGE. Many tumor cells express RAGE (45), and the binding of HMGB1 to RAGE promotes tumor cell autophagy, inhibits tumor cell apoptosis, and increases tumor cell invasiveness (46, 47). Collectively these effects produce an immune suppressive and pro-tumor environment. MDSC contribute to tumor growth through their immune suppressive mechanisms. However, their elimination may not be sufficient for tumor rejection, and active immunization of T cells and/or repolarization of macrophages to a M1-like phenotype may also be required (17). The studies reported here demonstrate that HMGB1 affects MDSC development and function. Since HMGB1 impacts tumor progression through multiple mechanisms that act on both tumor cells and immune cells, its effects on MDSC represent only one of its modes of action.

Paradoxically, under some conditions HMGB1 facilitates the activation of tumor-reactive T cells. HMGB1 facilitates dendritic cell maturation (48) and enhances DC-

mediated antigen presentation during chemotherapy and radiotherapy (49). In contrast to the pro-tumor effects of HMGB1 which are thought to be transmitted through RAGE, the enhancement of DC function requires the release of HMGB1 by dead tumor cells and is mediated through DC-expressed TLR4. Whether the in vivo pro-tumor or anti-tumor effects of HMGB1 balance each other, or whether one dominates is unclear. However, the potential for HMGB1 to both inhibit and promote anti-tumor immunity makes it difficult to evaluate whether neutralization of HMGB1 will be beneficial or harmful.

The quantity of HMGB1 within different solid tumors differs significantly (**see Supplementary Table 1**). MDSC, macrophages, tumor-infiltrating cells, and tumor cells themselves all contribute to the amount of HMGB1 in the tumor microenvironment. Live tumor cells secrete HMGB1, while necrotic tumor cells induced by suboptimal vascularization and hypoxia release nuclear HMGB1. Because the quantity of tumor-infiltrating cells and the extent of vascularization and hypoxia differ in different types of tumors, it is not unexpected that the quantity of HMGB1 within solid tumors does not correlate with tumor mass.

HMGB1 binds to both TLR4 and RAGE, and MDSC express both receptors (20, 50). TLR4 and RAGE signaling converges at NF-κB (9, 10, 28, 51), so that activation through either receptor may produce similar effects. Previous studies demonstrated that MDSC production of IL-10 is regulated by TLR4 (50). In the current report, the RAGE antagonist, A Box, partially restores T cell expression of L-selectin, suggesting that this effect of MDSC may be regulated through RAGE. The HMGB1 inhibitors ethyl pyruvate and glycyrrhizin reduced MDSC production of IL-10 during MDSC-macrophage crosstalk and the differentiation of MDSC from bone marrow progenitor

cells, and ethyl pyruvate restored T cell activation in the presence of MDSC. These reagents either bind exogenous HMGB1 (glycyrrhizin) or inhibit NF-κB signaling (ethyl pyruvate) and therefore do not distinguish whether HMGB1 is acting through TLR4 or RAGE. Regardless of which receptor is utilized, HMGB1 is a potent inducer of MDSC and immune suppression, and both its pro-tumor and anti-tumor activities must be considered when designing cancer immunotherapies.

Figures

Figure 1

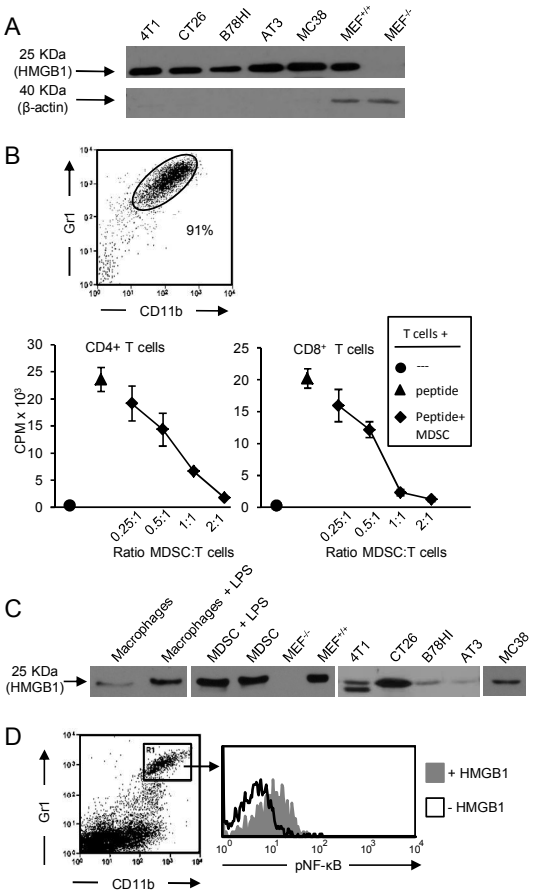

Figure 1: **HMGB1 is ubiquitously present in the tumor microenvironment, is secreted by MDSC, and activates the NF-κB signaling pathway in MDSC.** ***A***, 4T1, CT26, B78H1, AT3 and MC38 tumor cells were cultured in serum-free medium and their supernatants assessed by western blot for secreted HMGB1. Lysates of wild type and HMGB1-knocked-out MEF cells served as positive and negative controls. ***B*****,** BALB/c 4T1-induced $Gr1^{+}CD11b^{+}$ MDSC were obtained from the blood of tumor-bearing mice, stained for Gr1 and CD11b to assess purity, and co-cultured with transgenic $CD4^{+}$ (DO11.10) or $CD8^{+}$ (clone4) splenocytes. Splenocytes were activated with OVA or HA

peptide for DO11.10 and clone4 cells, respectively. T cell proliferation was measured by [^{3}H] thymidine incorporation. Data are expressed as cpm of triplicate cultures. ***C,*** LPS-treated and untreated macrophages and MDSC, and excised, dissociated tumors of BALB/c (4T1, CT26) and C57BL/6 (B78HI, AT3, MC38) mice were cultured overnight in serum-free medium. Resulting supernatants were assessed by western blot for HMGB1. ***D,*** Leukocytes from tumor-free BALB/c mice were treated with or without HMGB1 and stained for Gr1, CD11b, and pNF-κB. $Gr1^+CD11b^+$ cells were gated and analyzed for pNF-κB. Data are from one of three, two, three, and three independent experiments for panels A, B, C, and D, respectively.

Figure 2

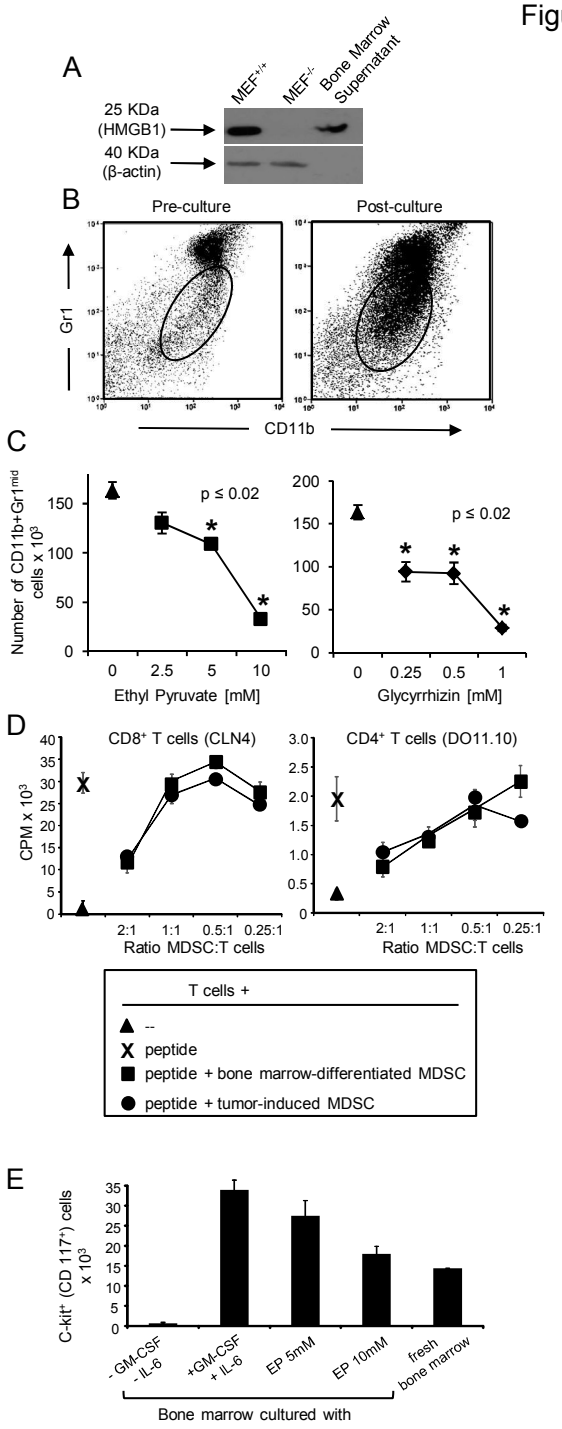

Figure 2: HMGB1 drives the differentiation of MDSC from bone marrow progenitor cells. Bone marrow cells were harvested from the femurs of healthy BALB/c mice and cultured with IL-6 and GM-CSF with or without ethyl pyruvate, glycyrrhizin,

or vehicle. After four days of culture, the absolute number of MDSC was determined. ***A,*** HMGB1 western blot of supernatants of bone marrow cultures. ***B*****,** Gating logic of $Gr1^{mid}CD11b^{+}$ MDSC from pre-cultured and post-cultured bone marrow cells. ***C,*** Absolute number of $Gr1^{mid}CD11b^{+}$ MDSC in the bone marrow cultures after incubation with ethyl pyruvate or glycyrrhizin. ***D,*** MDSC generated in the bone marrow cultures were assessed for suppressive activity against antigen-specific MHC-restricted transgenic $CD4^{+}$ and $CD8^{+}$ T cells. ***E,*** Bone marrow cells were cultured under MDSC differentiation conditions (GM-CSF+IL-6) ± ethyl pyruvate (EP) and analyzed for the percent of c-kit^{+} ($CD117^{+}$) progenitor cells. p values were obtained by Student's *t* test. Data are from one of three and two independent experiments for panels A-C and D-E, respectively.

Figure 3

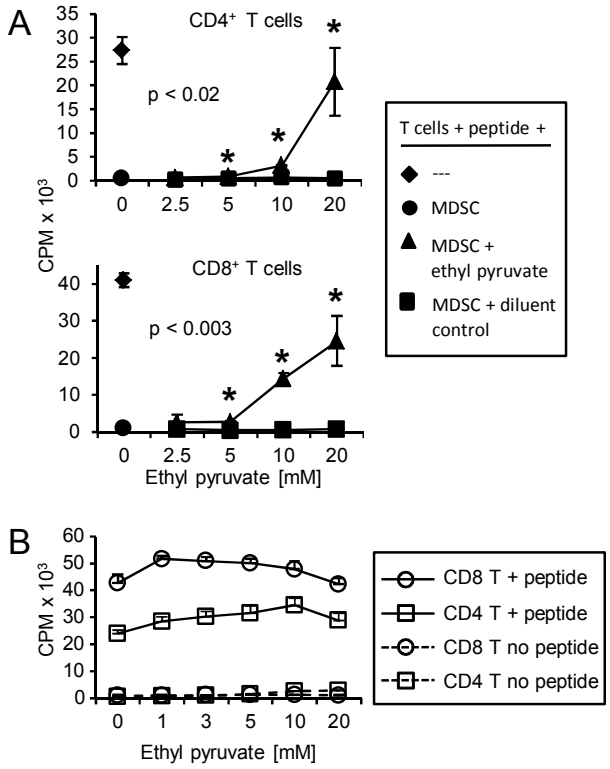

Figure 3: HMGB1 contributes to the ability of MDSC to suppress antigen-driven T cell activation. Splenocytes from $CD4^+$ DO11.10 TcR or $CD8^+$ clone4 TcR transgenic mice were co-cultured with irradiated 4T1-induced MDSC from BALB/c mice and cognate peptide (OVA or HA peptide for DO11.10 and clone 4 T cells, respectively). ***A***, T cell proliferation was measured by [^{3}H]-thymidine incorporation in the presence of titered amounts of ethyl pyruvate or vehicle control. ***B***, Ethyl pyruvate does not directly affect T cell activation. Transgenic DO11.10 and clone4 T cells were activated with cognate peptide in the presence of titered amounts of ethyl pyruvate. Data are from one of two independent experiments. p values were obtained by Student's *t* test comparing ethyl pyruvate treated samples versus the respective diluent control samples.

Figure 4

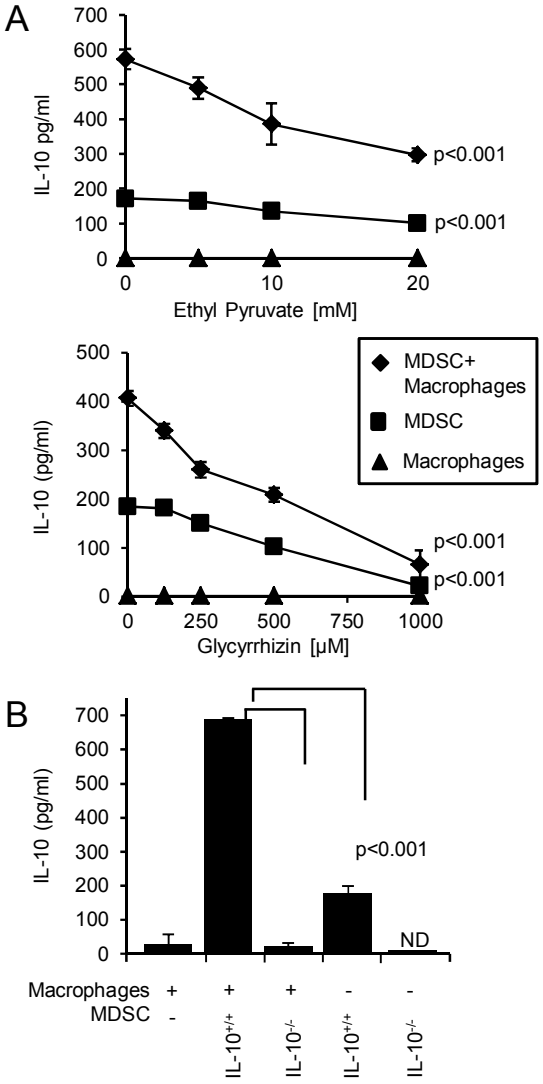

Figure 4: HMGB1 increases MDSC production of IL-10 and MDSC-macrophage crosstalk. ***A,*** Co-cultures of 4T1-induced BALB/c MDSC and macrophages from tumor-free mice were incubated with or without ethyl pyruvate or glycyrrhizin, and the supernatants were assayed by ELISA for IL-10. ***B,*** MDSC from 4T1-tumor-bearing BALB/c and BALB/c IL-$10^{-/-}$ mice and peritoneal macrophages from tumor-free BALB/c mice were co-cultured and the supernatants were assayed by ELISA for IL-10. ND indicates non-detectable levels of protein. Data are from one of six and three independent

experiments for panels A and B, respectively. p values were obtained by single-factor ANOVA.

Figure 5

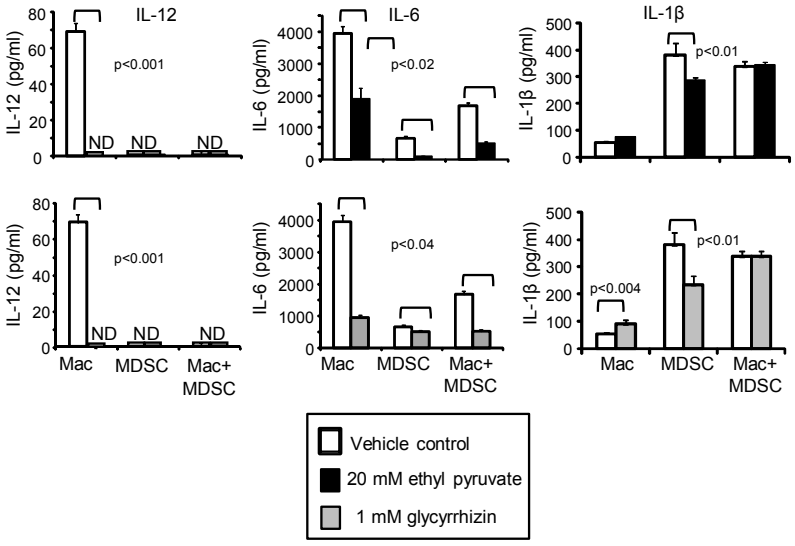

Figure 5: HMGB1 facilitates down-regulation of IL-6 and MDSC production of IL-1β, but does not alter MDSC-mediated down-regulation of macrophage production of IL-12. Co-cultures of 4T1-induced BALB/c MDSC and macrophages from tumor-free mice were incubated with or without ethyl pyruvate or glycyrrhizin and the supernatants were assayed by ELISA for IL-12, IL-6, and IL-1β. ND indicates non-detectable levels of protein. Data are from one of four, five, and two independent experiments for IL-12, IL-6, and IL-1β, respectively. p values were obtained by Student's *t* test.

Figure 6

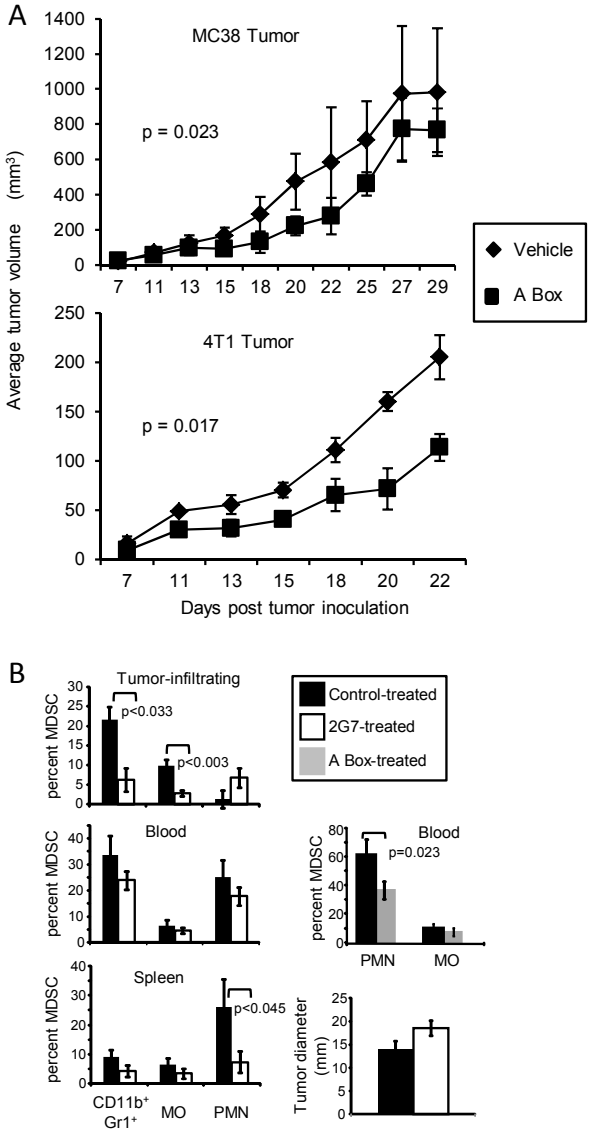

Figure 6: Tumor-bearing mice treated with mAbs to HMGB1 or with A Box have reduced levels of MDSC. ***A,*** C57BL/6 and BALB/c mice were inoculated s.c. with 5 x 10^5 MC38 colon carcinoma cells or in the mammary fat pad with 7 x 10^3 4T1 mammary carcinoma cells, respectively. Mice were given recombinant A box (300μg/mouse) or vehicle (PBS) three times per week starting when tumors were first palpable (day 7-9 post inoculation). p values were obtained by log rank test. ***B,*** C57BL/6 mice were

inoculated as in panel A. Treatment with 2G7 (5μg/200μl/mouse, 3x/week), irrelevant IgG, or A Box was started on day 10-13 when tumors were first palpable. Treatment was terminated on day 45 and blood leukocytes were analyzed by flow cytometry for total ($Gr1^+CD11b^+$), monocytic (MO; $CD11b^+Ly6G^-Ly6C^+$), and granulocytic (PMN; $CD11b^+Ly6G^+Ly6C^-$) MDSC. Mice were sacrificed on day 50 when their tumors were approximately the same size, and spleen and tumor-infiltrating leukocytes ($CD45^+$ cells) were analyzed by flow cytometry. n = 7 (blood, control-treated for 2G7), 4 (A Box, PBS-treated), 6 (tumor-infiltrating and spleen, control-treated; blood, 2G7-treated), 4 (tumor-infiltrating and spleen, 2G7-treated), and 4 (A Box-treated) mice/group. Data for 2G7 and their control-treated mice are pooled from two independent experiments; data for A Box and their control-treated mice are from a single experiment. . p values were obtained by Student's *t* test.

Figure 7

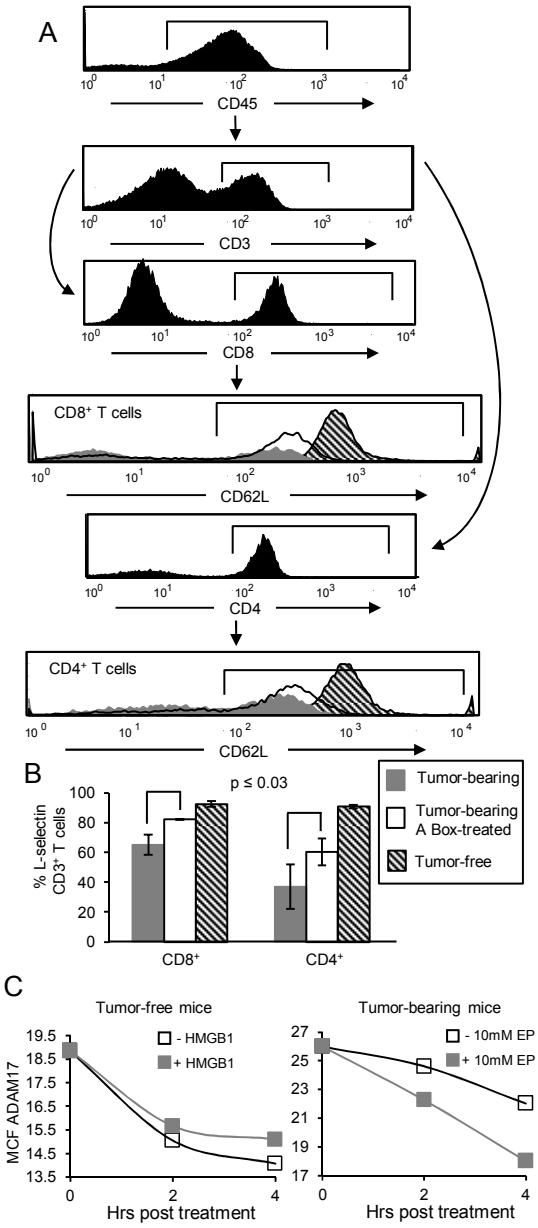

Figure 7: ***HMGB1 down-regulates T cell expression of L-selectin. A,*** Twenty-nine days after tumor inoculation the MC38 tumor-bearing mice from figure 6A were sacrificed and blood leukocytes were analyzed by flow cytometry for L-selectin expression and compared to blood leukocytes from tumor-free C57BL/6 mice. Representative histograms showing L-selectin expression from gated $CD45^{+}CD3^{+}CD4^{+}$ and

$CD45^+CD3^+CD8^+$ T cells from tumor-free, A box-treated, or control-treated (PBS) C56BL/6 tumor-bearing mice. ***B,*** Average percent ± SD of $CD45^+CD3^+CD4^+$ or $CD45^+CD3^+CD8^+$ T cells expressing L-selectin. n= 5 mice/group (PBS-treated and tumor-free groups); n= 3 mice/group (A Box-treated group). p values were obtained by Student's *t* test. Data are from one of two independent experiments. ***C,*** $Gr1^+CD11b^+$ cells from tumor-free (left-hand panels) or tumor-bearing (right-hand panels) mice were incubated in vitro for zero, two, or four hours with exogenous HMGB1 (left-hand panels) or ethyl pyruvate (right-hand panels), and stained for Gr1, CD11b, and ADAM17. Gated $Gr1^+CD11b^+$ cells were analyzed for ADAM17 expression. Graphs represent MCF of ADAM17 on $Gr1^+CD11b^+$ cells. Data are representative of three independent experiments.

Supp Figure S1

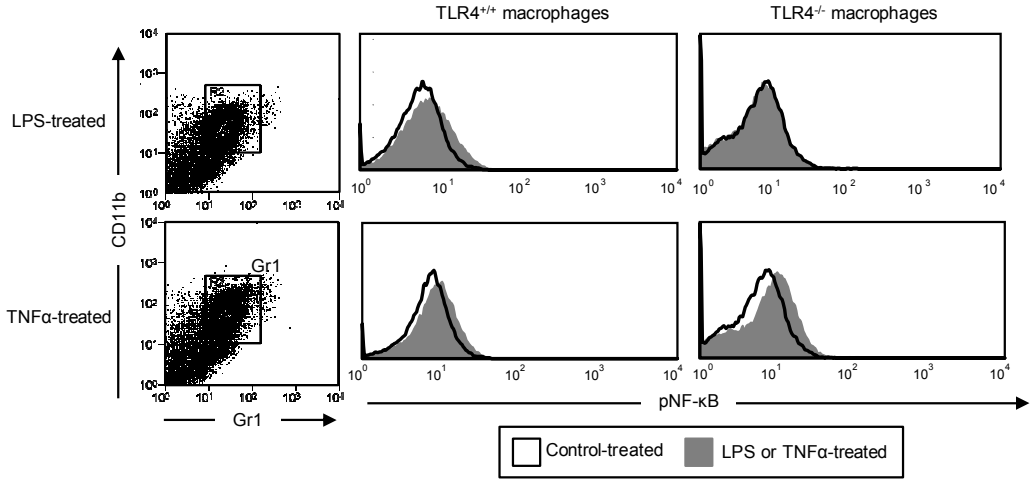

Supplementary Fig. S1. pNF-κB mAb is specific for activated NF-κB. Macrophages were harvested from the peritoneal cavity of $TLR4^{+/+}$ or $TLR4^{-/-}$ tumor-free mice treated with thioglycolate, rested in vitro for two hours, incubated with or without LPS or TNFα, and stained with mAbs to CD11b, F4/80, and pNF-κB. Gated CD11b+F4/80+ macrophages were analyzed for pNF-κB.

Supp Figure S2

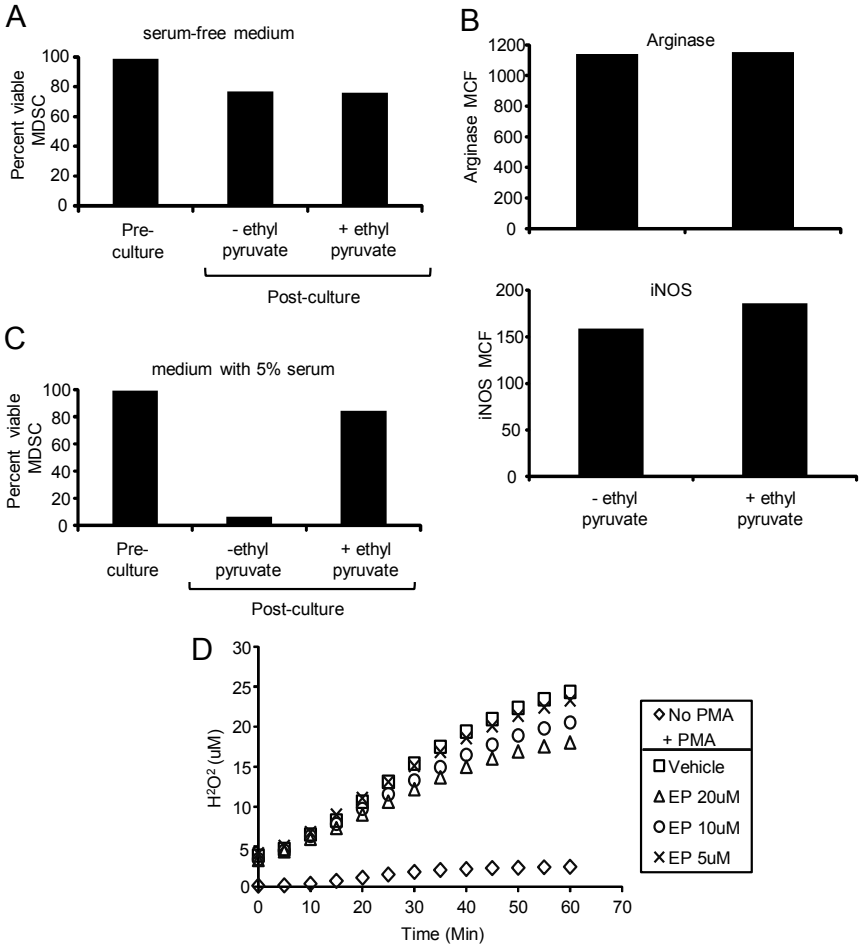

Supplementary Fig. S2. Treatment with ethyl pyruvate does not alter arginase or iNOS expression or induce MDSC apoptosis as compared to control-treated MDSC. MDSC were harvested from BALB/c mice with 4T1 tumor. **A,** MDSC were not cultured (pre-culture) or cultured overnight in serum-free HL-1 medium with or without 10mM EP and then stained with fluorescently coupled mAbs to Gr1 and CD11b, and Annexin V and PI, and the gated $Gr1^+CD11b^+$ cells analyzed by flow cytometry. Percent viable cells = 100% - $\%Gr1^+CD11b^+AnneinV^+PI^+$ **B,** MDSC were incubated overnight in serum-free media. The following day cells were stained with unlabeled mAbs to arginase or iNOS and goat-anti-mouse IgG-AlexaF647, followed by fluorescently labeled mAbs to Gr1 and CD11b. Gated $Gr1^+CD11b^+$ cells were analyzed by flow cytometry **C,** MDSC were treated as in panel A except cultured in DMEM with 5% serum. Data for each panel are representative of two independent experiments. **D,** HMGB1 increases MDSC content of H_2O_2. MDSC were activated with PMA and treated with vehicle or escalating doses of ethyl pyruvate. H_2O_2 levels were measured using an Amplex Red Hydrogen Peroxide Assay kit.

Supp Figure S3

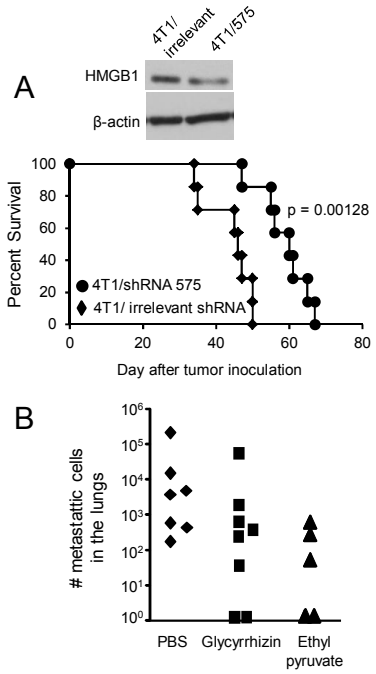

Supplementary Fig. S3: **HMGB1 produced by tumor cells promotes tumor growth and metastasis.** ***A,*** BALB/c mice were inoculated in the mammary fat pad with 7 x 10^3 4T1/575 (shRNA knockdown for HMGB1) or 4T1/irrelevant (shRNA knockdown for Invariant chain) mammary carcinoma cells and monitored for survival. Methods: HMGB1 Oligonucleotides: hm575sense– 5' GATCGGCAGCCCTA TGAGAAGAAATTCAAGAGATTTCTTCTCATAGGGCTGCTTTTTTG 3', hm575anti-sense – 5' AATTCAAAAA AGCAGCCCTATGAGAAGAAATCTCTTGAATTTCTTCTCATAGGGCTGCC 3' (IDTDNA). Invariant chain oligos: sense-5'GATCCGCTTGTTATCAGCTTTCAGTTCAAGAGACTGAAA GCTGATAACAAGCTTTTTTCTAGAG 3' Ii 54 anti-sense- 5' ATTCTCTAGAAAAAAGCTTGTTAT CAGCTTTCAGTCTCTTGAACTGAAAGCTGATAACAAGCG 3'. Double stranded DNA was generated by annealing 5 μM each of sense and anti-sense primers at 80°C.and subsequently cloned into pSiren RetroQ vector (Clonetech) utilizing the BamHI and EcoR1 sites. Constructs were confirmed by DNA sequencing. Plasmid DNA was prepared using a Macherey-Nagel Nucleo Bond Xtra Midi Kit and 4T1 cells were transfected with 3μg of DNA using Amaxa Nucleofactor program T-024. Stable transfectants were obtained after three weeks of culture in 1.8 μg/ml puromycin. Transfected and parental cells were lysed in 500μl of M-Per buffer Mammalian Protein Extraction Reagent (Thermo Scientific) using a GentleMACS M tube and program protein 01.01 on the GentleMACS Dissociator (Milltenyl Biotec). Protein concentrations of supernatants were determined at 280 absorbance. Fifty μg of protein/cell line was heated for 5 minutes at 95°C and run on a 12% polyacrylamide gel for 60 minutes at 100V. Protein was transferred to a PVDF membrane overnight at 30V and probed with antibody to HMGB1. Blots were stripped with Restore buffer (Thermoscientific) and reprobed for β-actin. ***B,*** BALB/c mice were inoculated s.c. with 7 x 10^3 4T1 mammary carcinoma cells. When tumors were first palpable (7-9 days post tumor inoculation), mice were treated i.p. with ethyl pyruvate (40 mg/kg, twice daily), glycyrrhizin (2mg/kg twice daily), or vehicle (PBS; twice a week). Four weeks after tumor inoculation when tumors were >10mm in diameter, mice were sacrificed and the number of metastatic cells in the lungs was quantified by clonogenic assay (20) with the following modification: Lung tissue was dissociated using a Gentle MACS Dissociator (Milltenyl Biotec) fitted with a C tube running program m_lung_02.01. Data are pooled from two experiments and are combined from two independent experiments. n=7, 5, and 8 for the PBS, ethyl pyruvate, and glycyrrhizin groups, respectively.

Supp Figure S4

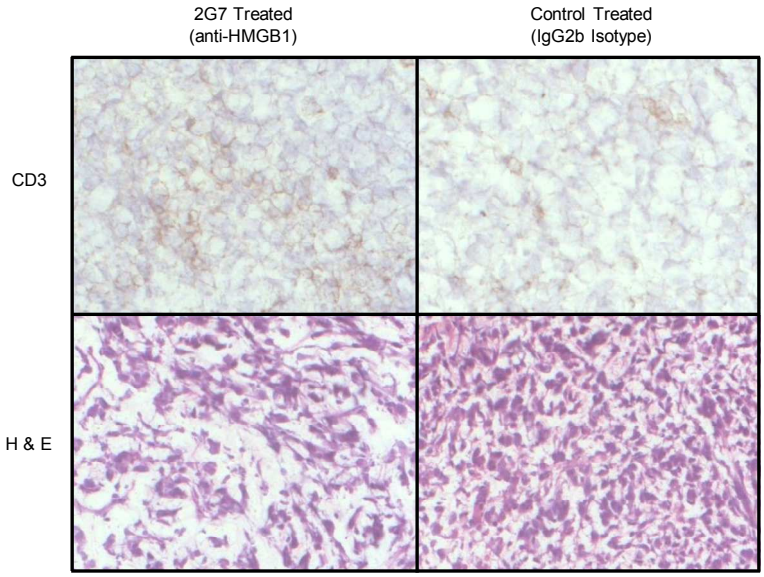

Supplementary Fig. S4: Tumors from mice treated with anti-HMGB1 mAb tend to have more tumor-infiltrating $CD3^+$ cells. Tumors from the HMGB1-treated (2G7 mAb) and isotype control-treated mice of Figure 6 were frozen and embedded in OCT medium and subsequently stained for CD3 or with H&E. Slides were examined at a magnification of 250X using a Zeiss microscope fitted with an AxioCamMRc5 camera. Images are representative of fields from each of two mice per group.

Supplementary Table 1. Quantitation of HMGB1 secreted by cultured tumor cells, ex vivo macrophages and MDSC, in vivo grown tumors, and cultures of MDSC differentiated from bone marrow progenitor cells.

In vitro cultured tumor cells	ng/ml/10^6 cells[a]
4T1	36.95
CT26	16.23
MC38	123.23
AT3	36.95
B78H1	12.61
	ng/ml/10^6 cells[b]
Bone marrow differentiation cultures	98.61
Ex vivo cells	ng/ml/10^7 cells[a]
Macrophages	0.31
LPS-treated macrophages	0.31
MDSC	3.29
LPS-treated MDSC	4.24

In vivo grown tumors	Tumor weight (mg)	Tumor diameter (mm)	ng/ml/1g tumor[a]
4T1	1140	13.54	85.89
CT26	1770	9.55	173.39
B78H1	840	8.84	216.86
AT3	127	3.96	0.63

[a] Amount of HMGB1 after 18 hrs of culture
[b] Amount of HMGB1 at the end of the four day incubation

Supplementary Table 2: HMGB1 drives the differentiation of MDSC from bone marrow progenitor cells

	Pre-culture	Post-culture						
		Vehicle	Ethyl Pyruvate (mM)			Glycyrrhizin (mM)		
			2.5	5	10	0.25	0.5	1
Total cells [a]	$4.2x10^5$	$5.5x10^5$	4.1 $x10^5$	3.4 $x10^5$	1.2 $x10^5$	3.1 $x10^5$	2.8 $x10^5$	9.6 $x10^4$
$Gr1^{mid}CD11b^{+}$ [b]	$5.5x10^4$	$1.6x10^5$	1.3 $x10^5$	1.08 $x10^5$	$3.2x10^4$	9.4 $x10^4$	9.2 $x10^4$	2.9 $x10^4$
$\%Gr1^{mid}CD11b^{+}$ [c]	13.11	29.6	31.72	32.12	25.25	30.58	32.14	30.13
% change								
$Gr1^{mid}CD11b^{+}$ [d]		0	20.23	33.46	80.12	42.26	43.49	82.26
$CD3^{+}$ [d]		0	-6.98	19.52	12.14	-22.19	30.44	-33.1
$B220^{+}$ [d]		0	3.89	33.05	36.29	-27.76	29.52	-4.87
$F4/80^{+}CD11b^{+}$ [d]		0	32.69	57.89	68.43	-2.92	58.28	66.08
$CD11c^{+}$ [d]		0	19.37	32.03	67.0	-4.96	51.97	43.07

[a] *Total number of cells was obtained by trypan blue cell counts*

[b] $Gr1^{mid}CD11b^{+}$ cells = *total cells x* % $Gr1^{mid}CD11b^{+}$ cells

[c] $Gr1^{mid}CD11b^{+}$ cells *were identified by flow cytometry*

[d] *% change = [(vehicle – treated)/vehicle] x 100*

References

1. Gabrilovich, D. I., V. Bronte, S. H. Chen, M. P. Colombo, A. Ochoa, S. Ostrand-Rosenberg, and H. Schreiber. 2007. The terminology issue for myeloid-derived suppressor cells. *Cancer Res* 67: 425; author reply 426.
2. Gabrilovich, D. I., and S. Nagaraj. 2009. Myeloid-derived suppressor cells as regulators of the immune system. *Nat Rev Immunol* 9: 162-174.
3. Sinha, P., V. K. Clements, S. K. Bunt, S. M. Albelda, and S. Ostrand-Rosenberg. 2007. Cross-talk between myeloid-derived suppressor cells and macrophages subverts tumor immunity toward a type 2 response. *J Immunol* 179: 977-983.
4. Hanson, E. M., V. K. Clements, P. Sinha, D. Ilkovitch, and S. Ostrand-Rosenberg. 2009. Myeloid-derived suppressor cells down-regulate L-selectin expression on CD4+ and CD8+ T cells. *J Immunol* 183: 937-944.
5. Yang, L., L. M. DeBusk, K. Fukuda, B. Fingleton, B. Green-Jarvis, Y. Shyr, L. M. Matrisian, D. P. Carbone, and P. C. Lin. 2004. Expansion of myeloid immune suppressor Gr+CD11b+ cells in tumor-bearing host directly promotes tumor angiogenesis. *Cancer Cell* 6: 409-421.
6. Yang, L., J. Huang, X. Ren, A. E. Gorska, A. Chytil, M. Aakre, D. P. Carbone, L. M. Matrisian, A. Richmond, P. C. Lin, and H. L. Moses. 2008. Abrogation of TGF beta signaling in mammary carcinomas recruits Gr-1+CD11b+ myeloid cells that promote metastasis. *Cancer Cell* 13: 23-35.
7. Balkwill, F., and A. Mantovani. 2001. Inflammation and cancer: back to Virchow? *Lancet* 357: 539-545.
8. Ostrand-Rosenberg, S., and P. Sinha. 2009. Myeloid-derived suppressor cells: linking inflammation and cancer. *J Immunol* 182: 4499-4506.

9. Sims, G. P., D. C. Rowe, S. T. Rietdijk, R. Herbst, and A. J. Coyle. 2010. HMGB1 and RAGE in inflammation and cancer. *Annu Rev Immunol* 28: 367-388.

10. Lotze, M. T., and K. J. Tracey. 2005. High-mobility group box 1 protein (HMGB1): nuclear weapon in the immune arsenal. *Nat Rev Immunol* 5: 331-342.

11. Wang, H., O. Bloom, M. Zhang, J. M. Vishnubhakat, M. Ombrellino, J. Che, A. Frazier, H. Yang, S. Ivanova, L. Borovikova, K. R. Manogue, E. Faist, E. Abraham, J. Andersson, U. Andersson, P. E. Molina, N. N. Abumrad, A. Sama, and K. J. Tracey. 1999. HMG-1 as a late mediator of endotoxin lethality in mice. *Science* 285: 248-251.

12. Li, J., R. Kokkola, S. Tabibzadeh, R. Yang, M. Ochani, X. Qiang, H. E. Harris, C. J. Czura, H. Wang, L. Ulloa, H. S. Warren, L. L. Moldawer, M. P. Fink, U. Andersson, K. J. Tracey, and H. Yang. 2003. Structural basis for the proinflammatory cytokine activity of high mobility group box 1. *Mol Med* 9: 37-45.

13. Yang, H., and K. J. Tracey. 2010. Targeting HMGB1 in inflammation. *Biochim Biophys Acta* 1799: 149-156.

14. Yang, H., M. Ochani, J. Li, X. Qiang, M. Tanovic, H. E. Harris, S. M. Susarla, L. Ulloa, H. Wang, R. DiRaimo, C. J. Czura, J. Roth, H. S. Warren, M. P. Fink, M. J. Fenton, U. Andersson, and K. J. Tracey. 2004. Reversing established sepsis with antagonists of endogenous high-mobility group box 1. *Proc Natl Acad Sci U S A* 101: 296-301.

15. Stewart, T. J., and S. I. Abrams. 2007. Altered immune function during long-term host-tumor interactions can be modulated to retard autochthonous neoplastic growth. *J Immunol* 179: 2851-2859.

16. Calogero, S., F. Grassi, A. Aguzzi, T. Voigtlander, P. Ferrier, S. Ferrari, and M. E. Bianchi. 1999. The lack of chromosomal protein Hmg1 does not disrupt cell growth but causes lethal hypoglycaemia in newborn mice. *Nat Genet* 22: 276-280.

17. Sinha, P., V. K. Clements, and S. Ostrand-Rosenberg. 2005. Reduction of myeloid-derived suppressor cells and induction of M1 macrophages facilitate the rejection of established metastatic disease. *J Immunol* 174: 636-645.

18. Marigo, I., E. Bosio, S. Solito, C. Mesa, A. Fernandez, L. Dolcetti, S. Ugel, N. Sonda, S. Bicciato, E. Falisi, F. Calabrese, G. Basso, P. Zanovello, E. Cozzi, S. Mandruzzato, and V. Bronte. 2010. Tumor-induced tolerance and immune suppression depend on the C/EBPbeta transcription factor. *Immunity* 32: 790-802.

19. Sinha, P., and S. Ostrand-Rosenberg. 2013. Myeloid-derived suppressor cell function is reduced by Withaferin A, a potent and abundant component of Withania somnifera root extract. *Cancer Immunol Immunother* 62: 1663-1673.

20. Sinha, P., C. Okoro, D. Foell, H. H. Freeze, S. Ostrand-Rosenberg, and G. Srikrishna. 2008. Proinflammatory S100 proteins regulate the accumulation of myeloid-derived suppressor cells. *J Immunol* 181: 4666-4675.

21. Andersson, U., H. Wang, K. Palmblad, A. C. Aveberger, O. Bloom, H. Erlandsson-Harris, A. Janson, R. Kokkola, M. Zhang, H. Yang, and K. J. Tracey. 2000. High mobility group 1 protein (HMG-1) stimulates proinflammatory cytokine synthesis in human monocytes. *J Exp Med* 192: 565-570.

22. Park, J. S., D. Svetkauskaite, Q. He, J. Y. Kim, D. Strassheim, A. Ishizaka, and E. Abraham. 2004. Involvement of toll-like receptors 2 and 4 in cellular activation by high mobility group box 1 protein. *J Biol Chem* 279: 7370-7377.

23. Kokkola, R., A. Andersson, G. Mullins, T. Ostberg, C. J. Treutiger, B. Arnold, P. Nawroth, U. Andersson, R. A. Harris, and H. E. Harris. 2005. RAGE is the major receptor for the proinflammatory activity of HMGB1 in rodent macrophages. *Scand J Immunol* 61: 1-9.

24. Sinha, P., V. K. Clements, A. M. Fulton, and S. Ostrand-Rosenberg. 2007. Prostaglandin E2 promotes tumor progression by inducing myeloid-derived suppressor cells. *Cancer Res* 67: 4507-4513.

25. Cheng, P., C. A. Corzo, N. Luetteke, B. Yu, S. Nagaraj, M. M. Bui, M. Ortiz, W. Nacken, C. Sorg, T. Vogl, J. Roth, and D. I. Gabrilovich. 2008. Inhibition of dendritic cell differentiation and accumulation of myeloid-derived suppressor cells in cancer is regulated by S100A9 protein. *J Exp Med* 205: 2235-2249.

26. Ulloa, L., M. Ochani, H. Yang, M. Tanovic, D. Halperin, R. Yang, C. J. Czura, M. P. Fink, and K. J. Tracey. 2002. Ethyl pyruvate prevents lethality in mice with established lethal sepsis and systemic inflammation. *Proc Natl Acad Sci U S A* 99: 12351-12356.

27. Yang, H., P. Lundback, L. Ottosson, H. Erlandsson-Harris, E. Venereau, M. E. Bianchi, Y. Al-Abed, U. Andersson, K. J. Tracey, and D. J. Antoine. 2012. Redox modification of cysteine residues regulates the cytokine activity of high mobility group box-1 (HMGB1). *Mol Med* 18: 250-259.

28. Bianchi, M. E., and A. A. Manfredi. 2007. High-mobility group box 1 (HMGB1) protein at the crossroads between innate and adaptive immunity. *Immunol Rev* 220: 35-46.

29. Bronte, V., E. Apolloni, A. Cabrelle, R. Ronca, P. Serafini, P. Zamboni, N. P. Restifo, and P. Zanovello. 2000. Identification of a CD11b(+)/Gr-1(+)/CD31(+) myeloid progenitor capable of activating or suppressing CD8(+) T cells. *Blood* 96: 3838-3846.

30. Gabrilovich, D. I., M. P. Velders, E. M. Sotomayor, and W. M. Kast. 2001. Mechanism of immune dysfunction in cancer mediated by immature Gr-1+ myeloid cells. *J Immunol* 166: 5398-5406.

31. Kontgen, F., R. J. Grumont, A. Strasser, D. Metcalf, R. Li, D. Tarlinton, and S. Gerondakis. 1995. Mice lacking the c-rel proto-oncogene exhibit defects in lymphocyte proliferation, humoral immunity, and interleukin-2 expression. *Genes Dev* 9: 1965-1977.

32. Huang, B., P. Y. Pan, Q. Li, A. I. Sato, D. E. Levy, J. Bromberg, C. M. Divino, and S. H. Chen. 2006. Gr-1+CD115+ Immature Myeloid Suppressor Cells Mediate the Development of Tumor-Induced T Regulatory Cells and T-Cell Anergy in Tumor-Bearing Host. *Cancer Res* 66: 1123-1131.

33. Bunt, S. K., P. Sinha, V. K. Clements, J. Leips, and S. Ostrand-Rosenberg. 2006. Inflammation induces myeloid-derived suppressor cells that facilitate tumor progression. *J Immunol* 176: 284-290.

34. Bunt, S. K., L. Yang, P. Sinha, V. K. Clements, J. Leips, and S. Ostrand-Rosenberg. 2007. Reduced inflammation in the tumor microenvironment delays

the accumulation of myeloid-derived suppressor cells and limits tumor progression. *Cancer Res* 67: 10019-10026.

35. Pulaski, B. A., and S. Ostrand-Rosenberg. 1998. Reduction of established spontaneous mammary carcinoma metastases following immunotherapy with major histocompatibility complex class II and B7.1 cell-based tumor vaccines. *Cancer Res* 58: 1486-1493.

36. Liu, Z., L. D. Falo, Jr., and Z. You. 2011. Knockdown of HMGB1 in tumor cells attenuates their ability to induce regulatory T cells and uncovers naturally acquired CD8 T cell-dependent antitumor immunity. *J Immunol* 187: 118-125.

37. Ellerman, J. E., C. K. Brown, M. de Vera, H. J. Zeh, T. Billiar, A. Rubartelli, and M. T. Lotze. 2007. Masquerader: high mobility group box-1 and cancer. *Clin Cancer Res* 13: 2836-2848.

38. Song, X., Y. Krelin, T. Dvorkin, O. Bjorkdahl, S. Segal, C. A. Dinarello, E. Voronov, and R. N. Apte. 2005. CD11b+/Gr-1+ immature myeloid cells mediate suppression of T cells in mice bearing tumors of IL-1beta-secreting cells. *J Immunol* 175: 8200-8208.

39. Sha, Y., J. Zmijewski, Z. Xu, and E. Abraham. 2008. HMGB1 develops enhanced proinflammatory activity by binding to cytokines. *J Immunol* 180: 2531-2537.

40. Liu, J. H., Z. J. Li, J. Tang, Y. W. Liu, L. Zhao, P. Deng, and Y. Jiang. 2006. [High mobility group box-1 protein activates endothelial cells to produce cytokines and has synergistic effect with lipopolysaccharide in inducing interleukin-6 release]. *Zhonghua Yi Xue Za Zhi* 86: 1191-1195.

41. Leclerc, P., H. Wahamaa, H. Idborg, P. J. Jakobsson, H. E. Harris, and M. Korotkova. 2013. IL-1beta/HMGB1 complexes promote The PGE2 biosynthesis pathway in synovial fibroblasts. *Scand J Immunol* 77: 350-360.

42. Rodriguez, P. C., C. P. Hernandez, D. Quiceno, S. M. Dubinett, J. Zabaleta, J. B. Ochoa, J. Gilbert, and A. C. Ochoa. 2005. Arginase I in myeloid suppressor cells is induced by COX-2 in lung carcinoma. *J Exp Med* 202: 931-939.

43. Sade-Feldman, M., J. Kanterman, E. Ish-Shalom, M. Elnekave, E. Horwitz, and M. Baniyash. 2013. Tumor necrosis factor-alpha blocks differentiation and enhances suppressive activity of immature myeloid cells during chronic inflammation. *Immunity* 38: 541-554.

44. Wild, C. A., C. Bergmann, G. Fritz, P. Schuler, T. K. Hoffmann, R. Lotfi, A. Westendorf, S. Brandau, and S. Lang. 2012. HMGB1 conveys immunosuppressive characteristics on regulatory and conventional T cells. *Int Immunol* 24: 485-494.

45. Gebhardt, C., A. Riehl, M. Durchdewald, J. Németh, G. Fürstenberger, K. Müller-Decker, A. Enk, B. Arnold, A. Bierhaus, P. P. Nawroth, J. Hess, and P. Angel. 2008. RAGE signaling sustains inflammation and promotes tumor development. *J Exp Med* 205: 275-285.

46. Taguchi, A., D. C. Blood, G. del Toro, A. Canet, D. C. Lee, W. Qu, N. Tanji, Y. Lu, E. Lalla, C. Fu, M. A. Hofmann, T. Kislinger, M. Ingram, A. Lu, H. Tanaka, O. Hori, S. Ogawa, D. M. Stern, and A. M. Schmidt. 2000. Blockade of RAGE-amphoterin signalling suppresses tumour growth and metastases. *Nature* 405: 354-360.

47. Livesey, K. M., D. Tang, H. J. Zeh, and M. T. Lotze. 2008. Not just nuclear proteins: 'novel' autophagy cancer treatment targets - p53 and HMGB1. *Curr Opin Investig Drugs* 9: 1259-1263.

48. Messmer, D., H. Yang, G. Telusma, F. Knoll, J. Li, B. Messmer, K. J. Tracey, and N. Chiorazzi. 2004. High mobility group box protein 1: an endogenous signal for dendritic cell maturation and Th1 polarization. *J Immunol* 173: 307-313.

49. Apetoh, L., F. Ghiringhelli, A. Tesniere, M. Obeid, C. Ortiz, A. Criollo, G. Mignot, M. C. Maiuri, E. Ullrich, P. Saulnier, H. Yang, S. Amigorena, B. Ryffel, F. J. Barrat, P. Saftig, F. Levi, R. Lidereau, C. Nogues, J. P. Mira, A. Chompret, V. Joulin, F. Clavel-Chapelon, J. Bourhis, F. Andre, S. Delaloge, T. Tursz, G. Kroemer, and L. Zitvogel. 2007. Toll-like receptor 4-dependent contribution of the immune system to anticancer chemotherapy and radiotherapy. *Nat Med* 13: 1050-1059.

50. Bunt, S. K., V. K. Clements, E. M. Hanson, P. Sinha, and S. Ostrand-Rosenberg. 2009. Inflammation enhances myeloid-derived suppressor cell cross-talk by signaling through Toll-like receptor 4. *J Leukoc Biol* 85: 996-1004.

51. Coffelt, S. B., and A. B. Scandurro. 2008. Tumors sound the alarmin(s). *Cancer Res* 68: 6482-6485.

Chapter 3: High Mobility Group Box Protein 1 Promotes the Survival of Myeloid-derived Suppressor Cells by Inducing Autophagy

Abstract

Myeloid-derived suppressor cells (MDSC) are immune suppressive cells that are elevated in most individuals with cancer where their accumulation and suppressive activity are driven by inflammation. Because MDSC inhibit anti-tumor immunity, and promote tumor progression, we are determining how their viability is regulated. Previous studies have established that the damage-associated molecular pattern molecule (DAMP) High Mobility Group Box protein 1(HMGB1) drives MDSC accumulation and suppressive potency and is ubiquitously present in the tumor microenvironment. Since HMGB1 also facilitates tumor cell survival by inducing autophagy, we sought to determine if HMGB1 regulates MDSC survival through induction of autophagy. Inhibition of autophagy increased the quantity of apoptotic MDSC demonstrating that autophagy extends the survival and increases the viability of MDSC. Inhibition of HMGB1 similarly increased the level of apoptotic MDSC and reduced MDSC autophagy demonstrating that in addition to inducing the accumulation of MDSC, HMGB1 sustains MDSC viability. Circulating MDSC have a default autophagic phenotype and tumor-infiltrating MDSC are more autophagic, consistent with the concept that inflammatory and hypoxic conditions within the microenvironment of solid tumors contribute to tumor progression by enhancing immune suppressive MDSC. Overall, these results demonstrate that in addition to previously recognized pro-tumor effects, HMGB1 also

contributes to tumor progression by increasing MDSC viability by driving them into a pro-autophagic state.

Introduction

Solid tumors often generate a harsh local environment containing multiple pro-inflammatory mediators (1). Tumor progression requires that tumor cells as well as immune suppressive host cells must survive in this tumor microenvironment (TME). Survival of malignant cells is at least partially due to autophagy. Many tumor cells are autophagic even under minimally stressful conditions, while non-malignant cells usually become autophagic only in response to stress (2). Autophagy is triggered by a variety of conditions present in the TME, including nutrient deprivation and hypoxia. It provides a survival advantage to stressed cells because it enables cells to maintain metabolic activity by engulfing cytoplasmic components that are degraded in autolysosomes (3). Degradation of cytoplasmic components through starvation-induced autophagy regenerates amino acids that are utilized in the trichloroacetic acid cycle to produce energy the cell needs to survive, thus allowing them to avoid death (4) .

Autophagy involves the formation of autophagosomes, mediated by a series of membrane rearrangements involving autophagy-related proteins (Atg) (5) (**Figure 1**). Autophagy is initiated when mTOR is down-regulated, resulting in the release of the transcription factor ULK1. ULK1 in turn induces vacuole formation by activating PI3KC3, Beclin1 (Atg6), and the Atg12, 5, and 16 complex. This complex then interacts with Atg9 to mediate the induction of an autophagosome (6). Once an autophagosome is formed, Atg4, 7, and 3 assist in modifying LC3 (Atg8), first into LC3-I through cleavage by a cysteine protease, and further into LC3-II by conjugation with a

phosphatidylethanolamine. LC3-II is then incorporated into the lumen of an autophagosome. Upon closure of the autophagosome, adaptor proteins, such as p62, are retained within the autophagosome and target cargo for degradation. An autophagosome will mature into an autolysosome by docking and fusing with a lysosome. The autolysosome allows for the breakdown and recycling of autophagosomal contents, which temporarily sustains survival.

Immune suppressive cells in the TME are important contributors to tumor progression because they prevent the host's immune system from eliminating malignant cells (7). Myeloid-derived suppressor cells (MDSC) are a major population of such suppressive cells and are present in the TME of most individuals with solid tumors (8). Studies by ourselves and others have established that multiple pro-inflammatory mediators induce the accumulation and suppressive potency of MDSC (9). The damage associated molecular pattern (DAMP) protein high mobility group box protein 1 (HMGB1) is ubiquitously present in the TME, is an established driver of MDSC development and function (10), and is also an inducer of tumor cell autophagy (11). These properties of HMGB1 raise the question of whether MDSC survival in the TME is prolonged due to autophagy.

Using inhibitors and inducers of autophagy and inhibitors of HMGB1, we have assessed the role of HMGB1 and autophagy in the survival of tumor-induced MDSC. Our results indicate that in addition to promoting MDSC development, HMGB1 also prolongs MDSC survival by driving MDSC autophagy, and that the TME promotes autophagy in MDSC.

Materials and methods

Mice

BALB/c, BALB/c DO11.10 (TCR-transgenic for the αβ-TCR specific for OVA peptide 323-339 restricted by I-A^d) and BALB/c clone 4 TCR-transgenic mice (αβ-TCR specific for influenza hemagglutinin 518-526 restricted by H-$2K^d$) mice were purchased from The Jackson Laboratory (Bar Harbor, ME) and/or bred in the University of Maryland Baltimore County Biology Department animal facility. Female mice <6 months of age were used for all experiments. All animal procedures were approved by the UMBC Institutional Animal Care and Use Committee.

Reagents, antibodies, and cells

Heparin sodium salt (grade IA), chloroquine, hyaluronidase, deoxyribonuclease I, and ethyl pyruvate were purchased from Sigma-Aldrich. Bafilomycin and rapamycin were purchased from Cayman Chemical. Collagenase type 4 was purchased from Worthington Biochemical. Ficoll-Paque PLUS was purchased from GE Healthcare Life Sciences. Fluorescently-coupled antibodies Gr1-APC (RB6-8C5), CD8-APC (53-6.7), CD4-PE (GK1.5), Vβ8.1 8.2-PE (MR5-2), Annexin V FITC, propidium iodide, and Annexin V binding buffer were from BD Biosciences. CD11b-PacB (M1/70) and CD45-APC-Cy7 (30-F11) were from BioLegend. DO11.10-APC (KJ1-26) was from eBiosciences. Murine 4T1 and human Jurkat cells were cultured in IMDM medium supplemented with 10% fetal bovine product, 1% penicillin, 1% streptomycin, 1% glutamax, and 1% gentamycin. HeLa cells were cultured in DMEM, supplemented with 10% fetal calf serum, 1% penicillin, 1% streptomycin, 1% glutamax, and 1% gentamycin.

Tumor inoculations

BALB/c mice were inoculated in the abdominal mammary fat pad with 7 x 10^3 4T1 mammary carcinoma cells. 4T1 cells have been in the authors' laboratory for >20 years. They were originally obtained from Dr. Fred Miller at the Karmanos Cancer Center.

Flow cytometry

Cells were labeled for immunofluorescence and analyzed by flow cytometry for cell surface molecules by staining with antibodies to Gr1 and CD11b. Antibodies were diluted in PBS containing 2% FCS (HyClone). Staining was conducted in the dark, on ice for thirty minutes. Staining for apoptosis or autophagy was conducted after surface staining. For apoptosis staining 1 x 10^6 cells were stained with PI and Annexin V for 15 minutes at room temperature as per the manufacturer's protocol (BD Biosciences). For cyto ID staining, cells were first stained for surface markers, Gr1 and CD11b, followed by staining with cyto ID for thirty minutes at 37°C as per the manufacturer's protocol (Enzo Life Sciences). Samples were run on a Cyan ADP flow cytometer and analyzed using Summit 4.3 Software (Beckman/Coulter).

MDSC

BALB/c mice with large 4T1 tumors (9-12 mm in diameter) were bled from the submandibular vein into 1ml of PBS containing 0.008% heparin. Red blood cells were removed by Gey's treatment as described (12). The remaining leukocytes were stained for Gr1 and CD11b and analyzed by flow cytometry. Populations that were >90%

$Gr1^+CD11b^+$ were used in experiments.

Isolation of tumor-infiltrating cells from solid tumors

Tumors were dissociated using a modified protocol from the Tissue Dissociation Kit (protocol 2.2.1; Miltenyi Biotech). 9-12 mm diameter tumors were excised from BALB/c mice, and minced with scissors into small pieces inside of GentleMACS C tubes containing DMEM media supplemented with 2,000U/ml DNase, 300U/ml collagenase, 0.1% hyaluronidase. Tumor chunks were then dissociated into single cell suspensions using a GentleMACS Dissociator (program m_imptumor _02;(Milltenyi Biotec) followed by rotation (10 rpm; Glas-Col Rotator) at 37°C for 40 minutes, and a second round of dissociation and rotation. Resulting cells were passed through 70μM filters, rinsed twice with PBS, resuspended in IMDM media, and then centrifuged on a Ficoll-Paque PLUS gradient at 1,230g (Eppendorf centrifuge 5810R) (20°C for 20 minutes). Tumor-infiltrating cells were harvested from the interphase of the gradient and then rinsed twice with PBS.

Starvation-induced autophagy

To induce autophagy cells were cultured in Hank's balanced salt solution (HBSS) for three hours or in Earl's balanced salt solution (EBSS) for four hours at 37°C in a 5% CO_2-95% air incubator. Non-starved control cell lines were maintained in their culture media under the same conditions as starved cells. Non-starved control MDSC were cultured in their growth medium (HL-1) without additional supplements.

MDSC viability

MDSC survival was assessed according to the procedure of (13). Briefly, MDSC from 4T1 tumor-bearing BALB/c mice were harvested and incubated in HL-1 with or without ethyl pyruvate (20mM) or diluent control (PBS) at 37°C in a 5% CO_2-95% air incubator. After one hour, MDSC were transferred to HBSS, returned to the incubator, and starved for three hours with or without ethyl pyruvate (20mM) or diluent control. In some experiments MDSC were incubated overnight in growth medium, or for four hours in EBSS with the autophagy inducer rapamycin (1μM), autophagy inhibitors chloroquine (5μM) or bafilomycin (0.1μM), or the respective diluent controls (water for chloroquine or DMSO for rapamycin and bafilomycin). Data were normalized so that the untreated sample represented 100% viability. Percent MDSC viability = [(experimental % viable)-(diluent control % viable-untreated % viable)].

Autophagy activity

4T1-induced MDSC, 4T1, Jurkat, and HeLa cells were starved for four hours in EBSS in the presence of ethyl pyruvate (20mM), bafilomycin (0.1μM), or their respective diluent controls (PBS for ethyl pyruvate; DMSO for bafilomycin). After starvation, autophagic vacuoles were detected by staining with cyto ID as per the manufacturer's protocol (Enzo Life Sciences). Data were normalized so that autophagy activity (mean channel fluorescence (MCF)) following starvation (EBSS only) = 100%. Percent autophagy activity = [$(\text{experimental}_{MCF}) - (\text{diluent control}_{MCF}\text{-untreated}_{MCF})$]. Fold increase in autophagy activity = $(\text{experimental}_{MCF})/(\text{tumor-free}_{MCF})$.

T cell activation

MDSC were isolated from 4T1-tumor-bearing BALB/c mice and starved in EBSS in the presence of rapamycin (1μM), chloroquine (5μM), bafilomycin (0.1μM), or the respective diluent control (water for chloroquine; DMSO for rapamycin and bafilomycin), and immediately used in T cell activation assays as previously described (12). Briefly, splenocytes from TCR-transgenic mice (1 x 10^5 cells) and irradiated (25 Gy) MDSC (2,1,0.5, or 0.25 x 10^5 cells) were co-cultured in flat bottom 96 well plates in 200μl HL-1 media containing 1% penicillin, 1% streptomycin, 1% glutamax, and 5 x 10^{-5} M β-mercaptoethanol/well. 14uM $OVA_{323-339}$ peptide or 28 μM $HA_{518-526}$ peptide was included for DO11.10 and clone4 cells, respectively. On day 3, 1μCi [^{3}H]-thymidine in 50μl medium was added to each well. Eighteen hours later the cells were harvested and [^{3}H]-thymidine incorporation was measured by scintillation counter. Data are expressed as cpm ± SD of triplicate cultures.

Western blots

Jurkat, HeLa, and 4T1 cells were harvested when 75% confluent. After harvesting, 1x10^7 cells were starved in 25 ml EBBS for four hours in the presence of ethyl pyruvate (10mM), rapamycin (1μM), chloroquine (500μM for 4T1 and 10μM for HeLa and Jurkat), bafilomycin (0.1μM), or the respective diluent controls (PBS for ethyl pyruvate, DMSO for rapamycin and bafilomycin, water for chloroquine). After starvation cells were rinsed with PBS and then lysed in 300μl of M-PERM protein extraction reagent (Thermo Scientific). 50 μg of whole cell lysate were then mixed with 6x sample buffer (0.375mM Tris HCl, 9% SDS, 50% glycerol, 0.03% bromophenol blue, and 9% β-

mercaptoethanol), boiled for five minutes at 95°C, and electrophoresed on 14% SDS-PAGE gels (SDS running buffer (BioRad), 150 volts, one hour)). Proteins were transferred to PVDF membranes (GE Healthcare) using a mini trans-blot cell (30 volts, BioRad transfer buffer, overnight). Membranes were blocked with 5% non-fat dried milk or 0.2% I block (Applied Biosystems) in TBST. LC3 was detected with anti-LC3B antibody (Novus; 1.4ug/ml in 7ml of 1% BSA/5% milk/TBS) followed by goat-anti-rabbit secondary antibody (Millipore) (40ng/ml in 10ml of 1% BSA/ 5% milk/TBS). p62 was detected with anti-p62 antibody (Novus; 22.8ng/ml in 10ml of 0.2% I Block/TBST) followed by goat-anti-rabbit secondary antibody (40ng/ml in 10ml of 5% milk/TBST). β-actin was detected with anti-β-actin antibody (Sigma; 50ng/ml in 10ml of 2.5% milk/TBST) followed by sheep-anti-mouse secondary antibody (Millipore; 40ng/ml in 10ml of 2.5% milk/TBST). Bands were visualized using an HRP detection kit on X-ray film (both from Denville Scientific, Inc).

Statistical analysis

Student's *t* test was used to determine statistical significance between two sets of data. p values <0.05 were considered significant. Single factor ANOVA was used to determine significance between groups of data.

Online Supplemental Material

HMGB1 promotes autophagy in 4T1 and HeLa cells as assessed by western blots and cyto ID immunofluorescence.

Results

Autophagy promotes MDSC survival

If MDSC survival is facilitated by autophagy, then inhibiting autophagy will reduce the viability of MDSC. To test this hypothesis, MDSC were obtained from the blood of BALB/c mice with large 4T1 tumors and cultured overnight in HL-1 medium. Autophagy inhibitors chloroquine and bafilomycin, the autophagy inducer, rapamycin (see **Figure 1**), or their diluent control solutions, were added to some cultures, and MDSC viability was assessed by staining cells for CD11b, Gr1, PI, and Annexin V (**Figure 2A**). Taking into account the effect of the diluents, chloroquine and bafilomycin reduced MDSC viability by 70% and 81% respectively, while rapamycin did not significantly alter MDSC viability. These results establish that under non-stressed conditions, MDSC utilize autophagy to enhance viability, and that the default condition of tumor-induced MDSC is as pro-autophagic cells.

To assess if MDSC in starved settings use autophagy to survive, MDSC were starved for four hours in serum- free EBSS medium to induce autophagy. The autophagy inhibitors chloroquine and bafilomycin reduced the viability of $CD11b^{+}Gr1^{+}$ gated MDSC by 12% and 22% respectively, while the autophagy inducer rapamycin increased MDSC viability by 7% (**Figure 2B**). These results demonstrate that MDSC utilize autophagy to survive in starvation conditions.

HMGB1 promotes MDSC survival

Our previous studies established that HMGB1 is ubiquitously present in the TME and drives both the accumulation of MDSC from bone marrow progenitor cells, and the

immune suppressive potency of MDSC, thereby identifying HMGB1 as a pro-inflammatory mediator in MDSC development and function (10). Studies by others demonstrated that HMGB1 facilitates the survival of tumor cells by converting them to an autophagic state (13). These findings led us to hypothesize that HMGB1 may sustain MDSC viability by promoting MDSC autophagy. If HMGB1 promotes MDSC autophagy, then inhibition of HMGB1 during conditions that drive MDSC autophagy will reduce MDSC viability. Since HMGB1 is constitutively released by MDSC (10, 14), we assessed this possibility by culturing MDSC under starvation conditions in the presence or absence of the HMGB1 inhibitor ethyl pyruvate which blocks the release of HMGB1 (14) (**Figure 3**). MDSC subjected to starvation-induced autophagy in the presence of ethyl pyruvate were 84% less viable than control-treated cells, demonstrating that HMGB1 enhances the survival of autophagic MDSC.

HMGB1 promotes autophagy in MDSC

To assess if HMGB1 enhances MDSC survival by inducing autophagy, MDSC autophagic flux was assessed by flow cytometry using the fluorescent dye cyto ID that stains autophagic vacuoles (see **Figure 1**). The dye is a cationic amphiphilic tracer that partitions into cells and stains pre-autophagosomes and autophagosomes. It interacts with hydrophobic lamellar structures of autophagic vacuoles and therefore co-localizes with LC3, which is an essential marker for autophagosomes (15, 16). Bafilomycin-induced inhibition of autophagy reduces cyto ID staining and thus serves as a control (17, 18).

If HMGB1 promotes autophagy in MDSC, then inhibition of HMGB1 under conditions that drive autophagy will decrease autophagy activity. To test this possibility,

MDSC were cultured under starvation conditions in the presence or absence of the autophagy inhibitor bafilomycin, or HMGB1 inhibitor ethyl pyruvate, and subsequently stained with cyto ID and analyzed by flow cytometry. Treatment with the autophagy inhibitor bafilomycin served as a control (**Figure 4A**). Autophagy activity of MDSC was reduced 53% when ethyl pyruvate was included in the cultures. A 65% reduction in autophagy activity was observed when bafilomycin was included instead of ethyl pyruvate. Therefore inhibition of HMGB1 and treatment with bafilomycin similarly reduce the level of autophagy in MDSC, demonstrating that HMGB1 regulates autophagic flux in MDSC.

Western blotting for the autophagy markers LC3 and p62 is conventionally used to assess autophagy. We have used cyto ID and flow cytometry for the MDSC studies because cyto ID staining is more sensitive and MDSC material is limiting. To confirm that cyto ID staining concurs with western blotting analysis, cultured cell lines were analyzed in parallel by cyto ID staining and western blotting. Jurkat cells were either starved or not starved and treated with the autophagy inducer rapamycin, the autophagy inhibitors bafilomycin and chloroquine, or ethyl pyruvate, and subsequently analyzed by western blot for the autophagic markers LC3 and p62 (**Figure 4B**) or by cyto ID and flow cytometry (**Figure 4C**). As seen in the western blots, induction of autophagy by either starvation or treatment with rapamycin caused the turnover of LC3-I and the degradation of p62, indicative of increased autophagy. Inhibition of autophagy by bafilomycin or chloroquine blocked the turnover of LC3-II, causing accumulation of LC3-II, and prevented the degradation of p62, indicative of reduced autophagy. Cyto ID staining

similarly showed decreased autophagy in Jurkat cells following treatment with bafilomycin.

The cyto ID results with MDSC indicated that the HMGB1 inhibitor ethyl pyruvate reduced autophagy. To confirm this observation, Jurkat cells were starved or not starved in the presence or absence of ethyl pyruvate and in parallel analyzed by western blot (**Figure 4B**) and cyto ID flow cytometry (**Figure 4C**). As seen in the western blot, ethyl pyruvate reduced the accumulation of LC3-I and blocked the conversion of LC3-I into LC3-II in Jurkat cells, characteristics of autophagic flux. In contrast, p62 levels were not different in ethyl pyruvate-treated starved cells compared to untreated, not starved cells. Cyto ID staining similarly showed reduced autophagy in ethyl pyruvate-treated Jurkat cells, thus demonstrating the concurrence of the western blot and cyto ID techniques. Since p62 changes occur after LC3 degradation, the western blot analyses demonstrate that HMGB1 acts early to inhibit autophagy. This finding is consistent with the function of ethyl pyruvate which is to prevent the release of HMGB1 and thereby block autophagy at its onset.

To further confirm the concurrence of cyto ID and western blotting analyses, two additional tissue culture cell lines were tested. Murine 4T1 mammary carcinoma cells (**Supp Figure 1A**) and human HeLa cells (**Supp Figure 1B**) were starved or not starved and treated with rapamycin, bafilomycin, chloroquine, or ethyl pyruvate, and assayed in parallel by western blotting and flow cytometry. 4T1 and HeLa cells gave similar results as shown for Jurkat cells, further supporting the validity of the cyto ID findings for MDSC. Collectively, the cyto ID and western studies demonstrate that HMGB1 promotes autophagy in Jurkat, 4T1, and HeLa cells, as well as in tumor-induced MDSC.

Autophagy reduces MDSC suppressive potency

Suppression of T cell activation is the hallmark function of MDSC (8). To determine if autophagic status affects suppressive function, MDSC were not starved or starved, and treated with the autophagy inhibitors bafilomycin or chloroquine prior to their incubation with antigen-specific $CD4^+$ or $CD8^+$ transgenic T cells and cognate peptide (**Figure 5**). Treatment with either chloroquine or bafilomycin increased MDSC suppressive potency, indicating that autophagy reduces the suppressive activity of MDSC.

The tumor microenvironment promotes autophagy in MDSC

To confirm the in vitro autophagy findings in the tumor microenvironment, cells were isolated from the blood of tumor-free and 4T1 tumor-bearing BALB/c mice, and from 4T1 primary tumors of BALB/c mice, and stained with antibodies to CD45, CD11b, and Gr1, and cyto ID. Relative autophagy activity of gated $CD45^+CD11b^+Gr1^+$ cells was then determined using MDSC from the blood of tumor-free mice as the reference point (**Figure 6**). MDSC from the blood of tumor-bearing mice express elevated levels of autophagy activity compared to MDSC from tumor-free mice, while tumor-infiltrating MDSC are the most autophagic. These results demonstrate that the tumor microenvironment enhances autophagy in MDSC.

Discussion

MDSC are profoundly immune suppressive cells that promote tumor progression by inhibiting anti-tumor immunity. In solid tumors they mediate many of their effects while residing in a tumor microenvironment that challenges their survival due to less than optimal growth conditions. The ability of MDSC to survive under these harsh conditions is likely due to multiple adaptations. Here, we demonstrate that one of the adaptations invoked by tumor-induced MDSC is to become autophagic and thereby avoid apoptosis, resulting in an increase in MDSC survival. This condition is mediated by the alarmin and DAMP, HMGB1, which is ubiquitously present in solid tumors.

Various apoptotic mechanisms have been implicated in MDSC survival. MDSC express the death receptor Fas and can be killed by FasL-expressing activated T cells (19). Inflammation in tumor-bearing mice increases MDSC levels (20, 21) by rendering them more resistant to Fas-FasL-mediated apoptosis (22, 23). Signaling through TNF receptor 2 drives MDSC survival by increasing cellular FLICE-inhibitory protein (c-FLIP). c-FLIP in turn inhibits the activation of caspase 8 thereby disrupting apoptosis (24). Activation through the IL-4Rα (CD124), which is expressed on some MDSC, has also been implicated in extending MDSC survival by inhibiting STAT6 phosphorylation and blocking MDSC apoptosis (25). MDSC survival is also regulated by the transcription factor IRF8 (26, 27). MDSC down-regulate IRF8 which modulates expression of the anti-apoptotic molecules Bax and Bcl-xL, thereby preventing apoptosis. Whether any of these effector molecules or transcription factors are regulated by HMGB1 or vice-versa, or whether HMGB1 identifies a distinct regulatory pathway remains to be determined.

Autophagy has not previously been examined as a mechanism for sustaining the survival of MDSC, yet many of the conditions and effector molecules that are known to facilitate MDSC survival can be linked to autophagy. For example, hypoxia, an established inducer of autophagy (28), promotes MDSC survival by redirecting MDSC in the TME towards a tumor-associated macrophage phenotype (29). Reactive oxygen species (ROS), a family of effector molecules that regulate autophagy (30), also drive MDSC accumulation and survival. ROS mediate their effects by regulating the cellular stress sensor C/EBP homologous protein (CHOP) in MDSC (31), and activation of CHOP has been linked to autophagy in that CHOP promotes increased transcription of essential autophagy proteins Atg5 and LC3 (32). ER stress also induces autophagy (33, 34), and ER stress regulates MDSC half-life by controlling TRAIL receptor expression on MDSC (35). Therefore, autophagy may be a unifying mechanism by which many MDSC inducers increase MDSC quantity and half-life.

Many of the conditions that have the potential to induce autophagy are present in the TME and are linked to HMGB1, so it is not unexpected that HMGB1 regulates the survival of MDSC by driving autophagy. For example, the TME of solid tumors is frequently an inflammatory environment, and inflammation promotes autophagy (36). HMGB1 is one of the pro-inflammatory molecules that contributes to the inflammatory milieu and HMGB1 drives the accumulation of MDSC (10). MDSC themselves release ROS and ROS are common within solid tumors. ROS promotes the extracellular release of HMGB1 (37) and HMGB1 release is enhanced by autophagy (13). Given the prevalence of ROS and HMGB1 in the TME, it is likely that tumor-induced MDSC are pro-autophagic as a result of exposure to these two molecules.

Conditions in the TME, including inflammation and hypoxia promote autophagy (30, 38, 39) and MDSC suppressive potency (9, 29, 40, 41). Since tumor-infiltrating MDSC have heightened suppressor function relative to circulating MDSC (19, 29), our finding that autophagy decreases MDSC function appears to be contradictory. This apparent inconsistency could be due to other factors in the TME that drive MDSC potency and over-ride the effects of autophagy on MDSC function. Metabolism and the use of energy could possibly explain the increase in MDSC suppressive potency when autophagy is blocked. Chloroquine and bafilomycin, the reagents used here to inhibit autophagy and increase MDSC-mediated suppression, block lysosomal acidification and autophagosome-lysosome fusion, thus limiting protein degradation (42). Under these conditions the energy expended on protein degradation might be redirected and used to drive immune suppressive functions.

The role of autophagy in promoting tumor progression is well established and has been attributed to its ability to increase the survival of tumor cells (3, 43). The studies reported here demonstrate that autophagy also supports tumor progression by sustaining the survival of MDSC. Therefore autophagy not only enhances tumor progression due to direct impact on tumor cells, but also by facilitating tumor-induced immune suppression and inhibiting anti-tumor immunity.

Figures

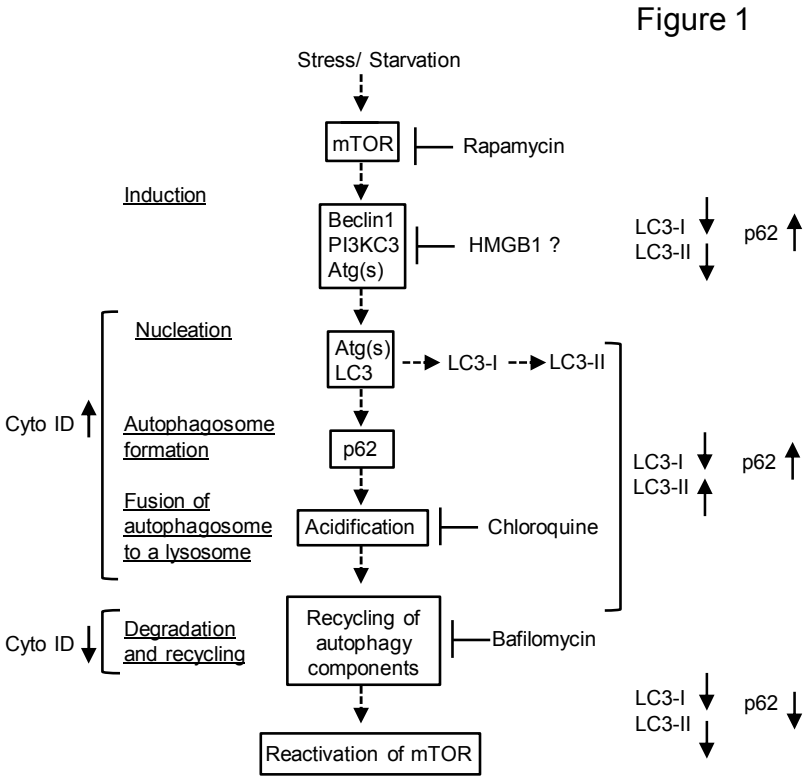

Figure 1: Autophagic flux. Autophagy is initiated by inhibition of mTOR which is caused by stress, starvation, or treatment with rapamycin. Following inactivation of mTOR, Beclin1, PI3KC3 and Atg proteins are activated and nucleation occurs with the assistance of additional Atg proteins. LC3 is then modified to give rise to LC3-1 which generates LC3-II and aids in forming the double membraned autophagosome. The autophagosome contains adaptor proteins such as p62 which aid in targeting cargo proteins. An autophagosome will mature into an autolysosome following fusion with a lysosome, creating an acidic internal environment. The acidic environment of the autolysosome allows for degradation and recycling of autophagosome components,

eventually leading to the reactivation of mTOR once stress/starvation are resolved. Autophagic flux can be monitored in live cells using a cyto ID stain (left side), or by western blot analysis of LC3 and p62 (right side). Chloroquine and bafilomycin block autophagy at the acidification and recycling stages, respectively. ↓ indicates molecules that are down-regulated; ↑ indicates molecules that are up-regulated; ⇣ indicates the direction of events in autophagy.

Figure 2

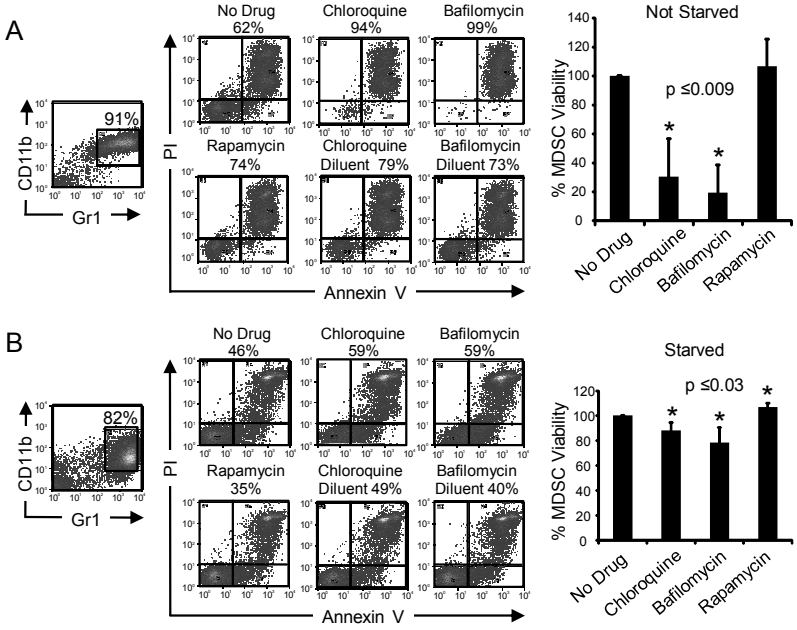

Figure 2: Autophagy promotes MDSC survival. (A) MDSC were obtained from the blood of 4T1 tumor-bearing BALB/c mice and an aliquot was assessed for purity by flow cytometry analysis of Gr1 and CD11b expression (left panel). MDSC were incubated overnight under non-starvation conditions (HL-1 medium) in the presence or absence of autophagy inhibitors chloroquine (5μM) or bafilomycin (0.1μM), autophagy inducer rapamycin (1μM), or the respective diluent controls. After incubation, MDSC were stained for Gr1, CD11b, Annexin V, and PI, and the gated $Gr1^{+}CD11b^{+}$ cells analyzed

for Annexin V and PI. Staining of MDSC from an individual mouse (left -side histograms); average percent MDSC viability for three mice (right-side graphs). (**B**) MDSC were obtained and treated as in (A), except, cells were incubated for four hours under starvation conditions (EBSS medium). * indicates statistical significant difference compared to non-treated samples. p values were obtained by Student's *t* test. Data were normalized so that the no treatment (A) or no drug (B) control groups were 100% viability. Flow cytometry profiles are from one of three independent experiments, Graphs are averaged from three independent experiments.

Figure 3

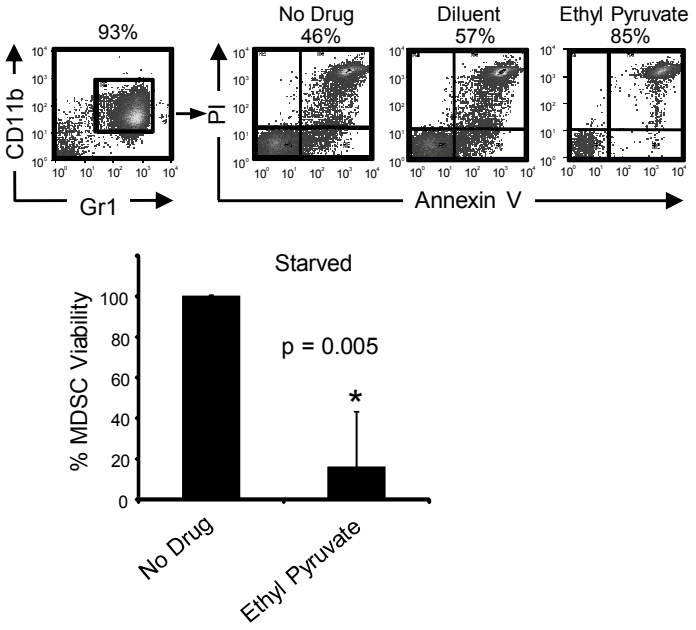

Figure 3: HMGB1 promotes MDSC survival. MDSC were obtained from the blood of 4T1 tumor-bearing BALB/c mice and an aliquot was assessed for purity by flow cytometry analysis of Gr1 and CD11b expression (top left histogram). MDSC were incubated for one hour in HL-1 medium in the presence or absence of the HMGB1 inhibitor ethyl pyruvate (20mM) or diluent control (PBS), and subsequently starved in HBSS for three hours with or without ethyl pyruvate or diluent control. After incubation MDSC were stained and analyzed as in figure 2. PI and Annexin V staining of MDSC from a representative individual mouse (top histograms); average percent MDSC viability for three mice (bottom). * indicates statistical significant difference compared to starved samples. p values were obtained by Student's *t* test. Data were normalized so that the no treatment control group was 100% viability. Flow profiles are from one of three

independent experiments. Graph represents the average from three independent experiments.

Figure 4

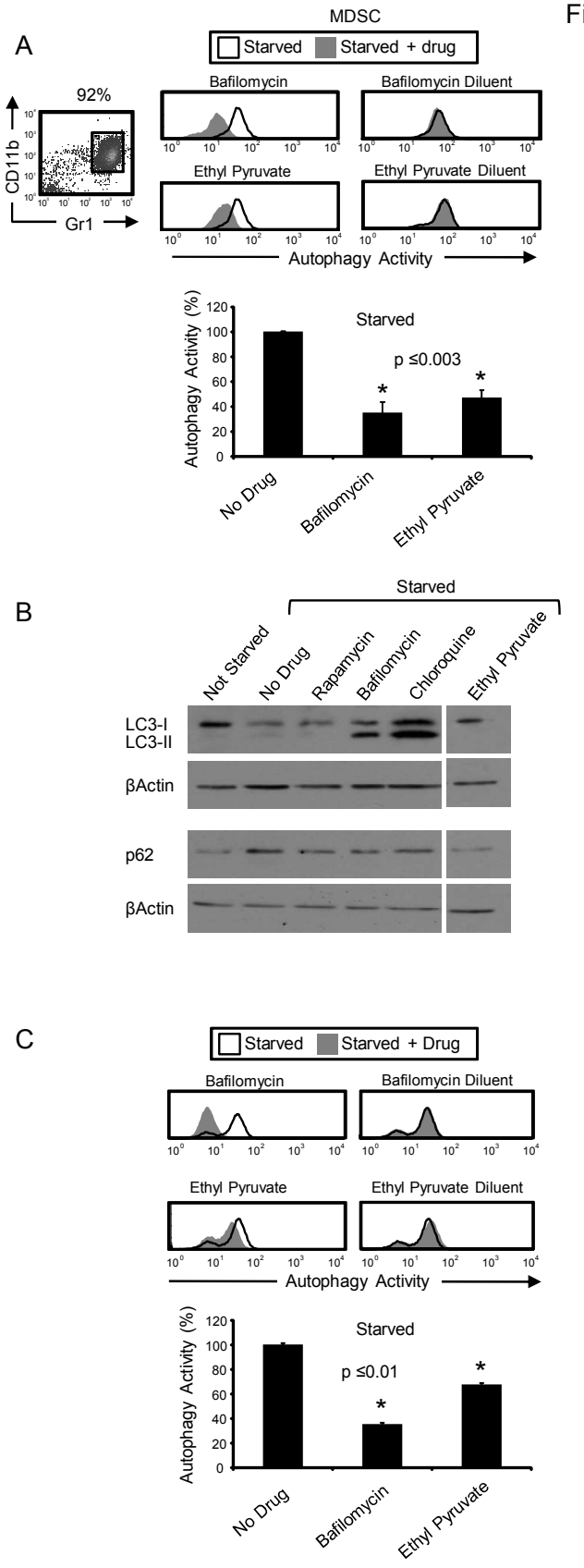
A
MDSC
Starved
Starved + drug
92%
CD11b
Gr1
Bafilomycin
Bafilomycin Diluent
Ethyl Pyruvate
Ethyl Pyruvate Diluent
Autophagy Activity
Autophagy Activity (%)
Starved
p ≤0.003
No Drug
Bafilomycin
Ethyl Pyruvate
B
Starved
Not Starved
No Drug
Rapamycin
Bafilomycin
Chloroquine
Ethyl Pyruvate
LC3-I
LC3-II
βActin
p62
βActin
C
Starved
Starved + Drug
Bafilomycin
Bafilomycin Diluent
Ethyl Pyruvate
Ethyl Pyruvate Diluent
Autophagy Activity
Autophagy Activity (%)
Starved
p ≤0.01
No Drug
Bafilomycin
Ethyl Pyruvate

Figure 4: HMGB1 promotes autophagy in MDSC. (A) MDSC were obtained from the blood of 4T1 tumor-bearing BALB/c mice and an aliquot was assessed for purity by flow cytometry analysis of Gr1 and CD11b (top left histogram). MDSC were incubated in EBSS for four hours in the presence of autophagy inhibitor bafilomycin (0.1μM), HMGB1 inhibitor ethyl pyruvate (20mM), or the respective diluent controls. After incubation, MDSC were stained for Gr1 and CD11b and with cyto ID, and the gated $Gr1^+CD11b^+$ cells were analyzed by flow cytometry for cyto ID expression. Cyto ID staining for MDSC from a representative individual mouse (top right histograms); average percent MDSC autophagy activity for three mice (bottom graph). **(B)** Jurkat cells were not starved or starved and treated with rapamycin (1μM), bafilomycin (0.1μM), chloroquine (10μM), or ethyl pyruvate (10mM), lysed, and assessed by western blot for LC3, p62, and β-actin expression. **(C)** Jurkat cells were starved, treated, and stained as in (A). Cyto ID staining on an individual sample of Jurkat cells (top histograms); average percent autophagy activity for three independent samples (bottom). * indicates statistical significant difference compared to starved samples. p values were obtained by Student's *t* test. Data were normalized so the starved control group is 100% autophagy activity. Data are from one of five, three, and two independent experiments for A, B, and C, respectively.

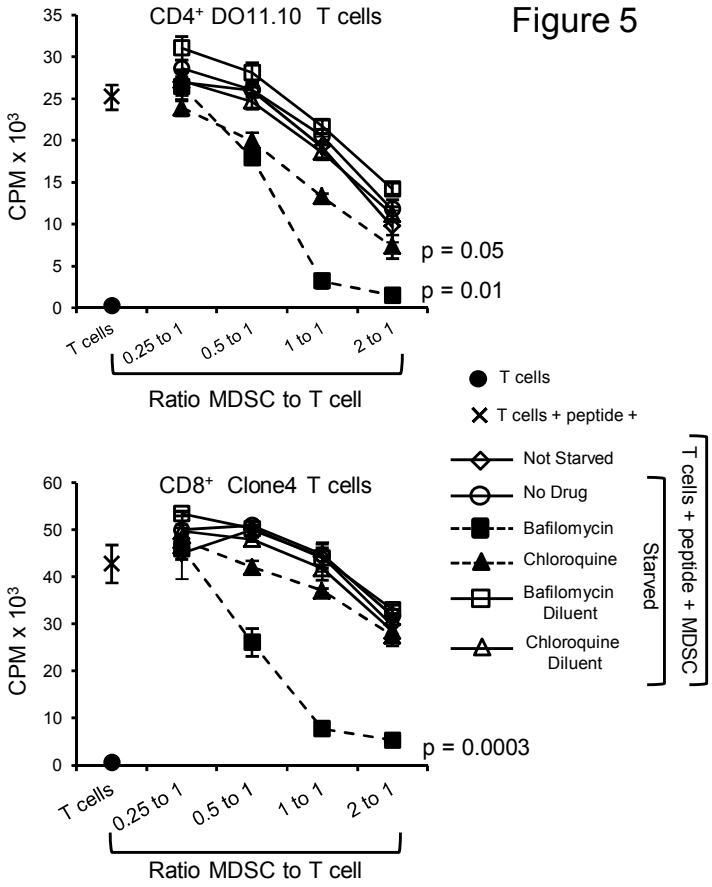

Figure 5: Autophagy decreases MDSC-mediated suppression of antigen-activated T-cells. MDSC (>87% $Gr1^+CD11b^+$) were obtained from the blood of 4T1 tumor-bearing BALB/c mice and not starved, or starved in the presence of autophagy inhibitors chloroquine (5μM) or bafilomycin (1μM), or the respective diluent controls. After starvation MDSC were rinsed with PBS and then irradiated prior to being cultured with splenocytes. Splenocytes from $CD4^+$ DO11.10 (Top) or $CD8^+$ clone4 (bottom) TCR transgenic mice were co-cultured with irradiated 4T1-induced MDSC and cognate peptide (OVA or HA peptide for DO11.10 and clone 4 T cells, respectively). T cell proliferation was measured by [^{3}H]-thymidine incorporation. * indicates statistical

significant difference compared to starved samples as assessed by single factor ANOVA. Data are from one of two independent experiments.

Figure 6

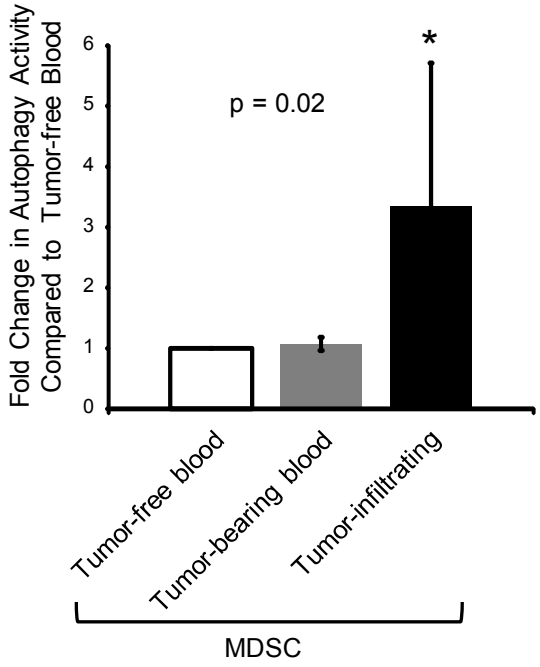

Figure 6: The tumor microenvironment promotes autophagy in MDSC. Cells were obtained from the blood of tumor-free BALB/c mice or from the blood and tumors of 4T1 tumor-bearing (tumor-infiltrating) BALB/c mice. Cells were stained for CD45, Gr1, and CD11b along with cyto ID, and the gated $CD45^{+}Gr1^{+}CD11b^{+}$ cells (MDSC) were analyzed by flow cytometry for cyto ID expression. Data are the average fold change in autophagy activity compared to the naïve blood sample. * indicates statistical significant difference compared to tumor-free samples. p values were obtained by Student's *t* test. Data are averaged from seven mice in three independent experiments.

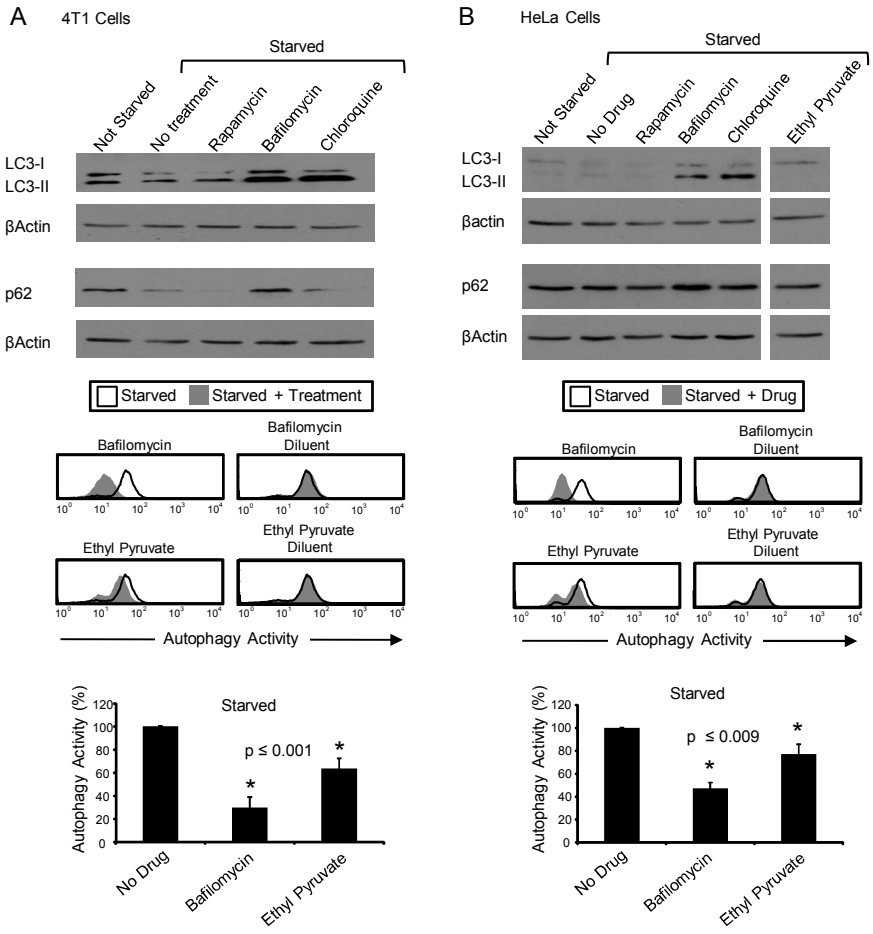

Supplemental Figure 1: HMGB1 promotes autophagy in 4T1 and HeLa cells. (A) upper panel: 4T1 cells were not starved or starved for four hours in the presence of rapamycin (1μM), bafilomycin (0.1μM), or chloroquine (500μM), and subsequently lysed, and analyzed by western blot for LC3, p62, and β-actin. Middle panel: 4T1 cells were starved in the presence of bafilomycin (0.1μM), ethyl pyruvate (20mM), or the respective diluent controls, followed by staining with cyto ID. 4T1 cells from an individual mouse (left histograms); bottom panel: average percent autophagy activity for three mice (bottom histograms and graph). **(B)** upper panel: HeLa cells were treated and analyzed by western blot as in (A), except that cells were also incubated with ethyl pyruvate (10mM). Middle and bottom panels: HeLa cells were starved as in (A) and assessed for autophagy by cyto ID staining. * indicates statistical significant difference compared to starved samples. Data are from one of three independent experiments for each cell line for the cyto ID staining, and one of two independent experiments for the westerns.

References

1. Balkwill, F., and A. Mantovani. 2001. Inflammation and cancer: back to Virchow? *Lancet* 357: 539-545.
2. White, E. 2012. Deconvoluting the context-dependent role for autophagy in cancer. *Nat Rev Cancer* 12: 401-410.
3. Yang, X., D. D. Yu, F. Yan, Y. Y. Jing, Z. P. Han, K. Sun, L. Liang, J. Hou, and L. X. Wei. 2015. The role of autophagy induced by tumor microenvironment in different cells and stages of cancer. *Cell Biosci* 5: 14.
4. Lum, J. J., D. E. Bauer, M. Kong, M. H. Harris, C. Li, T. Lindsten, and C. B. Thompson. 2005. Growth factor regulation of autophagy and cell survival in the absence of apoptosis. *Cell* 120: 237-248.
5. Tang, D., R. Kang, C. B. Coyne, H. J. Zeh, and M. T. Lotze. 2012. PAMPs and DAMPs: signal 0s that spur autophagy and immunity. *Immunol Rev* 249: 158-175.
6. Yorimitsu, T., and D. J. Klionsky. 2005. Autophagy: molecular machinery for self-eating. *Cell Death Differ* 12 Suppl 2: 1542-1552.
7. Quail, D. F., and J. A. Joyce. 2013. Microenvironmental regulation of tumor progression and metastasis. *Nat Med* 19: 1423-1437.
8. Gabrilovich, D. I., S. Ostrand-Rosenberg, and V. Bronte. 2012. Coordinated regulation of myeloid cells by tumours. *Nat Rev Immunol* 12: 253-268.
9. Ostrand-Rosenberg, S., and P. Sinha. 2009. Myeloid-derived suppressor cells: linking inflammation and cancer. *J Immunol* 182: 4499-4506.
10. Parker, K. H., P. Sinha, L. A. Horn, V. K. Clements, H. Yang, J. Li, K. J. Tracey, and S. Ostrand-Rosenberg. 2014. HMGB1 enhances immune suppression by

facilitating the differentiation and suppressive activity of myeloid-derived suppressor cells. *Cancer Res* 74: 5723-5733.

11. Tang, D., R. Kang, K. M. Livesey, C. W. Cheh, A. Farkas, P. Loughran, G. Hoppe, M. E. Bianchi, K. J. Tracey, H. J. Zeh, and M. T. Lotze. 2010. Endogenous HMGB1 regulates autophagy. *J Cell Biol* 190: 881-892.

12. Sinha, P., V. K. Clements, and S. Ostrand-Rosenberg. 2005. Reduction of myeloid-derived suppressor cells and induction of M1 macrophages facilitate the rejection of established metastatic disease. *J Immunol* 174: 636-645.

13. Tang, D., R. Kang, C. W. Cheh, K. M. Livesey, X. Liang, N. E. Schapiro, R. Benschop, L. J. Sparvero, A. A. Amoscato, K. J. Tracey, H. J. Zeh, and M. T. Lotze. 2010. HMGB1 release and redox regulates autophagy and apoptosis in cancer cells. *Oncogene* 29: 5299-5310.

14. Ulloa, L., M. Ochani, H. Yang, M. Tanovic, D. Halperin, R. Yang, C. J. Czura, M. P. Fink, and K. J. Tracey. 2002. Ethyl pyruvate prevents lethality in mice with established lethal sepsis and systemic inflammation. *Proc Natl Acad Sci U S A* 99: 12351-12356.

15. Guo, S., Y. Liang, S. F. Murphy, A. Huang, H. Shen, D. F. Kelly, P. Sobrado, and Z. Sheng. 2015. A rapid and high content assay that measures cyto-ID-stained autophagic compartments and estimates autophagy flux with potential clinical applications. *Autophagy* 11: 560-572.

16. Oeste, C. L., E. Seco, W. F. Patton, P. Boya, and D. Pérez-Sala. 2013. Interactions between autophagic and endo-lysosomal markers in endothelial cells. *Histochem Cell Biol* 139: 659-670.

17. Luu, K. Response Profiles of Known Autophagy - Modulators Across Multiple Cell Lines. W. Luty, ed, Life Sciences.

18. Porter, K., J. Nallathambi, Y. Lin, and P. B. Liton. 2013. Lysosomal basification and decreased autophagic flux in oxidatively stressed trabecular meshwork cells: implications for glaucoma pathogenesis. *Autophagy* 9: 581-594.

19. Sinha, P., O. Chornoguz, V. K. Clements, K. A. Artemenko, R. A. Zubarev, and S. Ostrand-Rosenberg. 2011. Myeloid-derived suppressor cells express the death receptor Fas and apoptose in response to T cell-expressed FasL. *Blood* 117: 5381-5390.

20. Bunt, S. K., L. Yang, P. Sinha, V. K. Clements, J. Leips, and S. Ostrand-Rosenberg. 2007. Reduced inflammation in the tumor microenvironment delays the accumulation of myeloid-derived suppressor cells and limits tumor progression. *Cancer Res* 67: 10019-10026.

21. Bunt, S. K., P. Sinha, V. K. Clements, J. Leips, and S. Ostrand-Rosenberg. 2006. Inflammation induces myeloid-derived suppressor cells that facilitate tumor progression. *J Immunol* 176: 284-290.

22. Chornoguz, O., L. Grmai, P. Sinha, K. A. Artemenko, R. A. Zubarev, and S. Ostrand-Rosenberg. 2011. Proteomic pathway analysis reveals inflammation increases myeloid-derived suppressor cell resistance to apoptosis. *Mol Cell Proteomics* 10: M110.002980.

23. Ostrand-Rosenberg, S., P. Sinha, O. Chornoguz, and C. Ecker. 2012. Regulating the suppressors: apoptosis and inflammation govern the survival of tumor-induced

myeloid-derived suppressor cells (MDSC). *Cancer Immunol Immunother* 61: 1319-1325.

24. Zhao, X., L. Rong, X. Li, X. Liu, J. Deng, H. Wu, X. Xu, U. Erben, P. Wu, U. Syrbe, J. Sieper, and Z. Qin. 2012. TNF signaling drives myeloid-derived suppressor cell accumulation. *J Clin Invest* 122: 4094-4104.

25. Roth, F., A. C. De La Fuente, J. L. Vella, A. Zoso, L. Inverardi, and P. Serafini. 2012. Aptamer-mediated blockade of IL4Rα triggers apoptosis of MDSCs and limits tumor progression. *Cancer Res* 72: 1373-1383.

26. Waight, J. D., C. Netherby, M. L. Hensen, A. Miller, Q. Hu, S. Liu, P. N. Bogner, M. R. Farren, K. P. Lee, K. Liu, and S. I. Abrams. 2013. Myeloid-derived suppressor cell development is regulated by a STAT/IRF-8 axis. *J Clin Invest* 123: 4464-4478.

27. Messmer, M. N., C. S. Netherby, D. Banik, and S. I. Abrams. 2015. Tumor-induced myeloid dysfunction and its implications for cancer immunotherapy. *Cancer Immunol Immunother* 64: 1-13.

28. Bellot, G., R. Garcia-Medina, P. Gounon, J. Chiche, D. Roux, J. Pouysségur, and N. M. Mazure. 2009. Hypoxia-induced autophagy is mediated through hypoxia-inducible factor induction of BNIP3 and BNIP3L via their BH3 domains. *Mol Cell Biol* 29: 2570-2581.

29. Corzo, C. A., T. Condamine, L. Lu, M. J. Cotter, J. I. Youn, P. Cheng, H. I. Cho, E. Celis, D. G. Quiceno, T. Padhya, T. V. McCaffrey, J. C. McCaffrey, and D. I. Gabrilovich. 2010. HIF-1α regulates function and differentiation of myeloid-

derived suppressor cells in the tumor microenvironment. *J Exp Med* 207: 2439-2453.

30. Scherz-Shouval, R., and Z. Elazar. 2011. Regulation of autophagy by ROS: physiology and pathology. *Trends Biochem Sci* 36: 30-38.

31. Thevenot, P. T., R. A. Sierra, P. L. Raber, A. A. Al-Khami, J. Trillo-Tinoco, P. Zarreii, A. C. Ochoa, Y. Cui, L. Del Valle, and P. C. Rodriguez. 2014. The stress-response sensor chop regulates the function and accumulation of myeloid-derived suppressor cells in tumors. *Immunity* 41: 389-401.

32. Rouschop, K. M., T. van den Beucken, L. Dubois, H. Niessen, J. Bussink, K. Savelkouls, T. Keulers, H. Mujcic, W. Landuyt, J. W. Voncken, P. Lambin, A. J. van der Kogel, M. Koritzinsky, and B. G. Wouters. 2010. The unfolded protein response protects human tumor cells during hypoxia through regulation of the autophagy genes MAP1LC3B and ATG5. *J Clin Invest* 120: 127-141.

33. Ogata, M., S. Hino, A. Saito, K. Morikawa, S. Kondo, S. Kanemoto, T. Murakami, M. Taniguchi, I. Tanii, K. Yoshinaga, S. Shiosaka, J. A. Hammarback, F. Urano, and K. Imaizumi. 2006. Autophagy is activated for cell survival after endoplasmic reticulum stress. *Mol Cell Biol* 26: 9220-9231.

34. Yorimitsu, T., U. Nair, Z. Yang, and D. J. Klionsky. 2006. Endoplasmic reticulum stress triggers autophagy. *J Biol Chem* 281: 30299-30304.

35. Condamine, T., V. Kumar, I. R. Ramachandran, J. I. Youn, E. Celis, N. Finnberg, W. S. El-Deiry, R. Winograd, R. H. Vonderheide, N. R. English, S. C. Knight, H. Yagita, J. C. McCaffrey, S. Antonia, N. Hockstein, R. Witt, G. Masters, T. Bauer,

and D. I. Gabrilovich. 2014. ER stress regulates myeloid-derived suppressor cell fate through TRAIL-R-mediated apoptosis. *J Clin Invest* 124: 2626-2639.

36. Mathew, R., V. Karantza-Wadsworth, and E. White. 2007. Role of autophagy in cancer. *Nat Rev Cancer* 7: 961-967.

37. Tang, D., R. Kang, K. M. Livesey, H. J. Zeh, and M. T. Lotze. 2011. High mobility group box 1 (HMGB1) activates an autophagic response to oxidative stress. *Antioxid Redox Signal* 15: 2185-2195.

38. Joven, J., M. Guirro, R. Mariné-Casadó, E. Rodríguez-Gallego, and J. A. Menéndez. 2014. Autophagy is an inflammation-related defensive mechanism against disease. *Adv Exp Med Biol* 824: 43-59.

39. Martinez-Outschoorn, U. E., C. Trimmer, Z. Lin, D. Whitaker-Menezes, B. Chiavarina, J. Zhou, C. Wang, S. Pavlides, M. P. Martinez-Cantarin, F. Capozza, A. K. Witkiewicz, N. Flomenberg, A. Howell, R. G. Pestell, J. Caro, M. P. Lisanti, and F. Sotgia. 2010. Autophagy in cancer associated fibroblasts promotes tumor cell survival: Role of hypoxia, HIF1 induction and NFκB activation in the tumor stromal microenvironment. *Cell Cycle* 9: 3515-3533.

40. Lu, T., and D. I. Gabrilovich. 2012. Molecular pathways: tumor-infiltrating myeloid cells and reactive oxygen species in regulation of tumor microenvironment. *Clin Cancer Res* 18: 4877-4882.

41. Lu, T., R. Ramakrishnan, S. Altiok, J. I. Youn, P. Cheng, E. Celis, V. Pisarev, S. Sherman, M. B. Sporn, and D. Gabrilovich. 2011. Tumor-infiltrating myeloid cells induce tumor cell resistance to cytotoxic T cells in mice. *J Clin Invest* 121: 4015-4029.

42. Tanida, I., N. Minematsu-Ikeguchi, T. Ueno, and E. Kominami. 2005. Lysosomal turnover, but not a cellular level, of endogenous LC3 is a marker for autophagy. *Autophagy* 1: 84-91.

43. Fung, C., R. Lock, S. Gao, E. Salas, and J. Debnath. 2008. Induction of autophagy during extracellular matrix detachment promotes cell survival. *Mol Biol Cell* 19: 797-806.

Chapter 4: Discussion

Introduction

The goal of this dissertation was to investigate whether a master upstream regulator of inflammation exists, since it is well appreciated that inflammation plays a large role in promoting immune suppression and immune suppression has such a profound inhibitory impact on immunotherapy.

Almost a decade ago, the connection between MDSC and inflammation was established when it was found that the pro-inflammatory cytokines IL-1β, IL-6 and PGE_2 promote MDSC accumulation and suppressive function (1-4). Subsequent studies demonstrated that additional pro-inflammatory cytokines and DAMPs, including but not limited to C5a, PGE_2, COX_2, VEGF, GM-CSF, G-CSF, IL-1β, IL-6, IL-17, IDO, S100A8/A9, C/EBPβ, and chop, also drive MDSC (1-14).

Various pro-inflammatory mediators that have been shown to encourage MDSC accumulation and function are induced by HMGB1, including IL-1β (1, 2, 15). Three other pro-inflammatory mediators that drive MDSC – IL-6, TNF-α, and PGE_2 (3, 4, 16, 17) – are also induced by HMGB1 (18-20).

In addition to HMGB1's pro-inflammatory properties, it also promotes tumor progression through direct interaction with tumor cells as well as induction of immune suppressive Tregs and TAMs. HMGB1 can enhance tumor progression by binding to

tumor cell expressed RAGE, which induces autophagy, inhibits apoptosis, and increases tumor cell invasiveness (21, 22). The association between HMGB1 and RAGE has also been linked to angiogenesis and metastasis, as blockade of either of these molecules impairs tumor angiogenesis and metastasis (23, 24). Furthermore, HMGB1 can promote tumor cell proliferation and invasion by increasing ATP production (25). HMGB1 induces the accumulation of immune suppressive Tregs and the induction of a pro-tumor environment (26, 27). TAM accumulation is promoted by tumor-infiltrating T cells expressing lymphotoxinα1β2, which is induced by HMGB1 (28). Therefore, given HMGB1's ability to induce inflammation and regulate several inflammatory inducers of MDSC, combined with its ability to induce immune suppression, we hypothesized that HMGB1 is an upstream regulator of inflammatory molecules that promote MDSC.

Summary of the major findings

The major findings reported here establish HMGB1 as an inducer of MDSC differentiation, accumulation, and immune suppressive functions. Therefore, HMGB1 contributes to the elevation and suppressive potency of MDSC in tumor-bearing mice and suggests that this pro-inflammatory mediator can be targeted to regulate MDSC. Identifying HMGB1 as a major regulator of tumor-induced immune suppression led to deciphering the way HMGB1 is able to regulate MDSC differentiation and accumulation.

It is well appreciated that HMGB1 helps to maintain tumor cell survival by promoting autophagy in tumor cells. Autophagy had not been previously examined as a

promoter of MDSC survival; however, data described here establish autophagy as an enhancer of tumor-induced immune suppression through the promotion of MDSC survival. HMGB1 induces autophagy activity in MDSC. It is not surprising that tumor-infiltrating MDSC exhibit elevated levels of autophagy activity as there is an increased presence of inflammatory inducers in the TME, including HMGB1.

Questions left unaddressed and limitations to answering these questions.

What receptor(s) on MDSC are responsible for HMGB1 mediated signaling?

As mentioned in the introduction (Chapter 1 section H6), HMGB1 can signal through a multitude of receptors. This dissertation has not assessed if HMGB1 signaling occurs in MDSC in response to a specific receptor. However, if a specific receptor could be identified as being responsible for HMGB1 signaling in MDSC, then this would supply another avenue for targeting MDSC.

Literature supports the pro-inflammatory effect of HMGB1 associating with TLR4 or RAGE, and interestingly, several of these interactions have a tumor-promoting effect. The interaction between HMGB1 and RAGE on tumor cells induces autophagy, inhibits apoptosis, promotes angiogenesis, and increases tumor cell invasiveness (21-24). Blockade of RAGE binding in tumor-bearing mice is able to reduce the levels of MDSC in the circulating blood and secondary lymphoid organs (12). Therefore, RAGE is an established pro-tumor receptor that possibly drives MDSC accumulation.

HMGB1 signaling through TLR4 on macrophages promotes the release of pro-inflammatory cytokines including IL-1β, IL-6, MIP-2, and IL-10 (29). In DC, HMGB1 signaling through TLR4 stimulates their activation and maturation (30). TLR4 signaling in MDSC is responsible for IL-10 production and MDSC-macrophage crosstalk interactions (31). Therefore, TLR4 is a critical immune receptor that regulates MDSC-macrophage cross-talk. Additionally, expression of CXCR4 in human MDSC has been shown to regulate MDSC accumulation in an ovarian cancer model (32). However, a connection has not been made with mouse MDSC as of yet. While other receptors are expressed by immune cells and mediate HMGB1 signaling, including TLR2, TLR9, and CD24, none of these receptors have been connected to MDSC function. Given that TLR4 and RAGE regulate MDSC accumulation and function, TLR4 and RAGE are the most likely mediators of HMGB1 signaling in MDSC.

To assess if HMGB1 signals through TLR4 or RAGE, tumor-bearing mice deficient in both TLR4 and RAGE could be treated with HMGB1 inhibitors and assessed for MDSC accumulation. In the absence of HMGB1 responsive receptors and reduced levels of HMGB1, MDSC accumulation should be significantly reduced. However, since MDSC are not the only cells expressing HMGB1 receptors, there could be deleterious side effects, as TLR4 and RAGE respond to other stimuli besides HMGB1 and do not solely possess tumor promoting characteristics. Therefore, the global knockout of TLR4 and RAGE could impede the overall immune response and weaken the immune system as a whole.

Does HMGB1 regulate other molecules in the TME that impact MDSC or other cells in the TME?

With HMGB1 able to impact several molecules in the TME that regulate MDSC function and accumulation, including IL-10, IL-6 and IL-1β, it would be interesting to determine if HMGB1 impacts other molecules in the TME that also modulate MDSC function such as VEGF, TNF-α, or PGE_2 (4, 7, 16, 17). To address this possibility, tumor-bearing mice could be treated with HMGB1 inhibitors and assessed for expression of VEGF, TNF-α, or PGE_2 and compared to control treated mice. If HMGB1 increases these inflammatory molecules then their expression could be reduced in HMGB1 inhibitor treated mice. Reduced expression of VEGF, TNF-α and PGE_2 would impede MDSC accumulation and weaken their suppressive potency.

To address if HMGB1 regulates other cells in the TME, tumor-bearing mice treated with HMGB1 inhibitors could be assessed for levels of macrophages, NK cells, DC, pDC, CAFs, and Bregs within the solid tumor and surrounding lymph nodes. Ideally, cells with anti-tumor function such as NK cells, DC, and macrophages would be elevated, while immune suppressive cells such as pDC, CAFs, and Bregs would be reduced. It has been previously established that HMGB1 induces the accumulation of immune suppressive Tregs and TAMs (26-28). Data from this dissertation established that HMGB1 regulates the levels of MDSC in the spleen, circulating blood, and tumor-infiltrating populations of tumor-bearing mice. This dissertation has also demonstrated that the inhibition of HMGB1 in tumor-bearing mice increases the amount of tumor-

infiltrating T cells. However, the infiltration of other immune cells was not assessed. If HMGB1 is a global driver of immune suppression, then inhibition of HMGB1 should reduce the levels of immune suppressive cells such as pDC, CAFs, and Bregs and promote the accumulation of immune reactive cells such as macrophages, DC, and NK cells.

Determining if HMGB1 impacts other molecules or cells in the TME would provide valuable information that could help determine its effectiveness as an immunotherapeutic. If inhibition of HMGB1 impedes the function or accumulation of macrophages, DC, or NK cells or perhaps promotes the accumulation or function of pDC, CAFs, or Bregs, then HMGB1 would not be an ideal molecule to target for therapeutic use. Ideally, immunotherapies stimulate cells with anti-tumor activity and subdue cells that are immune suppressive.

Does HMGB1-induced inflammation promote MDSC survival?

HMGB1 promotes autophagy in tumor cells and MDSC as well as inflammatory cytokines IL-6 and GM-CSF, both of which promote autophagy. Since IL-6 and GM-CSF are inducers of MDSC accumulation (3, 8, 33, 34), it would be interesting to determine if HMGB1 is acting in a pro-inflammatory manner to promote autophagy. To address whether HMGB1-promoted IL-6 and GM-CSF induce autophagy in MDSC, tumor-bearing mice could be treated with HMGB1 inhibitors and assessed for autophagy activity. If autophagy activity is reduced in MDSC from these mice as a result of

decreased inflammation, then treating these mice with recombinant IL-6 or GM-CSF should restore autophagy activity. However, this question presents the age-old predicament of whether the chicken or the egg came first. In this case, the question is if HMGB1 or inflammation is first. Ideally, mice that are knocked out for HMGB1 would be utilized for these experiments; however, global knockouts of HMGB1 are not viable (35). Therefore, tissue specific knockouts of HMGB1 solely in myeloid cells should be generated to determine if HMGB1 is induced by inflammation, or if inflammation induces HMGB1 expression which in turn promotes autophagy in MDSC.

Would the global targeting of HMGB1 be beneficial for cancer treatment?

This dissertation has described HMGB1 as a pro-inflammatory alarmin that promotes tumor-induced immune suppression. Therefore, it would be logical to use HMGB1 inhibitors therapeutically to reduce tumor-induced immune suppression. However, HMGB1 does not solely function as a driver of tumor-induced immune suppression. HMGB1 is also a regulator of the immune response to sepsis, viral infection, and arthritis (15, 36, 37). Therefore, globally targeting HMGB1 could negatively impact the immune system as a whole and weaken immune responses to sepsis, viral infection, and arthritis.

The global targeting of HMGB1 must be done with caution, as HMGB1 knockout mice are not viable (35). While the knockout offspring survive birth, they die within 24 hours as a result of hypoglycemia. Therefore, HMGB1 inhibitors must be used with caution so as not to be toxic. These HMGB1 inhibitors, while useful, display varying

degrees of specificity. The most specific inhibitors of HMGB1 are a neutralizing antibody called 2G7, and a recombinant form of half of the molecule called A box utilized in chapter 2 (19, 38). While the logical progression of this research is to conduct extended in vivo experiments and determine the long-term effects of inhibiting HMGB1 in tumor-bearing mice, the logistics behind obtaining these reagents are complicated.

Less specific chemical inhibitors of HMGB1 are commercially available for purchase and have proven extremely useful (chapter 2), yet they exhibit limitations as well. Ethyl pyruvate is a simple derivative of the metabolite pyruvic acid. Ethyl pyruvate is established as a potent anti-inflammatory agent in that it improves survival and organ function in animal models of sepsis, ischemia-reperfusion, and pancreatitis resulting from the inhibition of NF-κB as well as reduced release of TNF-α, IL-1β, and IL-6 (39-42). Additionally, ethyl pyruvate inhibits the release of HMGB1 in lung adenocarcinoma cells, which induces a shift from necrosis to apoptosis (43). While ethyl pyruvate inhibits the release of HMGB1, it is not a specific inhibitor of HMGB1. In fact, ethyl pyruvate's inhibition of the promiscuous transcription factor NF-κB suggests that ethyl pyruvate could be a global inhibitor of inflammation solely as a result of NF-κB inhibition.

Glycyrrhizin is a glycol conjugated triterpene produced by the licorice plant. Glycyrrhizin inhibits HMGB1 by binding to two distinct regions of the molecule and preventing HMGB1 from having chemoattractant activity (44). While I have established glycyrrhizin as a potent inhibitor of tumor-induced immune suppression (chapter 2), its impact on other cells in the TME has not been assessed. Before glycyrrhizin can be

deemed to have any therapeutic potential, its impact on other immune cells must be established.

While there are logistical limitations in the targeting of HMGB1, there are also fundamental limitations present. This dissertation has focused on the pro-tumor implications of HMGB1; however, HMGB1 also has anti-tumor effects. These anti-tumor effects include increasing genome stability, promoting maturation of APC, and promoting autophagy. Therefore, inhibiting HMGB1 could result in sponsoring tumor progression, which is not a desired effect.

This dissertation has identified another means by which autophagy promotes tumor progression: by maintaining MDSC viability and, consequently, driving tumor-induced immune suppression (chapter 3). However, autophagy, like HMGB1, has pro- and anti-tumor implications that are directly related to the stage of tumor progression (45, 46). The mechanism by which autophagy can reduce tumor formation is linked to the degradation of impaired mitochondria that would otherwise cause DNA damage or genomic instability (47). While initial tumor development is impeded by autophagy, once a tumor is established, autophagy promotes tumor development. Tumor cells utilize autophagy for survival during dissemination (48).Tumor cell resistance to chemotherapy or irradiation is also attributed to autophagy (49).

Interestingly, HMGB1 and autophagy exhibit a similar relationship with tumor progression in that the initial anti-tumor immune response requires HMGB1. However,

established tumors utilize HMGB1 to induce inflammation and promote immune suppression. Therefore, it is possible that the function of HMGB1 is dependent on the stage of tumor progression as well. Perhaps inhibition of HMGB1 should only be implemented with established tumors that have generated a highly pro-inflammatory environment. In this instance, inhibition of HMGB1 would weaken the pro-inflammatory environment that is driving immune suppressive cells as well as tumor development and aid in the restoration of immune competence.

How could HMGB1 be used in combination therapy treatment?

In recent years, a combination approach involving the inhibition of HMGB1 has been utilized in murine tumor models. Neutralization of HMGB1 by glycyrrhizin, combined with an anti-cancer peptide (CAMEL) that induces necrotic cell death, was able to reduce tumor growth in a B16-F10 murine melanoma model (50). The logic behind using CAMEL in combination with glycyrrhizin was that CAMEL-induced necrosis would result in the release of HMGB1, which would induce pro-inflammatory cytokines that could aid tumor progression. However, by combining CAMEL with an HMGB1 inhibitor, the pro-tumor effects of necrotic released HMGB1 are removed. A similar approach was taken employing tumor cells knocked down siRNA for HMGB1 expression. Tumor lines CT26, EL4, and MCA205 were knocked down for HMGB1 and inoculated in mice. These tumor-bearing mice were then treated with one of two chemotherapy agents, doxorubicin or oxaliplatin, in combination with a TLR4 agonist dendrophilin. This combination treatment successfully induced the accumulation of IFN-

γ producing $CD4^+$ and $CD8^+$ T cells, which resulted in reduced tumor progression (51). Therefore, in this instance, the levels of HMGB1 were reduced, tumor cells were killed via chemotherapy, and the immune system was stimulated via TLR4 activation. This combination is successful because HMGB1-induced TLR4 activation is required for DC-dependent T cell priming by tumor-associated antigens, and dendrophilin compensates for the absence of HMGB1 (30). In both of these scenarios, HMGB1 was targeted as a means of reducing inflammation brought on by cell death and combined with an immune activating treatment.

With HMGB1 established as a driver of tumor-induced immune suppression, it would be interesting to know if the neutralization of HMGB1 could be used therapeutically as a method to weaken tumor-induced immune suppression. Neutralization of HMGB1 in combination with anti-angiogenesis treatment or immune checkpoint inhibitors could trigger a robust anti-tumor immune response. To achieve a successful anti-tumor immune response, there are four main steps that are required: (**1**) DC must present a tumor antigen to a naïve T cell, (**2**) this T cell must then differentiate into an effector T cell, (**3**) the effector T cell must find its compatible tumor cell with which it can react with and cause the release of cytotoxic granules, and (**4**) during this entire process, T cells and other immune reactive cells must overcome tumor-induced immune suppression. Given that these four events are necessary, it is reasonable to create an immunotherapy regimen that ensures these four steps occur.

For instance, treatment could begin with a therapy that promotes antigen presentation by DC, followed by a therapy that enhances anti-tumor T cell function. Finally, a therapy that reduces tumor-induced immune suppression could be given throughout the treatment process. In this design, the DC boosting agent could be sunitinib or bevacizumab. Sunitinib blocks multiple tumor-associated tyrosine kinases including VEGFR, which aids in DC activation and inhibits the accumulation and function of immune suppressive Tregs and MDSC (52, 53). Bevacizumab is a VEGF neutralizing antibody that promotes DC maturation and increases DC priming of T cells (54, 55). Enhancers of T cell function could be in the form of immune checkpoint inhibitors, or co-stimulatory molecules. Co-stimulation by CD80 is an effective CD28 stimulant and inhibitor of PD-1 induced apoptosis (56). Inhibition of checkpoint molecule CTLA-4 by ipilimumab provides durable survival advantages in metastatic melanoma patients (57-59). Lastly, systemic inhibition of tumor-induced immune suppression could be accomplished by using an HMGB1 inhibitor. Implementation of this kind of therapeutic regimen, which focuses on achieving a natural anti-tumor immune response, would provide a platform in which inhibition of HMGB1 could be used to its full potential.

Concluding remarks

The goal of this dissertation was to determine whether HMGB1 functions as a master upstream regulator of inflammation and driver of tumor-induced immune suppression. This dissertation concludes that HMGB1 is indeed an upstream regulator as well as inducer of MDSC. Yet, it's not the sole regulator of inflammation in TME that promotes

MDSC; rather, it appears that HMGB1 works in parallel with other inflammatory inducers to promote an immune suppressive TME. That said, HMGB1 remains an important inducer of MDSC that not only regulates their accumulation and function but also promotes their survival. Therefore, HMGB1is an appealing target for use in comprehensive immunotherapy treatment.

1. Bunt, S. K., P. Sinha, V. K. Clements, J. Leips, and S. Ostrand-Rosenberg. 2006. Inflammation induces myeloid-derived suppressor cells that facilitate tumor progression. *J Immunol* 176: 284-290.
2. Song, X., Y. Krelin, T. Dvorkin, O. Bjorkdahl, S. Segal, C. A. Dinarello, E. Voronov, and R. N. Apte. 2005. CD11b+/Gr-1+ immature myeloid cells mediate suppression of T cells in mice bearing tumors of IL-1beta-secreting cells. *J Immunol* 175: 8200-8208.
3. Bunt, S. K., L. Yang, P. Sinha, V. K. Clements, J. Leips, and S. Ostrand-Rosenberg. 2007. Reduced inflammation in the tumor microenvironment delays the accumulation of myeloid-derived suppressor cells and limits tumor progression. *Cancer Res* 67: 10019-10026.

4. Sinha, P., V. K. Clements, A. M. Fulton, and S. Ostrand-Rosenberg. 2007. Prostaglandin E2 promotes tumor progression by inducing myeloid-derived suppressor cells. *Cancer Res* 67: 4507-4513.

5. Markiewski, M. M., R. A. DeAngelis, F. Benencia, S. K. Ricklin-Lichtsteiner, A. Koutoulaki, C. Gerard, G. Coukos, and J. D. Lambris. 2008. Modulation of the antitumor immune response by complement. *Nat Immunol* 9: 1225-1235.

6. Eruslanov, E., I. Daurkin, J. Ortiz, J. Vieweg, and S. Kusmartsev. 2010. Pivotal Advance: Tumor-mediated induction of myeloid-derived suppressor cells and M2-polarized macrophages by altering intracellular PGE_2 catabolism in myeloid cells. *J Leukoc Biol* 88: 839-848.

7. Gabrilovich, D., T. Ishida, T. Oyama, S. Ran, V. Kravtsov, S. Nadaf, and D. P. Carbone. 1998. Vascular endothelial growth factor inhibits the development of dendritic cells and dramatically affects the differentiation of multiple hematopoietic lineages in vivo. *Blood* 92: 4150-4166.

8. Serafini, P., R. Carbley, K. A. Noonan, G. Tan, V. Bronte, and I. Borrello. 2004. High-dose granulocyte-macrophage colony-stimulating factor-producing vaccines impair the immune response through the recruitment of myeloid suppressor cells. *Cancer Res* 64: 6337-6343.

9. Okazaki, T., S. Ebihara, M. Asada, A. Kanda, H. Sasaki, and M. Yamaya. 2006. Granulocyte colony-stimulating factor promotes tumor angiogenesis via increasing circulating endothelial progenitor cells and Gr1+CD11b+ cells in cancer animal models. *Int Immunol* 18: 1-9.

10. Wang, L., T. Yi, M. Kortylewski, D. M. Pardoll, D. Zeng, and H. Yu. 2009. IL-17 can promote tumor growth through an IL-6-Stat3 signaling pathway. *J Exp Med* 206: 1457-1464.

11. Smith, C., M. Y. Chang, K. H. Parker, D. W. Beury, J. B. DuHadaway, H. E. Flick, J. Boulden, E. Sutanto-Ward, A. P. Soler, L. D. Laury-Kleintop, L. Mandik-Nayak, R. Metz, S. Ostrand-Rosenberg, G. C. Prendergast, and A. J. Muller. 2012. IDO is a nodal pathogenic driver of lung cancer and metastasis development. *Cancer Discov* 2: 722-735.

12. Sinha, P., C. Okoro, D. Foell, H. H. Freeze, S. Ostrand-Rosenberg, and G. Srikrishna. 2008. Proinflammatory S100 proteins regulate the accumulation of myeloid-derived suppressor cells. *J Immunol* 181: 4666-4675.

13. Marigo, I., E. Bosio, S. Solito, C. Mesa, A. Fernandez, L. Dolcetti, S. Ugel, N. Sonda, S. Bicciato, E. Falisi, F. Calabrese, G. Basso, P. Zanovello, E. Cozzi, S. Mandruzzato, and V. Bronte. 2010. Tumor-induced tolerance and immune suppression depend on the C/EBPbeta transcription factor. *Immunity* 32: 790-802.

14. Thevenot, P. T., R. A. Sierra, P. L. Raber, A. A. Al-Khami, J. Trillo-Tinoco, P. Zarreii, A. C. Ochoa, Y. Cui, L. Del Valle, and P. C. Rodriguez. 2014. The stress-response sensor chop regulates the function and accumulation of myeloid-derived suppressor cells in tumors. *Immunity* 41: 389-401.

15. Yang, H., M. Ochani, J. Li, X. Qiang, M. Tanovic, H. E. Harris, S. M. Susarla, L. Ulloa, H. Wang, R. DiRaimo, C. J. Czura, J. Roth, H. S. Warren, M. P. Fink, M. J. Fenton, U. Andersson, and K. J. Tracey. 2004. Reversing established sepsis

with antagonists of endogenous high-mobility group box 1. *Proc Natl Acad Sci U S A* 101: 296-301.

16. Rodriguez, P. C., C. P. Hernandez, D. Quiceno, S. M. Dubinett, J. Zabaleta, J. B. Ochoa, J. Gilbert, and A. C. Ochoa. 2005. Arginase I in myeloid suppressor cells is induced by COX-2 in lung carcinoma. *J Exp Med* 202: 931-939.

17. Sade-Feldman, M., J. Kanterman, E. Ish-Shalom, M. Elnekave, E. Horwitz, and M. Baniyash. 2013. Tumor necrosis factor-alpha blocks differentiation and enhances suppressive activity of immature myeloid cells during chronic inflammation. *Immunity* 38: 541-554.

18. Liu, J. H., Z. J. Li, J. Tang, Y. W. Liu, L. Zhao, P. Deng, and Y. Jiang. 2006. [High mobility group box-1 protein activates endothelial cells to produce cytokines and has synergistic effect with lipopolysaccharide in inducing interleukin-6 release]. *Zhonghua Yi Xue Za Zhi* 86: 1191-1195.

19. Yang, H., M. Ochani, J. Li, X. Qiang, M. Tanovic, H. E. Harris, S. M. Susarla, L. Ulloa, H. Wang, R. DiRaimo, C. J. Czura, J. Roth, H. S. Warren, M. P. Fink, M. J. Fenton, U. Andersson, and K. J. Tracey. 2004. Reversing established sepsis with antagonists of endogenous high-mobility group box 1. *Proc Natl Acad Sci U S A* 101: 296-301.

20. Leclerc, P., H. Wahamaa, H. Idborg, P. J. Jakobsson, H. E. Harris, and M. Korotkova. 2013. IL-1beta/HMGB1 complexes promote The PGE2 biosynthesis pathway in synovial fibroblasts. *Scand J Immunol* 77: 350-360.

21. Taguchi, A., D. C. Blood, G. del Toro, A. Canet, D. C. Lee, W. Qu, N. Tanji, Y. Lu, E. Lalla, C. Fu, M. A. Hofmann, T. Kislinger, M. Ingram, A. Lu, H. Tanaka,

O. Hori, S. Ogawa, D. M. Stern, and A. M. Schmidt. 2000. Blockade of RAGE-amphoterin signalling suppresses tumour growth and metastases. *Nature* 405: 354-360.

22. Livesey, K. M., D. Tang, H. J. Zeh, and M. T. Lotze. 2008. Not just nuclear proteins: 'novel' autophagy cancer treatment targets - p53 and HMGB1. *Curr Opin Investig Drugs* 9: 1259-1263.

23. Sasahira, T., T. Kirita, U. K. Bhawal, M. Ikeda, A. Nagasawa, K. Yamamoto, and H. Kuniyasu. 2007. The expression of receptor for advanced glycation end products is associated with angiogenesis in human oral squamous cell carcinoma. *Virchows Arch* 450: 287-295.

24. van Beijnum, J. R., P. Nowak-Sliwinska, E. van den Boezem, P. Hautvast, W. A. Buurman, and A. W. Griffioen. 2013. Tumor angiogenesis is enforced by autocrine regulation of high-mobility group box 1. *Oncogene* 32: 363-374.

25. Vernon, P. J., H. J. Zeh Iii, and M. T. Lotze. 2013. The myeloid response to pancreatic carcinogenesis is regulated by the receptor for advanced glycation end-products. *Oncoimmunology* 2: e24184.

26. Wild, C. A., C. Bergmann, G. Fritz, P. Schuler, T. K. Hoffmann, R. Lotfi, A. Westendorf, S. Brandau, and S. Lang. 2012. HMGB1 conveys immunosuppressive characteristics on regulatory and conventional T cells. *Int Immunol* 24: 485-494.

27. Liu, Z., L. D. Falo, Jr., and Z. You. 2011. Knockdown of HMGB1 in tumor cells attenuates their ability to induce regulatory T cells and uncovers naturally acquired CD8 T cell-dependent antitumor immunity. *J Immunol* 187: 118-125.

28. He, Y., J. Zha, Y. Wang, W. Liu, X. Yang, and P. Yu. 2013. Tissue damage-associated "danger signals" influence T-cell responses that promote the progression of preneoplasia to cancer. *Cancer Res* 73: 629-639.

29. Yang, H., H. S. Hreggvidsdottir, K. Palmblad, H. Wang, M. Ochani, J. Li, B. Lu, S. Chavan, M. Rosas-Ballina, Y. Al-Abed, S. Akira, A. Bierhaus, H. Erlandsson-Harris, U. Andersson, and K. J. Tracey. 2010. A critical cysteine is required for HMGB1 binding to Toll-like receptor 4 and activation of macrophage cytokine release. *Proc Natl Acad Sci U S A* 107: 11942-11947.

30. Apetoh, L., F. Ghiringhelli, A. Tesniere, A. Criollo, C. Ortiz, R. Lidereau, C. Mariette, N. Chaput, J. P. Mira, S. Delaloge, F. André, T. Tursz, G. Kroemer, and L. Zitvogel. 2007. The interaction between HMGB1 and TLR4 dictates the outcome of anticancer chemotherapy and radiotherapy. *Immunol Rev* 220: 47-59.

31. Bunt, S. K., V. K. Clements, E. M. Hanson, P. Sinha, and S. Ostrand-Rosenberg. 2009. Inflammation enhances myeloid-derived suppressor cell cross-talk by signaling through Toll-like receptor 4. *J Leukoc Biol* 85: 996-1004.

32. Obermajer, N., R. Muthuswamy, K. Odunsi, R. P. Edwards, and P. Kalinski. 2011. PGE(2)-induced CXCL12 production and CXCR4 expression controls the accumulation of human MDSCs in ovarian cancer environment. *Cancer Res* 71: 7463-7470.

33. Morales, J. K., M. Kmieciak, K. L. Knutson, H. D. Bear, and M. H. Manjili. 2010. GM-CSF is one of the main breast tumor-derived soluble factors involved in the differentiation of CD11b-Gr1- bone marrow progenitor cells into myeloid-derived suppressor cells. *Breast Cancer Res Treat* 123: 39-49.

34. Nefedova, Y., M. Huang, S. Kusmartsev, R. Bhattacharya, P. Cheng, R. Salup, R. Jove, and D. Gabrilovich. 2004. Hyperactivation of STAT3 is involved in abnormal differentiation of dendritic cells in cancer. *J Immunol* 172: 464-474.

35. Calogero, S., F. Grassi, A. Aguzzi, T. Voigtländer, P. Ferrier, S. Ferrari, and M. E. Bianchi. 1999. The lack of chromosomal protein Hmg1 does not disrupt cell growth but causes lethal hypoglycaemia in newborn mice. *Nat Genet* 22: 276-280.

36. Jungas, T., P. Verbeke, T. Darville, and D. M. Ojcius. 2004. Cell death, BAX activation, and HMGB1 release during infection with Chlamydia. *Microbes Infect* 6: 1145-1155.

37. Andersson, U., and H. Erlandsson-Harris. 2004. HMGB1 is a potent trigger of arthritis. *J Intern Med* 255: 344-350.

38. Li, J., R. Kokkola, S. Tabibzadeh, R. Yang, M. Ochani, X. Qiang, H. E. Harris, C. J. Czura, H. Wang, L. Ulloa, H. S. Warren, L. L. Moldawer, M. P. Fink, U. Andersson, K. J. Tracey, and H. Yang. 2003. Structural basis for the proinflammatory cytokine activity of high mobility group box 1. *Mol Med* 9: 37-45.

39. Ulloa, L., M. Ochani, H. Yang, M. Tanovic, D. Halperin, R. Yang, C. J. Czura, M. P. Fink, and K. J. Tracey. 2002. Ethyl pyruvate prevents lethality in mice with established lethal sepsis and systemic inflammation. *Proc Natl Acad Sci U S A* 99: 12351-12356.

40. Cheng, B. Q., C. T. Liu, W. J. Li, W. Fan, N. Zhong, Y. Zhang, X. Q. Jia, and S. Z. Zhang. 2007. Ethyl pyruvate improves survival and ameliorates distant organ injury in rats with severe acute pancreatitis. *Pancreas* 35: 256-261.

41. Tsung, A., T. Kaizu, A. Nakao, L. Shao, B. Bucher, M. P. Fink, N. Murase, and D. A. Geller. 2005. Ethyl pyruvate ameliorates liver ischemia-reperfusion injury by decreasing hepatic necrosis and apoptosis. *Transplantation* 79: 196-204.

42. Han, Y., J. A. Englert, R. Yang, R. L. Delude, and M. P. Fink. 2005. Ethyl pyruvate inhibits nuclear factor-kappaB-dependent signaling by directly targeting p65. *J Pharmacol Exp Ther* 312: 1097-1105.

43. Lim, S. C., J. E. Choi, C. H. Kim, H. Q. Duong, G. A. Jeong, H. S. Kang, and S. I. Han. 2007. Ethyl pyruvate induces necrosis-to-apoptosis switch and inhibits high mobility group box protein 1 release in A549 lung adenocarcinoma cells. *Int J Mol Med* 20: 187-192.

44. Mollica, L., F. De Marchis, A. Spitaleri, C. Dallacosta, D. Pennacchini, M. Zamai, A. Agresti, L. Trisciuoglio, G. Musco, and M. E. Bianchi. 2007. Glycyrrhizin binds to high-mobility group box 1 protein and inhibits its cytokine activities. *Chem Biol* 14: 431-441.

45. Degenhardt, K., R. Mathew, B. Beaudoin, K. Bray, D. Anderson, G. Chen, C. Mukherjee, Y. Shi, C. Gélinas, Y. Fan, D. A. Nelson, S. Jin, and E. White. 2006. Autophagy promotes tumor cell survival and restricts necrosis, inflammation, and tumorigenesis. *Cancer Cell* 10: 51-64.

46. Yang, X., D. D. Yu, F. Yan, Y. Y. Jing, Z. P. Han, K. Sun, L. Liang, J. Hou, and L. X. Wei. 2015. The role of autophagy induced by tumor microenvironment in different cells and stages of cancer. *Cell Biosci* 5: 14.

47. Maycotte, P., and A. Thorburn. 2014. Targeting autophagy in breast cancer. *World J Clin Oncol* 5: 224-240.

48. Fung, C., R. Lock, S. Gao, E. Salas, and J. Debnath. 2008. Induction of autophagy during extracellular matrix detachment promotes cell survival. *Mol Biol Cell* 19: 797-806.

49. Kimmelman, A. C. 2011. The dynamic nature of autophagy in cancer. *Genes Dev* 25: 1999-2010.

50. Smolarczyk, R., T. Cichoń, S. Matuszczak, I. Mitrus, M. Lesiak, M. Kobusińska, W. Kamysz, M. Jarosz, A. Sieroń, and S. Szala. 2012. The role of Glycyrrhizin, an inhibitor of HMGB1 protein, in anticancer therapy. *Arch Immunol Ther Exp (Warsz)* 60: 391-399.

51. Yamazaki, T., D. Hannani, V. Poirier-Colame, S. Ladoire, C. Locher, A. Sistigu, N. Prada, S. Adjemian, J. P. Catani, M. Freudenberg, C. Galanos, F. André, G. Kroemer, and L. Zitvogel. 2014. Defective immunogenic cell death of HMGB1-deficient tumors: compensatory therapy with TLR4 agonists. *Cell Death Differ* 21: 69-78.

52. Ozao-Choy, J., G. Ma, J. Kao, G. X. Wang, M. Meseck, M. Sung, M. Schwartz, C. M. Divino, P. Y. Pan, and S. H. Chen. 2009. The novel role of tyrosine kinase inhibitor in the reversal of immune suppression and modulation of tumor microenvironment for immune-based cancer therapies. *Cancer Res* 69: 2514-2522.

53. Bose, A., J. L. Taylor, S. Alber, S. C. Watkins, J. A. Garcia, B. I. Rini, J. S. Ko, P. A. Cohen, J. H. Finke, and W. J. Storkus. 2011. Sunitinib facilitates the activation and recruitment of therapeutic anti-tumor immunity in concert with specific vaccination. *Int J Cancer* 129: 2158-2170.

54. Yang, D. H., J. S. Park, C. J. Jin, H. K. Kang, J. H. Nam, J. H. Rhee, Y. K. Kim, S. Y. Chung, S. J. Choi, H. J. Kim, I. J. Chung, and J. J. Lee. 2009. The dysfunction and abnormal signaling pathway of dendritic cells loaded by tumor antigen can be overcome by neutralizing VEGF in multiple myeloma. *Leuk Res* 33: 665-670.

55. Shrimali, R. K., Z. Yu, M. R. Theoret, D. Chinnasamy, N. P. Restifo, and S. A. Rosenberg. 2010. Antiangiogenic agents can increase lymphocyte infiltration into tumor and enhance the effectiveness of adoptive immunotherapy of cancer. *Cancer Res* 70: 6171-6180.

56. Haile, S. T., S. P. Dalal, V. Clements, K. Tamada, and S. Ostrand-Rosenberg. 2013. Soluble CD80 restores T cell activation and overcomes tumor cell programmed death ligand 1-mediated immune suppression. *J Immunol* 191: 2829-2836.

57. Hodi, F. S., S. J. O'Day, D. F. McDermott, R. W. Weber, J. A. Sosman, J. B. Haanen, R. Gonzalez, C. Robert, D. Schadendorf, J. C. Hassel, W. Akerley, A. J. van den Eertwegh, J. Lutzky, P. Lorigan, J. M. Vaubel, G. P. Linette, D. Hogg, C. H. Ottensmeier, C. Lebbé, C. Peschel, I. Quirt, J. I. Clark, J. D. Wolchok, J. S. Weber, J. Tian, M. J. Yellin, G. M. Nichol, A. Hoos, and W. J. Urba. 2010. Improved survival with ipilimumab in patients with metastatic melanoma. *N Engl J Med* 363: 711-723.

58. Wolchok, J. D., B. Neyns, G. Linette, S. Negrier, J. Lutzky, L. Thomas, W. Waterfield, D. Schadendorf, M. Smylie, T. Guthrie, J. J. Grob, J. Chesney, K. Chin, K. Chen, A. Hoos, S. J. O'Day, and C. Lebbé. 2010. Ipilimumab

monotherapy in patients with pretreated advanced melanoma: a randomised, double-blind, multicentre, phase 2, dose-ranging study. *Lancet Oncol* 11: 155-164.

59. Phan, G. Q., J. C. Yang, R. M. Sherry, P. Hwu, S. L. Topalian, D. J. Schwartzentruber, N. P. Restifo, L. R. Haworth, C. A. Seipp, L. J. Freezer, K. E. Morton, S. A. Mavroukakis, P. H. Duray, S. M. Steinberg, J. P. Allison, T. A. Davis, and S. A. Rosenberg. 2003. Cancer regression and autoimmunity induced by cytotoxic T lymphocyte-associated antigen 4 blockade in patients with metastatic melanoma. *Proc Natl Acad Sci U S A* 100: 8372-8377.

Appendix 1: High Mobility Group Box Protein 1 enhances immune suppression by facilitating the differentiation and suppressive activity of myeloid-derived suppressor cells. Katherine Parker, Pratima Sinha, Lucas Horn, Virginia Clements, Huan Yang, Jianhua Li, Kevin Tracey, Suzanne Ostrand-Rosenberg Cancer Research, 2014.

Published OnlineFirst August 27, 2014; DOI: 10.1158/0008-5472.CAN-13-2347

Microenvironment and Immunology

Cancer Research

HMGB1 Enhances Immune Suppression by Facilitating the Differentiation and Suppressive Activity of Myeloid-Derived Suppressor Cells

Katherine H. Parker[1], Pratima Sinha[1], Lucas A. Horn[1], Virginia K. Clements[1], Huan Yang[2], Jianhua Li[2], Kevin J. Tracey[2], and Suzanne Ostrand-Rosenberg[1]

Abstract

Chronic inflammation often precedes malignant transformation and later drives tumor progression. Likewise, subversion of the immune system plays a role in tumor progression, with tumoral immune escape now well recognized as a crucial hallmark of cancer. Myeloid-derived suppressor cells (MDSC) are elevated in most individuals with cancer, where their accumulation and suppressive activity are driven by inflammation. Thus, MDSCs may define an element of the pathogenic inflammatory processes that drives immune escape. The secreted alarmin HMGB1 is a proinflammatory partner, inducer, and chaperone for many proinflammatory molecules that MDSCs develop. Therefore, in this study, we examined HMGB1 as a potential regulator of MDSCs. In murine tumor systems, HMGB1 was ubiquitous in the tumor microenvironment, activating the NF-κB signal transduction pathway in MDSCs and regulating their quantity and quality. We found that HMGB1 promotes the development of MDSCs from bone marrow progenitor cells, contributing to their ability to suppress antigen-driven activation of $CD4^+$ and $CD8^+$ T cells. Furthermore, HMGB1 increased MDSC-mediated production of IL-10, enhanced crosstalk between MDSCs and macrophages, and facilitated the ability of MDSCs to down-regulate expression of the T-cell homing receptor L-selectin. Overall, our results revealed a pivotal role for HMGB1 in the development and cancerous contributions of MDSCs. *Cancer Res; 74(20); 5723–33. ©2014 AACR.*

Introduction

Antitumor immunity and immunotherapies that activate innate and/or adaptive immunity have potential for the prevention and/or treatment of primary and metastatic cancers. However, immunotherapies are frequently ineffective because patients with cancer contain immunosuppressive cells. Myeloid-derived suppressor cells (MDSC; ref. 1) are present in virtually all patients with solid tumors and are major contributors to immune suppression. They facilitate tumor progression through multiple immune mechanisms, including the inhibition of T- and NK-cell activation (2), polarization of immunity toward a tumor-promoting type II phenotype through their production of IL-10 (3), and by perturbing the trafficking of naïve T cells by downregulating L-selectin (4). MDSCs also use nonimmune mechanisms to enhance tumor growth. They produce VEGF and matrix metalloproteases that promote tumor vascularization (5) as well as invasion and metastasis (6).

Chronic inflammation has long been associated with tumor onset and progression (7). The role of chronic inflammation was originally attributed to its ability to foster genetic mutations, enhance tumor cell proliferation and survival, and promote metastases. Chronic inflammation also facilitates malignancy by inducing the accumulation and increasing the potency of MDSCs, which prevent adaptive and innate immunity from delaying tumor progression (8). Multiple redundant proinflammatory molecules drive MDSCs. Because the damage-associated molecular pattern molecule (DAMP) and alarmin high mobility group box protein I (HMGB1) is proinflammatory and is a binding partner, inducer, and/or chaperone for many of the proinflammatory molecules that drive MDSCs (9), we have studied HMGB1 as a potential regulator of MDSCs. HMGB1 was originally identified as a DNA-binding protein in the nucleus. It performs multiple functions within the nucleus, including changing the conformation of DNA to allow for the binding of regulatory proteins, facilitating the integration of transposons into DNA, and stabilizing nucleosome formation (10). Its role as a secreted protein and an immune modulator has only been recognized within the past 15 years (11).

We now report that in addition to many other cells, MDSCs release HMGB1 and that HMGB1 activates MDSCs through NF-κB and facilitates several immune suppressive mechanisms used by MDSCs to inhibit antitumor immunity. HMGB1 drives the differentiation of MDSCs from bone marrow progenitor cells, enhances crosstalk between MDSCs and macrophages by increasing MDSC production of IL-10, and reduces the expression of L-selectin on circulating naïve T cells. Collectively, these

[1]Department of Biological Sciences, University of Maryland Baltimore County, Baltimore, Maryland. [2]Laboratory of Biomedical Science, The Feinstein Institute for Medical Research, Manhasset, New York.

Note: Supplementary data for this article are available at Cancer Research Online (http://cancerres.aacrjournals.org/).

Corresponding Author: Suzanne Ostrand-Rosenberg, Department of Biological Sciences, University of Maryland Baltimore County, 1000 Hilltop Circle, Baltimore, MD 21250. Phone: 410-455-2237; Fax: 410-455-3875; E-mail: srosenbe@umbc.edu

doi: 10.1158/0008-5472.CAN-13-2347

results suggest that HMGB1 contributes to immune suppression by inducing and activating MDSCs.

Materials and Methods

Mice

BALB/c, C57BL/6, BALB/c IL-10$^{-/-}$, BALB/c TLR4$^{-/-}$, BALB/c DO11.10 (TCR-transgenic for the αβ-TCR specific for OVA peptide 323-339 restricted by I-A^{d}) and BALB/c clone 4 TCR-transgenic (αβ-TCR specific for influenza hemagglutinin 518–526 restricted by H-2K^{d}) mice were from The Jackson Laboratory and/or bred in the UMBC animal facility. Mice <6 months of age were used for all experiments. All animal procedures were approved by the University of Maryland Baltimore County (Baltimore, MD) Institutional Animal Care and Use Committee.

Reagents and antibodies

Heparin sodium salt (grade IA) and ethyl pyruvate were from Sigma-Aldrich. Glycyrrhizin (ammonium salt) was from Calbiochem. Recombinant mouse IL-6 and GM-CSF were from BioLegend. Recombinant mouse IFNγ, HMGB1, and TNFα were from R&D Systems. Recombinant LPS was from Difco. Monoclonal antibodies (mAb) Gr1-APC-Cy7, Gr1-APC (RB6-8C5), CD45-PE (30-F11), CD8-FITC (53-6.7), CD4-PE (L3T4/GK1.5), CD3-PE-Cy7 (145-2C11), CD11b-PE (M1/70), CD11c-FITC (HL3), CD45R-B220-PE (RA3-6B2), CD62L-APC (MEL14), c-kit-PE (CD117; ACK45), iNOS, arginase, rat IgG2b isotype, and annexin V were from BD Biosciences. CD11b-PacB (M1/70), F4/80-PE (BM8), F4/80-PacB (BM8), rat IgG1a-APC (RTK2758), and CD16/32 (93) were from BioLegend. CD45-TxR (MCD4517) was from Invitrogen. Anti-mouse ADAM17 mAb was from Abcam (ab2051). Secondary for ADAM17 antibody (goat-anti-rabbit; 554020) was from BD Biosciences. Anti-CD3 was from Dako (clone F7.2.38). Recombinant A box (12, 13) and 2G7 (14) were produced as described.

Tumor inoculations, tumor measurements, 2G7, and A box treatment

C57BL/6 mice were inoculated subcutaneously in the flank with 5×10^5 MC38 colon carcinoma cells, 1×10^6 B78H1 melanoma cells, or 1×10^6 AT3 mammary carcinoma cells (15). BALB/c mice were inoculated in the abdominal mammary fat pad with 7×10^3 4T1 mammary carcinoma cells or subcutaneously with 1×10^6 CT26 colon carcinoma cells. With the exception of AT3, which was obtained from Dr. S. Abrams (Roswell Park Cancer Center, Buffalo, NY) approximately 5 years ago, all tumor cell lines have been in the authors' laboratory for >15 years. Cell lines are routinely checked for mycoplasma and early freeze-downs are preferentially used. Recombinant A box (300 μg/100 μL/mouse), vehicle (PBS), 2G7 mAb (5 μg/200 μL/mouse), or control IgG2b antibody (MOPC 195; 5 μg/200 μL/mouse; Sigma Aldrich) were administered intraperitoneally 3×/week starting when tumors were first palpable (day 7–9 postinoculation). Tumors were measured in two perpendicular diameters every 2 to 3 days. Tumor volume = (4/3) πr^3, where r = (diameter 1 + diameter 2)/4. IHC for tumor-infiltrating T cells was performed by CD3 staining of O.C.T. embedded tumors.

Tumors, MDSCs, and macrophage supernatants; MEF cell lysates

The 4T1, CT26, B78H1, MC38, and AT3 tumor cells were cultured at 5×10^6 cells/mL in 6-well plates in serum-free HL-1 medium at 37°C, 5% CO_2. MDSCs and thioglycolate-elicited macrophages were similarly cultured except some wells contained 100 ng/mL LPS. Supernatants were harvested after 18 hours and concentrated 10× using 10 kDa Centricon filters (Millipore). Excised tumors were minced into small pieces using scissors, and placed in 10 mL of serum-free HL-1 media containing 0.8 μg/mL DNase. Tumor chunks were then dissociated into single cell suspensions using a GentleMACS Dissociator equipped with a GentleMACS C tube and program m_tumor 01.01 (Miltenyi Biotec). Dissociated material, including medium, was then plated in 10 cm dishes and incubated at 37°C, 5% CO_2 for 18 hours, after which the supernatants were collected and concentrated to 2 mL using 10 kDa Centricon filters. Wild-type and HMGB1-knocked out MEF cells (16) were lysed in 300 μL of M-Per buffer Mammalian Protein Extraction Reagent (Thermo Scientific) using a GentleMACS Dissociator fitted with an M tube and program protein 01.01. Lysates were centrifuged at 10°C and 650 × g for 5 minutes, and the supernatants removed and centrifuged at 10°C and 160 × g for 15 minutes. Protein concentration of the supernatants was determined at 280 absorbance.

Blood MDSCs

Mice were bled from the submandibular vein into 1 mL of PBS containing 0.008% heparin. RBCs were removed by Gey's treatment (17). The remaining white blood cells were stained for Gr1 and CD11b and analyzed by flow cytometry. White blood cells that were >90% Gr1^{+}CD11b^{+} were used in experiments.

MDSC–macrophage cocultures

Peritoneal macrophage (>80%CD11b^{+}F4/80^{+} cells) and MDSC cocultures were performed as described elsewhere (3). Briefly, cells were plated at 7.5×10^5 MDSCs and 7.5×10^5 macrophages/well in 500 μL of DMEM with 5% FBS, 100 ng/mL LPS, and 20 U/mL IFNγ in 24-well plates. Cocultures were incubated at 37°C, 5% CO_2 for 16 to 18 hours. Supernatants were stored at −80°C until analyzed by ELISA.

Cytokine detection

IL-10, IL-6, IL-12, and IL-1β were measured by ELISA according to the manufacturer's protocol (R&D Systems). Plates were read at 450 nm using a Bio-Tek synergy microplate reader. Data are the mean ± SD of triplicate wells.

MDSC generation from bone marrow cells

MDSCs were generated (18) with the following adaptations: Bone marrow was flushed aseptically from femurs with RPMI medium using a syringe fitted with a 27 g needle. RBCs were lysed with Gey's solution. Resulting cells were cultured at 37°C, 5% CO_2 at 4.2×10^5 cells/2 mL in 6-well plates containing RPMI medium supplemented with 10% FCS, 40 ng/mL IL-6, and 40 ng/mL GM-CSF. After 4 days of culture, percent decrease in Gr1^{mid}CD11b^{+} cells was determined (Gr1^{mid}CD11b^{+} cells = 100% [(number of vehicle-treated cells − number of inhibitor

treated cells)/(number of vehicle-treated cells)]. Absolute number of cells = (total number of cells) × % of a given cell type as determined by flow cytometry.

T-cell activation assays

T-cell activation assays were performed as described (17). Briefly, splenocytes and irradiated (2500 Rad) 4T1-induced MDSCs or bone marrow generated MDSCs were cocultured in 96-well plates at 10^5 cells/200 μL/well of HL-1 media containing 1% penicillin, 1% streptomycin, 1% Glutamax, and 5×10^{-5} M β-mercaptoethanol. Of note, 14 μmol/L $OVA_{323-339}$ peptide or 28 μmol/L $HA_{518-526}$ peptide was included for DO11.10 and clone 4 cells, respectively. Wells were pulsed with 1 μCi of [^{3}H] thymidine/well on day 3, and 18 hours later, the cells were harvested. Data are expressed as cpm ± SD of triplicate cultures. Hydrogen peroxide levels were measured as described (19).

HMGB1 Western blot analyses and ELISA

Of note, 50 μL of equivalent quantities of concentrated supernatants of cultured tumor cells, *in vivo* grown tumors, MDSCs, macrophages, or 60 μg of MEF cell lysates were mixed with 10 μL or the appropriate amount of 6× sample buffer and electrophoresed on 12% SDS-PAGE gels in SDS running buffer (Bio-Rad) at 150 volts for 1 hour, and transferred overnight in transfer buffer (Bio-Rad) at 30 volts to PVDF membranes (GE Healthcare). Membranes were blocked with 5% milk in TBST. HMGB1 was detected with anti-HMGB1 antibody (Epitomics; 5 ng/mL in 10 mL of 2.5% milk/TBST) followed by goat-anti-rabbit-HRP (Millipore; 40 ng/mL in 10 mL of 2.5% milk/TBST). Protein was visualized using an HRP detection kit (Denville Scientific, Inc). HMGB1 levels were measured by ELISA according to the manufacturer's directions (IBL International).

Flow cytometry

Cells were labeled and analyzed by flow cytometry for cell surface molecules as described (17). For bone marrow experiments, cells were first stained using the LIVE/DEAD fixable yellow dead cell stain kit (Invitrogen) as per the manufacture's protocol, followed by staining for cell surface markers with antibodies diluted in PBS/2% FCS (HyClone). For NF-κB staining of MDSCs, 3×10^6 to 5×10^6 leukocytes/mL RPMI were incubated with/without 50 ng/mL HMGB1 for 15 minutes at 37°C, fixed and permeabilized, and then stained with rabbit mAb phospho-NF-κB p65 (Ser536; clone 93H1) and goat-anti-rabbit (Fab')$_2$-AlexaFluor 647 (Cell Signaling Technology, Inc.) according to the manufacturer's protocol, followed by staining for Gr1 and CD11b. Peritoneal macrophages (5×10^6/5 mL DMEM) were similarly stained, except they were rested for 2 hours at 37°C before stimulation with 20 ng/mL TNFα or 100 μg/mL LPS, and subsequently incubated with Fc block (CD16/32) for 15 minutes, followed by staining with NF-κB, CD11b, and F4/80 mAbs. For ADAM17 staining, 3×10^6 to 5×10^6 leukocytes were incubated with or without HMGB1 (50 ng/ml) or ethyl pyruvate (10 mmol/L) for 0, 2, and 4 hours and stained with mAb to ADAM17. For tumor-infiltrating MDSCs, solid tumors were prepared as they were for tumor supernatants, except collagenase (300 U/mL) was included in the dissociation medium, and the resulting cells were centrifuged through ficoll to remove dead cells. Samples were run on a Cyan ADP flow cytometer and analyzed using Summit Software (Beckman/Coulter).

Statistical analysis

Statistical analysis of tumor growth rate was conducted utilizing the compare Growth Curves function of the Statmod software package (http://bioinf.wehi.edu.au/software/compareCurves). A Student *t* test was used to determine statistical significance between two sets of data. Single-factor ANOVA was used to determine statistical significance between groups of data.

Results

HMGB1 is ubiquitously present in the tumor microenvironment and activates MDSCs via the NF-κB pathway

If HMGB1 is associated with the induction of MDSCs, then HMGB1 will be present in the tumor microenvironment. To test this hypothesis, BALB/c-derived 4T1 mammary carcinoma and CT26 colon carcinoma cells, and C57BL/6-derived B78H1 melanoma, MC38 colon carcinoma, and PyMT-MMTV–derived AT3 mammary carcinoma cells were cultured in serum free-media, and the supernatants assessed by Western blot analysis for HMGB1. Whole-cell lysates of wild-type MEF cells and their HMGB1-knocked out counterparts served as positive and negative controls, respectively. All tumors constitutively secreted HMGB1 (Fig. 1A). Secretion of HMGB1 was confirmed and quantified by ELISA (Supplementary Table S1).

Because MDSCs are driven by inflammation and themselves produce proinflammatory mediators (8, 20), we tested MDSCs for secretion of HMGB1. MDSCs generated in 4T1 tumor-bearing BALB/c mice were harvested from the blood, stained for Gr1 and CD11b, and assessed for their ability to suppress T-cell activation (Fig. 1B). More than 90% of the blood leukocytes were $CD11b^+Gr1^+$ and they were suppressive. We then tested MDSCs for their ability to secrete HMGB1 by culturing them overnight and assaying the supernatant for HMGB1 by Western blot analysis and ELISA (Fig. 1C and Supplementary Table S1). Macrophages are established producers of HMGB1 (11), and LPS is reported to increase their secretion of HMGB1 (21). To determine whether LPS similarly affects MDSCs, MDSCs were cultured with and without LPS. Both LPS-treated and untreated MDSCs produced more HMGB1 than equivalent numbers of LPS-treated macrophages, demonstrating that MDSCs constitutively secrete HMGB1.

To determine whether HMGB1 is present *in vivo* within the tumor microenvironment, 4T1, CT26, B78H1, MC38, and AT3 tumors of BALB/c and C57BL/6 tumor-bearing mice were measured, and then excised and weighed. Explanted tumors were then dissociated into single cell suspensions without disrupting cell integrity, and incubated in serum-free medium. The resulting supernatants were assessed by Western blot analysis and ELISA for HMGB1 (Fig. 1C right-hand five lanes and Supplementary Table S1). All excised tumors released HMGB1; however, the quantity of HMGB1 released did not directly correlate with tumor burden. Because different types of tumors contain

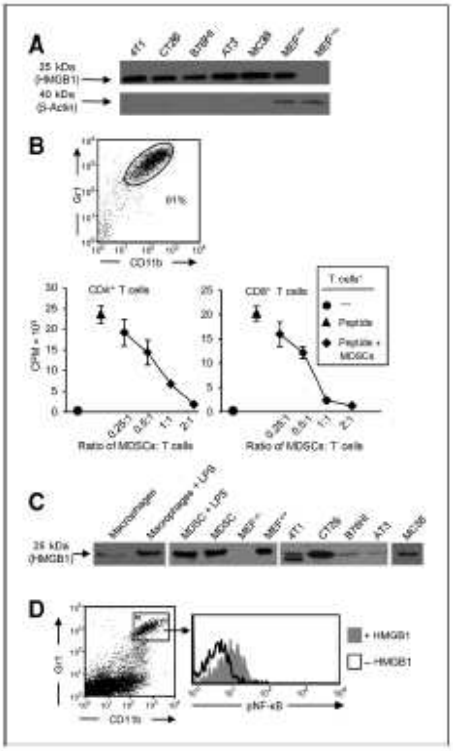

Figure 1. HMGB1 is ubiquitously present in the tumor microenvironment, is secreted by MDSCs, and activates the NF-κB signaling pathway in MDSCs. A, 4T1, CT26, B78H1, AT3, and MC38 tumor cells were cultured in serum-free medium and their supernatants assessed by Western blot analysis for secreted HMGB1. Lysates of wild-type and HMGB1-knocked out MEF cells served as positive and negative controls. B, BALB/c 4T1-induced Gr1$^+$CD11b$^+$ MDSCs were obtained from the blood of tumor-bearing mice, stained for Gr1 and CD11b to assess purity, and cocultured with transgenic CD4$^+$ (DO11.10) or CD8$^+$ (clone 4) splenocytes. Splenocytes were activated with OVA or HA peptide for DO11.10 and clone 4 cells, respectively. T-cell proliferation was measured by [^{3}H] thymidine incorporation. Data are expressed as cpm of triplicate cultures. C, LPS-treated and untreated macrophages and MDSCs, and excised, dissociated tumors of BALB/c (4T1, CT26) and C57BL/6 (B78H, AT3, MC38) mice were cultured overnight in serum-free medium. Resulting supernatants were assessed by Western blot analysis for HMGB1. D, leukocytes from tumor-free BALB/c mice were treated with or without HMGB1 and stained for Gr1, CD11b, and pNF-κB. Gr1$^+$CD11b$^+$ cells were gated and analyzed for pNF-κB. Data are from one of three, two, three, and three independent experiments for A, B, C, and D, respectively.

different quantities of HMGB1-producing cells and necrotic cells (i.e., tumor cells, macrophages, MDSCs, etc.), it is not unexpected that HMGB1 levels are not proportional to tumor mass.

HMGB1 binds to multiple receptors, including two receptors that are expressed by MDSCs: TLR4 (2,2) and Receptor for Advanced Glycation Endproducts (RAGE; ref. 23). Signaling through both of these receptors converges on the NF-κB signal transduction pathway. To determine whether HMGB1 activates MDSCs, leukocytes from the blood of tumor-free BALB/c mice were cultured with or without HMGB1, subsequently stained for phosphorylated NF-κB (pNF-κB), and the Gr1$^+$ CD11b$^+$ cells gated and analyzed for pNF-κB (Fig. 1D). HMGB1 treatment caused phosphorylation of NF-κB.

To confirm the specificity of the pNF-κB staining, macrophages from either TLR4$^{+/+}$ or TLR4$^{-/-}$ mice were treated with either LPS or TNFα. If the pNF-κB mAb is specific, then TNFα will activate NF-κB in both TLR4$^{+/+}$ and TLR4$^{-/-}$ cells because it acts via the TNFα receptor. In contrast, NF-κB will only be activated by LPS in TLR4$^{+/+}$ cells, because LPS activates NF-κB via TLR4. TNFα activated NF-κB in both TLR4$^{+/+}$ and TLR4$^{-/-}$ cells, whereas LPS activated NF-κB in TLR4$^{+/+}$, but not TLR4$^{-/-}$ cells, confirming the specificity of the pNF-κB mAb (Supplementary Fig. S1).

These data indicate that HMGB1 is ubiquitously present *in vivo* in the tumor microenvironment, multiple cell populations within the tumor microenvironment produce HMGB1, MDSCs contribute to the production of HMGB1, and HMGB1 activates the NF-κB signal transduction pathway in MDSCs.

HMGB1 drives the differentiation of MDSCs from bone marrow progenitor cells

Because the differentiation, accumulation, and function of MDSCs are driven by inflammation (8, 20, 24, 25), HMGB1 may regulate MDSCs by either controlling their accumulation and/or affecting their functional activities. To assess whether HMGB1 affects MDSC differentiation, bone marrow cells from the femurs of healthy BALB/c mice were cultured under conditions that drive the differentiation of MDSCs (18). The HMGB1 inhibitors ethyl pyruvate and glycyrrhizin were included in some cultures. Ethyl pyruvate prevents extracellular secretion of HMGB1 from activated monocytes and macrophages by blocking NF-κB signaling (26). Glycyrrhizin prevents the binding of extracellular HMGB1 by attaching to two distinct regions of HMGB1 (27). At the end of the 4-day culture period, the presence of HMGB1 was confirmed by Western blot analysis (Fig. 2A) and quantified by ELISA (Supplementary Table S1), and the absolute number of Gr1^{mid}CD11b$^+$ cells was determined by cell counting and flow cytometry (Fig. 2B). At the start of culture, 5.5×10^4 cells were Gr1^{mid}CD11b$^+$. At the end of the culture period, the vehicle control–treated cultures contained 16×10^5 Gr1^{mid}CD11b$^+$ cells, indicating that MDSCs had expanded by almost 3-fold. Both HMGB1 inhibitors significantly reduced the absolute number of MDSCs (Fig. 2C and Supplementary Table S2). The highest dose of glycyrrhizin reduced the number of Gr1^{mid}CD11b$^+$ cells by 82%, whereas ethyl pyruvate reduced the number by 80%. Gr1$^+$CD11b$^+$ MDSCs induced under these conditions were just as suppressive as tumor-induced MDSCs isolated from mice with 4T1 tumors (Fig. 2D). Glycyrrhizin and ethyl pyruvate also decreased the generation of DC (CD11c$^+$ cells, 43% and 67%, respectively) and macrophages (F4/80$^+$CD11b$^+$ cells, 66% and 68%, respectively), consistent with published reports showing that HMGB1 also drives the maturation of these cells (28). In contrast, B cells (B220$^+$ cells) and T cells (CD3$^+$ cells) were either not affected or only minimally decreased.

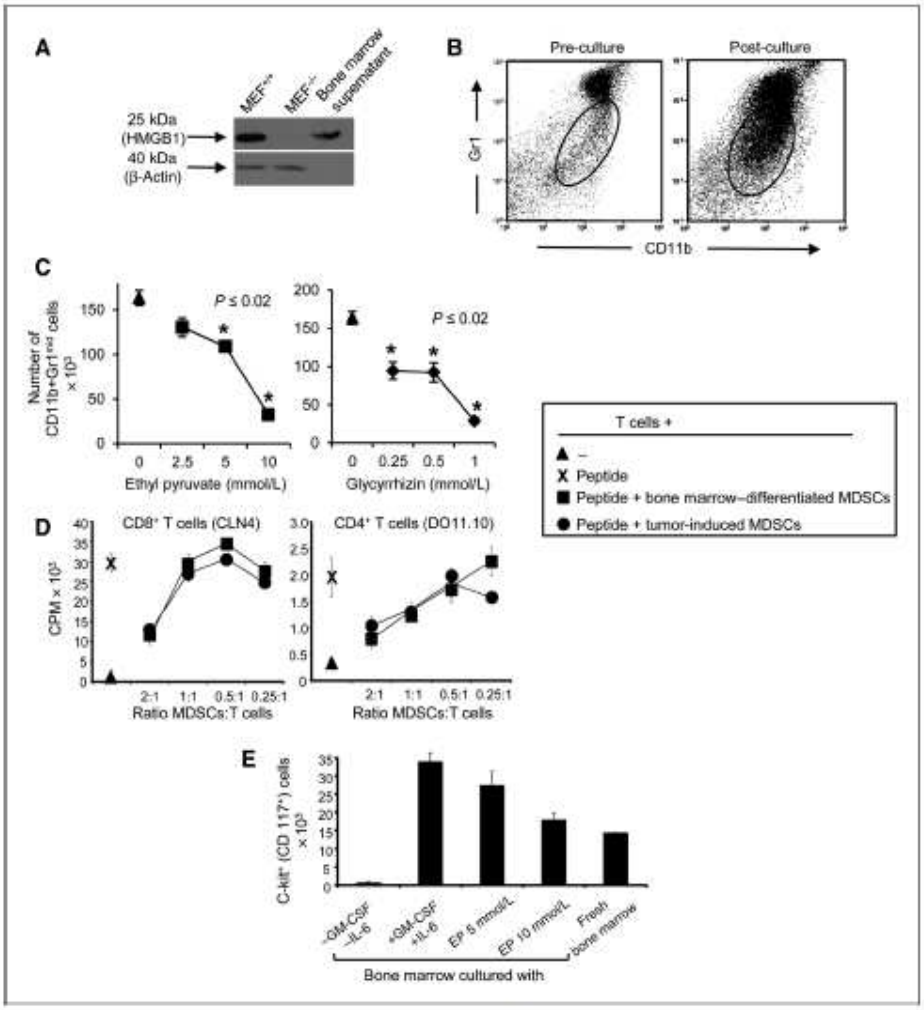

Figure 2. HMGB1 drives the differentiation of MDSCs from bone marrow progenitor cells. Bone marrow cells were harvested from the femurs of healthy BALB/c mice and cultured with IL-6 and GM-CSF with or without ethyl pyruvate, glycyrrhizin, or vehicle. After 4 days of culture, the absolute number of MDSCs was determined. A, HMGB1 Western blot analysis of supernatants of bone marrow cultures. B, gating logic of $Gr1^{mid}CD11b^{+}$ MDSCs from precultured and postcultured bone marrow cells. C, absolute number of $Gr1^{mid}CD11b^{+}$ MDSCs in the bone marrow cultures after incubation with ethyl pyruvate or glycyrrhizin. D, MDSCs generated in the bone marrow cultures were assessed for suppressive activity against antigen-specific MHC-restricted transgenic $CD4^{+}$ and $CD8^{+}$ T cells. E, bone marrow cells were cultured under MDSC differentiation conditions (GM-CSF + IL-6) ± ethyl pyruvate (EP) and analyzed for the percent of c-kit^{+} ($CD117^{+}$) progenitor cells. *P* values were obtained by the Student *t* test. Data are from one of three and two independent experiments for A–C and D and E, respectively. *, $P < 0.02$ versus vehicle-treated control.

To determine whether inhibition of HMGB1 reduces MDSC accumulation by inhibiting the proliferation of MDSC progenitor cells or by causing apoptosis of differentiated MDSCs, bone marrow cells and matured MDSCs were vehicle or ethyl pyruvate treated, and the levels of c-kit^{+} (CD117) progenitor cells and Annexin $V^{+}PI^{+}$ apoptotic cells were determined by flow cytometry (Fig. 2E and Supplementary Fig. S2A). Ethyl pyruvate reduced the level of progenitor cells but did not

induce apoptosis as compared with vehicle treatment. These data indicate that HMGB1 facilitates the expansion of myeloid cells, including MDSCs, from bone marrow progenitor cells.

HMGB1 contributes to the ability of MDSCs to suppress antigen-driven T-cell activation

MDSCs use multiple mechanisms to suppress antitumor immunity. Suppression of antigen-driven T-cell activation was one of the first mechanisms identified (29, 30). To determine whether HMGB1 impacts MDSC suppression of T-cell activation, MDSCs from 4T1 tumor-bearing BALB/c mice were tested for their ability to prevent the proliferation of transgenic $CD4^+$ (DO11.10) or $CD8^+$ (clone 4) T cells activated with cognate peptides (Fig. 3A). Increasing concentrations of the HMGB1 inhibitor ethyl pyruvate restored T-cell activation in the presence of MDSCs. Because ethyl pyruvate prevents signaling through NF-κB and T-cell activation requires NF-κB signaling (31), transgenic T cells were treated with ethyl pyruvate to ascertain that these doses were not affecting T-cell proliferation (Fig. 3B). Ethyl pyruvate did not increase T-cell activation in the absence of MDSCs, demonstrating that the increase in T-cell activation seen in Fig. 3A is an effect of ethyl pyruvate on MDSCs and not an effect on T cells.

To determine how ethyl pyruvate inhibits MDSCs, vehicle and ethyl pyruvate–treated MDSCs were assayed by flow cytometry for their content of molecules that mediate T-cell suppression (arginase, iNOS, and H_2O_2), and for its impact on MDSC viability. Ethyl pyruvate did not decrease arginase or iNOS levels or alter MDSC apoptosis levels (Supplementary Fig. S2B and S2C), but modestly reduced H_2O_2 levels (Supplementary Fig. S2D) as compared with vehicle-treated cells. In previous studies, another NF-κB inhibitor, Withaferin A, also reduced the suppressive potency of MDSCs (19). These results suggest that HMGB1 contributes to MDSC-mediated T-cell suppression by increasing their expression of H_2O_2.

HMGB1 increases MDSC production of IL-10 and MDSC–macrophage crosstalk

One of the mechanisms MDSCs use to inhibit antitumor immunity is their production of IL-10. MDSC-produced IL-10 reduces macrophage production of IL-12, thereby skewing macrophages toward a type II tumor–promoting phenotype (3). Crosstalk between MDSCs and macrophages increases MDSC production of IL-10, thereby contributing to MDSC suppression. MDSC-produced IL-10 also drives the differentiation and accumulation of T regulatory cells (32), further increasing immune suppression. To determine whether HMGB1 drives MDSC production of IL-10 or MDSC–macrophage crosstalk with respect to IL-10, MDSCs and macrophages were cocultured with or without ethyl pyruvate and glycyrrhizin and IL-10 production was measured (Fig. 4A). Both ethyl pyruvate and glycyrrhizin dose dependently reduced the production of IL-10 by MDSCs and by mixtures of MDSCs plus macrophages. To ascertain that MDSCs, rather than macrophages, are the producers of IL-10, macrophages and MDSCs from IL-10–deficient BALB/c mice were used in conjunction with MDSCs or macrophages, respectively, from wild-type BALB/c mice (Fig. 4B). Only marginal

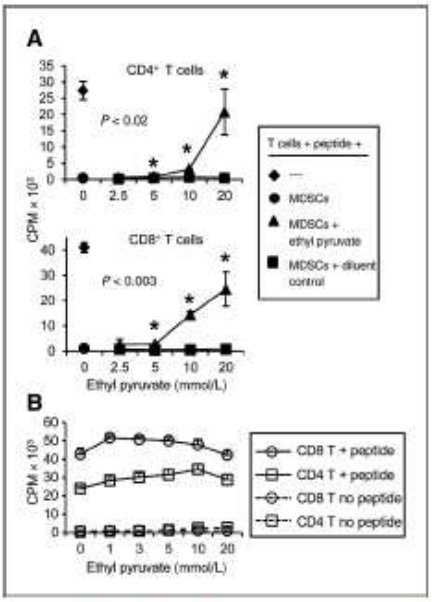

Figure 3. HMGB1 contributes to the ability of MDSCs to suppress antigen-driven T-cell activation. Splenocytes from $CD4^+$ DO11.10 TCR or $CD8^+$ clone 4 TCR transgenic mice were cocultured with irradiated 4T1-induced MDSCs from BALB/c mice and cognate peptide (OVA or HA peptide for DO11.10 and clone 4 T cells, respectively). A, T-cell proliferation was measured by (^{3}H)-thymidine incorporation in the presence of titered amounts of ethyl pyruvate or vehicle control. B, ethyl pyruvate does not directly affect T-cell activation. Transgenic DO11.10 and clone 4 T cells were activated with cognate peptide in the presence of titered amounts of ethyl pyruvate. Data are from one of two independent experiments. *P* values were obtained by the Student *t* test comparing ethyl pyruvate–treated samples versus the respective diluent control samples. *, $P < 0.02$ or $P < 0.003$ versus vehicle-treated control.

levels of IL-10 were detected in cultures containing $IL\text{-}10^{-/-}$ MDSCs with wild-type macrophages, demonstrating that MDSCs are the cells producing the IL-10. The reduction of IL-10 is not due to reduced MDSC viability because ethyl pyruvate–treated MDSCs cultured under the crosstalk conditions (with 5% serum) are more viable than vehicle-treated MDSCs (Supplementary Fig. S2C). These findings indicate that HMGB1 regulates MDSC production of IL-10 and macrophage-induced increases in MDSC production of IL-10.

MDSCs also promote a type II immune response by down regulating macrophage production of IL-12 (3) and IL-6 (unpublished). To determine whether HMGB1 mediates either of these effects, MDSCs and macrophages were cocultured with or without ethyl pyruvate and glycyrrhizin and IL-12 and IL-6 were quantified by ELISA (Fig. 5). Ethyl pyruvate and glycyrrhizin reduced macrophage production of IL-12 and IL-6, and did not restore production of these cytokines in MDSC–macrophage cocultures. IL-1β, a

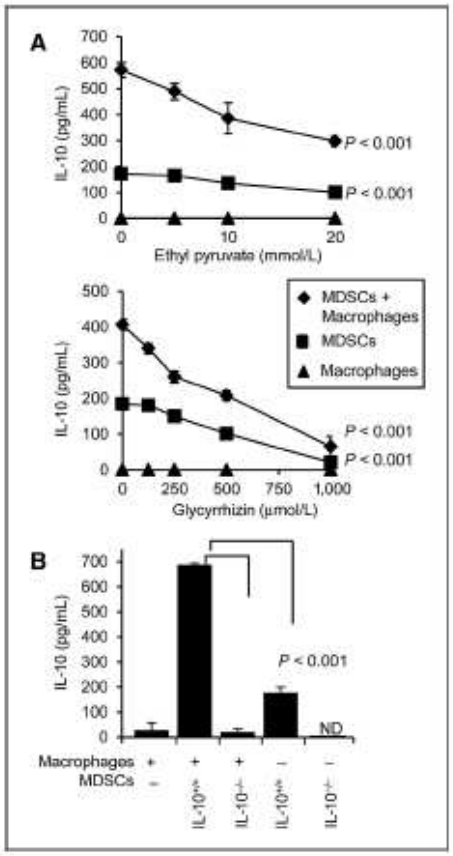

Figure 4. HMGB1 increases MDSC production of IL-10 and MDSC–macrophage crosstalk. A, cocultures of 4T1-induced BALB/c MDSCs and macrophages from tumor-free mice were incubated with or without ethyl pyruvate or glycyrrhizin, and the supernatants were assayed by ELISA for IL-10. B, MDSCs from 4T1-tumor-bearing BALB/c and BALB/c IL-10$^{-/-}$ mice and peritoneal macrophages from tumor-free BALB/c mice were cocultured and the supernatants were assayed by ELISA for IL-10. ND, nondetectable levels of protein. Data are from one of six and three independent experiments for A and B, respectively. *P* values were obtained by single-factor ANOVA.

proinflammatory cytokine that is produced by MDSCs and also drives the suppressive potency of MDSCs (33, 34), was also assessed. Ethyl pyruvate and glycyrrhizin decreased MDSC production of IL-1β; however, HMGB1 inhibition restored IL-1β levels in cocultures of MDSCs and macrophages. These results indicate that HMGB1 regulates MDSC production of IL-1β during MDSC–macrophage crosstalk; however, it is not involved in MDSC-mediated downregulation of macrophage-produced IL-12 or IL-6.

Neutralization of HMGB1 delays tumor growth and reduces MDSCs in tumor-bearing mice

HMGB1 includes two functional domains: the proinflammatory B box and the anti-inflammatory A box. The B box is a RAGE agonist, whereas the A box is an HMGB1 antagonist (13). Although the A box is a competitor for the B box, the B box of HMGB1 is dominant *in vivo* (27). However, if administered *in vivo* as a recombinant protein, A box neutralizes endogenous HMGB1 (14). To determine whether A box impacts tumor progression, BALB/c and C57BL/6 mice bearing 4T1 or MC38 tumor, respectively, were treated with A box or vehicle control starting when the tumors were first palpable (approximate day 7–9 after tumor cell inoculation; Fig. 6A). In both strains, A box delayed tumor progression, supporting the concept that HMGB1 facilitates tumor growth. 4T1 tumor cells were also knocked down by shRNA for HMGB1 (4T1/575 cells) and their tumorigenicity compared with that of 4T1 cells transfected with an irrelevant shRNA (4T1/irrelevant; Supplementary Fig. S3A). The effect of HMGB1 on spontaneous metastatic disease was assessed by treating 4T1 tumor-bearing mice with glycyrrhizin and ethyl pyruvate and assessing the number of metastatic cells by clonogenic assay (Supplementary Fig. S3B; ref. 35). 4T1/575 tumor–bearing mice survived significantly longer than mice with 4T1/irrelevant cells supporting previously published work (36). Tumor-bearing mice treated with the inhibitors trended toward fewer metastatic cells; however, the values were not statistically significantly different. These results further confirm that HMGB1 enhances tumor progression.

To determine whether HMGB1 drives MDSC accumulation *in vivo*, tumor-bearing mice were treated with a neutralizing HMGB1 mAb (2G7), and tumor-infiltrating MDSCs and MDSCs from the blood and spleen were compared with MDSCs in vehicle-treated tumor-bearing mice. C57BL/6 mice were inoculated with the MC38 tumor on day 1 and 2G7 treatment was started on days 10 to 13. Mice were sacrificed at a late stage of disease when their primary tumors were approximately the same diameter, and total MDSCs, monocytic MDSCs, and granulocytic MDSC levels in the blood, spleen, and infiltrating the tumors were determined by flow cytometry (Fig. 6B). Total, monocytic, and granulocytic MDSCs were reduced in the spleens, blood, and tumors of 2G7-treated mice with the exception of tumor-infiltrating granulocytic MDSCs. These decreases were not a secondary effect of reduced tumor size since, at the time of analysis, the 2G7-treated and control-treated mice had similar-sized primary tumors. MDSCs were similarly reduced in the blood of A box–treated tumor-bearing mice. These results indicate that *in vivo*, neutralization of HMGB1 reduces the accumulation of MDSCs in tumor-bearing mice.

Tumors from the HMGB1 mAb–treated (2G7) and isotype control–treated mice of Fig. 6 were assessed by IHC for the presence of CD3$^+$ T cells (Supplementary Fig. S4). Both types of tumors contained few T cells; however, there was a trend toward more CD3$^+$ cells in the tumors of 2G7-treated mice.

HMGB1 downregulates T-cell expression of L-selectin

MDSCs also impair T-cell immunity by perturbing the homing of naïve T cells to lymph nodes where they could become activated. To enter lymph nodes, naïve T cells must first be tethered via

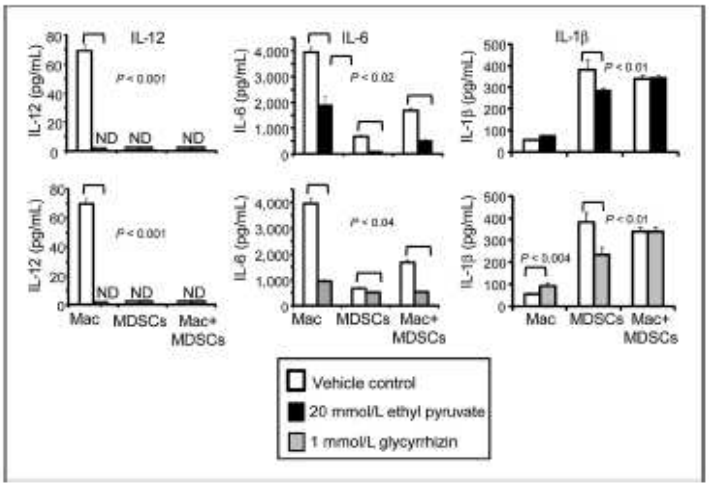

Figure 5. HMGB1 facilitates downregulation of IL-6 and MDSC production of IL-1β, but does not alter MDSC-mediated downregulation of macrophage production of IL-12. Cocultures of 4T1-induced BALB/c MDSCs and macrophages from tumor-free mice were incubated with or without ethyl pyruvate or glycyrrhizin and the supernatants were assayed by ELISA for IL-12, IL-6, and IL-1β. ND, nondetectable levels of protein. Data are from one of four, five, and two independent experiments for IL-12, IL-6, and IL-1β, respectively. *P* values were obtained by the Student *t* test.

L-selectin (CD62L) to the walls of high endothelial venules (HEV) so they can extravasate from the bloodstream. Our previous *in vitro* studies showed that MDSCs reduce T cell levels of L-selectin through their constitutive expression of ADAM17 (a disintegrin and metalloproteinase domain 17), an enzyme that cleaves the ectodomain of L-selectin (4). Subsequent *in vivo* vital imaging studies showed that T cells with reduced expression of L-selectin do not enter HEVs (J. Mulnich, S. Ostrand-Rosenberg, S. Abrams, and S. Evans; unpublished data). To determine whether HMGB1 impacts MDSC-mediated downregulation of T cell-expressed L-selectin, A box and control-treated mice were sacrificed 29 days after tumor inoculation and circulating $CD45^+CD3^+CD4^+$ and $CD45^+CD3^+CD8^+$ T cells were analyzed for L-selectin by flow cytometry (Fig. 7A). Circulating $CD4^+$ and $CD8^+$ T cells from tumor-free mice were controls for normal L-selectin expression. L-selectin was reduced in $CD4^+$ and $CD8^+$ T cells of tumor-bearing vehicle-treated mice, whereas A box treatment partially restored L-selectin expression (Fig. 7B). To confirm that HMGB1 acts on MDSCs to reduce L-selectin, $Gr1^+CD11b^+$ cells from tumor-free and tumor-bearing mice were treated for 0, 2, or 4 hours with HMGB1 or ethyl pyruvate, respectively. The cells were then stained with mAbs to Gr1, CD11b, and ADAM17, and the gated $Gr1^+CD11b^+$ cells were analyzed for plasma membrane expression of ADAM17 (Fig. 7C). HMGB1-treated $Gr1^+CD11b^+$ cells from tumor-free mice expressed more ADAM17, whereas ethyl pyruvate–treated MDSCs from tumor-bearing mice had less ADAM17, as compared with vehicle-treated cells. These observations indicate that plasma membrane ADAM17 turns over on MDSCs and that HMGB1 contributes to the downregulation of L-selectin on T cells by sustaining MDSC expression of ADAM17.

Discussion

The DAMP and alarmin HMGB1 is released by many tumor cells, is elevated in the serum of many patients with cancer (37), and is recognized as an enhancer of tumor progression by its direct action on tumor cells (9, 10, 28). The studies reported here identify MDSCs, along with tumor cells and macrophages, as producers of HMGB1. The observed decrease in MDSCs of tumor-bearing mice following treatment with HMGB1 inhibitors, combined with the *in vitro* mechanistic studies demonstrate that HMGB1 (i) promotes the differentiation of MDSCs from bone marrow progenitor cells; (ii) increases MDSC–macrophage crosstalk and MDSC production of IL-10; and (iii) increases MDSC-mediated downregulation of L-selectin on naïve T cells. These findings support the conclusion that HMGB1 contributes to the elevation and suppressive potency of MDSCs in tumor-bearing mice, and identify a new proinflammatory mediator that regulates MDSCs.

HMGB1 is likely to activate and drive MDSCs because it induces, chaperones, and/or enhances the activity of several proinflammatory molecules that regulate MDSCs. For example, IL-1β drives MDSC accumulation and T-cell suppressive activity (33, 38) and is induced by HMGB1 (14). Complexes of HMGB1 and IL-1β have increased proinflammatory activity relative to either molecule alone (39). HMGB1 also enhances the proinflammatory activity of IL-6 (40), TNFα (14), and prostaglandin E2 (41), three other proinflammatory mediators that drive MDSCs (24, 34, 42, 43). Although neutralization of HMGB1 significantly downregulates MDSC-suppressive activity, it does not globally neutralize MDSCs, most likely because the multiple proinflammatory mediators that drive MDSCs are redundant and can also be regulated by molecules other than HMGB1.

HMGB1 is known to facilitate tumor progression by co-opting other immune cells and by directly affecting tumor cell growth (9, 10, 28). It increases the accumulation of T regulatory cells and diverts type I T helper cells to a protumor type II phenotype (36, 44). HMGB1 also acts directly on tumor cells to enhance tumor progression by binding to tumor cell–expressed RAGE. Many tumor cells express RAGE (45), and the binding of

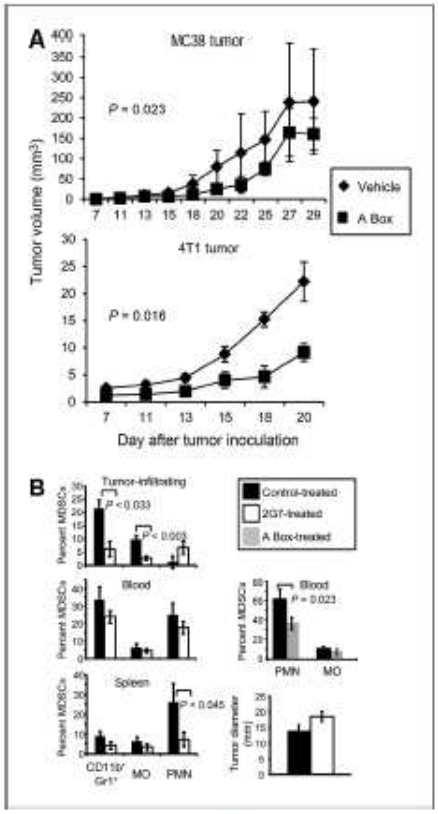

Figure 6. Tumor-bearing mice treated with mAbs to HMGB1 or with A box have reduced levels of MDSCs. A, C57BL/6 and BALB/c mice were inoculated subcutaneously with 5×10^5 MC38 colon carcinoma cells or in the mammary fat pad with 7×10^3 4T1 mammary carcinoma cells, respectively. Mice were given recombinant A box (300 μg/mouse) or vehicle (PBS) three times per week starting when tumors were first palpable (day 7–9 postinoculation). *P* values were obtained by the log-rank test. B, C57BL/6 mice were inoculated as in A. Treatment with 2G7 (5 μg/200 μL/mouse, 3×/week), irrelevant IgG, or A box was started on days 10 to 13 when tumors were first palpable. Treatment was terminated on day 45 and blood leukocytes were analyzed by flow cytometry for total ($Gr1^+CD11b^+$), monocytic (MO; $CD11b^+Ly6G^-Ly6C^+$), and granulocytic (PMN; $CD11b^+Ly6G^+Ly6C^-$) MDSCs. Mice were sacrificed on day 50 when their tumors were approximately the same size, and spleen and tumor-infiltrating leukocytes ($CD45^+$ cells) were analyzed by flow cytometry. $n = 7$ (blood, control treated for 2G7), 4 (A box, PBS treated), 6 (tumor-infiltrating and spleen, control-treated; blood, 2G7-treated), 4 (tumor-infiltrating and spleen, 2G7-treated), and 4 (A box-treated) mice/group. Data for 2G7 and their control-treated mice are pooled from two independent experiments; data for A box and their control-treated mice are from a single experiment.

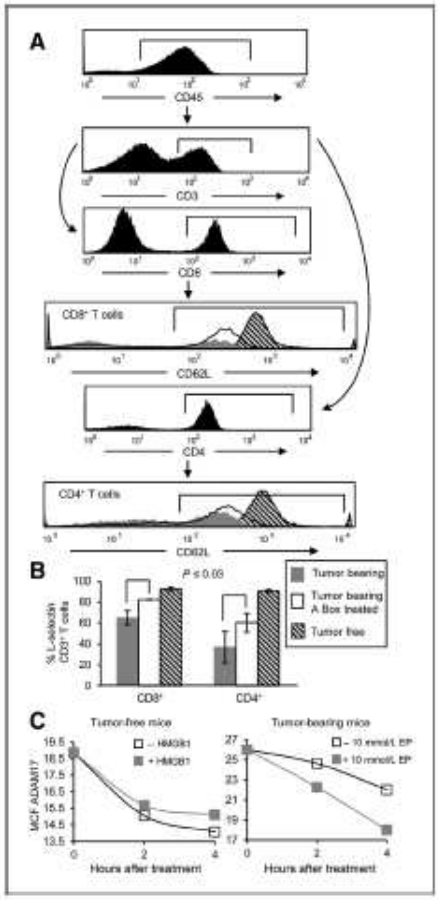

Figure 7. HMGB1 downregulates T-cell expression of L-selectin. A, twenty-nine days after tumor inoculation, the MC38 tumor-bearing mice from Fig. 6A were sacrificed and blood leukocytes were analyzed by flow cytometry for L-selectin expression and compared with blood leukocytes from tumor-free C57BL/6 mice. Representative histograms showing L-selectin expression from gated $CD45^+CD3^+CD4^+$ and $CD45^+CD3^+CD8^+$ T cells from tumor-free, A box–treated, or control-treated (PBS) C56BL/6 tumor-bearing mice. B, average percent ± SD of $CD45^+CD3^+CD4^+$ or $CD45^+CD3^+CD8^+$ T cells expressing L-selectin. $n = 5$ mice/group (PBS-treated and tumor-free groups); $n = 3$ mice/group (A box–treated group). *P* values were obtained by the Student *t* test. Data are from one of two independent experiments. C, $Gr1^+CD11b^+$ cells from tumor-free (left) or tumor-bearing (right) mice were incubated *in vitro* for 0, 2, or 4 hours with exogenous HMGB1 (left) or ethyl pyruvate (right) and stained for Gr1, CD11b, and ADAM17. Gated $Gr1^+CD11b^+$ cells were analyzed for ADAM17 expression. Graphs represent MCF of ADAM17 on $Gr1^+$ $CD11b^+$ cells. Data are representative of three independent experiments.

HMGB1 to RAGE promotes tumor cell autophagy, inhibits tumor cell apoptosis, and increases tumor cell invasiveness (46, 47). Collectively, these effects produce an immune suppressive and protumor environment. MDSCs contribute to tumor growth through their immune suppressive mechanisms. However, their elimination may not be sufficient for tumor rejection, and active immunization of T cells and/or repolarization of macrophages to a M1-like phenotype may also be required (17). The studies reported here demonstrate that HMGB1 affects MDSC development and function. Because HMGB1 affects tumor progression through multiple mechanisms that act on both tumor cells and immune cells, its effects on MDSCs represent only one of its modes of action.

Paradoxically, under some conditions, HMGB1 facilitates the activation of tumor-reactive T cells. HMGB1 facilitates dendritic cell maturation (48) and enhances DC-mediated antigen presentation during chemotherapy and radiotherapy (49). In contrast with the protumor effects of HMGB1, which are thought to be transmitted through RAGE, the enhancement of DC function requires the release of HMGB1 by dead tumor cells and is mediated through DC-expressed TLR4. Whether the *in vivo* protumor or antitumor effects of HMGB1 balance each other, or whether one dominates is unclear. However, the potential for HMGB1 to both inhibit and promote antitumor immunity makes it difficult to evaluate whether neutralization of HMGB1 will be beneficial or harmful.

The quantity of HMGB1 within different solid tumors differs significantly (see Supplementary Table S1). MDSCs, macrophages, tumor-infiltrating cells, and tumor cells themselves all contribute to the amount of HMGB1 in the tumor microenvironment. Live tumor cells secrete HMGB1, whereas necrotic tumor cells induced by suboptimal vascularization and hypoxia release nuclear HMGB1. Because the quantity of tumor-infiltrating cells and the extent of vascularization and hypoxia differ in different types of tumors, it is not unexpected that the quantity of HMGB1 within solid tumors does not correlate with tumor mass.

HMGB1 binds to both TLR4 and RAGE, and MDSCs express both receptors (20, 50). TLR4 and RAGE signaling converges at NF-κB (9, 10, 28, 51), so that activation through either receptor may produce similar effects. Previous studies demonstrated that MDSC production of IL-10 is regulated by TLR4 (50). In the current report, A box partially restores T-cell expression of L-selectin, suggesting that this effect of MDSCs may be regulated through RAGE. The HMGB1 inhibitors ethyl pyruvate and glycyrrhizin reduced MDSC production of IL-10 during MDSC–macrophage crosstalk and the differentiation of MDSCs from bone marrow progenitor cells, and ethyl pyruvate restored T-cell activation in the presence of MDSCs. These reagents either bind exogenous HMGB1 (glycyrrhizin) or inhibit NF-κB signaling (ethyl pyruvate) and therefore do not distinguish whether HMGB1 is acting through TLR4 or RAGE. Regardless of which receptor is utilized, HMGB1 is a potent inducer of MDSCs and immune suppression, and both its protumor and antitumor activities must be considered when designing cancer immunotherapies.

Disclosure of Potential Conflicts of Interest

No potential conflicts of interest were disclosed.

Authors' Contributions

Conception and design: K. Parker, P. Sinha, S. Ostrand-Rosenberg
Development of methodology: K. Parker, P. Sinha, J. Li, K.J. Tracey, S. Ostrand-Rosenberg
Acquisition of data (provided animals, acquired and managed patients, provided facilities, etc.): K. Parker, P. Sinha, L.A. Horn, V.K. Clements, J. Li, S. Ostrand-Rosenberg
Analysis and interpretation of data (e.g., statistical analysis, biostatistics, computational analysis): K. Parker, P. Sinha, L.A. Horn, S. Ostrand-Rosenberg
Writing, review, and/or revision of the manuscript: K. Parker, P. Sinha, H. Yang, S. Ostrand-Rosenberg
Administrative, technical, or material support (i.e., reporting or organizing data, constructing databases): K. Parker, P. Sinha, H. Yang, S. Ostrand-Rosenberg
Study supervision: S. Ostrand-Rosenberg

Acknowledgments

The authors thank Ms. Inna Berkhatmer for her excellent care of their mice, Ms. Julie Wolf for help with the cloning, Dr. James Thompson for generating the original shRNA irrelevant control construct, and Dr. Michael Iotze for providing the wild-type and HMGB1-knockout MEF cells.

Grant Support

This work was supported by NIH grants RO1CA115880, RO1CA84232 (S. Ostrand-Rosenberg), and RO1GM090446 (H. Yang). K. Parker and L.A. Horn were partially supported by U.S. Department of Education grant P200A090094-11.

The costs of publication of this article were defrayed in part by the payment of page charges. This article must therefore be hereby marked advertisement in accordance with 18 U.S.C. Section 1734 solely to indicate this fact.

Received August 15, 2013; revised June 26, 2014; accepted July 24, 2014; published OnlineFirst August 27, 2014.

References

1. Gabrilovich DI, Bronte V, Chen SH, Colombo MP, Ochoa A, Ostrand-Rosenberg S, et al. The terminology issue for myeloid-derived suppressor cells. Cancer Res 2007;67:425.
2. Gabrilovich DI, Nagaraj S. Myeloid-derived suppressor cells as regulators of the immune system. Nat Rev Immunol 2009;9:162–74.
3. Sinha P, Clements VK, Bunt SK, Albelda SM, Ostrand-Rosenberg S. Cross-talk between myeloid-derived suppressor cells and macrophages subverts tumor immunity toward a type 2 response. J Immunol 2007;179:977–83.
4. Hanson EM, Clements VK, Sinha P, Ilkovitch D, Ostrand-Rosenberg S. Myeloid-derived suppressor cells down-regulate L-selectin expression on CD4+ and CD8+ T cells. J Immunol 2009;183:937–44.
5. Yang L, DeBusk LM, Fukuda K, Fingleton B, Green-Jarvis B, Shyr Y, et al. Expansion of myeloid immune suppressor Gr+CD11b+ cells in tumor-bearing host directly promotes tumor angiogenesis. Cancer Cell 2004;6:409–21.
6. Yang L, Huang J, Ren X, Gorska AE, Chytil A, Aakre M, et al. Abrogation of TGF beta signaling in mammary carcinomas recruits Gr-1+CD11b+ myeloid cells that promote metastasis. Cancer Cell 2008;13:23–35.
7. Balkwill F, Mantovani A. Inflammation and cancer: back to Virchow? Lancet 2001;357:539–45.
8. Ostrand-Rosenberg S, Sinha P. Myeloid-derived suppressor cells: linking inflammation and cancer. J Immunol 2009;182:4499–506.
9. Sims GP, Rowe DC, Rietdijk ST, Herbst R, Coyle AJ. HMGB1 and RAGE in inflammation and cancer. Annu Rev Immunol 2010;28:367–88.
10. Lotze MT, Tracey KJ. High-mobility group box 1 protein (HMGB1): nuclear weapon in the immune arsenal. Nat Rev Immunol 2005;5:331–42.

11. Wang H, Bloom O, Zhang M, Vishnubhakat JM, Ombrellino M, Che J, et al. HMG-1 as a late mediator of endotoxin lethality in mice. Science 1999;285:248–51.
12. Li J, Kokkola R, Tabibzadeh S, Yang R, Ochani M, Qiang X, et al. Structural basis for the proinflammatory cytokine activity of high mobility group box 1. Mol Med 2003;9:37–45.
13. Yang H, Tracey KJ. Targeting HMGB1 in inflammation. Biochim Biophys Acta 2010;1799:149–56.
14. Yang H, Ochani M, Li J, Qiang X, Tanovic M, Harris HE, et al. Reversing established sepsis with antagonists of endogenous high-mobility group box 1. Proc Natl Acad Sci U S A 2004;101:296–301.
15. Stewart TJ, Abrams SI. Altered immune function during long-term host-tumor interactions can be modulated to retard autochthonous neoplastic growth. J Immunol 2007;179:2851–9.
16. Calogero S, Grassi F, Aguzzi A, Voigtlander T, Ferrier P, Ferrari S, et al. The lack of chromosomal protein Hmg1 does not disrupt cell growth but causes lethal hypoglycaemia in newborn mice. Nat Genet 1999;22:276–80.
17. Sinha P, Clements VK, Ostrand-Rosenberg S. Reduction of myeloid-derived suppressor cells and induction of M1 macrophages facilitate the rejection of established metastatic disease. J Immunol 2005;174:636–45.
18. Marigo I, Bosio E, Solito S, Mesa C, Fernandez A, Dolcetti L, et al. Tumor-induced tolerance and immune suppression depend on the C/EBPbeta transcription factor. Immunity 2010;32:790–802.
19. Sinha P, Ostrand-Rosenberg S. Myeloid-derived suppressor cell function is reduced by Withaferin A, a potent and abundant component of Withania somnifera root extract. Cancer Immunol Immunother 2013;62:1663–73.
20. Sinha P, Okoro C, Foell D, Freeze HH, Ostrand-Rosenberg S, Srikrishna G. Proinflammatory S100 proteins regulate the accumulation of myeloid-derived suppressor cells. J Immunol 2008;181:4666–75.
21. Andersson U, Wang H, Palmblad K, Aveberger AC, Bloom O, Erlandsson-Harris H, et al. High mobility group 1 protein (HMG-1) stimulates proinflammatory cytokine synthesis in human monocytes. J Exp Med 2000;192:565–70.
22. Park JS, Svetkauskaite D, He Q, Kim JY, Strassheim D, Ishizaka A, et al. Involvement of toll-like receptors 2 and 4 in cellular activation by high mobility group box 1 protein. J Biol Chem 2004;279:7370–7.
23. Kokkola R, Andersson A, Mullins G, Ostberg T, Treutiger CJ, Arnold B, et al. RAGE is the major receptor for the proinflammatory activity of HMGB1 in rodent macrophages. Scand J Immunol 2005;61:1–9.
24. Sinha P, Clements VK, Fulton AM, Ostrand-Rosenberg S. Prostaglandin E2 promotes tumor progression by inducing myeloid-derived suppressor cells. Cancer Res 2007;67:4507–13.
25. Cheng P, Corzo CA, Luetteke N, Yu B, Nagaraj S, Bui MM, et al. Inhibition of dendritic cell differentiation and accumulation of myeloid-derived suppressor cells in cancer is regulated by S100A9 protein. J Exp Med 2008;205:2235–49.
26. Ulloa L, Ochani M, Yang H, Tanovic M, Halperin D, Yang R, et al. Ethyl pyruvate prevents lethality in mice with established lethal sepsis and systemic inflammation. Proc Natl Acad Sci U S A 2002;99:12351–6.
27. Yang H, Lundback P, Ottosson L, Erlandsson-Harris H, Venereau E, Bianchi ME, et al. Redox modification of cysteine residues regulates the cytokine activity of high mobility group box-1 (HMGB1). Mol Med 2012;18:250–9.
28. Bianchi ME, Manfredi AA. High-mobility group box 1 (HMGB1) protein at the crossroads between innate and adaptive immunity. Immunol Rev 2007;220:35–46.
29. Bronte V, Apolloni E, Cabrelle A, Ronca R, Serafini P, Zamboni P, et al. Identification of a CD11b(+)/Gr-1(+)/CD31(+) myeloid progenitor capable of activating or suppressing CD8(+) T cells. Blood 2000;96:3838–46.
30. Gabrilovich DI, Velders MP, Sotomayor EM, Kast WM. Mechanism of immune dysfunction in cancer mediated by immature Gr-1+ myeloid cells. J Immunol 2001;166:5398–406.
31. Kontgen F, Grumont RJ, Strasser A, Metcalf D, Li R, Tarlinton D, et al. Mice lacking the c-rel proto-oncogene exhibit defects in lymphocyte proliferation, humoral immunity, and interleukin-2 expression. Genes Dev 1995;9:1965–77.
32. Huang B, Pan PY, Li Q, Sato AI, Levy DE, Bromberg J, et al. Gr-1+CD115+ immature myeloid suppressor cells mediate the development of tumor-induced T regulatory cells and T-cell anergy in tumor-bearing host. Cancer Res 2006;66:1123–31.
33. Bunt SK, Sinha P, Clements VK, Leips J, Ostrand-Rosenberg S. Inflammation induces myeloid-derived suppressor cells that facilitate tumor progression. J Immunol 2006;176:284–90.
34. Bunt SK, Yang L, Sinha P, Clements VK, Leips J, Ostrand-Rosenberg S. Reduced inflammation in the tumor microenvironment delays the accumulation of myeloid-derived suppressor cells and limits tumor progression. Cancer Res 2007;67:10019–26.
35. Pulaski BA, Ostrand-Rosenberg S. Reduction of established spontaneous mammary carcinoma metastases following immunotherapy with major histocompatibility complex class II and B7.1 cell-based tumor vaccines. Cancer Res 1998;58:1486–93.
36. Liu Z, Falo LD Jr, You Z. Knockdown of HMGB1 in tumor cells attenuates their ability to induce regulatory T cells and uncovers naturally acquired CD8T cell-dependent antitumor immunity. J Immunol 2011;187:118–25.
37. Bierman JE, Brown CK, de Vera M, Zeh HJ, Billiar T, Rubartelli A, et al. Masquerader: high mobility group box-1 and cancer. Clin Cancer Res 2007;13:2836–48.
38. Song X, Kraft Y, Dvorkin T, Bjorkdahl O, Segal S, Dinarello CA, et al. CD11b+/Gr-1+ immature myeloid cells mediate suppression of T cells in mice bearing tumors of IL-1beta-secreting cells. J Immunol 2005;175:8200–8.
39. Sha Y, Zmijewski J, Xu Z, Abraham E. HMGB1 develops enhanced proinflammatory activity by binding to cytokines. J Immunol 2008;180:2531–7.
40. Liu JH, Li ZJ, Tang J, Liu YW, Zhao L, Dang P, et al. [High mobility group box-1 protein activates endothelial cells to produce cytokines and has synergistic effect with lipopolysaccharide in inducing interleukin-6 release]. Zhonghua Yi Xue Za Zhi 2006;86:1191–5.
41. Lederer P, Wahamaa H, Idborg H, Jakobsson PJ, Harris HE, Korotkova M. IL-1beta/HMGB1 complexes promote The PGE2 biosynthesis pathway in synovial fibroblasts. Scand J Immunol 2013;77:350–60.
42. Rodriguez PC, Hernandez CP, Quiceno D, Dubinett SM, Zabaleta J, Ochoa JB, et al. Arginase I in myeloid suppressor cells is induced by COX-2 in lung carcinoma. J Exp Med 2005;202:931–9.
43. Sade-Feldman M, Kanterman J, Ish-Shalom E, Elnekave M, Horwitz E, Baniyash M. Tumor necrosis factor-alpha blocks differentiation and enhances suppressive activity of immature myeloid cells during chronic inflammation. Immunity 2013;38:541–54.
44. Wild CA, Bergmann C, Fritz G, Schuler P, Hoffmann TK, Lotfi R, et al. HMGB1 conveys immunosuppressive characteristics on regulatory and conventional T cells. Int Immunol 2012;24:485–94.
45. Gebhardt C, Riehl A, Durchdewald M, Nemeth J, Furstenberger G, Muller-Decker K, et al. RAGE signaling sustains inflammation and promotes tumor development. J Exp Med 2008;205:275–85.
46. Taguchi A, Blood DC, del Toro G, Canet A, Lee DC, Qu W, et al. Blockade of RAGE-amphoterin signalling suppresses tumour growth and metastases. Nature 2000;405:354–60.
47. Livesey KM, Tang D, Zeh HJ, Lotze MT. Not just nuclear proteins: 'novel' autophagy cancer treatment targets - p53 and HMGB1. Curr Opin Investig Drugs 2008;9:1259–63.
48. Messmer D, Yang H, Telusma G, Knoll F, Li J, Messmer B, et al. High mobility group box protein 1: an endogenous signal for dendritic cell maturation and Th1 polarization. J Immunol 2004;173:307–13.
49. Apetoh L, Ghiringhelli F, Tesniere A, Obeid M, Ortiz C, Criollo A, et al. Toll-like receptor 4-dependent contribution of the immune system to anticancer chemotherapy and radiotherapy. Nat Med 2007;13:1050–9.
50. Bunt SK, Clements VK, Hanson EM, Sinha P, Ostrand-Rosenberg S. Inflammation enhances myeloid-derived suppressor cell cross-talk by signaling through Toll-like receptor 4. J Leukoc Biol 2009;85:996–1004.
51. Coffelt SB, Scandurro AB. Tumors sound the alarmin(s). Cancer Res 2008;68:6482–5.

Supp Figure S1

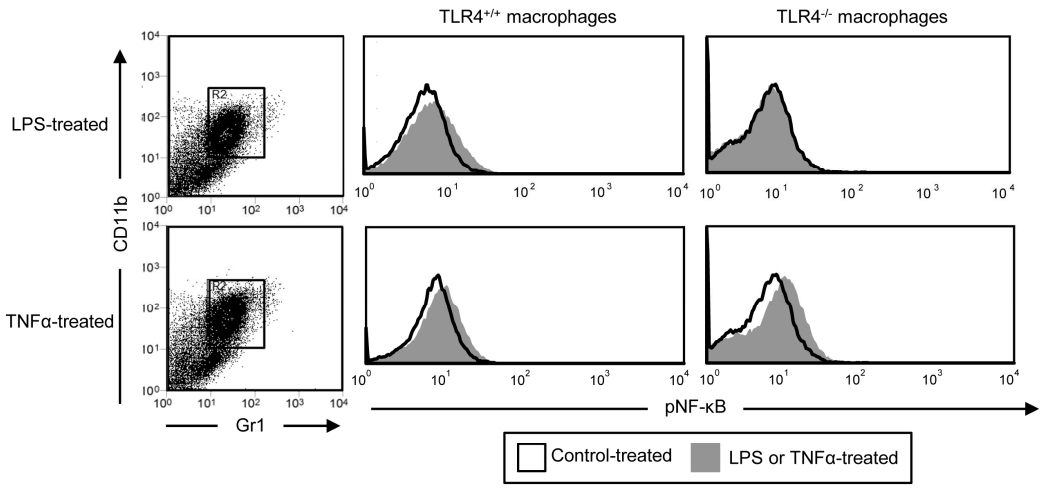

Supplementary Fig. S1. pNF-κB mAb is specific for activated NF-κB. Macrophages were harvested from the peritoneal cavity of TLR4$^{+/+}$ or TLR4$^{-/-}$ tumor-free mice treated with thioglycolate, rested in vitro for two hours, incubated with or without LPS or TNFα, and stained with mAbs to CD11b, F4/80, and pNF-κB. Gated CD11b+F4/80+ macrophages were analyzed for pNF-κB.

Supp Figure S2

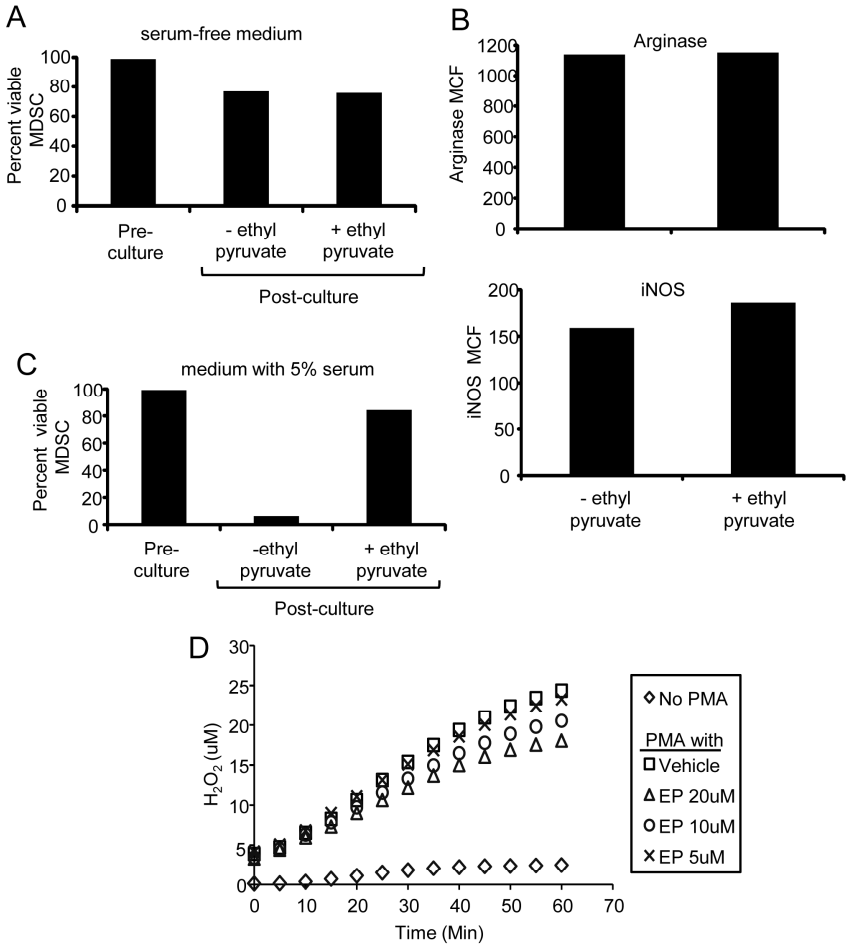

Supplementary Fig. S2. Treatment with ethyl pyruvate does not alter arginase or iNOS expression or induce MDSC apoptosis as compared to control-treated MDSC. MDSC were harvested from BALB/c mice with 4T1 tumor. **A,** MDSC were not cultured (pre-culture) or cultured overnight in serum-free HL-1 medium with or without 10mM EP and then stained with fluorescently coupled mAbs to Gr1 and CD11b, and Annexin V and PI, and the gated $Gr1^+CD11b^+$ cells analyzed by flow cytometry. Percent viable cells = 100%- $\%Gr1^+CD11b^+AnneinV^+ PI^+$. **B,** MDSC were incubated overnight in serum-free media and stained the following day with unlabeled mAbs to arginase or iNOS and goat-anti-mouse IgG-AlexaF647, followed by fluorescently labeled mAbs to Gr1 and CD11b. Gated $Gr1^+CD11b^+$ cells were analyzed by flow cytometry **C,** MDSC were treated as in panel A except cultured in DMEM with 5% serum. Data for each panel are representative of two independent experiments. **D,** HMGB1 increases MDSC content of H_2O_2. MDSC were activated with PMA and treated with vehicle or escalating doses of ethyl pyruvate. H_2O_2 levels were measured using an Amplex Red Hydrogen Peroxide Assay kit.

Supp Figure S3

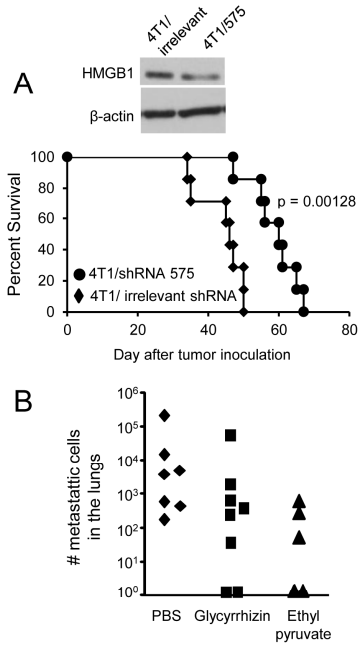

Supplementary Fig. S3: **HMGB1 produced by tumor cells promotes tumor growth and metastasis.** ***A,*** BALB/c mice were inoculated in the mammary fat pad with 7 x 10^3 4T1/575 (shRNA knockdown for HMGB1) or 4T1/irrelevant (shRNA knockdown for Invariant chain) mammary carcinoma cells and monitored for survival. Methods: HMGB1 Oligonucleotides: hm575sense– 5' GATCGGCAGCCCTA TGAGAAGAAATTCAAGAGATTTCTTCTCATAGGGCTGCTTTTTTG 3', hm575anti-sense – 5' AATTCAAAAA AGCAGCCCTATGAGAAGAAATCTCTTGAATTTCTTCTCATAGGGCTGCC 3' (IDTDNA). Invariant chain oligos: sense-5'GATCCGCTTGTTATCAGCTTTCAGTTCAAGAGACTGAAA GCTGATAACAAGCTTTTTTCTAGAG 3' Ii 54 anti-sense- 5' ATTCTCTAGAAAAAAGCTTGTTAT CAGCTTTCAGTCTCTTGAACTGAAAGCTGATAACAAGCG 3'. Double stranded DNA was generated by annealing 5 μM each of sense and anti-sense primers at 80°C.and subsequently cloned into pSiren RetroQ vector (Clonetech) utilizing the BamHI and EcoR1 sites. Constructs were confirmed by DNA sequencing. Plasmid DNA was prepared using a Macherey-Nagel Nucleo Bond Xtra Midi Kit and 4T1 cells were transfected with 3μg of DNA using Amaxa Nucleofactor program T-024. Stable transfectants were obtained after three weeks of culture in 1.8 μg/ml puromycin. Transfected and parental cells were lysed in 500μl of M-Per buffer Mammalian Protein Extraction Reagent (Thermo Scientific) using a GentleMACS M tube and program protein 01.01 on the GentleMACS Dissociator (Milltenyl Biotec). Protein concentrations of supernatants were determined at 280 absorbance. Fifty μg of protein/cell line was heated for 5 minutes at 95°C and run on a 12% polyacrylamide gel for 60 minutes at 100V. Protein was transferred to a PVDF membrane overnight at 30V and probed with antibody to HMGB1. Blots were stripped with Restore buffer (Thermoscientific) and reprobed for β-actin. ***B,*** BALB/c mice were inoculated s.c. with 7 x 10^3 4T1 mammary carcinoma cells. When tumors were first palpable (7-9 days post tumor inoculation), mice were treated i.p. with ethyl pyruvate (40 mg/kg, twice daily), glycyrrhizin (2mg/kg twice daily), or vehicle (PBS; twice a week). Four weeks after tumor inoculation when tumors were >10mm in diameter, mice were sacrificed and the number of metastatic cells in the lungs was quantified by clonogenic assay (20) with the following modification: Lung tissue was dissociated using a Gentle MACS Dissociator (Milltenyl Biotec) fitted with a C tube running program m_lung_02.01. Data are pooled from two experiments and are combined from two independent experiments. n=7, 5, and 8 for the PBS, ethyl pyruvate, and glycyrrhizin groups, respectively.

Supp Figure S4

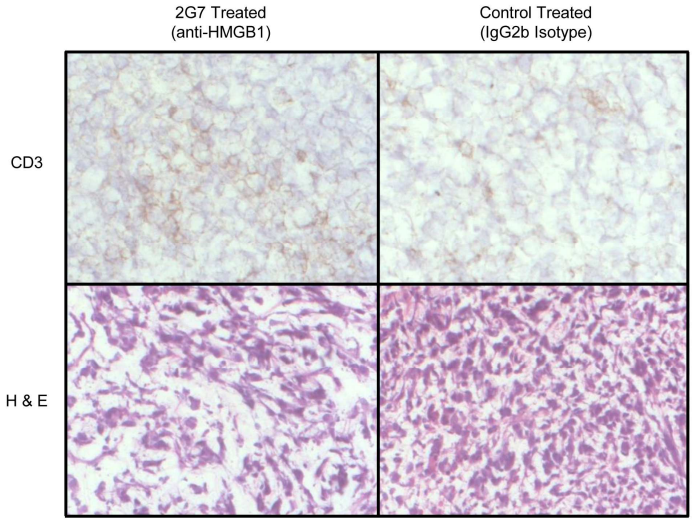

Supplementary Fig. S4: Tumors from mice treated with anti-HMGB1 mAb tend to have more tumor-infiltrating $CD3^+$ cells. Tumors from the HMGB1-treated (2G7 mAb) and isotype control-treated mice of Figure 6 were frozen and embedded in OCT medium and subsequently stained for CD3 or with H&E. Slides were examined at a magnification of 250X using a Zeiss microscope fitted with an AxioCamMRc5 camera. Images are representative of fields from each of two mice per group.

Supplementary Table 1. Quantitation of HMGB1 secreted by cultured tumor cells, ex vivo macrophages and MDSC, in vivo grown tumors, and cultures of MDSC differentiated from bone marrow progenitor cells.

In vitro cultured tumor cells	ng/ml/10^6 cells[a]
4T1	36.95
CT26	16.23
MC38	123.23
AT3	36.95
B78H1	12.61

	ng/ml/10^6 cells[b]
Bone marrow differentiation cultures	98.61

Ex vivo cells	ng/ml/10^7 cells[a]
Macrophages	0.31
LPS-treated macrophages	0.31
MDSC	3.29
LPS-treated MDSC	4.24

In vivo grown tumors	Tumor weight (mg)	Tumor diameter (mm)	ng/ml/1g tumor[a]
4T1	1140	13.54	85.89
CT26	1770	9.55	173.39
B78H1	840	8.84	216.86
AT3	127	3.96	0.63

[a] Amount of HMGB1 after 18 hrs of culture

[b] Amount of HMGB1 at the end of the four day incubation

Supplementary Table 2: HMGB1 drives the differentiation of MDSC from bone marrow progenitor cells

	Pre-culture	Post-culture						
		Vehicle	Ethyl Pyruvate (mM)			Glycyrrhizin (mM)		
			2.5	5	10	0.25	0.5	1
Total cells [a]	$4.2x10^5$	$5.5x10^5$	$4.1 x10^5$	$3.4 x10^5$	$1.2 x10^5$	$3.1 x10^5$	$2.8 x10^5$	$9.6 x10^4$
$Gr1^{mid}CD11b^{+}$ [b]	$5.5x10^4$	$1.6x10^5$	$1.3 x10^5$	$1.08 x10^5$	$3.2x10^4$	$9.4 x10^4$	$9.2 x10^4$	$2.9 x10^4$
$\%Gr1^{mid}CD11b^{+}$ [c]	13.11	29.6	31.72	32.12	25.25	30.58	32.14	30.13
% change								
$Gr1^{mid}CD11b^{+}$ [d]		0	20.23	33.46	80.12	42.26	43.49	82.26
$CD3^{+}$ [d]		0	-6.98	19.52	12.14	-22.19	30.44	-33.1
$B220^{+}$ [d]		0	3.89	33.05	36.29	-27.76	29.52	-4.87
$F4/80^{+}CD11b^{+}$ [d]		0	32.69	57.89	68.43	-2.92	58.28	66.08
$CD11c^{+}$ [d]		0	19.37	32.03	67.0	-4.96	51.97	43.07

[a] *Total number of cells was obtained by trypan blue cell counts*

[b] $Gr1^{mid}CD11b^{+}$ cells = *total cells x* % $Gr1^{mid}CD11b^{+}$ cells

[c] $Gr1^{mid}CD11b^{+}$ cells *were identified by flow cytometry*

[d] *% change = [(vehicle – treated)/vehicle] x 100*

Appendix 2: Cross-talk among myeloid-derived suppressor cells, macrophages, and tumor cells impacts the inflammatory milieu of solid tumor. Daniel Beury, Katherine Parker, Maeva Nyandjo, Pratima Sinha, Kayla Carter, Suzanne Ostrand-Rosenberg, Journal of Leukocyte Biology, 2014.

Epub ahead of print August 28, 2014 - doi:10.1189/jlb.3A0414-210R

JLB

Article

Cross-talk among myeloid-derived suppressor cells, macrophages, and tumor cells impacts the inflammatory milieu of solid tumors

Daniel W. Beury, Katherine H. Parker, Maeva Nyandjo, Pratima Sinha, Kayla A. Carter, and Suzanne Ostrand-Rosenberg[1]

Department of Biological Sciences, University of Maryland, Baltimore County, Baltimore, Maryland, USA

RECEIVED APRIL 17, 2014; REVISED AUGUST 4, 2014; ACCEPTED AUGUST 11, 2014. DOI: 10.1189/jlb.3A0414-210R

ABSTRACT

MDSC and macrophages are present in most solid tumors and are important drivers of immune suppression and inflammation. It is established that cross-talk between MDSC and macrophages impacts anti-tumor immunity; however, interactions between tumor cells and MDSC or macrophages are less well studied. To examine potential interactions between these cells, we studied the impact of MDSC, macrophages, and four murine tumor cell lines on each other, both in vitro and in vivo. We focused on IL-6, IL-10, IL-12, TNF-α, and NO, as these molecules are produced by macrophages, MDSC, and many tumor cells; are present in most solid tumors; and regulate inflammation. In vitro studies demonstrated that MDSC-produced IL-10 decreased macrophage IL-6 and TNF-α and increased NO. IL-6 indirectly regulated MDSC IL-10. Tumor cells increased MDSC IL-6 and vice versa. Tumor cells also increased macrophage IL-6 and NO and decreased macrophage TNF-α. Tumor cell-driven macrophage IL-6 was reduced by MDSC, and tumor cells and MDSC enhanced macrophage NO. In vivo analysis of solid tumors identified IL-6 and IL-10 as the dominant cytokines and demonstrated that these molecules were produced predominantly by stromal cells. These results suggest that inflammation within solid tumors is regulated by the ratio of tumor cells to MDSC and macrophages and that interactions of these cells have the potential to alter significantly the inflammatory milieu within the tumor microenvironment. *J. Leukoc. Biol.* 96: 000–000; 2014.

Introduction

Solid tumors are a complex and frequently inflamed environment. The inflammation is driven by proinflammatory mediators that are secreted by tumor cells, various tumor-infiltrating lymphocytes, tumor-associated fibroblasts, and myeloid cells, such as macrophages, dendritic cells, and MDSC [1]. Some of these cells engage in cross-talk with each other, resulting in the release of proinflammatory cytokines (e.g., IL-1, IL-6, IL-17, TNF-α), chemokines (e.g., CCL2, CXCL5, CXCL12), growth factors (e.g., TGF-β, GM-CSF, VEGF), and other effector molecules (e.g., S100A8/A9, high-mobility group box 1) [2–4]. These factors, in turn, induce the accumulation and enhance the function of immune-suppressive cells, such as regulatory T cells, plasmacytoid dendritic cells, tumor-associated macrophages, and MDSC [3, 5, 6]. Although the cellular interactions contributing to some of the protumor factors present in the tumor microenvironment have been identified, the etiology of others remains unknown.

Macrophages and MDSC are present within most solid tumors, where they are major drivers of immune suppression and inflammation [3]. We have reported previously that these cells participate in cross-talk with each other that results in increased MDSC production of IL-10 and decreased macrophage production of IL-12, thereby polarizing the immune system toward a protumor type 2 environment [7, 8]. Additional factors are also likely to be impacted by cross-talk between MDSC and macrophages, as well as by interactions with tumor cells. Therefore, we have investigated how tumor cells, macrophages, and MDSC interact with respect to IL-6, TNF-α, IL-10, and NO. We have focused on these four molecules, as they are chronically present in many solid tumors and play important roles in tumor progression. IL-6 promotes tumor progression by enhancing tumor cell development, growth, and metastasis and by inhibiting apoptosis and enhancing tumor vascularization [9–11]. TNF-α causes DNA damage, inhibits apoptosis, and induces the production of matrix metalloproteases, cytokines, and chemokines that facilitate tumor cell invasion and metastasis [12]. In contrast to IL-6 and TNF-α, which when chronically present, are exclusively protumor, NO can have pro- and anti-tumor activity. When produced by M1-like macrophages, NO induces tumor cell apoptosis [13]. However,

Abbreviations: $^{-/-}$=deficient, HSD=honestly significant difference, MDSC=myeloid-derived suppressor cell or cells, PB=Pacific Blue, UMB=University of Maryland Baltimore, UMBC=University of Maryland Baltimore County, VEGF=vascular endothelial growth factor, WT=wild-type

The online version of this paper, found at www.jleukbio.org, includes supplemental information.

1. Correspondence: Dept. of Biological Sciences, UMBC, 1000 Hilltop Circle, Baltimore, MD 21250, USA. E-mail: srosenbe@umbc.edu

0741-5400/14/0096-0001 © Society for Leukocyte Biology

when produced by MDSC, NO drives immune suppression [14]. IL-10 has also been associated with pro- and anti-tumor activity [15]. Here, we report that macrophages, MDSC, and tumor cells participate in a network of cross-talk, resulting in differential production of IL-6, IL-10, TNF-α, and NO, suggesting that the interaction of these cells has the potential to alter significantly the inflammatory milieu within the tumor microenvironment.

MATERIALS AND METHODS

Mice, tumor cells, tumor growth

BALB/c, C57BL/6, BALB/c IL-6$^{-/-}$, and BALB/c IL-10$^{-/-}$ mice were bred in the UMBC animal facility from stock obtained from The Jackson Laboratory (Bar Harbor, ME, USA; C57BL/6 and BALB/c) or provided by Dr. Manfred Kopf (Zürich, Switzerland; IL-6$^{-/-}$). BALB/c-derived 4T1 and TS/A mammary carcinomas, CT26 colon carcinoma, and C57BL/6-derived MC38 colon carcinoma were maintained as described [16]. Mice were inoculated in the abdominal mammary gland with 100 μl DMEM containing 7×10^4 (WT and IL-10$^{-/-}$ mice) or 10^5 (WT and IL-6$^{-/-}$ mice) 4T1 cells or 10^6 TS/A cells or s.c. in the flank with 5×10^5, 1×10^5, or 1×10^4 CT26 cells. Primary tumors were measured as described [17]. Survival time was recorded when mice became moribund and were euthanized. All animal procedures were approved by the UMBC Institutional Animal Care and Use Committee.

Flow cytometry and antibodies

Gr1-FITC, Gr1-allophycocyanin, Ly6C-FITC, Ly6G-PB, CD11b-PE, CD11b-PB, F4/80-allophycocyanin, F4/80-PB, pSTAT3-PB, IL-6R-PE, and IL-10R-PE mAb and rat IgG1-PE and IgG2b-PE isotypes were from BD PharMingen (San Diego, CA, USA) or BioLegend (San Diego, CA, USA). Cells were stained for surface markers as described [18]. For phosphoflow experimenta, cells were stimulated with 50 ng/mL rIL-10 (BioLegend) or supernatants from MDSC and macrophage cocultures, fixed with Lyse/Fix Buffer (BD Biosciences, San Jose, CA, USA), permeabilized with Perm Buffer III (BD Biosciences), and stained with antibodies diluted in Stain Buffer (BD Biosciences). Samples were analyzed on a Beckman/Coulter CyAn ADP flow cytometer using Summit software.

T Cell proliferation assays

CD4$^+$ and CD8$^+$ T cell proliferation assays were performed as described [18]. Briefly, DO11.10 (ovalbumin peptide$_{323-339}$-specific, I-A^d-restricted) or Clone 4 (hemagglutinin peptide$_{518-526}$-specific, H-2K^d-restricted) splenocytes were cultured with their respective cognate peptides and irradiated blood MDSC from 4T1-bearing WT, IL-6$^{-/-}$, or IL-10$^{-/-}$ mice. Cultures were pulsed with ^{3}H-thymidine on Day 4 and harvested on Day 5. Peptides were synthesized at the UMB Biopolymer Core Facility.

MDSC, macrophage, MDSC-macrophage-tumor cell cross-talk

MDSC were isolated from the peripheral blood of 4T1 tumor-bearing mice [16]. Peritoneal macrophages were prepared from tumor-free mice [8]. MDSC and macrophages in all experiments were >90% Gr1$^+$CD11b$^+$ cells and >95% CD11b$^+$ F4/80$^+$ cells, respectively, as assessed by flow cytometry. MDSC and macrophage cross-talk experiments were performed as described [7] with the following modifications: 4T1, MC38, TS/A, or CT26 tumor cells (1×10^5 cells) were cultured with or without 7.5×10^5 MDSC and/or macrophages in 500 μl macrophage media (5% FCS in DMEM, 1% penicillin-streptomycin, 1% glutamax, 0.1% gentamycin) for 16 h at 37°C with 100 ng/mL LPS (Difco Laboratories, Franklin Lakes, NJ, USA) and 20 U/mL IFN-γ (R&D Systems, Minneapolis, MN, USA). In some experiments, macrophages and/or MDSC were cultured with LPS, IFN-γ, rIL-6 and rIL-10 (both from BioLegend) and IL-10 that was denatured by boiling at 95°C for 15 min or in the presence of neutralizing antibodies to IL-10 (1 μg/ml; Clone JES5-2A5; eBioscience, San Diego, CA, USA). Cells were harvested by scraping and analyzed by flow cytometry. Supernatants were analyzed for IL-10, IL-6, and TNF-α using ELISA kits (R&D Systems and eBioscience), per the manufacturers' protocol, or by multiplex analysis in the UMB Cytokine Core Facility. NO production was quantified by Griess assay [18]. Values were normalized between experiments using the following formulas:

- production of IL-6 by macrophages or MDSC in response to tumor cells = (IL-6 from WT MDSC or macrophages with tumor cells) − (IL-6 from IL-6$^{-/-}$ macrophages or MDSC with tumor cells)
- percent increase in IL-6 or NO by MDSC or macrophages in response to tumor cells = {[(IL-6 or NO from macrophages and MDSC ± tumor cells)/(IL-6 or NO from macrophages or MDSC)] × 100%} − 100%
- percent decrease in IL-6 or TNF-α by macrophages in response to tumor cells and/or MDSC = 1 − {(IL-6 or TNF-α from macrophages ± tumor cells)/(IL-6 or TNF-α from WT macrophages ± tumor cells ± MDSC)} × 100%
- percent increase in IL-10 by MDSC in response to macrophages = {[(IL-10 from macrophages + MDSC)/(IL-10 from MDSC)] × 100%} − 100%

If IL-6 was not detected, then the lowest value detectable on the standard curve was used for the calculations.

Macrophages and MDSC were stained with 5 μM CellTrace Violet (Life Technologies, Carlsbad, CA, USA) and 4T1 tumor cells with 1 μM CFSE (Life Technologies). MDSC or macrophages were cultured for 16 h in macrophage media with 100 ng/mL LPS and 20 U/mL IFN-γ in a six-well dish at 3×10^6 cells/well/2 mL, with or without 4×10^5 4T1 cells. Cells were then harvested using Detachin (Genlantis, San Diego, CA, USA) and scraping, washed, and stained for Gr1, CD11b, and with 7-amino-actinomycin D; and analyzed by flow cytometry.

Ex vivo tumor cultures

4T1, CT26, and TS/A tumors >8 mm in diameter were surgically resected from euthanized mice and placed on sterile #50 Whatman filter paper to remove excess liquid. The tumors were then transferred to 6 cm culture dishes and finely minced using a sterile scalpel, and the resulting pieces weighed. 4T1 and TS/A pieces were resuspended in 5 mL prewarmed 4T1 media (10% Fetal Clone I in IMDM, 1% penicillin-streptomycin, 1% glutamax, 0.1% gentamycin) containing 100 ng/mL LPS and 20 U/mL IFN-γ for IL-10 studies or without LPS and IFN-γ for IL-6 studies. Resuspended tumor pieces were incubated for 16 h at 37°C, 5% CO_2, and supernatants were analyzed for cytokine production by ELISA. Cytokine levels were normalized to one gram of tumor tissue/mL media using the following formula: cytokine production (normalized) = cytokine (pg/mL) × [(tumor weight/1 g) × 5 mL].

Statistical analyses

Student's t-test and Tukey's HSD test were performed using Microsoft Excel 2013. Values denoted with different letters (e.g., a, b, c, etc.) are significantly different from each other; values with the same letter are not significantly different. Tumor growth and exogenous IL-10 data were analyzed using the Mann-Whitney test on the VassarStats website (www.VassarStats.net). Survival data were analyzed using the log-rank test from the Walter and Eliza Hall Institute of Medical Research Bioinformatics webpage (http://bioinf.wehi.edu.au/software/russell/logrank/). Values of $P < 0.05$ were considered statistically significant.

RESULTS

IL-6 and IL-10 promote tumor progression

Increased levels of serum IL-6 are correlated with chronic inflammation, increased tumor burden, and poor prognosis in some human and mouse systems [19]. IL-6 also promotes MDSC-mediated inhibition of Th1 responses in mice [20]. In contrast, IL-10 correlates with tumor progression in some systems but with tumor regression in other systems [15, 21–25].

To determine if IL-6 and/or IL-10 contribute to progression of the 4T1 mammary carcinoma or CT26 colon carcinoma, we inoculated syngeneic WT, IL-$6^{-/-}$, and IL-$10^{-/-}$ mice with 4T1 (**Fig. 1A**) or CT26 (Fig. 1B) tumor cells and followed the mice for tumor onset, growth, and engraftment. In the absence of host-produced IL-6, 4T1 tumor progression was delayed, and survival time was increased. IL-$10^{-/-}$ mice showed a similar, although less dramatic, delay in tumor progression and extension of survival time. 4T1 tumor engraftment in WT BALB/c and IL-$10^{-/-}$ mice was 90–100%, whereas only 40% of IL-$6^{-/-}$ mice developed tumor. Tumor progression was also delayed, and survival time increased in IL-$6^{-/-}$ mice with CT26 tumors. In contrast, IL-$10^{-/-}$ mice inoculated with 5×10^5 CT26 tumor cells had similar tumor progression, survival time, and percent engraftment as WT mice. Tumor progression, survival time, and engraftment were also similar in WT and IL-$10^{-/-}$ BALB/c mice inoculated with 1×10^5 or 1×10^4 cells (Supplemental Fig. 1A). These results demonstrate that stromal cell-derived IL-6 and IL-10 facilitate progression of 4T1 and CT26 tumors in their syngeneic hosts.

MDSC production of IL-10 decreases macrophage IL-6 and TNF-α and increases NO; IL-6 indirectly regulates MDSC production of IL-10

We have shown previously that MDSC production of IL-10 is enhanced by cross-talk with macrophages and polarizes macrophages toward a tumor-promoting phenotype by inhibiting macrophage production of IL-12 [7, 8]. To determine if IL-10 produced by MDSC impacts the production of additional proinflammatory mediators, we cocultured $CD11b^+F4/80^+$ peritoneal macrophages and 4T1-induced $Gr1^+CD11b^+$ immunesuppressive MDSC (**Fig. 2A**) and assayed the supernatants for IL-10 and the proinflammatory cytokine IL-6 (Fig. 2B). Consistent with our previous reports, production of IL-10 was increased significantly in the presence of macrophages (average increase in IL-10 of 116±19.4% for 30 experiments). IL-10 was produced exclusively by MDSC, as macrophage cultures containing IL-$10^{-/-}$ MDSC produced no IL-10. In the same cocultures, macrophages were the sole producers of IL-6, and MDSC decreased macrophage IL-6 (average decrease in IL-6 of 24±3.8% for 30 experiments).

To determine if IL-6 regulates MDSC production of IL-10, we cocultured WT or IL-$6^{-/-}$ macrophages with WT or IL-$6^{-/-}$ MDSC (Fig. 2C). IL-$6^{-/-}$ MDSC produced significantly more IL-10 than WT MDSC. Macrophage cocultures with IL-$6^{-/-}$ MDSC had significantly more IL-10 than cocultures with WT MDSC. Macrophage IL-6 had no effect on MDSC IL-10, as WT MDSC cocultured with WT or IL-$6^{-/-}$ macrophages produced similar amounts of IL-10. The lack of a direct effect by IL-6 on MDSC IL-10 was confirmed by incubation of MDSC with exogenous IL-6 (Supplemental Fig. 1B). These results indicate that MDSC do not produce IL-6 in the coculture setting; however, their development in vivo in the presence of IL-6 down-regulates their production of IL-10.

To determine if IL-10 produced by MDSC decreased macrophage IL-6 or regulated other molecules characteristic of tumor-rejecting M1 macrophages, WT or IL-$10^{-/-}$ MDSC were cocultured with WT macrophages (Fig. 2D). There was no decrease in

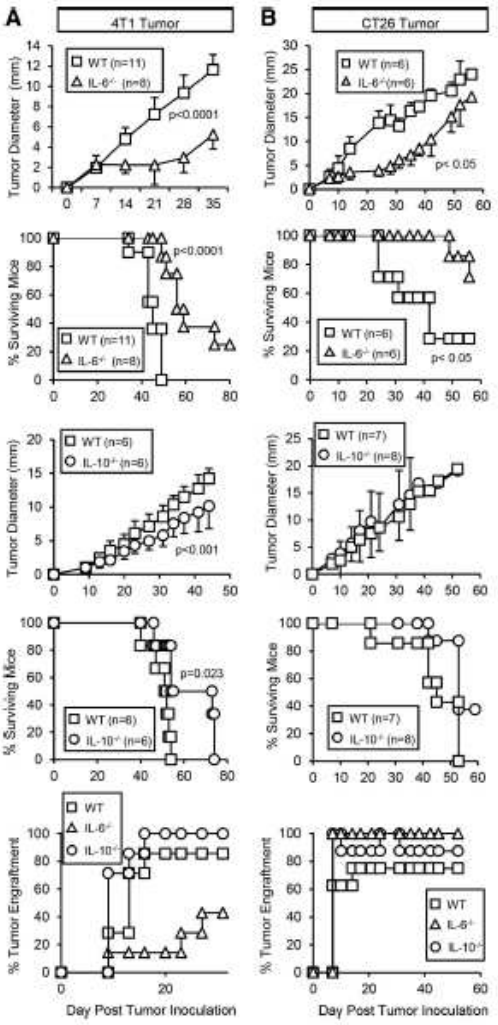

Figure 1. IL-6 and IL-10 produced by host cells enhance primary tumor growth and decrease survival time. WT, IL-$6^{-/-}$, and IL-$10^{-/-}$ BALB/c mice were inoculated with (A) 4T1 or (B) CT26 tumor cells and monitored for tumor diameter, survival, and tumor engraftment. Mice in the WT versus IL-$6^{-/-}$ graphs and WT versus IL-$10^{-/-}$ graphs (tumor diameter and percent survival) were inoculated with 1×10^5 and 7000 4T1 cells, respectively. Mice in the engraftment graph were inoculated with 1×10^5 4T1 cells. All CT26 inoculations were 5×10^5 cells. For tumor engraftment, n = 7 for each 4T1 group; n = 6 for each CT26 group. Statistical significance was tested by Mann-Whitney (tumor growth) or log-rank test (survival). Data are pooled from three independent experiments.

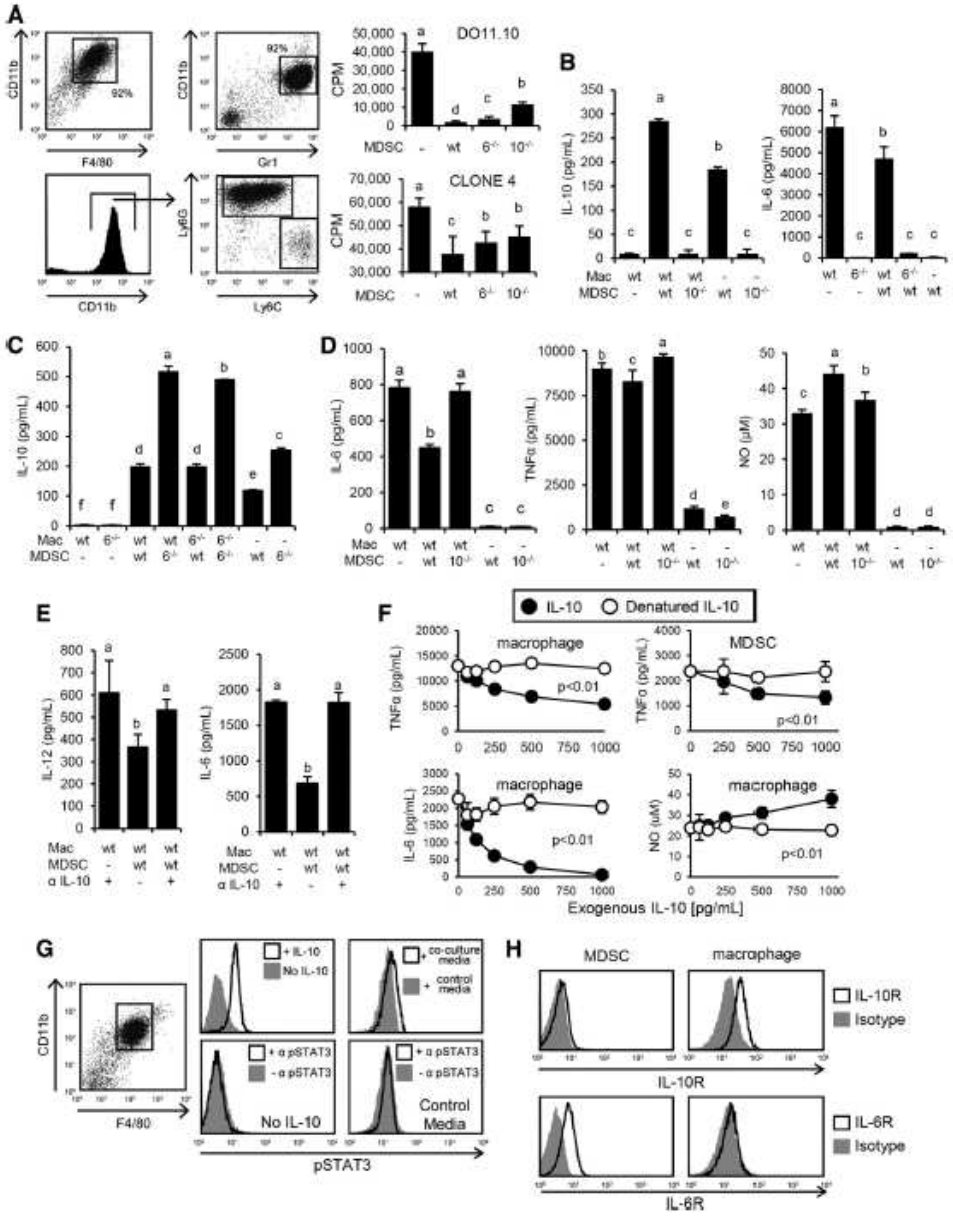

Figure 2. Cross-talk between MDSC and macrophages regulates production of IL-10, IL-6, and NO. (A) Peritoneal macrophages from healthy mice and MDSC from tumor-bearing mice were stained with mAb to CD11b, F4/80, Gr1, Ly6C, and/or Ly6G and analyzed by flow cytometry.

(*continued on next page*)

IL-6 in the presence of IL-10$^{-/-}$ MDSC, suggesting that IL-10 from WT MDSC reduced macrophage IL-6. To confirm the role of IL-10, neutralizing antibodies to IL-10 were added to MDSC-macrophage cocultures. As previous studies demonstrated that MDSC IL-10 also decreases macrophage IL-12 [8], IL-12 levels served as a positive control (Fig. 2E). IL-10 neutralizing antibodies reduced the MDSC-mediated decrease of IL-6 and IL-12. Thus, a feedback loop exists between macrophages and MDSC, in which macrophages increase MDSC production of IL-10, and MDSC IL-10 regulates macrophage synthesis of IL-6.

We also assessed the role of MDSC IL-10 on macrophage NO and TNF-α production (Fig. 2D). MDSC IL-10 decreased TNF-α in the cocultures; however, this decrease was minimal. In contrast, macrophage production of NO was increased by coculture with MDSC. The increase was predominantly a result of MDSC IL-10, as only a minimal increase in NO was observed in the presence of IL-10$^{-/-}$ MDSC.

To confirm further that IL-10 regulated macrophage production of IL-6 and NO, and macrophage and MDSC production of TNF-α, macrophages or MDSC were cultured in the presence of exogenous IL-10, and culture supernatants were assessed for TNF-α, IL-6, and NO (Fig. 2F). Exogenous IL-10 reduced MDSC and macrophage TNF-α and macrophage IL-6 but increased macrophage NO. As STAT3 is activated by signaling through IL-10R, macrophages were cultured with exogenous IL-10 or with supernatants from MDSC-macrophage cocultures and subsequently stained for phosphorylated STAT3 (Fig. 2G). STAT3 was phosphorylated under both conditions, further confirming the regulatory role of IL-10 produced by MDSC.

MDSC and macrophages express IL-6R and IL-10R, respectively (Fig. 2H), so these cells have the potential to respond directly to these cytokines. The results of Fig. 2F suggest that IL-10 directly impacts macrophages. However, IL-10-deficiency and IL-6-deficiency could also cause other changes in MDSCs and/or macrophages so that the effects are only mediated indirectly by IL-10 or IL-6. To distinguish these possibilities, we compared cytokine/chemokine production by WT, IL-10$^{-/-}$, and IL-6$^{-/-}$ MDSC to determine if gene deficiency impacts MDSC phenotype (Supplemental Table 1). TGF-β3, GM-CSF, IL-4, IL-13, and IL-23 were not detectable in WT MDSC. TGF-β2, IL-1-β, CCL2, and VEGF production was similar for WT, IL-10$^{-/-}$, and IL-6$^{-/-}$ MDSC. TGF-β1 trended higher in IL-10$^{-/-}$ and IL-6$^{-/-}$ MDSC, and MIP-1α trended lower in IL-10$^{-/-}$ and IL-6$^{-/-}$ MDSC compared with WT MDSC. These results suggest that IL-10-deficiency and IL-6-deficiency may alter the phenotype of MDSC.

These results, together with our earlier studies on IL-12 [7, 8], demonstrate that MDSC production of IL-10 increases some M2-like characteristics of macrophages (i.e., IL-12^{low}IL-6^{low}) but also increases some M1-like properties (NO^{high}).

Other cytokines are also impacted by interactions between MDSC and macrophages

In addition to IL-10, TNF-α, IL-12, NO, and IL-6, other immune-regulatory molecules are present in solid tumors. Of particular note are cytokines that drive effector and regulatory T cells (e.g., IL-23, IL-27, IL-4, and IL-13), growth factors that regulate neovascularization (e.g., VEGF) and myeloid cell differentiation (e.g., GM-CSF), proinflammatory mediators (e.g., IL-1β), and immune-suppressive molecules (e.g., TGF-β). To determine if any of these molecules are affected by cross-talk between MDSC and macrophages, supernatants from cocultures of 4T1-induced WT MDSC and WT BALB/c macrophages were assayed by multiplex analysis (Supplemental Table 1). Neither MDSC nor macrophages produced TGF-β3, GM-CSF, IL-4, IL-13, or IL-23, whereas both cell types produced TGF-β1, TGF-β2, IL-1β, CCL2, MIP-1α, and VEGF. Cocultures using WT MDSC reduced the production of TGF-β1, TGF-β2, and MIP-1α and modestly increased the production of VEGF. Cocultures of WT macrophages with IL-10$^{-/-}$ or IL-6$^{-/-}$ MDSC displayed similar trends, except for CCL2, where we observed a decrease in CCL2 production.

Tumor cells increase MDSC production of IL-6 and vice versa

Tumor cells produce proinflammatory mediators and therefore, may contribute to the polarization of myeloid cells in the tumor microenvironment. To assess if there is cross-talk between MDSC and tumor cells, 4T1, CT26, TS/A, or MC38 murine tumor cells were cultured by themselves or cocultured with MDSC (**Fig. 3**). When cultured alone, 4T1 and CT26 cells produced IL-6, and TS/A, MC38, and MDSC produced no detectable IL-6. Cultures containing WT MDSC plus 4T1, CT26, TS/A, or MC38 tumor cells contained more IL-6 than cultures of tumor cells alone, whereas cultures of 4T1, CT26, and TS/A tumor cells plus IL-6$^{-/-}$ MDSC produced intermediate

MDSC from WT, IL-10$^{-/-}$, and IL-6$^{-/-}$ BALB/c mice with 4T1 tumors were assayed for their ability to suppress the antigen-driven activation of peptide-specific, MHC-restricted, transgenic CD4$^+$ (DO11.10) and CD8$^+$ (Clone 4) T cells. (B–D) 4T1-induced MDSC and peritoneal macrophages (Mac) from WT, IL-10$^{-/-}$ (10$^{-/-}$), or IL-6$^{-/-}$ (6$^{-/-}$) BALB/c mice were cocultured, and supernatants were assayed for IL-10, IL-6, and NO. (B) Macrophages enhance MDSC IL-10, and MDSC decrease macrophage IL-6. (C) IL-6 decreases MDSC IL-10. (D) IL-10 production by MDSC decreases macrophage IL-6 and TNF-α and increases macrophage NO. (E) Neutralizing antibodies to IL-10 prevent the down-regulation of macrophage IL-6 and IL-12. (F) Exogenous IL-10 decreases MDSC and macrophage TNF-α, decreases macrophage IL-6, and enhances macrophage NO. Macrophages or MDSC were cultured with IL-10 or denatured IL-10. (G) Macrophages activate STAT3 in response to IL-10. Macrophages (left) were cultured for 5 min in the presence or absence of exogenous IL-10 (middle) or with supernatants (media) from MDSC-macrophage cocultures (right), subsequently fixed and permeabilized, and then stained for F4/80, CD11b, and pSTAT3. (H) Macrophages and MDSC express the receptors for IL-10 and IL-6, respectively. (A–H) Data are from one of two, 30, three, five, four, three, two, and two experiments, respectively. Statistical significance was determined by (A–E) Tukey's HSD test and (F) the Mann-Whitney test. Different lower case letters above each value indicate that those values are statistically, significantly different; values that share the same lowercase letter are not statistically, significantly different.

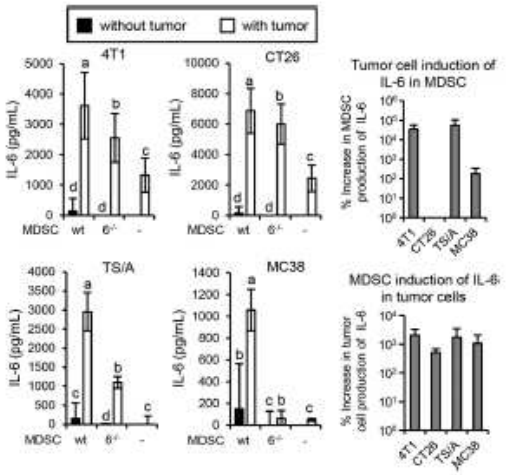

Figure 3. Tumor cells induce MDSC to produce IL-6 and vice versa. WT or IL-6$^{-/-}$ 4T1-induced MDSC were cultured with or without 4T1, CT26, TS/A, or MC38 tumor cells, and the supernatants were assayed for IL-6 by ELISA. One of three independent experiments (left four graphs); average percent increase of three independent experiments comparing tumor cells with IL-6$^{-/-}$ and WT MDSC (right two graphs). Statistical significance for the independent experiments was determined by Tukey's HSD test.

levels of IL-6. Cultures of MC38 tumor cells plus IL-6$^{-/-}$ MDSC produced very low levels of IL-6. Increases in IL-6 production in the presence of IL-6$^{-/-}$ MDSC indicate that in vitro, MDSC enhanced tumor cell production of IL-6. However, as IL-6 levels in cocultures of WT MDSC plus tumor cells were even higher than IL-6 production in cocultures with IL-6$^{-/-}$ MDSC, MDSC may also be induced by tumor cells to synthesize IL-6. Interestingly, MDSC, but not tumor cells, proliferated during the overnight culture (Supplemental Fig. 1C), so the increase in IL-6 in this setting could be a result of higher numbers of MDSC. In contrast, tumor cells did not impact MDSC production of TNF-α, IL-12, or IL-10 (Supplemental Fig. 2). These results demonstrate that in vitro, reciprocal cross-talk between MDSC and most tumor cells increases IL-6 production, and there is no cross-talk between MDSC and tumor cells with respect to IL-10, IL-12, or TNF-α.

Tumor cells increase macrophage IL-6 and NO and decrease macrophage TNF-α

To assess if there is cross-talk between macrophages and tumor cells, 4T1, CT26, TS/A, or MC38 tumor cells were cultured with macrophages and the culture supernatants assayed for IL-6, NO, and TNF-α (**Fig. 4**). All four tumor lines increased macrophage production of IL-6. Macrophages also increased IL-6 produced by 4T1, CT26, and TS/A tumor cells, as cultures containing tumor cells plus IL-6$^{-/-}$ macrophages produced more IL-6 than tumor cells alone. In cocultures of WT

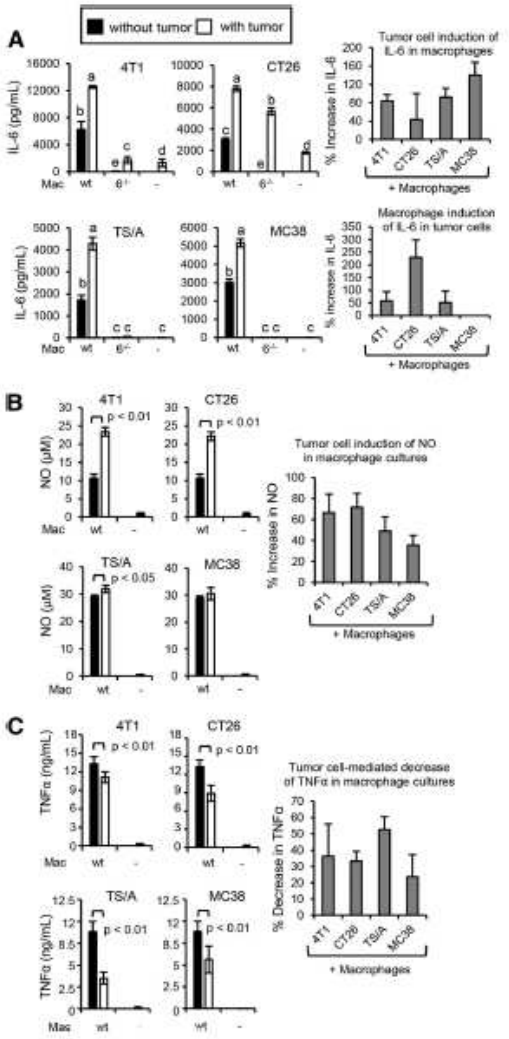

Figure 4. Tumor cells induce macrophages to produce IL-6 and NO but decrease macrophage TNF-α. WT or IL-6$^{-/-}$ macrophages were cultured with or without 4T1, CT26, TS/A, or MC38 tumor cells, and the supernatants were assayed for (A) IL-6, (B) NO, or (C) TNF-α. Representative data (left graphs) from one of four, three, and four independent experiments, respectively. Average percent change of pooled data from all experiments (right graphs). (A) Comparison of tumor cells with IL-6$^{-/-}$ and WT macrophages. (B and C) Comparison of tumor cells with WT macrophages. (A–C) Statistical significance was determined by *t*-test.

or IL-6$^{-/-}$ macrophages with 4T1, TS/A, or MC38 tumor cells, macrophages were the dominant producers of IL-6 (Fig. 4A). In contrast, tumor cells were the dominant producers of IL-6 in cultures of macrophages plus CT26 tumor cells, indicating that some tumor cells have a greater response to macrophages. Cross-talk-induced increases in IL-6 ranged from 43% to 230%. These results indicate that tumor cell production of IL-6 is differentially affected by macrophages and that macrophages produce IL-6 in response to tumor cells.

4T1, CT26, and TS/A cells also increased macrophage production of NO, and increases in NO ranged from 36% to 72% (Fig. 4B). In contrast, macrophage production of TNF-α was decreased significantly in the presence of the four tumors, as cultures of macrophages plus tumor cells produced significantly less TNF-α compared with macrophages cultured alone. Tumor cell-mediated decreases in TNF-α ranged from 24% to 53% (Fig. 4C). Macrophage production of IL-10 and IL-12 was not affected by tumor cells (Supplemental Fig. 2). Increases in macrophage NO and IL-6 were a result of increased production by individual macrophages, as the macrophages did not proliferate during the overnight culture period (Supplemental Fig. 1C). These results show that macrophages and tumor cells participate in cross-talk with each other, resulting in differential production of proinflammatory mediators, which are characteristic of M1 (NO^{hi}) and M2 (TNF-α^{low}) macrophages.

MDSC prevent most tumor cells from increasing macrophage IL-6

As MDSC and macrophages are present in the tumor microenvironment, we next tested if MDSC alter cross-talk between tumor cells and macrophages. MDSC, macrophages, and/or tumor cells were cocultured, and IL-6 levels were assessed (**Fig. 5A**). Cultures containing 4T1, TS/A, or MC38 tumor cells plus MDSC and macrophages produced less IL-6 than cultures without MDSC. MDSC-mediated decreases of IL-6 ranged from 0% to 37%. In contrast, MDSC did not decrease IL-6 in cultures of macrophages and CT26 tumor cells. These results demonstrate that in the presence of most tumors, MDSC modestly reduce macrophage IL-6.

MDSC increase macrophage NO in the presence of tumor cells

To determine if MDSC affect the tumor-driven increase in macrophage NO, tumor cells, macrophages, and MDSC were cocultured (Fig. 5B). Cultures of 4T1 or CT26 tumor cells with macrophages and MDSC contained more NO than cultures without MDSC. MDSC-mediated increases in NO ranged from 0% to 30%. In contrast, TNF-α, IL-10, and IL-12 were not affected by MDSC (Supplemental Fig. 2). These results indicate

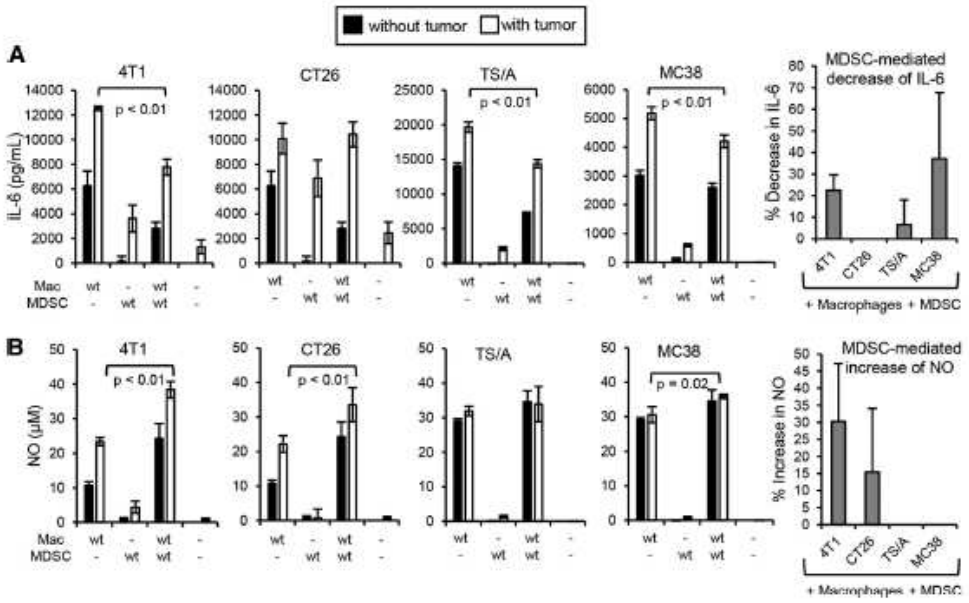

Figure 5. MDSC decrease tumor cell-mediated enhancement of IL-6 and increase tumor cell-mediated enhancement of macrophage NO. WT macrophages were cultured with or without 4T1-induced MDSC and/or 4T1, CT26, TS/A, or MC38 tumor cells. Supernatants were assayed for (A) IL-6 and (B) NO. (A and B, left four graphs of each) One of three independent experiments. (Right) Average of the three independent experiments. (A and B) Statistical significance was determined by *t*-test.

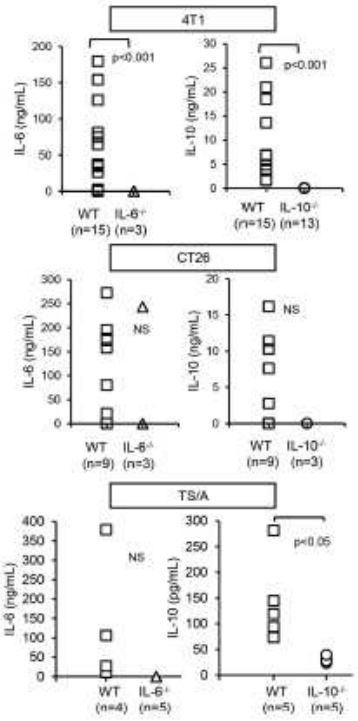

Figure 6. Host cells are the dominant producers of IL-6 and IL-10 in the tumor microenvironment. Eight- to 10-mm diameter 4T1, CT26, and TS/A tumors were excised from WT, IL-6$^{-/-}$, and IL-10$^{-/-}$ BALB/c mice, manually teased into small pieces, and incubated overnight and the supernatants analyzed by ELISA for IL-6 and IL-10. Cytokine levels were normalized to 1 g tumor tissue/mL media. Data are pooled from four independent experiments. Statistical significance was assessed by *t*-test.

that MDSC alter the dynamic of tumor cell and macrophage cross-talk by enhancing NO production.

Stromal cells are the dominant producers of IL-6 and IL-10 in the tumor microenvironment

Our in vitro findings suggest that tumor-infiltrating cells and not tumor cells are the dominant producers of IL-6 and IL-10. To determine if this in vitro finding occurs in vivo, we harvested 4T1, CT26, and TS/A tumors from WT, IL-6$^{-/-}$, and IL-10$^{-/-}$ mice and assayed the tumors for IL-6 and IL-10 (**Fig. 6**). Tumors in all WT mice contained IL-6 and IL-10, whereas all tumors from IL-10$^{-/-}$ mice contained very little or no IL-10. With the exception of one mouse with CT26 tumor, tumors from IL-6$^{-/-}$ mice did not have IL-6. Isolated tumors did not contain detectable levels of TNF-α or NO (data not shown). These results demonstrate that in vivo in the tumor microenvironment, stromal cells and not tumor cells are the dominant sources of IL-6 and IL-10.

DISCUSSION

Solid tumors include multiple, diverse host cells that contribute to an inflammatory tumor microenvironment and facilitate tumor progression. As macrophages and MDSC are present in most solid tumors, we have examined the interplay of these cells to determine if and how their interactions may influence the intratumor environment. The studies reported here on IL-6, IL-10, TNF-α, and NO, plus our previous reports on IL-12, address some of the most common molecules produced by MDSC and macrophages that contribute to tumor progression. Our findings are summarized in **Fig. 7A**. Collectively, our results indicate that the levels of IL-6, IL-10, IL-12, TNF-α, and NO are modulated by interactions among MDSC, macrophages, and tumor cells. MDSC induce some M2 macrophage characteristics (IL-6^{low}IL-12^{low}TNF-α^{low}) but simultaneously induce NO, which is characteristic of M1 macrophages. These apparently opposing activities are both regulated by MDSC production of IL-10. Tumor cells

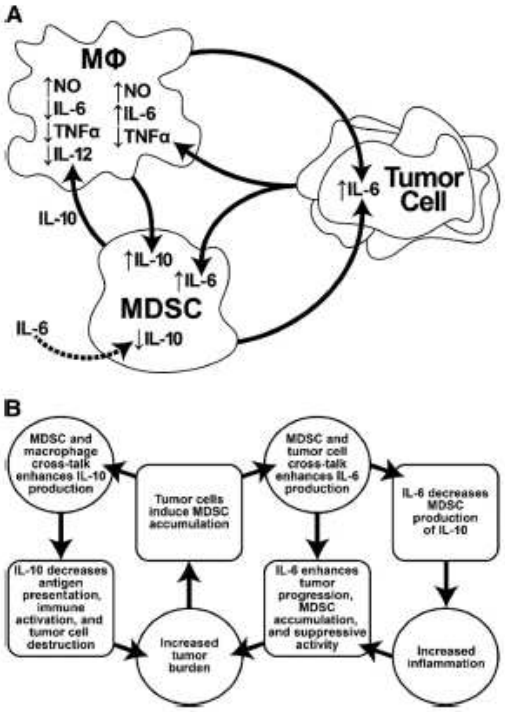

Figure 7. Summary of cross-talk among MDSC, macrophages (MΦ), and tumor cells. (A) Cross-talk with respect to IL-10, IL-6, IL-12, TNF-α, and NO. Solid arrows indicate direct effects mediated by the cell type or IL-10. Dashed arrow indicates an indirect effect by IL-6. (B) Potential cycle by IL-6, IL-10, and MDSC cross-talk promotes inflammation and tumor progression.

also regulate macrophage expression of molecules characteristic of M1 ($IL\text{-}6^{hi}NO^{hi}$) and M2 ($TNF\text{-}\alpha^{low}$) phenotypes, whereas tumor cells and macrophages enhance MDSC production of IL-6 and IL-10, respectively. As stromal cells are the dominant producers in vivo of several of these cytokines, the complex pattern of cross-talk among MDSCs, macrophages, and tumor cells is likely to have profound effects on tumor progression.

NO is an important effector molecule that is differentially impacted by IL-10 and promotes or inhibits tumor progression depending on the tumor model. NO is produced by eNOS and iNOS, which are up-regulated [26] and down-regulated [27], respectively, by macrophage-produced IL-10. Pro- and anti-tumor roles have been attributed to NO/iNOS in multiple tumor systems (Supplemental Table 2). It is likely that the apparent conflicting effects of NO are a result of many variables, including, but not limited to, the production of NO by different types of cells, the location of the producer cells, neighboring cells that might be altered by the released NO, and the concentration of NO. As a result of the complexity of NO on tumor progression and the presence of multiple cell types in the tumor microenvironment that may participate in cross-talk, elucidating the role of NO in tumor progression will be challenging.

IL-6 is a pivotal cytokine that promotes tumor progression directly by enhancing tumor cell development, growth, metastasis, vascularization, and inhibiting apoptosis [9–11]. MDSC were reported to be a primary producer of IL-6 in the tumor microenvironment [20]. This observation is consistent with our finding that stromal cells and not tumor cells are the major producer of IL-6 in vivo and that tumor cells drive MDSC IL-6 production. IL-6 also enhances MDSC accumulation and suppressive activity [28–30] and decreases MDSC production of IL-10, an anti-inflammatory cytokine [31]. Therefore, positive feedback between MDSC and tumor cells will potentially maintain chronic inflammation and promote tumor progression through the cycle shown in Fig. 7B.

Pro- and anti-tumor roles have been attributed to IL-10. It down-regulates numerous immune-modulatory molecules that are essential for an anti-tumor immune response and is considered an anti-inflammatory cytokine [15, 31]. For example, IL-10 impairs antigen presentation by dendritic cells and macrophages by down-regulating expression of MHC class II, CD80, and CD86. IL-10 also decreases production of IFN-γ and IL-12, cytokines that are characteristic of and facilitate the development of type I anti-tumor effector and helper cells, and IL-10 overexpressing tumor cells have increased growth rates in vivo [32]. In cancer patients, secretion of IL-10 from basal or squamous cell carcinoma cells prevents in vitro lysis of tumor cells by tumor-infiltrating lymphocytes. In vitro, pretreatment of tumor cells (e.g., melanoma, lymphoma) with IL-10 confers resistance to CTL-mediated lysis by decreasing expression of transporter associated with antigen processing 1 and 2 and subsequent surface expression of MHC I. IL-10 also contributes to tumor progression by enhancing angiogenesis and tumor cell proliferation. As MDSC IL-10 is enhanced by macrophage cross-talk, and IL-10 is produced predominantly by tumor-infiltrating stromal cells, cross-talk by macrophages and MDSCs is most likely a source of IL-10 in the tumor microenvironment.

However, IL-10 has also been linked to enhancing anti-tumor immunity [15]. For example, the reduction in MHC I by IL-10 renders tumor cells more susceptible to NK-mediated killing, and a tumor cell-based glioma vaccine induced more effective anti-tumor immunity in WT mice than in $IL\text{-}10^{-/-}$ mice. IL-10 also activated tumor-resident $CD8^+$ T cells directly, facilitated tumor rejection of PDV6 squamous carcinoma [23], and served as an adjuvant in immunotherapy. Treatment of mice with pegylated IL-10, a form of IL-10 that has an increased serum half-life, induced IFN-γ and granzyme-B production by tumor-infiltrating $CD8^+$ T cells in a mouse mammary tumor virus tumor model [24]. IL-10 also inhibited tumorigenesis in mice with colon carcinoma and patients with B cell lymphoma [21, 22]. Ablation of IL-10 from $CD4^+$ T cells enhanced tumor burden in $APC^{\Delta 468}$ mice [33], whereas $IL\text{-}10^{-/-}$ mice bearing MC38 tumors displayed increased tumor growth, metastasis, MDSC accumulation, and enhanced susceptibility to chemical carcinogenesis [34]. Therefore, as reported in the literature and shown in this report, the role of IL-10 in the promotion of tumor progression is dependent on the tumor model.

STAT3 is activated by IL-6 and IL-10; however, the two cytokines can result in different biological effects as a result of the complexity of the STAT3 pathway [35]. There are 1.3×10^6 potential binding sites for STAT3 in the mouse genome [36]; however, STAT3 only binds a few thousand sites in a given cell type [37]. STAT3 is a pleiotropic transcription factor that regulates target genes by acting in conjunction with a variety of transcriptional coactivators. The expression of these coactivators is dependent on the cell type and signaling events that occur in a cell's lifetime. Many of these coactivators are prebound to STAT3 target sites (reviewed in ref. [37]). Therefore, a cell's phenotype following STAT3 signaling depends on its previous history with respect to STAT3 activation. The tumor microenvironment is a complex milieu, so differential expression of transcriptional coactivators is likely. As MDSC-macrophage-tumor cell cross-talk involves activation of STAT3 via IL-6 and IL-10, and the relative amounts of these cytokines differ depending on the type of tumor, cross-talk is likely to contribute to the differential effects of IL-10 on tumor progression.

In addition to the cells examined here, other stromal cells also contribute to inflammation within the tumor microenvironment through their cross-talk with MDSC [38, 39]. However, MDSC and macrophages are present at significant levels in most solid tumors, and therefore, their contributions to the inflammatory milieu are likely to be important.

AUTHORSHIP

D.W.B., K.H.P., P.S., and S.O-R. designed experiments and analyzed data. D.W.B., K.H.P., M.N., K.A.C., and P.S. performed experiments. D.W.B. and S.O-R. wrote the manuscript. All authors approved the manuscript.

ACKNOWLEDGMENTS

This work was supported by grants from the U.S. National Institutes of Health (RO1CA115880, RO1CA84232). D.W.B. was partially supported by a predoctoral fellowship from the Congressionally Directed Medical Research Programs Breast Can-

cer Program (W81XWH-11-1-0115). We thank Dr. Manfred Kopf for providing breeding stock of BALB/c IL-6$^{-/-}$, Ms. Lisa Burkheimer for her excellent care of our mice, Ms. Virginia Clements for excellent technical support, and Ms. Katelyn Beury for help with the schematic figures.

DISCLOSURES

The authors declare no conflicts of interest.

REFERENCES

1. Shiao, S. L., Ganesan, A. P., Rugo, H. S., Coussens, L. M. (2011) Immune microenvironments in solid tumors: new targets for therapy. *Genes Dev.* **25,** 2559–2572.
2. Yang, L., Pang, Y., Moses, H. L. (2010) TGF-beta and immune cells: an important regulatory axis in the tumor microenvironment and progression. *Trends Immunol.* **31,** 220–227.
3. Gabrilovich, D. I., Ostrand-Rosenberg, S., Bronte, V. (2012) Coordinated regulation of myeloid cells by tumours. *Nat. Rev. Immunol.* **12,** 253–268.
4. Viola, A., Sarukhan, A., Bronte, V., Molon, B. (2012) The pros and cons of chemokines in tumor immunology. *Trends Immunol.* **33,** 496–504.
5. Sica, A., Larghi, P., Mancino, A., Rubino, L., Porta, C., Totaro, M. G., Rimoldi, M., Biswas, S. K., Allavena, P., Mantovani, A. (2008) Macrophage polarization in tumour progression. *Semin. Cancer Biol.* **18,** 349–355.
6. Ostrand-Rosenberg, S., Sinha, P. (2009) Myeloid-derived suppressor cells: linking inflammation and cancer. *J. Immunol.* **182,** 4499–4506.
7. Bunt, S. K., Clements, V. K., Hanson, E. M., Sinha, P., Ostrand-Rosenberg, S. (2009) Inflammation enhances myeloid-derived suppressor cell cross-talk by signaling through Toll-like receptor 4. *J. Leukoc. Biol.* **85,** 996–1004.
8. Sinha, P., Clements, V. K., Bunt, S. K., Albelda, S. M., Ostrand-Rosenberg, S. (2007) Cross-talk between myeloid-derived suppressor cells and macrophages subverts tumor immunity toward a type 2 response. *J. Immunol.* **179,** 977–983.
9. Becker, C., Fantini, M. C., Wirtz, S., Nikolaev, A., Lehr, H. A., Galle, P. R., Rose-John, S., Neurath, M. F. (2005) IL-6 signaling promotes tumor growth in colorectal cancer. *Cell Cycle* **4,** 217–220.
10. Su, Y. W., Xie, T. X., Sano, D., Myers, J. N. (2011) IL-6 stabilizes Twist and enhances tumor cell motility in head and neck cancer cells through activation of casein kinase 2. *PLoS One* **6,** e19412.
11. Samier, F. R., Malinowska, K., Culig, Z., Cavarretta, I. T. (2010) Interleukin-6 trans-signalling differentially regulates proliferation, migration, adhesion and matrix expression in human prostate cancer cells. *Endocr. Relat. Cancer* **17,** 241–253.
12. Balkwill, F. (2006) TNF-alpha in promotion and progression of cancer. *Cancer Metastasis Rev.* **25,** 409–416.
13. Hussain, S. P., Trivers, G. E., Hofseth, L. J., He, P., Shaikh, I., Mechanic, L. E., Doja, S., Jiang, W., Subleski, J., Shoura, L., Haines, D., Laukach, V. E., Wilcox, R. H., Djurickovic, D., Harris, C. C. (2004) Nitric oxide, a mediator of inflammation, suppresses tumorigenesis. *Cancer Res.* **64,** 6849–6853.
14. Bronte, V., Zanovello, P. (2005) Regulation of immune responses by L-arginine metabolism. *Nat. Rev. Immunol.* **5,** 641–654.
15. Mocellin, S., Marincola, F. M., Young, H. A. (2005) Interleukin-10 and the immune response against cancer: a counterpoint. *J. Leukoc. Biol.* **78,** 1043–1051.
16. Sinha, P., Parker, K. H., Horn, L., Ostrand-Rosenberg, S. (2012) Tumor-induced myeloid-derived suppressor cell function is independent of IFN-gamma and IL-4Ralpha. *Eur. J. Immunol.* **42,** 2052–2059.
17. Bunt, S. K., Sinha, P., Clements, V. K., Leips, J., Ostrand-Rosenberg, S. (2006) Inflammation induces myeloid-derived suppressor cells that facilitate tumor progression. *J. Immunol.* **176,** 284–290.
18. Sinha, P., Clements, V. K., Ostrand-Rosenberg, S. (2005) Reduction of myeloid-derived suppressor cells and induction of M1 macrophages facilitate the rejection of established metastatic disease. *J. Immunol.* **174,** 636–645.
19. Lippitz, B. E. (2013) Cytokine patterns in patients with cancer: a systematic review. *Lancet Oncol.* **14,** e218–28.
20. Tsukamoto, H., Nishikata, R., Senju, S., Nishimura, Y. (2013) Myeloid-derived suppressor cells attenuate TH1 development through IL-6 production to promote tumor progression. *Cancer Immunol. Res.* **1,** 64–76.
21. Berg, D. J., Davidson, N., Kühn, R., Muller, W., Menon, S., Holland, G., Thompson-Snipes, L., Leach, M. W., Rennick, D. (1996) Enterocolitis and colon cancer in interleukin-10-deficient mice are associated with aberrant cytokine production and CD4(+) TH1-like responses. *J. Clin. Invest.* **98,** 1010–1020.
22. Neven, B., Mamessier, E., Bruneau, J., Kaluzenbach, S., Kodiatz, D., Suarez, F., Masliah-Planchon, J., Billot, K., Canioni, D., Frange, P., Radford-Weiss, I., Asnafi, V., Murugan, D., Bole, C., Nitschke, P., Goules, O., Casanova, J. L., Blanche, S., Picard, C., Hermine, O., Rieux-Laucat, F., Brousse, N., Davi, F., Raud, V., Klein, C., Nadel, B., Ruemmele, F., Fischer, A. (2013) A Mendelian predisposition to B-cell lymphoma caused by IL-10R deficiency. *Blood* **122,** 3713–3722.
23. Emmerich, J., Mumm, J. B., Chan, I. H., LaFace, D., Truong, H., McClanahan, T., Gorman, D. M., Oft, M. (2012) IL-10 directly activates and expands tumor-resident CD8(+) T cells without de novo infiltration from secondary lymphoid organs. *Cancer Res.* **72,** 3570–3581.
24. Mumm, J. B., Emmerich, J., Zhang, X., Chan, I., Wu, L., Mauze, S., Blaisdell, S., Basham, B., Dai, J., Grein, J., Sheppard, C., Hong, K., Cutler, C., Turner, S., LaFace, D., Kleinschek, M., Judo, M., Ayanoglu, G., Langowski, J., Gu, D., Paporello, B., Murphy, E., Sriram, V., Naravula, S., Desai, B., Medicherla, S., Seghezzi, W., McClanahan, T., Cannon-Carlson, S., Beebe, A. M., Oft, M. (2011) IL-10 elicits IFNgamma-dependent tumor immune surveillance. *Cancer Cell* **20,** 781–796.
25. Sato, T., Terai, M., Tamura, Y., Alexeev, V., Mastrangelo, M. J., Selvan, S. R. (2011) Interleukin 10 in the tumor microenvironment: a target for anticancer immunotherapy. *Immunol. Res.* **51,** 170–182.
26. Jacobs, F., Chaussabel, D., Truyens, C., Leclercq, V., Carlier, Y., Goldman, M., Vray, B. (1998) IL-10 up-regulates nitric oxide (NO) synthesis by lipopolysaccharide (LPS)-activated macrophages: improved control of *Trypanosoma cruzi* infection. *Clin. Exp. Immunol.* **113,** 59–64.
27. Qasimi, P., Ming-Lum, A., Ghanipour, A., Ong, C. J., Cox, M. E., Ihle, J., Cacalano, N., Yoshimura, A., Mui, A. L. (2006) Divergent mechanisms utilized by SOCS3 to mediate interleukin-10 inhibition of tumor necrosis factor alpha and nitric oxide production by macrophages. *J. Biol. Chem.* **281,** 6316–6324.
28. Smith, C., Chang, M. Y., Parker, K. H., Beury, D. W., DuHadaway, J. B., Flick, H. E., Boulden, J., Sutanto-Ward, E., Soler, A. P., Laury-Kleintop, L. D., Mandik-Nayak, L., Metz, R., Ostrand-Rosenberg, S., Prendergast, G. C., Muller, A. J. (2012) IDO is a nodal pathogenic driver of lung cancer and metastasis development. *Cancer Discov.* **2,** 722–735.
29. Marigo, I., Bosio, E., Solito, S., Mesa, C., Fernandez, A., Dolcetti, L., Ugel, S., Sonda, N., Bicciato, S., Falisi, E., Calabrese, F., Basso, G., Zanovello, P., Cozzi, E., Mandruzzato, S., Bronte, V. (2010) Tumor-induced tolerance and immune suppression depend on the C/EBPbeta transcription factor. *Immunity* **32,** 790–802.
30. Bunt, S. K., Yang, L., Sinha, P., Clements, V. K., Leips, J., Ostrand-Rosenberg, S. (2007) Reduced inflammation in the tumor microenvironment delays the accumulation of myeloid-derived suppressor cells and limits tumor progression. *Cancer Res.* **67,** 10019–10026.
31. Ouyang, W., Ruiz, S., Crellin, N. K., Valdez, P. A., Hymowitz, S. G. (2011) Regulation and functions of the IL-10 family of cytokines in inflammation and disease. *Annu. Rev. Immunol.* **29,** 71–109.
32. Lee, J. H., Lee, G. T., Woo, S. H., Ha, Y. S., Kwon, S. J., Kim, W. J., Kim, I. Y. (2013) BMP-6 in renal cell carcinoma promotes tumor proliferation through IL-10-dependent M2 polarization of tumor-associated macrophages. *Cancer Res.* **73,** 3604–3614.
33. Dennis, K. L., Wang, Y., Blatner, N. R., Wang, S., Saadalla, A., Trudeau, E., Roers, A., Weaver, C. T., Lee, J. J., Gilbert, J. A., Chang, E. B., Khazaie, K. (2013) Adenomatous polyps are driven by microbe-instigated focal inflammation and are controlled by IL-10-producing T cells. *Cancer Res.* **73,** 5905–5913.
34. Tamakawa, T., Wilke, C. M., Kryczek, I., Chen, G. Y., Kao, J., Nunez, G., Zou, W. (2012) Interleukin-10 ablation promotes tumor development, growth, and metastasis. *Cancer Res.* **72,** 420–429.
35. Niemand, C., Nimmesgern, A., Haan, S., Fischer, P., Schaper, F., Rossaint, R., Heinrich, P. C., Muller-Newen, G. (2003) Activation of STAT3 by IL-6 and IL-10 in primary human macrophages is differentially modulated by suppressor of cytokine signaling 3. *J. Immunol.* **170,** 3263–3272.
36. Vallania, F., Schiavone, D., Dewilde, S., Pupo, E., Carbay, S., Calogero, R., Pomoglio, M., Provero, P., Poli, V. (2009) Genome-wide discovery of functional transcription factor binding sites by comparative genomics: the case of Stat3. *Proc. Natl. Acad. Sci. USA* **106,** 5117–5122.
37. Huchins, A. P., Diez, D., Miranda-Saavedra, D. (2013) The IL-10/STAT3-mediated anti-inflammatory response: recent developments and future challenges. *Brief Funct. Genomics* **12,** 489–498.
38. Morales, J. K., Saleem, S. J., Martin, R. K., Saunders, B. L., Barnstein, B. O., Faber, T. W., Pullen, N. A., Kolawole, E. M., Brooks, K. B., Norton, S. K., Sturgill, J., Graham, L., Bear, H. D., Urban J. F., Jr., Lamz, C. S., Conrad, D. H., Ryan, J. J. (2014) Myeloid-derived suppressor cells enhance IgE-mediated mast cell responses. *J. Leukoc. Biol.* **95,** 643–650.
39. Saleem, S. J., Martin, R. K., Morales, J. K., Sturgill, J. L., Gibb, D. R., Graham, L., Bear, H. D., Manjili, M. H., Ryan, J. J., Conrad, D. H. (2012) Cutting edge: mast cells critically augment myeloid-derived suppressor cell activity. *J. Immunol.* **189,** 511–515.

KEY WORDS:
cancer · cytokines · tumor microenvironment · IL-6 · IL-10 · nitric oxide

Appendix 3: IDO is a nodal pathogenic driver of lung cancer and metastasis development. Courtney Smith, Mee Young Chang, Katherine Parker, Daniel Beury, James DuHadaway, Hollie Flick, Janette Boulden, Erika Sutanto-Ward, Alejandro Peralta Soler, Lisa Laury-Kleitop, Laura Mandik-Nayak, Richard Metz, Suzanne Ostrand-Rosenberg, George Prendergast, Alexander J. Muller, Cancer Discovery, 2012.

Published OnlineFirst July 18, 2012; DOI: 10.1158/2159-8290.CD-12-0014

RESEARCH ARTICLE

IDO Is a Nodal Pathogenic Driver of Lung Cancer and Metastasis Development

Courtney Smith[1], Mee Young Chang[1], Katherine H. Parker[3], Daniel W. Beury[3], James B. DuHadaway[1], Hollie E. Flick[1,4], Janette Boulden[1], Erika Sutanto-Ward[1], Alejandro Peralta Soler[1,7], Lisa D. Laury-Kleintop[1], Laura Mandik-Nayak[1], Richard Metz[2], Suzanne Ostrand-Rosenberg[3], George C. Prendergast[1,5,6], and Alexander J. Muller[1,6]

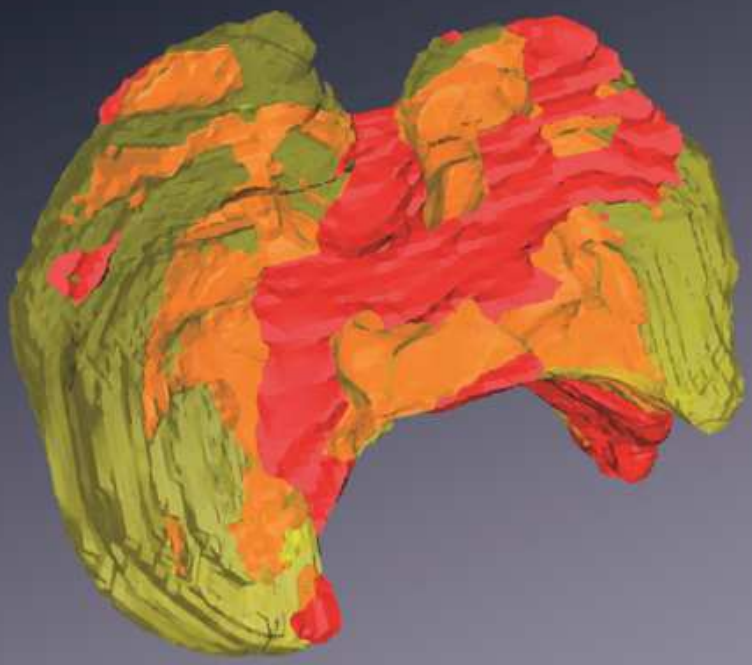

Published OnlineFirst July 19, 2012; DOI: 10.1158/2159-8290.CD-12-0014

ABSTRACT Indoleamine 2,3-dioxygenase (IDO) enzyme inhibitors have entered clinical trials for cancer treatment based on preclinical studies, indicating that they can defeat immune escape and broadly enhance other therapeutic modalities. However, clear genetic evidence of the impact of IDO on tumorigenesis in physiologic models of primary or metastatic disease is lacking. Investigating the impact of *Ido1* gene disruption in mouse models of oncogenic KRAS-induced lung carcinoma and breast carcinoma–derived pulmonary metastasis, we have found that IDO deficiency resulted in reduced lung tumor burden and improved survival in both models. Micro-computed tomographic (CT) imaging further revealed that the density of the underlying pulmonary blood vessels was significantly reduced in Ido1-nullizygous mice. During lung tumor and metastasis outgrowth, interleukin (IL)-6 induction was greatly attenuated in conjunction with the loss of IDO. Biologically, this resulted in a consequential impairment of protumorigenic myeloid-derived suppressor cells (MDSC), as restoration of IL-6 recovered both MDSC suppressor function and metastasis susceptibility in Ido1-nullizygous mice. Together, our findings define IDO as a prototypical integrative modifier that bridges inflammation, vascularization, and immune escape to license primary and metastatic tumor outgrowth.

SIGNIFICANCE: This study provides preclinical, genetic proof-of-concept that the immunoregulatory enzyme IDO contributes to autochthonous carcinoma progression and to the creation of a metastatic niche. IDO deficiency in vivo negatively impacted both vascularization and IL-6–dependent, MDSC-driven immune escape, establishing IDO as an overarching factor directing the establishment of a protumorigenic environment. *Cancer Discov; 2(8); 722–35. ©2012 AACR.*

INTRODUCTION

Inflammatory tissue microenvironments contribute strongly to tumor progression, but due to the complex multifactorial nature of inflammation, there remains limited understanding of specific pathogenic components that might be targeted to effectively treat cancer (1). In this context, the tryptophan-catabolizing enzyme indoleamine 2,3-dioxygenase (IDO) has emerged as an intriguing target implicated in tumoral immune escape (2, 3). IDO-inhibitory compounds have entered clinical trials based on evidence of immune-based antitumor responses in a variety of preclinical models of cancer (4–10). Meanwhile, inadvertent IDO targeting may already be providing benefits to patients as illustrated by recent evidence that the clinically approved tyrosine kinase inhibitor imatinib dampens IDO induction as a key mechanism for achieving therapeutic efficacy in the treatment of gastrointestinal stromal tumors (11).

Authors' Affiliations: [1]Lankenau Institute for Medical Research; [2]NewLink Genetics Corporation, Wynnewood, Pennsylvania; [3]Department of Biological Sciences, University of Maryland Baltimore County, Baltimore, Maryland; [4]Department of Biochemistry, Drexel University College of Medicine; [5]Department of Pathology, Anatomy, and Cell Biology, [6]Kimmel Cancer Center, Thomas Jefferson University, Philadelphia, Pennsylvania; and [7]Richfield Laboratory of Dermatopathology, Cincinnati, Ohio

Note: Supplementary data for this article are available at Cancer Discovery Online (http://cancerdiscovery.aacrjournals.org/).

C. Smith and M.Y. Chang contributed equally to this study.

Corresponding Authors: Alexander J. Muller and George C. Prendergast, Lankenau Institute for Medical Research, 100 Lancaster Avenue, Wynnewood, PA 19096. Phone: 484-476-8034 or 8475; Fax: 484-476-8533; E-mail: mullera@mlhs.org or prendergast@limr.org

doi: 10.1158/2159-8290.CD-12-0014

Although results with IDO pathway inhibitors are provocative, the conclusions that can be drawn are inherently limited by drug specificity concerns, especially in the absence of independent genetic validation. Addressing this issue, our studies on the impact of *Ido1* gene deletion on 7,12-dimethylbenz(*a*)anthracene/12-O-tetradecanoylphorbol-13-acetate (DMBA/TPA)-elicited skin papillomagenesis established that IDO has an integral tumor-promoting role in the context of phorbol ester–elicited inflammation (12, 13), but interpretation of these results is tempered by the possibility that the chemical exposures in this model may produce anomalies irrelevant to the majority of spontaneous tumors. The lungs present a particularly compelling physiologic context in which to further investigate the role of IDO in tumorigenesis as IDO is known to be highly inducible in this tissue (14, 15), and there is an urgent unmet medical need for effective therapeutic options to treat primary lung tumors and metastases. In this report, we investigated the consequences of IDO loss through genetic ablation in the context of well-established, pulmonary models of oncogenic KRAS-induced adenocarcinoma and orthotopic breast carcinoma metastasis. Our findings reveal previously unappreciated roles for IDO in vascularization and in the production of the proinflammatory cytokine interleukin (IL)-6 that in turn dictates the development of protumorigenic, myeloid-derived suppressor cells (MDSC).

RESULTS

IDO Deficiency Prolongs the Survival of Mice with Sporadic *Kras*^{G12D}-Driven Lung Carcinomas

LSL-Kras^{G12D} (*Lox-Stop-Lox Kras*^{G12D}) transgenic mice develop sporadic focal pulmonary adenocarcinomas following intranasal administration of Cre-expressing adenovirus vector

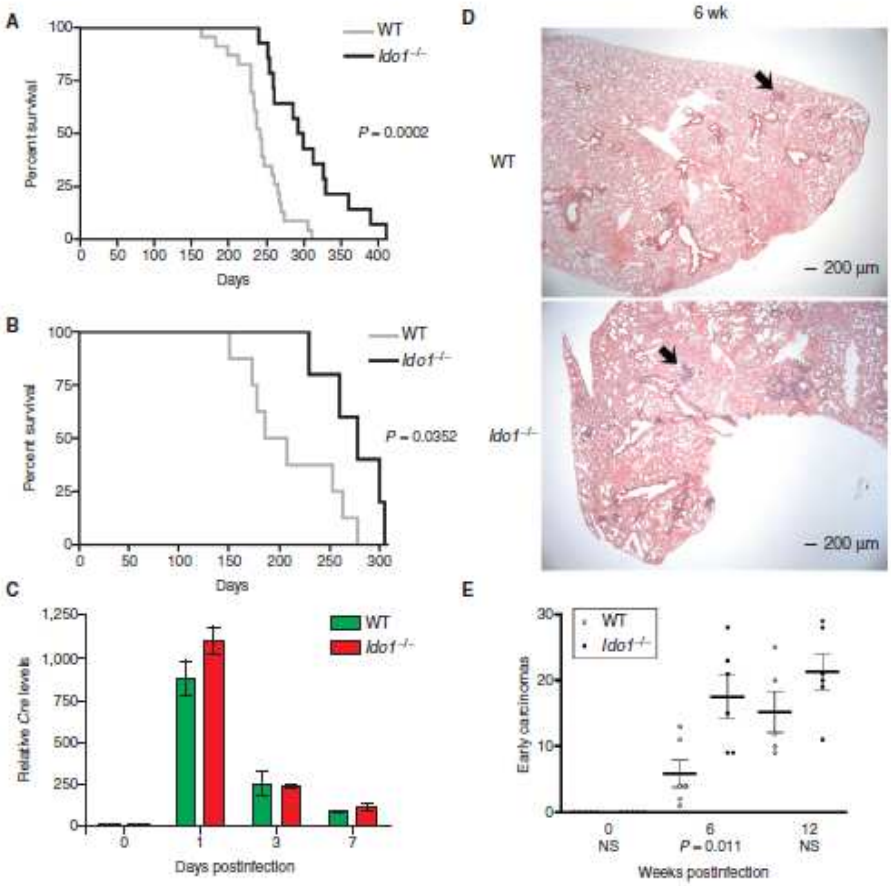

Figure 1. IDO deficiency extends the survival of mice with KRAS-induced lung adenocarcinomas despite an elevated number of early lesions. **A**, Kaplan–Meier survival curves for cohorts of *Lox-Kras*^{G12D} ($n = 23$) and *Ido1*$^{-/-}$ *Lox-Kras*^{G12D} ($n = 14$) mice infected with 2.5×10^7 plaque-forming units (pfu) of Ad-Cre virus. **B**, Kaplan–Meier survival curves for cohorts of *Lox-Kras*^{G12D} ($n = 8$) and *Ido1*$^{-/-}$ *Lox-Kras*^{G12D} ($n = 5$) mice infected with 1.25×10^8 pfu Ad-Cre virus. Significance for both data sets was assessed by 2-group log-rank test at $P < 0.05$. **C**, total lung DNA prepared from 3 mice per time point was analyzed for the presence of the viral *Cre* gene by real-time PCR at 0, 1, 3, and 7 days postinfection. Relative Cre levels determined from this analysis are plotted as means ± SEM. **D**, representative hematoxylin and eosin (H&E)–stained sections depicting the observed difference in early lesions between the lungs of *Lox-Kras*^{G12D} and *Ido1*$^{-/-}$ *Lox-Kras*^{G12D} mice at 6 weeks postinfection. **E**, quantitative histopathologic assessment of lesion frequency in H&E–stained sections of lung biopsies from *Lox-Kras*^{G12D} and *Ido1*$^{-/-}$ *Lox-Kras*^{G12D} mice at 6 and 12 weeks postinfection ($n \geq 5$). The number of lesions identifiable under low magnification within a defined region of each specimen are graphed on the scatter plot with the means ± SEM. Significance was determined by 2-tailed Student *t* test at $P < 0.05$. NS, not significant.

(Ad-Cre) to activate the latent oncogenic *Kras*^{G12D} allele (16). These RAS-induced adenocarcinomas elicit a robust inflammatory response (17) wherein IDO may impart a protumorigenic skew (2). To investigate this hypothesis in an autochthonous lung tumor setting, we introduced *Ido1*$^{-/-}$ (homozygous *Ido1*-null) alleles (18) into the *LSL-Kras*^{G12D} mouse strain. *Ido1*$^{-/-}$ *Lox-Kras*^{G12D} mice displayed significantly increased survival relative to *Lox-Kras*^{G12D} mice at 2 different multiplicities of Ad-Cre infection (Fig. 1A and B). Similar levels of *Cre* were present in the lungs of both strains at 0, 1, 3, and 7 days postinfection (Fig. 1C). Unexpectedly, histopathologic examination at 6 weeks revealed that the frequency of early precancerous lesions was actually about 3-fold higher in the *Ido1*$^{-/-}$ *Lox-Kras*^{G12D} mice (Fig. 1D and E), substantiating

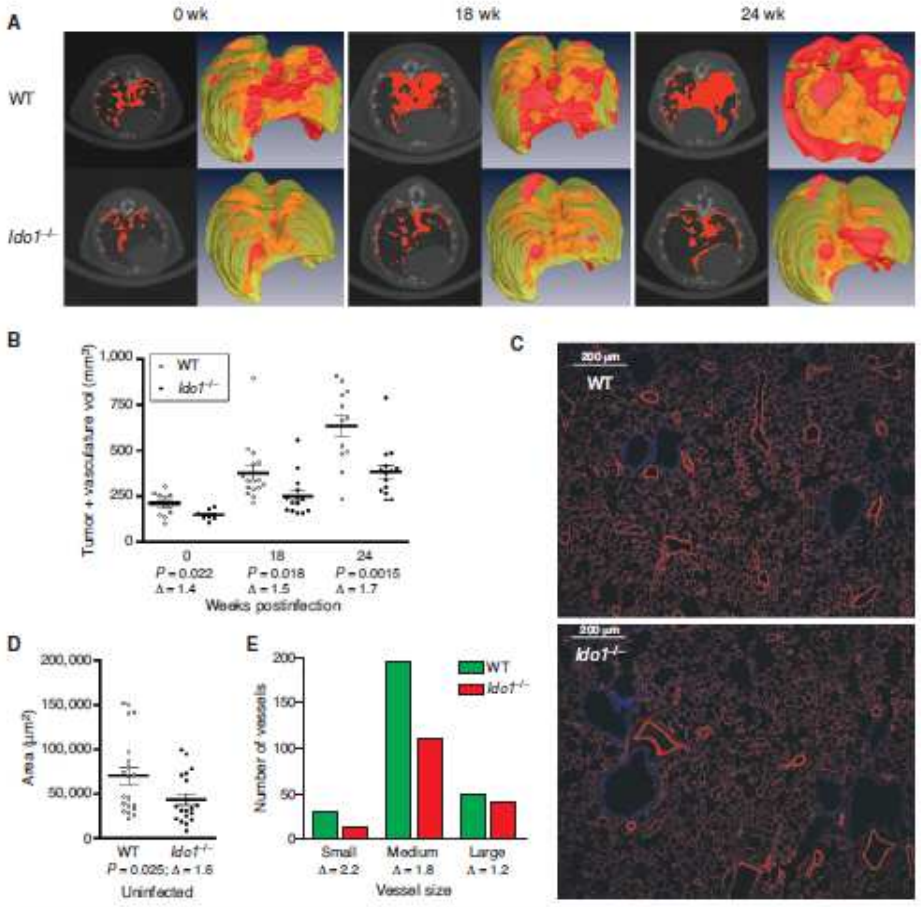

Figure 2. IDO deficiency impairs the outgrowth of overt lung adenocarcinomas and reduces normal pulmonary vascularization. **A,** representative axial micro-CT images and 3D reconstructions of *Lox-Kras*^{G12D} and *Ido1*$^{-/-}$ *Lox-Kras*^{G12D} mouse lungs acquired at 0, 18, and 24 weeks postinfection. Tumor and vasculature, which have indistinguishable x-ray densities, are designated in red in the individual CT images (left) or red/orange for exterior/interior location in the 3D reconstructions (right). **B,** volumetric image analysis of tumor and vasculature conducted on the 3D reconstructions of lung micro-CT images. The data are graphed as a scatter plot with the means ± SEM (Δ, fold difference). Significance was determined by 2-tailed Student *t* test at $P < 0.05$. **C,** immunofluorescent staining of blood vessels with antibody to caveolin 1 (red) and 4′,6-diamidino-2-phenylindole (DAPI) staining of nuclei (blue) in representative lung tissue specimens from BALB/cWT and *Ido1*$^{-/-}$ mice. **D,** quantitation of blood vessel areas. The vessel area totals measured within each field are graphed as a scatter plot with the means ± SEM (Δ, fold difference). Significance was determined by 2-tailed Student *t* test at $P < 0.05$. **E,** distribution of pulmonary vessels within specified size ranges. The total number of small (<500 μm²), medium (500–5,000 μm²), and large (>5,000 μm²) vessels identified within the defined fields evaluated in **D** are plotted on a bar graph (Δ, fold difference). Also see Supplementary Fig. S1C for a graph of individual vessel measurements rank ordered across the entire size range.

that IDO deficiency does not interfere at the stage of Ad-Cre–mediated oncogenic RAS activation required to initiate these tumors (ref. 16; Supplementary Fig. S1A). While early tumorigenesis may be negatively impacted by IDO-mediated tryptophan catabolism, as previously proposed (19), this phenomenon was transient with the differential no longer significant by 12 weeks (Fig. 1E).

IDO Deficiency Impairs Tumor Outgrowth and Vascular Development in the Lung

To assess the impact of *Ido1* loss on overt lung tumors, non-invasive micro-computed tomographic (CT) scans were conducted on groups of *Lox-Kras*^{G12D} and *Ido1*$^{-/-}$ *Lox-Kras*^{G12D} mice at 18 and 24 weeks following Ad-Cre administration (Fig. 2A).

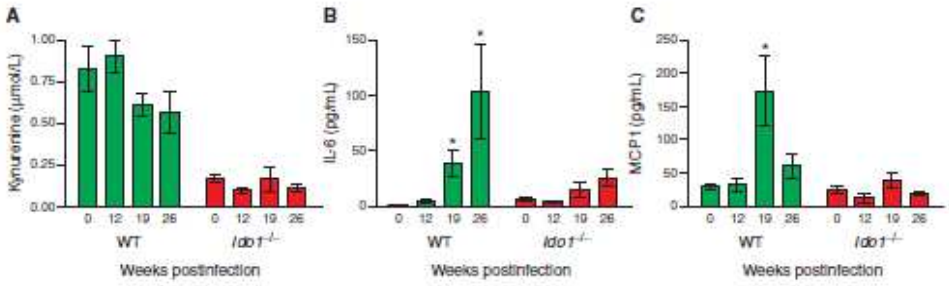

Figure 3. IDO deficiency is associated with attenuated induction of IL-6 and MCP1. **A**, kynurenine levels in the lungs of *Lox-Kras*^{G12D} and *Ido1*$^{-/-}$ *Lox-Kras*^{G12D} mice at 0, 12, 19, and 26 weeks postinfection ($n \geq 3$) assessed by LC/MS-MS analysis and plotted as the means ± SEM. **B** and **C**, IL-6 and MCP1 levels in the lungs of *Lox-Kras*^{G12D} and *Ido1*$^{-/-}$ *Lox-Kras*^{G12D} mice at 0, 12, 19, and 26 weeks postinfection ($n \geq 3$) assessed by multiplexed cytokine bead immunoassay–based analysis and plotted as the means ± SEM with significance relative to baseline determined by one-way ANOVA with Dunn test (*, $P < 0.05$).

Semiautomated quantitative image analysis (20) was conducted on 3-dimensional (3D) reconstructions of the thoracic cavity excluding the heart to assess the combined tumor and vasculature volume within this space. Although lung tumor burden did increase progressively in both cohorts, it was significantly reduced in the *Ido1*$^{-/-}$ *Lox-Kras*^{G12D} mice relative to the corresponding *Ido1*-competent *Lox-Kras*^{G12D} mice (Fig. 2B). Individual micro-CT scan images paired with 3D reconstructions of total chest space and functional lung volume visually highlight the difference in lung tumor burden between representative *Ido1*$^{-/-}$ *Lox-Kras*^{G12D} and *Kras*^{G12D} animals (Fig. 2A; Supplementary Videos). These results indicate that IDO deficiency mitigates overt lung tumor outgrowth, consistent with the increased survival exhibited by these mice.

Micro-CT analysis additionally revealed that the density of normal vasculature in the lungs of uninfected animals was substantially diminished in the *Ido1*$^{-/-}$ animals (Fig. 2A and B). Intriguingly, the difference in vascular density between IDO-deficient and IDO-competent cohorts was proportionately comparable with the difference in overt lung tumor burden at the 18- and 24-week time points (Supplementary Fig. S1B), suggesting an association between the extent of the underlying basal vasculature and the capacity of the lungs to support tumor formation. Immunofluorescent staining of blood vessels in the lungs confirmed the decrease in pulmonary vascular density in *Ido1*$^{-/-}$ animals (Fig. 2C). The area within the lungs occupied by vessels was reduced by about 1.6-fold in *Ido1*$^{-/-}$ animals (Fig. 2D), in line with the differential identified by micro-CT data analysis. Further analysis revealed that the reduction in vascular density occurred predominantly at the level of small- to medium-sized vessels, which were nearly twice as abundant in the wild-type (WT) animals, whereas there was little difference in the number of large vessels (Fig. 2E; Supplementary Fig. S1C).

IDO Promotes IL-6 Elevation during Lung Tumor Formation

In the lungs, IDO is highly responsive to pathogen or cytokine exposure (14, 15). To determine whether lung tumorigenesis also stimulates IDO, we compared steady-state levels of the tryptophan catabolite kynurenine at various times after *Kras*^{G12D} activation. Although baseline levels of kynurenine in the lungs of uninfected *Lox-Kras*^{G12D} mice were significantly higher than in their IDO-deficient counterparts (Fig. 3A), these levels remained constant during lung tumorigenesis (Fig. 3A). In contrast, a multiplexed analysis of inflammatory cytokines at 19 and 26 weeks revealed IL-6 to be elevated by about 25- and 68-fold, respectively, in lungs from tumor-bearing *Lox-Kras*^{G12D} mice but only by about 1- and 3-fold in *Ido1*$^{-/-}$ *Lox-Kras*^{G12D} mice (Fig. 3B). This finding was notable given the known tumor-promoting role of IL-6 in this model (21). Although not of the same magnitude, induction of CCL2/MCP1 [chemokine (C-C motif) ligand 2] was likewise attenuated in tumor-bearing *Lox-Kras*^{G12D} mice lacking *Ido1* (Fig. 3C). In contrast, *Ido1* loss did not significantly affect the relative levels of IL-10, IFN-γ, TNF-α, or IL-12p70 (data not shown).

IDO Deficiency Impedes the Development of Pulmonary Metastases

Given the evidence that *Ido1*$^{-/-}$ mice are resistant to the outgrowth of primary lung tumors, we asked whether *Ido1*$^{-/-}$ animals might exhibit reduced susceptibility to pulmonary metastasis development as well. This question was investigated by orthotopic engraftment of mice with highly malignant 4T1 breast carcinoma cells, which metastasize efficiently to the lungs. Survival was increased significantly in *Ido1*$^{-/-}$ hosts compared with WT hosts after challenge with either a 4T1-luciferase–expressing subclone or with parental 4T1 cells, despite an overall shift in the curves (Fig. 4A and B). No difference in primary tumor growth rate was observed (Supplementary Fig. S2A and S2B), but metastatic lung nodules at necropsy were unambiguously less pronounced in *Ido1*$^{-/-}$ mice (Fig. 4C). Noninvasive micro-CT imaging also confirmed a marked reduction in metastatic burden in *Ido1*$^{-/-}$ mice (Fig. 4C), which was quantified by an *ex vivo* colony-forming assay (ref. 22; Fig. 4D). The metastasis differential was not attributable to reduced intravasation because the same numbers of tumor cells were present in peripheral blood samples from both strains (Fig. 4D). In contrast to lung,

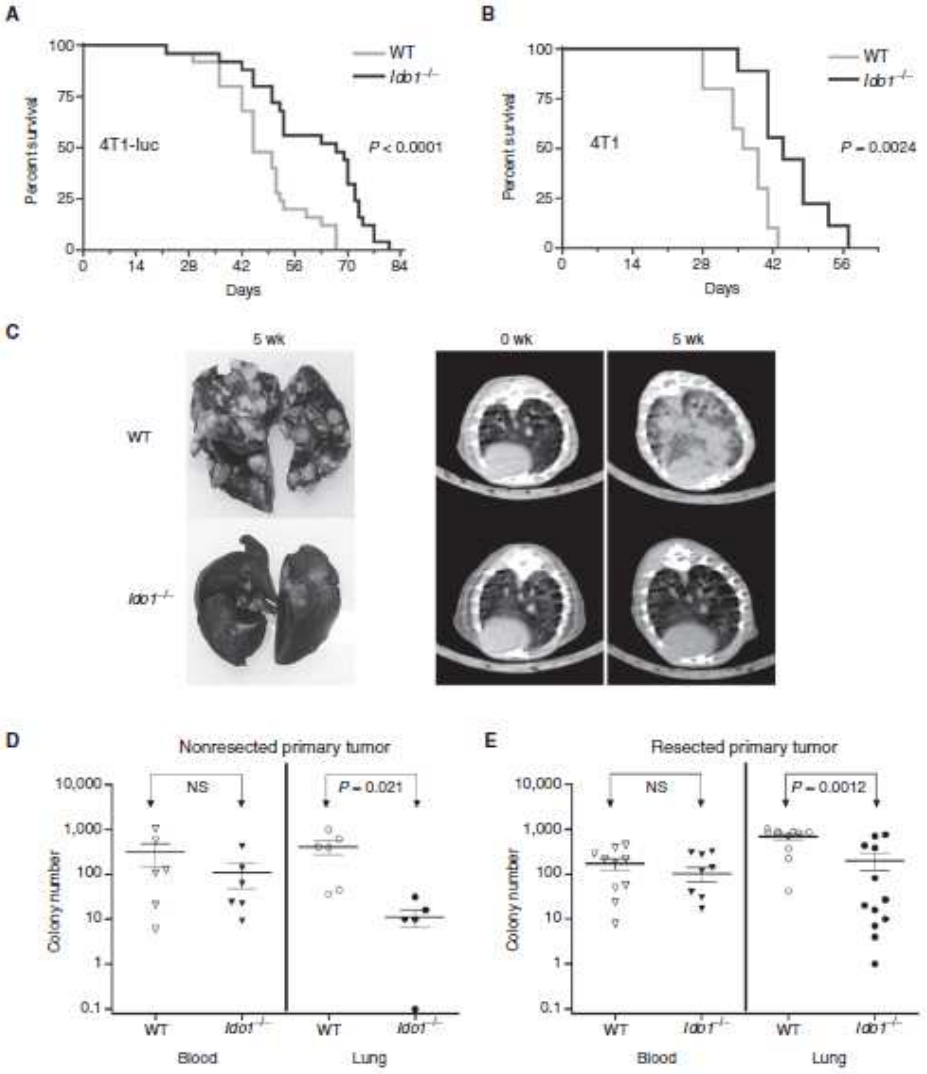

Figure 4. IDO deficiency delays the development of pulmonary metastases. Kaplan-Meier survival curves for cohorts of WT and *Ido1*$^{-/-}$ mice following orthotopic engraftment of 1×10^4 (**A**) 4T1-luc ($n = 25$) or (**B**) 4T1 ($n \geq 9$) tumor cells. Significance was assessed by 2-group log-rank test at $P < 0.05$. The survival benefit observed in *Ido1*$^{-/-}$ mice was independently replicated at University of Maryland Baltimore County. **C**, staining of lungs with India ink and axial images from micro-CT scans depicting the difference in pulmonary metastasis burden between WT and *Ido1*$^{-/-}$ mice at 5 weeks following orthotopic 4T1 tumor cell engraftment. At 5 weeks following (**D**) orthotopic engraftment of 4T1 cells ($n = 6$) or (**E**) orthotopic engraftment of 4T1 cells and resection of the primary tumor at 18 days postengraftment ($n \geq 11$), colony-forming assays were conducted to assess the relative tumor cell burden in the blood (neat) and lungs (1:1,000). Individual data points are graphed on a log scale scatter plot with the means ± SEM and significance assessed by 2-tailed Student *t* test at $P < 0.05$ (NS, not significant).

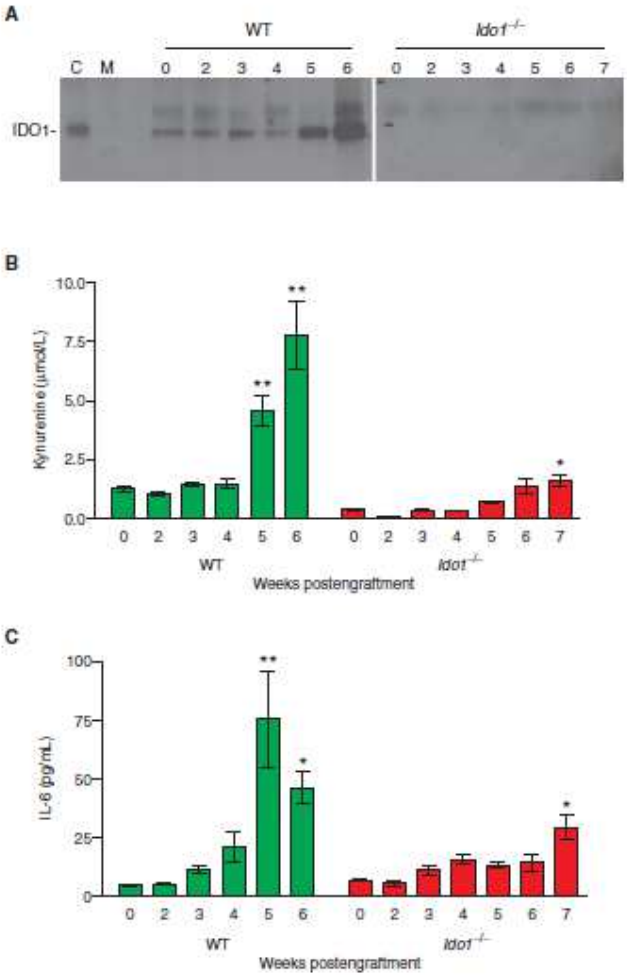

Figure 5. IDO deficiency is associated with attenuated induction of IL-6 during 4T1 tumor metastasis. **A,** evaluation of IDO1 protein levels by immunoprecipitation-Western blot analysis of lung tissue lysates from WT and *Ido1*$^{-/-}$ mice following orthotopic engraftment of 4T1 tumor cells at the time points in weeks indicated above each lane. C, epididymis lysate positive control lane; M, molecular weight marker lane. **B,** evaluation of kynurenine levels by LC/MS-MS–based analysis of homogenized lung samples from WT and *Ido1*$^{-/-}$ mice following orthotopic engraftment of 4T1 tumor cells at the time points in weeks indicted for each lane. Means ± SEM ($n \geq 6$) are graphed with significance relative to baseline determined by one-way ANOVA with Dunn test (*, $P < 0.05$; **, $P < 0.01$). **C,** IL-6 level determinations from cytokine bead array immunoassay–based analysis of homogenized lung samples from WT and *Ido1*$^{-/-}$ mice following orthotopic engraftment of 4T1 tumor cells at the time points in weeks indicted for each lane. Means ± SEM ($n \geq 3$) are graphed with significance relative to baseline determined by one-way ANOVA with Dunn test (*, $P < 0.05$; **, $P < 0.01$).

no difference in metastatic burden was observed in liver, although the presence of 4T1 cells was also nearly too low to detect in this tissue (Supplementary Fig. S2C). Because excision of the primary tumor can alter immune-based effects on metastasis (23), we evaluated the metastasis burden in resected mice. *Ido1*$^{-/-}$ mice continued to exhibit significant resistance to metastasis development (Fig. 4E), indicating that IDO-mediated support of metastatic development in lung is not dependent on the presence of the primary tumor. We also examined pulmonary VEGF levels but found that these increased comparably in both WT and *Ido1*$^{-/-}$ lungs during metastasis development and were actually somewhat higher at baseline in the *Ido1*$^{-/-}$ lungs (Supplementary Fig. S2D).

IDO Is Activated during Metastatic Lung Colonization and Potentiates IL-6 Induction

In WT mice, IDO1 protein and kynurenine levels both increased in the lungs during 4T1 metastasis development, particularly at 5 and 6 weeks postengraftment (Fig. 5A and B). The principal source of IDO1 expression in this context appears to be the native stroma rather than the engrafted 4T1 tumor cells because no IDO1 protein was detectable in the lungs of *Ido1*$^{-/-}$ mice (Fig. 5A), even at 7 weeks postengraftment when

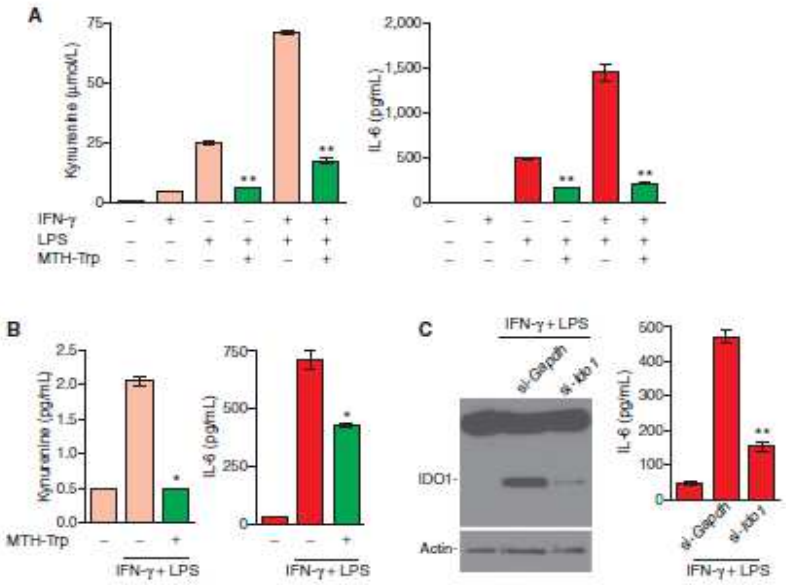

Figure 6. IDO-dependent potentiation of IL-6 production. **A**, supernatant from U937 cells stimulated for 24 hours with IFN-γ (100 ng/mL) and/or LPS (100 ng/mL) was analyzed for kynurenine and IL-6. Results from triplicate wells are plotted as the means ± SEM. Methylthiohydantoin tryptophan (MTH-Trp, 100 μmol/L) was included during induction where indicated and significance relative to the corresponding induced level without MTH-Trp was determined by 2-tailed Student *t* test (**, $P \leq 0.0001$). **B**, supernatant from HL-60 cells stimulated for 24 hours with IFN-γ (100 ng/mL) and LPS (100 ng/mL) was analyzed for kynurenine and IL-6. Results from duplicate wells are plotted as the means ± SEM. Methylthiohydantoin tryptophan (MTH-Trp, 100 μmol/L) was included during induction where indicated and significance relative to the corresponding induced level without MTH-Trp was determined by 2-tailed Student *t* test (*, $P < 0.05$). **C**, HL-60 cells treated in triplicate with Ido1-targeting (si-Ido1) or nontargeting (si-Gapdh) siRNAs were stimulated for 24 hours with IFN-γ (100 ng/mL) and LPS (100 ng/mL). Pooled cell lysates were analyzed by Western blot analysis for IDO1 and β-actin (left). IDO1 induction was suppressed by approximately 89.7% as assessed by densitometric analysis and normalization to actin. Individual cell supernatants were analyzed for IL-6 (right). The IL-6 data are plotted as the means ± SEM with the significance of the difference between specific Ido1-targeting versus nontargeting results determined by 2-tailed Student *t* test (**, $P < 0.0001$). Gapdh, glyceraldehyde-3-phosphate dehydrogenase.

the metastatic tumor burden was high. However, a weak but significant increase in kynurenine was observed in the lungs of *Ido1*$^{+/+}$ mice (Fig. 5B), suggesting that metastasis development may be associated with induction of an alternative mechanism of kynurenine production, such as IDO2 (24) or TDO2 (tryptophan 2,3-dioxygenase; ref. 25), either in conjunction with or in the absence of IDO1.

As in the *Kras*-driven primary lung tumor model, *Ido1* competence in the pulmonary metastatic setting was linked to enhanced elevation of IL-6, with levels increasing up to 15-fold over baseline in WT animals (Fig. 5C). On the other hand, the IL-6 levels in *Ido1*$^{+/+}$ lungs remained about 2- to 4-fold over baseline even when evaluated at an extended time point to account for the differential in tumor burden (Fig. 5C). Thus, like the autochthonous lung tumor studies, results from this lung metastasis model led us to infer a positive regulatory link between IDO and IL-6 production. Direct interrogation of this hypothesis was carried out in a cell-based assay with known IDO inducers. Lipopolysaccharide (LPS) induced both IDO activity and IL-6 production in monocytic U937 cells whereas IFN-γ on its own elicited little response but greatly elevated the level of IDO activity in combination with LPS that was mirrored by a comparable enhancement of IL-6 production (Fig. 6A). In both instances, inclusion of the competitive IDO-inhibitory compound MTH-tryptophan (8) significantly suppressed the observed increases in IDO activity as well as IL-6 production (Fig. 6A). MTH-tryptophan–mediated suppression of IL-6 induction was confirmed in a second monocytic cell line HL-60 (Fig. 6B). Likewise, siRNA-mediated interference with *Ido1* gene expression also significantly suppressed IL-6 induction (Fig. 6C). Taken together, these results are consistent with our *in vivo* findings suggesting that IDO activity can potentiate the elevated production of IL-6.

IDO Drives MDSC Expansion and Immunosuppressive Function

Studies in *Il1r*$^{-/-}$ (IL-1 receptor–nullizygous) mice have shown a crucial role for IL-6 in 4T1 pulmonary metastasis development (26). At the cellular level, IL-1β enhances development

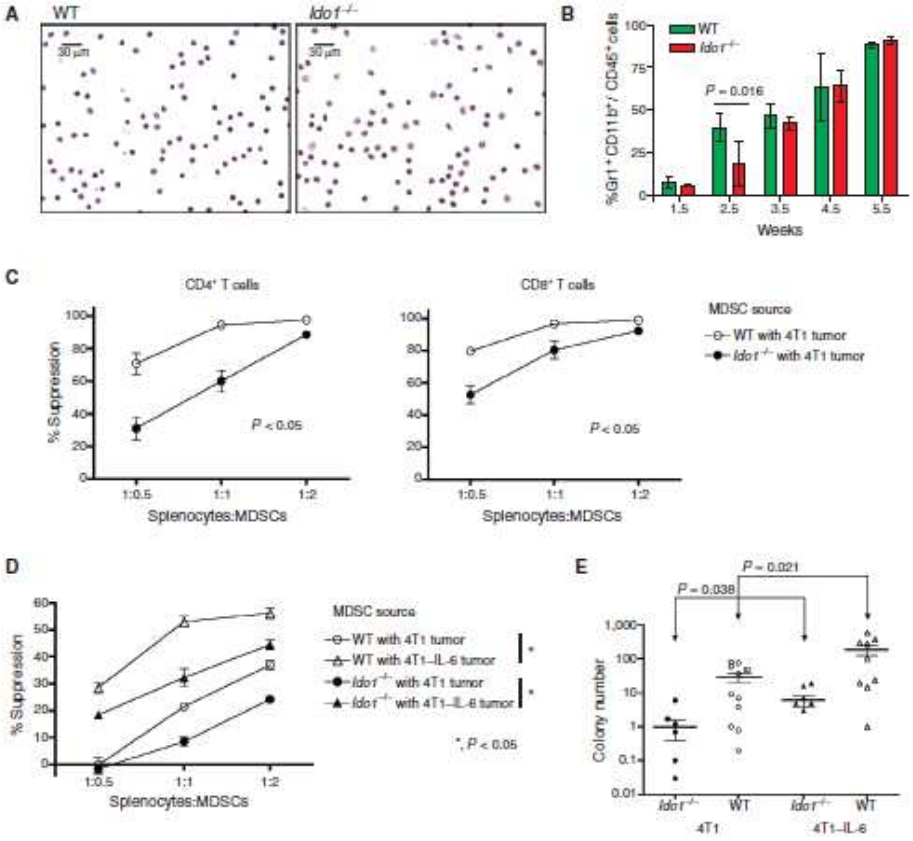

Figure 7. Attenuated MDSC-suppressive activity and metastasis development in IDO-deficient mice is rescued by IL-6. **A**, comparative microscopic images of hematoxylin and eosin (H&E)-stained MDSCs harvested from the blood of WT and Ido1$^{-/-}$ mice with primary 4T1 tumors that were not significantly different in size (12.2 ± 1.36 and 11. 5 ± 0.4 mm in diameter, respectively). **B**, single-cell suspensions of whole-lung tissues were prepared at the indicated time points following 4T1 engraftment into WT and Ido1$^{-/-}$ mice and evaluated by flow cytometry for MDSC infiltration by gating on CD45$^+$ cells and analyzing the Gr1$^+$CD11b$^+$ cell population. Means ± SEM are graphed with significance assessed by 2-tailed Student *t* test at $P < 0.05$. **C**, splenocytes from CD4$^+$ TS1 (left) or CD8$^+$ Clone 4 (right) mice were cocultured in triplicate with cognate peptide and increasing proportions of 4T1-induced peripheral blood MDSCs from WT or Ido1$^{-/-}$ mice. T-cell activation was quantified by uptake of ^{3}H-thymidine and graphed as percentage of suppression relative to activation in the absence of MDSCs. Significance was assessed by Wilcoxon rank test at $P < 0.05$. Outcomes are representative of a minimum of 3 independent experiments. **D**, splenocytes from CD8$^+$ clone 4 transgenic mice were cocultured with cognate peptide and increasing proportions of 4T1 or 4T1–IL-6 tumor-induced MDSCs from WT or Ido1$^{-/-}$ mice for analysis as in **B**. Outcomes are representative of 6 independent experiments using TS1, clone 4, or DO11.10 transgenic T cells. **E**, colony-forming assays to assess the relative tumor cell burden in the lungs conducted 6 weeks following intravenous injection of 4T1 or 4T1–IL-6 cells into WT and Ido1$^{-/-}$ mice. Results are presented on log scale scatter plot with means ± SEM. Significance was assessed by 2-tailed Student *t* test at $P < 0.05$.

of tumor-promoting MDSCs with IL-6 serving as a critical downstream mediator of this process (26). Because *Ido1* loss attenuated IL-6 induction and metastatic colonization in the lung, we hypothesized that MDSCs may be compromised at some level in tumor-bearing *Ido1*$^{-/-}$ mice. MDSCs isolated from WT and *Ido1*$^{-/-}$ mice did not differ phenotypically (Fig. 7A; Supplementary Fig. S3A); however, an early delay in the expansion of Gr1$^+$CD11b$^+$ cells in *Ido1*$^{-/-}$ mice, similar to that observed in *Il1r*$^{-/-}$ animals (26), was noted (Fig. 7B). Moreover, circulating MDSCs isolated from *Ido1*$^{-/-}$ hosts were functionally impaired in their ability to suppress T cells (Fig. 7C). We did not detect IDO1 protein in Gr1$^+$CD11b$^+$ cells

obtained from tumor-bearing WT hosts (Supplementary Fig. S3B), consistent with the hypothesis that the observed functional impairment of MDSCs is a non–cell-autonomous effect of IDO deficiency in which IL-6 may act as a key intermediary.

IL-6 Is Critical to IDO-Driven MDSC Activity and Pulmonary Metastasis

To directly test the ability of IL-6 to functionally restore MDSC-suppressive activity in *Ido1*$^{-/-}$ mice, orthotopic tumors were established using 4T1–IL-6 cells (26), a 4T1 cell population engineered to constitutively express IL-6. MDSCs isolated from *Ido1*$^{-/-}$ mice engrafted with 4T1–IL-6 cells exhibited an elevated T-cell–suppressive activity similar to that of MDSCs isolated from WT hosts engrafted with parental 4T1 cells (Fig. 7D). Further enhancement of MDSC-suppressive activity could be achieved by engrafting 4T1–IL-6 cells into WT mice (Fig. 7D), indicating that the endogenous IL-6 levels stimulated by parental 4T1 tumor cells in WT animals were not fully saturating with regard to promoting MDSC suppressor function.

We next asked whether restoring IL-6 levels could also reverse the metastatic resistance exhibited by *Ido1*$^{-/-}$ mice. In the orthotopic setting, high levels of IL-6 produced in primary tumors formed by 4T1–IL-6 cells complicated the analysis by impairing the efficiency of pulmonary metastasis [possibly reflecting the recruitment of metastatic cancer cells back to IL-6–expressing primary tumors as documented previously (ref. 27)]. However, as our results in orthotopically engrafted mice had indicated that the *Ido1* allelic status does not affect 4T1 intravasation, we reasoned that a valid assessment of the impact of IDO deficiency on pulmonary metastasis could be made by introducing the metastatic tumor cells directly into the circulation. Accordingly, we confirmed that intravenously engrafted *Ido1*$^{-/-}$ mice maintained their resistance to pulmonary metastasis formation, with the apparent mean metastatic tumor burden being 30.4- and 31.6-fold lower in *Ido1*$^{-/-}$ versus WT mice challenged with 4T1 and 4T1–IL-6 cells, respectively (Fig. 7E). The proportional increase in metastatic burden observed in the 4T1–IL-6 challenged cohorts is also in line with the proposed interpretation of the MDSC functional data that IL-6 is not being produced at saturating levels in the 4T1-challenged WT animals. Because of the significantly higher metastasis burden produced by 4T1–IL-6 cells, comparison of 4T1–IL-6 challenged *Ido1*$^{-/-}$ mice to 4T1 challenged WT mice yielded a differential in mean metastatic tumor burden of only 4.8-fold (Fig. 7E). Thus, IL-6 supplementation not only rescued WT levels of MDSC suppressor function in 4T1 tumor-challenged *Ido1*$^{-/-}$ mice but also markedly restored their susceptibility to pulmonary metastasis development.

DISCUSSION

The idea of immune escape as a "hallmark of cancer" (28, 29) represents a groundbreaking although still largely untested paradigm within the field of cancer biology. The presumption that tumors exploit IDO activity as a mechanism of immune escape, initially inferred from the pioneering studies on maternal immune tolerance of Munn and colleagues (30), has become increasingly accepted despite a fundamental deficit in genetic support for the role of IDO in tumor development. This study addresses this gap with direct genetic validation of the importance of IDO in well-established models of lung cancer and metastasis that offers novel insights into the impact of IDO on tumor pathogenesis. Moreover, these findings strongly encourage the prioritization of clinical investigations into the use of IDO pathway inhibitors for treating lung adenocarcinomas and pulmonary metastases where more effective modalities are urgently needed.

While IDO activity was not elevated in lung tissue beyond baseline levels during KRAS-driven lung tumor development, the observed reduction in pulmonary vascularization in *Ido1*$^{-/-}$ animals even before initiation of tumorigenesis implied that the loss of steady-state IDO in this context was sufficiently consequential to impact physiologic processes important to tumor outgrowth. Enhanced tumor vascularization has been reported in tumor xenograft models involving exogenous IDO overexpression (31, 32), but our study is the first to identify a role for IDO in supporting vascular development under native physiologic conditions. Our findings likewise genetically establish the importance of IDO activity in nontumor cells for supporting pulmonary metastasis. In this manner, IDO activity may influence metastatic dissemination to tissues such as the lung where its expression is particularly robust. This may, however, be less relevant when IDO [or tryptophan 2,3-dioxygenase (ref. 25)] activity is substantially elevated within the tumor cells themselves (8, 33), enabling the malignancy to preemptively shape its surroundings through intrinsic tryptophan catabolism. As such, IDO activity that originates from stromal cells of the tumor microenvironment or from the tumor cells themselves may contribute to directing tumor outgrowth.

The positive association between IDO and IL-6 in lung tumorigenesis and metastasis was not necessarily anticipated, given that it runs counter to expectations based on IDO-mediated induction of liver-enriched inhibitory protein (LIP), a negative regulatory isoform of the *Il6* gene expression promoting transcription factor C/EBPβ (24, 34). The precise regulatory impact of LIP on *Il6* expression is not clear cut, however, insofar as other findings have indicated that LIP can interact with NF-κB to induce rather than limit *Il6* transcription (35). Our findings are also consistent with evidence that a downstream product of IDO-mediated catabolism, kynurenic acid, can potentiate IL-6 production in the context of inflammation by signaling through the aryl hydrocarbon receptor (36). IL-6 is a pleiotropic cytokine that is widely implicated in supporting neoplastic outgrowth in the context of chronic inflammation (37). Clinically, IL-6 has been established as a marker of early relapse of resected lung tumors (38). Analyses of DNA polymorphisms in the IL-6 promoter region have identified positive correlations between IL-6 inducibility and lung cancer susceptibility in the context of concurrent inflammatory disease (39) as well as micrometastatic disease in patients with high-risk breast cancer (40). Functionally, IL-6 induction has been identified as an essential downstream component of RAS-induced tumorigenesis (41) that is directly linked to lung tumor development in the *Lox-Kras*^{G12D} transgenic mouse model (21). Numerous other studies indicate that IL-6 can also contribute to tumor promotion by supporting angiogenesis and neovascularization of tumors (42, 43). Thus, biologically,

the epidemiologic and functional data for IL-6 are consistent with the tumor-promoting activity that we have ascribed to IDO through mouse genetics.

Tumor responses to IDO-inhibitory compounds require functional host immunity (5, 6, 8, 9), but the mechanisms through which IDO promotes immune escape have yet to be fully delineated. Connecting IL-6 to IDO provides valuable insight in this regard. IL-6 has previously been identified in the 4T1 metastasis model as critical to the induction of MDSCs, which act as potent inhibitors of antitumor immunity (44). MDSC accumulation is known to be driven by several factors that are produced by tumor cells and the tumor stroma, including the potent inflammatory mediators prostaglandin E2 and IL-1β (45–47). Genetic ablation of IL-1β signaling can affect both the early accumulation of MDSCs as well as their immunosuppressive capability (26), and IL-6 has been determined to be a downstream mediator for the effects of IL-1β on MDSC populations in tumor-bearing animals (26). In this context, our findings identify IDO as a key determinant of IL-6–elicited MDSC accumulation and suppressor activity. Interestingly, IL-1β may dynamically potentiate the contribution of IDO to IL-6 induction given that IL-1β can promote the upregulation of IFNGR1 (48) that enhances *Ido1* inducibility in response to IFN-γ. In contrast, IL-6 may exert a counter-regulatory feedback effect by inducing SOCS3 (suppressor of cytokine signaling 3), which not only attenuates IL-6 signaling (49) but also limits IDO transcription and IDO enzyme stability (50, 51). Thus, IDO is well situated to act as a dynamic modifier of inflammatory states in the microenvironment of primary tumors or budding metastases.

Our results deepen the concept that IDO activity profoundly influences the pathogenic character of the tumor microenvironment by identifying the cytokine IL-6 as a crucial IDO effector for establishing "cancer-associated" inflammation. IL-6 is a far-reaching, pleiotropic signaling molecule that can elicit both intrinsic and extrinsic effects on tumor development (i.e., increased malignancy and survival as well as increased angiogenesis and immune escape). The ramifications of our results thus extend beyond the constrained effects that local IDO-mediated tryptophan catabolism might exert on the proximal microenvironment, and one would expect the potentiation of IL-6 expression by IDO to affect diverse aspects of tumor development with the relative weighting of each aspect being an important focus of future study. Indeed, further investigations of IDO as a nexus for control of tumorigenic inflammation, vascularization, and immune escape will be invaluable in formulating rational strategies to guide the best application of IDO inhibitors that have entered clinical development.

METHODS

Transgenic Mouse Strains

Congenic *Ido1*$^{-/-}$ mice on C57BL/6 and BALB/c strain backgrounds were provided by A. Mellor (Georgia Health Sciences University, GSHU, Augusta GA), and corresponding control strains were purchased from Jackson Laboratory. *LSL-Kras*^{G12D} *Cre*-inducible transgenic mice on a mixed 129Sv*J*-C57BL/6 strain background (16) were obtained through the Mouse Models of Human Cancer Consortium (NCI-Frederick, Frederick, MD). Administration of Ad-*Cre* virus to activate the latent *Kras*^{G12D} allele in lungs of *LSL-Kras*^{G12D} transgenic mice (referred to as *Lox-Kras*^{G12D} mice; ref. 16) was carried out as described (52). Doubly mutant *Ido1*$^{-/-}$ *LSL-Kras*^{G12D} mice were generated through breeding of the 2 transgenic strains. Mating pairs of BALB/c and T-cell receptor (TcR) transgenic DO11.10 BALB/c mice (I-A^d–restricted, specific for chicken ovalbumin$_{323-339}$) were obtained from The Jackson Laboratory. Mating pairs of TcR transgenic Clone 4 BALB/c mice [H-$2K^d$–restricted, specific to influenza hemagglutinin (HA) peptide$_{518-526}$] and TcR transgenic TS1 BALB/c mice (I-E^d–restricted, specific to HA peptide$_{110-119}$) were provided by E. Fuchs (Johns Hopkins, Baltimore, MD). All procedures involving mice were approved by either the Lankenau Institute for Medical Research (LIMR; Wynnewood, PA) or University of Maryland Baltimore County (UMBC) Institutional Animal Care and Use Committee (IACUC).

Micro-CT Scanning

Three-dimensional micro-CT images were acquired from anesthetized mice using an Imtek Micro-CT scanner operated at 40-kVp, 500-μA, 250-millisecond per frame, 5 frames per view, 360 views, and 1-degree increments per view. Contiguous axial DICOM-formatted images through each mouse thorax, with voxels of dimensions 91 μm × 91 μm × 91 μm were compiled into 3D format using Amira v5.1 software and normalized to Hounsfield units. Using the segmentation editor, manual selections of the chest cavity minus the heart were conducted on every other slice followed by interpolation of these selections. Magic wand tool selection was conducted at the threshold range defining air (determined to be between −750 and −350) to define the functional lung volume, which was automatically subtracted from the total chest space to identify the volume representing vasculature and tumors (20).

4T1 Tumor Cell Metastasis

Parental 4T1 mouse mammary carcinoma cells and 4T1-derived cell lines expressing luciferase (4T1-luc) or mouse *Il6* (4T1-IL-6) were maintained as described (5, 22, 26). Primary tumor growth was monitored by caliper measurements of orthogonal diameters. Tumor volume was calculated using the formula for determining a prolapsed elliptoid [$(d^2 \times l)0.52$], where d is the shorter of the 2 orthogonal measurements. To enhance visualization of metastatic nodules, lungs were insufflated with India ink dye, washed, and bleached in Fekete's solution. The clonogenic assay to assess metastatic burden was conducted as described (22).

Real-time PCR

Lung DNA was analyzed by Real Time-PCR containing SYBR green PCR master mix (Applied Biosystems) and primers to amplify *Cre* (5′-GGAGCCGCGCGAGATA-3′ and 5′-GCCACCAGCTTGCATGATC-3′) and endogenous mouse *Gd81* (5′-TCGCCAAGGATGTGAAGCA-3′ and 5′-CATTGTTGGCATCATCATCCA-3′). Assays were conducted in quadruplicate, and relative quantitation of the viral *Cre* gene present in lung tissue was calculated using the comparative threshold cycle (C_T) method (User Bulletin 2, Applied Biosystems) normalizing the target C_T values to the internal housekeeping gene (*Gd81*).

Histology

Tissues were isolated and fixed in 10% neutral-buffered formalin or 4% paraformaldehyde, sectioned, and stained for histopathologic analysis with hematoxylin and eosin using standard methods. For immunofluorescent staining, 4-μm paraffin sections were deparaffinized in xylene and rehydrated with a graded alcohol series. Following antigen retrieval (vector), sections were washed and placed in 0.1% Triton for 10 minutes. Tissue was blocked in 40 μg/mL goat anti-mouse IgG-Fab (H+L) (Jackson ImmunoResearch) followed by

10% normal goat serum (Jackson ImmunoResearch). Rabbit anti-mouse caveolin-1 (1:200; Cell Signaling) was incubated overnight at 4°C. Sections were washed and incubated with goat anti-rabbit Cy3 (1:200; Jackson ImmunoResearch). Tissues were mounted using Prolong Gold with DAPI (Invitrogen). To quantitate the blood vessel areas present within defined fields of caveolin-1–stained lung samples, 4 images were acquired per mouse from 5 WT and 5 *Ido1*$^{-/-}$ mice. Vessel boundaries were identified by caveolin-1 staining, and the area of every vessel within each field was determined using AxioVision Release 4.6 software.

Immunoprecipitation–Western Blot Analysis

Immunoprecipitation of IDO1 protein from mouse lung tissue with purified rabbit polyclonal antibody (7) followed by Western blotting–based detection with rat monoclonal antibody (clone mIDO-48; BioLegend) was carried out as described (9).

Flow Cytometry for Cytokine and Cell Analysis

Flow cytometric data were acquired on a FACSCanto II or Cyan ADP flow cytometer and analyzed using FACSDIVA (BD Biosciences) or Summit v4.3.02 (Beckman/Coulter) software. Multiplexed cytokine analysis was conducted using the Inflammation Bead Array (BD Biosciences). Lung homogenates were centrifuged and supernatant added to beads in the array according to the manufacturer's instructions. Flow cytometric analysis of MDSCs harvested from digested lung samples or from blood was conducted with the following antibodies as indicated: Gr1-FITC, Ly6G-PE, Ly6C-FITC, and CD124 (IL-4Rα)-PE (BD Biosciences); CD11b-PacB, CD115-PE, and F4/80-PE (BioLegend); Ly6C-PerCP (eBioscience); and arginase and iNOS (BD Transduction Labs). Second step goat anti-mouse IgG-Alexa 647 for arginase and inducible NO synthase (iNOS) was from Invitrogen. Isotype control antibodies were from BD Biosciences.

Kynurenine Assay

Lungs were homogenized in PBS containing dithiothreitol (DTT) and protease and phosphatase inhibitors (1:3 wt/vol). Deproteinated lysates were analyzed by high-performance liquid chromatography (HPLC) coupled to electrospray ionization liquid chromatography/tandem mass spectroscopy (LC/MS-MS) analysis as described (9).

Cell Culture

U937 and HL-60 monocytic cell lines (American Type Culture Collection) were expanded for frozen storage after receipt and freshly thawed cells cultured in Dulbecco's Modified Eagle's Media + 10% FBS were used at early passage for experiments. No additional authentication was conducted by the authors. Twenty-four–hour treatment of cells with LPS (100 ng/mL; Sigma) and/or IFN-γ (100 ng/mL; R&D systems) was carried out in triplicate on 1×10^6 cells per well in a 96-well dish. MTH-Trp (methylthiohydantoin-DL-tryptophan; 100 μmol/L; Sigma) was also included at the time of induction as indicated. Kynurenine and IL-6 levels in the supernatant were analyzed as described above. *Ido1* gene "knockdown" studies were conducted with siRNAs (Dharmacon) targeting *Ido1* (catalog no. E-010337-00) or *Gapdh* (catalog no. D-001930-01) using the Accell siRNA Delivery System (Dharmacon) as described by the manufacturer. HL-60 cells were plated at 1×10^4 per well in a 96-well dish and cultured with 1% FBS in the Accell growth media. Twenty-four–hour treatment of cells with LPS and IFN-γ was initiated at 48 hours following incubation with siRNA. Western blotting to detect IDO1 protein in cell lysates was conducted following standard procedures using rabbit polyclonal anti-IDO1 (7) and rabbit monoclonal anti-β-actin (13E5; Cell Signaling) as a loading control. Detection was carried out with goat anti-rabbit IgG, horseradish peroxidase (HRP)-linked secondary antibody (catalog no. 7074; Cell Signaling) using the SuperSignal West Femto Chemiluminescent substrate (Thermo Scientific).

T-cell Suppression Assay

MDSC-suppressive activity was measured as previously described (53) using transgenic splenocytes and their cognate peptides in the presence of 25 Gy–irradiated, blood-derived MDSCs from 4T1 tumor–bearing mice. $HA_{518\text{-}526}$, $HA_{333\text{-}339}$, and $Ova_{323\text{-}339}$ peptides were synthesized in the Biopolymer Core Facility at the University of Maryland, Baltimore, MD. ELISA duo set mAbs for mIL6 were from R&D Systems. Monoclonal antibody Vβ8.1,8.2-PE was from BD PharMingen.

Disclosure of Potential Conflicts of Interest

G.C. Prendergast, A.J. Muller, and J.B. DuHadaway declare a potential conflict of interest with regard to IDO due to intellectual property, financial interests, grant support, and consultancy roles with New Link Genetics Corporation, which is engaged in the clinical development of IDO inhibitors for the purpose of treating cancer and other diseases. R. Metz is an employee of New Link Genetics Corporation as Director of Research and has financial and intellectual property interests in the company. No potential conflicts of interest were disclosed by the other authors.

Authors' Contributions

Conception and design: C. Smith, S. Ostrand-Rosenberg, G.C. Prendergast, A.J. Muller

Development of methodology: C. Smith, J.B. DuHadaway, L.D. Laury-Kleintop, L. Mandik-Nayak, R. Metz, S. Ostrand-Rosenberg, A.J. Muller

Acquisition of data (provided animals, acquired and managed patients, provided facilities, etc.): C. Smith, M.Y. Chang, K.H. Parker, D.W. Beury, J.B. DuHadaway, J. Boulden, E. Sutanto-Ward, S. Ostrand-Rosenberg

Analysis and interpretation of data (e.g., statistical analysis, biostatistics, computational analysis): C. Smith, M.Y. Chang, K.H. Parker, D.W. Beury, H.E. Flick, A.P. Soler, L.D. Laury-Kleintop, L. Mandik-Nayak, S. Ostrand-Rosenberg, G.C. Prendergast, A.J. Muller

Writing, review, and/or revision of the manuscript: C. Smith, D.W. Beury, A.P. Soler, L.D. Laury-Kleintop, L. Mandik-Nayak, R. Metz, S. Ostrand-Rosenberg, G.C. Prendergast, A.J. Muller

Administrative, technical, or material support (i.e., reporting or organizing data, constructing databases): C. Smith, J. Boulden, A.P. Soler, S. Ostrand-Rosenberg

Study supervision: C. Smith, S. Ostrand-Rosenberg, A.J. Muller, G.C. Prendergast

Acknowledgments

The authors thank Gwen Guillard for tissue sectioning and histology and Lingling Yang for preliminary studies on MDSCs in IDO-deficient mice.

Grant Support

A.J. Muller is the recipient of grants from Susan G. Komen for the Cure and the W.W. Smith Foundation. G.C. Prendergast is the recipient of NIH grants CA109542, CA159337, and CA159315 with additional support from NewLink Genetics Corporation, the Sharpe-Strumia Foundation, the Lankenau Medical Center Foundation, and the Main Line Health System. S. Ostrand-Rosenberg is the recipient of NIH grants RO1CA115880, RO1CA84232, and RO1GM021248. C. Smith is the recipient of a postdoctoral fellowship through the Department of Defense Breast Cancer Research Program. D. Beury is the recipient of a predoctoral fellowship through the Department of Defense Breast Cancer Research Program.

Received January 12, 2012; revised May 31, 2012; accepted June 1, 2012; published OnlineFirst July 19, 2012.

REFERENCES

1. Peek RM Jr, Mobley S, DuBois RN. Inflammation in the genesis and perpetuation of cancer: summary and recommendations from a national cancer institute-sponsored meeting. Cancer Res 2005;65:8583–6.
2. Muller AJ, Mandik-Nayak L, Prendergast GC. Beyond immunosuppression: reconsidering indoleamine 2,3-dioxygenase as a pathogenic element of chronic inflammation. Immunotherapy 2010;2:293–7.
3. Muller AJ, Scherle PA. Targeting the mechanisms of tumoral immune tolerance with small-molecule inhibitors. Nat Rev Cancer 2006; 6:613–25.
4. Banerjee T, DuHadaway JB, Gaspari P, Sutanto-Ward E, Munn DH, Mellor AL, et al. A key *in vivo* antitumor mechanism of action of natural product-based brassinins is inhibition of indoleamine 2,3-dioxygenase. Oncogene 2008;27:2851–7.
5. Hou DY, Muller AJ, Sharma MD, DuHadaway J, Banerjee T, Johnson M, et al. Inhibition of indoleamine 2,3-dioxygenase in dendritic cells by stereoisomers of 1-methyl-tryptophan correlates with antitumor responses. Cancer Res 2007;67:792–801.
6. Kumar S, Malachowski WP, Duhadaway JB, Lalonde JM, Carroll PJ, Jaller D, et al. Indoleamine 2,3-dioxygenase is the anticancer target for a novel series of potent naphthoquinone-based inhibitors. J Med Chem 2008;51:1706–18.
7. Metz R, Duhadaway JB, Rust S, Munn DH, Muller AJ, Mautino M, et al. Zinc protoporphyrin IX stimulates tumor immunity by disrupting the immunosuppressive enzyme indoleamine 2,3-dioxygenase. Mol Cancer Ther 2010;9:1864–71.
8. Muller AJ, Duhadaway JB, Donover PS, Sutanto-Ward E, Prendergast GC. Inhibition of indoleamine 2,3-dioxygenase, an immunoregulatory target of the cancer suppression gene Bin1, potentiates cancer chemotherapy. Nat Med 2005;11:312–9.
9. Muller AJ, DuHadaway JB, Jaller D, Curtis P, Metz R, Prendergast GC. Immunotherapeutic suppression of indoleamine 2,3-dioxygenase and tumor growth with ethyl pyruvate. Cancer Res 2010;70:1845–53.
10. Koblish HK, Hansbury MJ, Bowman KJ, Yang G, Neilan CL, Haley PJ, et al. Hydroxyamidine inhibitors of indoleamine-2,3-dioxygenase potently suppress systemic tryptophan catabolism and the growth of IDO-expressing tumors. Mol Cancer Ther 2010;9:489–98.
11. Balachandran VP, Cavnar MJ, Zeng S, Bamboat ZM, Ocuin LM, Obaid H, et al. Imatinib potentiates antitumor T cell responses in gastrointestinal stromal tumor through the inhibition of Ido. Nat Med 2011;17:1094–100.
12. Muller AJ, Duhadaway JB, Chang MY, Ramalingam A, Sutanto-Ward E, Boulden J, et al. Non-hematopoietic expression of IDO is integrally required for inflammatory tumor promotion. Cancer Immunol Immunother 2010;59:1655–63.
13. Muller AJ, Sharma MD, Chandler PR, Duhadaway JB, Everhart ME, Johnson BA III, et al. Chronic inflammation that facilitates tumor progression creates local immune suppression by inducing indoleamine 2,3 dioxygenase. Proc Natl Acad Sci U S A 2008; 105:17073–8.
14. Yoshida R, Imanishi J, Oku T, Kishida T, Hayaishi O. Induction of pulmonary indoleamine 2,3-dioxygenase by interferon. Proc Natl Acad Sci U S A 1981;78:129–32.
15. Yoshida R, Urade Y, Tokuda M, Hayaishi O. Induction of indoleamine 2,3-dioxygenase in mouse lung during virus infection. Proc Natl Acad Sci U S A 1979;76:4084–6.
16. Jackson EL, Willis N, Mercer K, Bronson RT, Crowley D, Montoya R, et al. Analysis of lung tumor initiation and progression using conditional expression of oncogenic K-ras. Genes Dev 2001;15:3243–8.
17. Ji H, Houghton AM, Mariani TJ, Perera S, Kim CB, Padera R, et al. K-ras activation generates an inflammatory response in lung tumors. Oncogene 2006;25:2105–12.
18. Baban B, Chandler P, McCool D, Marshall B, Munn DH, Mellor AL. Indoleamine 2,3-dioxygenase expression is restricted to fetal trophoblast giant cells during murine gestation and is maternal genome specific. J Reprod Immunol 2004;61:67–77.
19. Ozaki Y, Edelstein MP, Duch DS. Induction of indoleamine 2,3-dioxygenase: a mechanism of the antitumor activity of interferon gamma. Proc Natl Acad Sci U S A 1988;85:1242–6.
20. Haines BB, Bettano KA, Chenard M, Sevilla RS, Ware C, Angagaw MH, et al. A quantitative volumetric micro-computed tomography method to analyze lung tumors in genetically engineered mouse models. Neoplasia 2009;11:39–47.
21. Ochoa CE, Mirabolfathinejad SG, Ruiz VA, Evans SE, Gagea M, Evans CM, et al. Interleukin 6, but not T helper 2 cytokines, promotes lung carcinogenesis. Cancer Prev Res (Phila) 2011;4:51–64.
22. Pulaski BA, Ostrand-Rosenberg S. Mouse 4T1 breast tumor model. In: Coligan JE, Kruisbeek AM, Margulies DH, Shevach EM, Strober W, editors. Current protocols in immunology. New York: John Wiley & Sons, Inc.; 2000. p. 20.2.1–16.
23. Ostrand-Rosenberg S, Clements VK, Terabe M, Park JM, Berzofsky JA, Dissanayake SK. Resistance to metastatic disease in STAT6-deficient mice requires hemopoietic and nonhemopoietic cells and is IFN-gamma dependent. J Immunol 2002;169:5796–804.
24. Metz R, Duhadaway JB, Kamasani U, Laury-Kleintop L, Muller AJ, Prendergast GC. Novel tryptophan catabolic enzyme IDO2 is the preferred biochemical target of the antitumor indoleamine 2,3-dioxygenase inhibitory compound D-1-methyl-tryptophan. Cancer Res 2007;67:7082–7.
25. Opitz CA, Litzenburger UM, Sahm F, Ott M, Tritschler I, Trump S, et al. An endogenous tumour-promoting ligand of the human aryl hydrocarbon receptor. Nature 2011;478:197–203.
26. Bunt SK, Yang L, Sinha P, Clements VK, Leips J, Ostrand-Rosenberg S. Reduced inflammation in the tumor microenvironment delays the accumulation of myeloid-derived suppressor cells and limits tumor progression. Cancer Res 2007;67:10019–26.
27. Kim MY, Oskarsson T, Acharyya S, Nguyen DX, Zhang XH, Norton L, et al. Tumor self-seeding by circulating cancer cells. Cell 2009;139:1315–26.
28. Luo J, Solimini NL, Elledge SJ. Principles of cancer therapy: oncogene and non-oncogene addiction. Cell 2009;136:823–37.
29. Prendergast GC. Immune escape as a fundamental trait of cancer: focus on IDO. Oncogene 2008;27:3889–900.
30. Munn DH, Zhou M, Attwood JT, Bondarev I, Conway SJ, Marshall B, et al. Prevention of allogeneic fetal rejection by tryptophan catabolism. Science 1998;281:1191–93.
31. Nonaka H, Saga Y, Fujiwara H, Akimoto H, Yamada A, Kagawa S, et al. Indoleamine 2,3-dioxygenase promotes peritoneal dissemination of ovarian cancer through inhibition of natural killer cell function and angiogenesis promotion. Int J Oncol 2011;38:113–20.
32. Li Y, Tredget EE, Ghaffari A, Lin X, Kilani RT, Ghahary A. Local expression of indoleamine 2,3-dioxygenase protects engraftment of xenogeneic skin substitute. J Invest Dermatol 2006;126:128–36.
33. Uyttenhove C, Pilotte L, Theate I, Stroobant V, Colau D, Parmentier N, et al. Evidence for a tumoral immune resistance mechanism based on tryptophan degradation by indoleamine 2,3-dioxygenase. Nat Med 2003;9:1269–74.
34. Sharma MD, Hou DY, Liu Y, Koni PA, Metz R, Chandler P, et al. Indoleamine 2,3-dioxygenase controls conversion of Foxp3+ Tregs to TH17-like cells in tumor-draining lymph nodes. Blood 2009;113:6102–11.
35. Hu HM, Tian Q, Baer M, Spooner CJ, Williams SC, Johnson PF, et al. The C/EBP bZIP domain can mediate lipopolysaccharide induction of the proinflammatory cytokines interleukin-6 and monocyte chemoattractant protein-1. J Biol Chem 2000;275:16373–81.

36. DiNatale BC, Murray IA, Schroeder JC, Flaveny CA, Lahoti TS, Laurenzana EM, et al. Kynurenic acid is a potent endogenous aryl hydrocarbon receptor ligand that synergistically induces interleukin-6 in the presence of inflammatory signaling. Toxicol Sci 2010;115:89–97.
37. Hodge DR, Hurt EM, Farrar WL. The role of IL-6 and STAT3 in inflammation and cancer. Eur J Cancer 2005;41:2502–12.
38. Kita H, Shiraishi Y, Watanabe K, Suda K, Ohtsuka K, Koshiishi Y, et al. Does postoperative serum interleukin-6 influence early recurrence after curative pulmonary resection of lung cancer? Ann Thorac Cardiovasc Surg 2011;17:454–60.
39. Seow A, Ng DP, Choo S, Eng P, Poh WT, Ming T, et al. Joint effect of asthma/atopy and an IL-6 gene polymorphism on lung cancer risk among lifetime non-smoking Chinese women. Carcinogenesis 2006;27:1240–4.
40. DeMichele A, Martin AM, Mick R, Gor P, Wray L, Klein-Cabral M, et al. Interleukin-6 -174G->C polymorphism is associated with improved outcome in high-risk breast cancer. Cancer Res 2003;63:8051–6.
41. Ancrile B, Lim KH, Counter CM. Oncogenic Ras-induced secretion of IL6 is required for tumorigenesis. Genes Dev 2007;21:1714–9.
42. Angelo LS, Kurzrock R. Vascular endothelial growth factor and its relationship to inflammatory mediators. Clin Cancer Res 2007;13:2825–30.
43. Grivennikov SI, Karin M. Inflammatory cytokines in cancer: tumour necrosis factor and interleukin 6 take the stage. Ann Rheum Dis 2011;70 Suppl 1: i104–8.
44. Ostrand-Rosenberg S, Sinha P. Myeloid-derived suppressor cells: linking inflammation and cancer. J Immunol 2009;182:4499–506.
45. Bunt SK, Sinha P, Clements VK, Leips J, Ostrand-Rosenberg S. Inflammation induces myeloid-derived suppressor cells that facilitate tumor progression. J Immunol 2006;176:284–90.
46. Sinha P, Clements VK, Fulton AM, Ostrand-Rosenberg S. Prostaglandin E2 promotes tumor progression by inducing myeloid-derived suppressor cells. Cancer Res 2007;67:4507–13.
47. Song X, Krelin Y, Dvorkin T, Bjorkdahl O, Segal S, Dinarello CA, et al. CD11b+/Gr-1+ immature myeloid cells mediate suppression of T cells in mice bearing tumors of IL-1beta-secreting cells. J Immunol 2005;175:8200–8.
48. Shirey KA, Jung JY, Maeder GS, Carlin JM. Upregulation of IFN-gamma receptor expression by proinflammatory cytokines influences IDO activation in epithelial cells. J Interferon Cytokine Res 2006;26:53–62.
49. Heinrich PC, Behrmann I, Haan S, Hermanns HM, Muller-Newen G, Schaper F. Principles of interleukin (IL)-6-type cytokine signalling and its regulation. Biochem J 2003;374:1–20.
50. Orabona C, Belladonna ML, Vacca C, Bianchi R, Fallarino F, Volpi C, et al. Cutting edge: silencing suppressor of cytokine signaling 3 expression in dendritic cells turns CD28-Ig from immune adjuvant to suppressant. J Immunol 2005;174:6582–6.
51. Orabona C, Pallotta MT, Volpi C, Fallarino F, Vacca C, Bianchi R, et al. SOCS3 drives proteasomal degradation of indoleamine 2,3-dioxygenase (IDO) and antagonizes IDO-dependent tolerogenesis. Proc Natl Acad Sci U S A 2008;105:20828–33.
52. Fasbender A, Lee JH, Walters RW, Moninger TO, Zabner J, Welsh MJ. Incorporation of adenovirus in calcium phosphate precipitates enhances gene transfer to airway epithelia *in vitro* and *in vivo*. J Clin Invest 1998;102:184–93.
53. Sinha P, Clements VK, Ostrand-Rosenberg S. Reduction of myeloid-derived suppressor cells and induction of M1 macrophages facilitate the rejection of established metastatic disease. J Immunol 2005;174:636–45.

Appendix 4: Tumor-induced myeloid-derived suppressor cell function is independent of IFN-γ and IL-4Rα. Pratima Sinha, Katherine Parker, Lucas Horn, Suzanne Ostrand-Rosenberg, European Journal of Immunology, 2012.

European Journal of Immunology

SHORT COMMUNICATION

Tumor-induced myeloid-derived suppressor cell function is independent of IFN-γ and IL-4Rα

Pratima Sinha, Katherine H. Parker, Lucas Horn and Suzanne Ostrand-Rosenberg

Department of Biological Sciences, University of Maryland Baltimore County, Baltimore, MD, USA

Myeloid-derived suppressor cells (MDSCs) are present in most cancer patients and experimental animals where they exert a profound immune suppression and are a significant obstacle to immunotherapy. IFN-γ and IL-4 receptor alpha (IL-4Rα) have been implicated as essential molecules for MDSC development and immunosuppressive function. If IFN-γ and IL-4Rα are critical regulators of MDSCs, then they are potential targets for preventing MDSC accumulation or inhibiting MDSC function. Because data supporting a role for IFN-γ and IL-4Rα are not definitive, we have examined MDSCs induced in IFN-γ-deficient, IFN-γR-deficient, and IL-4Rα-deficient mice carrying three C57BL/6-derived (B16 melanoma, MC38 colon carcinoma, and 3LL lung adenocarcinoma), and three BALB/c-derived (4T1 and TS/A mammary carcinomas, and CT26 colon carcinoma) tumors. We report that although MDSCs express functional IFN-γR and IL-4Rα, and have the potential to signal through the STAT1 and STAT6 pathways, respectively, neither IFN-γ nor IL-4Rα impacts the phenotype, accumulation, or T-cell suppressive potency of MDSCs, although IFN-γ and IL-4Rα modestly alter MDSC-macrophage IL-10 crosstalk. Therefore, neither IFN-γ nor IL-4Rα is a key regulator of MDSCs and targeting these molecules is unlikely to significantly alter MDSC accumulation or function.

Keywords: Cancer · Cellular immunology · T-cell activation · Tumor-induced immune suppression · Tumor immunology


Supporting Information available online

Introduction

Individuals with advanced cancer are frequently immunosuppressed, lack effective innate and adaptive antitumor immunity, and are poorly responsive to active immunotherapy. Assorted tumor-secreted factors drive the accumulation of multiple immune suppressive mechanisms [1]. Tumor-secreted factors act directly to activate suppressive mechanisms, or indirectly by inducing host cells that reduce immunocompetence [2]. Different cancers stimulate diverse inhibitory mechanisms; however, myeloid-derived suppressor cells (MDSCs) are induced by virtually all cancers and are an obstacle to antitumor immunity [3]. Mouse MDSCs are a heterogeneous cell population consisting of $CD11b^+Gr1^+$ cells. Two major subpopulations are defined based on the differential expression of Ly6C and Ly6G, the components of Gr1. Monocytic MDSCs (MO-MDSCs) are mononuclear and $CD11b^+Ly6G^-Ly6C^{hi}$, while granulocytic MDSCs (PMN-MDSCs, where PMN-MDSCs are defined as polymorphonuclear MDSCs) are polymorphonuclear and $CD11b^+Ly6G^+Ly6C^{low/-}$ [4, 5]. Gr1 levels roughly correlate with Ly6G levels, so that $CD11b^+Gr1^{hi/mod}$ cells tend to be $CD11b^+Ly6G^+Ly6C^{-/low}$ PMN-MDSCs [6]. Both subpopulations

Correspondence: Dr. Suzanne Ostrand-Rosenberg
e-mail: srosenbe@umbc.edu

suppress by the production of arginase, while MO-MDSCs also produce nitric oxide (NO) [4, 5]. Although not as well characterized, comparable subpopulations exist in cancer patients [7–9].

Various tumor-produced factors, including granulocyte-macrophage-colony stimulating factor (GM-CSF) [6, 8, 10–13], IL-1β [14, 15], IL-6 [16], cyclooxygenase-2 and prostaglandin E2 [17, 18], S100A8/A9 [19, 20], and vascular endothelial growth factor [21] facilitate MDSC development and/or suppressive activity. Because MDSCs are induced by any one of these factors, no single molecule is essential for generating MDSCs. In contrast, IFN-γ [10, 22] and IL-4 receptor alpha (IL-4Rα) [9, 23] have been reported as essential for MDSC development and/or suppressive activity. Two of these studies used MDSC "cell lines" [22, 23], so the applicability of the results to primary MDSCs is unclear. The requirement for IFN-γ [4] and IL-4Rα [9, 16] has been attributed to the development and suppressive activity of MO-MDSCs and PMN-MDSCs, respectively. IL-4Rα is also considered a marker for human MDSCs [9]. However, other studies demonstrated that IL-4Rα [5, 24] and IFN-γ [25] are not essential for murine MDSC accumulation or suppression. If IFN-γ and/or IL-4Rα are critical for MDSC development and function, then manipulation of these molecules could impact MDSC-mediated immune suppression. Therefore, it is important to clarify the role of IFN-γ and IL-4Rα in MDSC biology. Given the inconsistencies in the literature, we evaluated the role of these molecules using IFN-γ-deficient, IFN-γR-deficient (where IFN-γR is defined as interferon gamma receptor), and IL-4Rα-deficient mice using three C57BL/6-derived and three BALB/c-derived tumors that induce monocytic and granulocytic MDSCs. We now report that neither IFN-γ nor IL-4Rα is essential for murine MDSC development or suppression.

Results and discussion

MDSCs from wild-type, IFN-$\gamma^{-/-}$, IFN-$\gamma R^{-/-}$, and IL-4R$\alpha^{-/-}$ mice have similar phenotypes

To determine if IFN-γ or IL-4Rα impacts MDSC development, wild-type BALB/c, IFN-$\gamma^{-/-}$, IFN-$\gamma R^{-/-}$, and IL-4R$\alpha^{-/-}$ mice were inoculated with syngeneic TS/A, 4T1, or CT26 tumor cells, and wild-type C57BL/6, IFN-$\gamma^{-/-}$, and IFN-$\gamma R^{-/-}$ mice were inoculated with syngeneic MC38, 3LL, or B16 tumor cells. MDSCs were harvested from the blood when primary tumors within each group of wild-type and knockout mice carrying the same tumor were approximately equal in size, and analyzed by flow cytometry (Figs. 1, 2). Microscopy images were obtained to confirm morphology (Supporting Information Fig. 1). Percentages of total, MO-MDSCs, and PMN-MDSCs did not significantly differ between wild-type, IFN-$\gamma^{-/-}$, IFN-$\gamma R^{-/-}$, and IL-4R$\alpha^{-/-}$ mice with the same tumor (Fig. 1, 2A). As reported previously, MO-MDSCs ($CD11b^+Ly6G^-Ly6C^{hi}$) express more CD115, F4/80, and iNOS compared with PMN-MDSCs ($CD11b^+Ly6G^+Ly6C^{low/-}$), while all MDSC populations contain similar quantities of IL-4Rα and arginase [4, 5] (representative profiles for individual mice are in Fig. 2B; average mean channel fluorescence pooled from three mice per group are in Fig. 2C). MDSCs induced by the six tumors in their respective syngeneic wild-type, IFN-$\gamma^{-/-}$, and IFN-$\gamma R^{-/-}$ hosts do not substantially differ in expression of CD11b, Gr1, Ly6C, Ly6G, IL-4Rα, CD115, F4/80, arginase, iNOS, or ROS. MDSCs induced by the three tumors in BALB/c and IL-4R$\alpha^{-/-}$ mice express similar levels of CD11b, Gr1, Ly6C, Ly6G, CD115, F4/80, arginase, iNOS, and ROS. Therefore, IFN-γ and IL-4Rα do not alter the phenotype of MO-MDSCs or PMN-MDSCs with respect to the markers that define these cells, or impact the accumulation of MDSCs.

MDSC-mediated T-cell suppression is independent of IFN-γ and IL-4Rα

To determine if IFN-γ or IL-4Rα is essential for T-cell suppression by MDSCs, MDSCs were harvested from tumor-bearing wild-type and knockout mice, and tested for their ability to suppress the activation of antigen-specific transgenic T cells. MDSCs induced by the same tumor were similarly suppressive for $CD8^+$ and $CD4^+$ T cells regardless of whether they were generated in wild-type, IFN-$\gamma^{-/-}$, IFN-$\gamma R^{-/-}$, or IL-4R$\alpha^{-/-}$ mice (Fig. 3A). Therefore, the T-cell suppressive function of MDSCs is not affected by IFN-γ or IL-4Rα.

MDSC-macrophage crosstalk is independent of IFN-γ and IL-4Rα

MDSCs also promote tumor progression by polarizing immunity toward a type 2 response through their crosstalk with macrophages that reduces macrophage production of IL-12 and increases MDSCs production of IL-10 [24]. MDSCs from IFN-$\gamma^{-/-}$, IFN-$\gamma R^{-/-}$, and IL-4R$\alpha^{-/-}$ mice produced less IL-10 than MDSCs from wild-type mice when cocultured with or without wild-type BALB/c macrophages (Fig. 3B), indicating that MDSC production of IL-10 and macrophage-induced MDSC production of IL-10 is modestly affected by IFN-γ and IL-4Rα. Macrophage production of IL-12 was reduced >87% by MDSCs from wild-type, IFN-$\gamma^{-/-}$, IFN-$\gamma R^{-/-}$, and IL-4R$\alpha^{-/-}$ mice. Since MDSCs produced IL-10 downregulates macrophage production of IL-12 [24], and macrophage IL-12 expression is not impacted, it is likely that the modest decrease in IL-10, although statistically significant, is not physiologically relevant.

MDSCs have functional receptors for IFN-γ and IL-4

Synthesis of iNOS and NO by MO-MDSCs are attributed to IFN-γ signaling through STAT1 [4]. To determine if this pathway is active, B16- and 4T1-induced MDSCs were examined for STAT1 phosphorylation. $CD11b^+Gr1^+$ MDSCs from wild type, but not from IFN-$\gamma R^{-/-}$ mice, expressed IFN-γR and IFN-γ-deficiency did not affect expression of IFN-γR (Supporting Information Fig. 2).

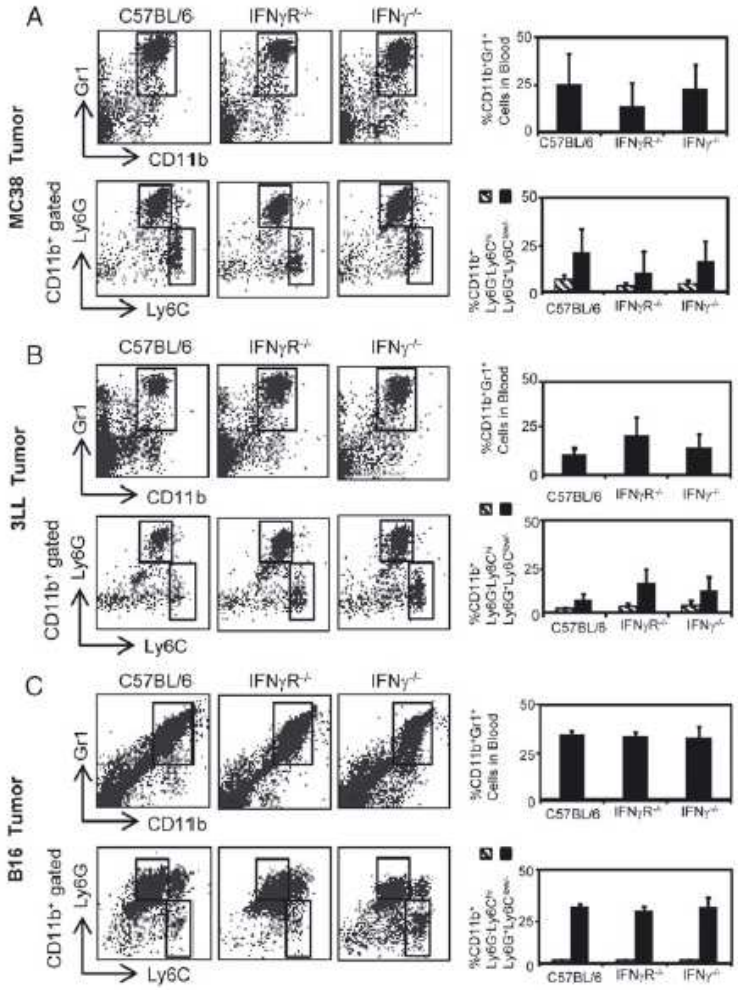

Figure 1. MO-MDSCs and PMN-MDSCs from wild-type, IFN-γ$^{-/-}$, IFN-γR$^{-/-}$, and IL-4Rα$^{-/-}$ mice have similar phenotypes. Wild-type, IFN-γ$^{-/-}$, and IFN-γR$^{-/-}$ mice on a C57BL/6 background or wild-type, IFN-γ$^{-/-}$, IFN-γR$^{-/-}$, and IL-4Rα$^{-/-}$ mice on a BALB/c background were inoculated with MC38 (A), 3LL (B), or B16 (C) tumor cells (C57BL/6) or TS/A (D), 4T1 (E), or CT26 (F) tumor cells (BALB/c). Mice with 4T1 and B16 tumors were bled on days 21–28 when primary tumors for each group of wild-type and knockout mice with the same tumor were 11.38 ± 0.94 and 6.29 ± 0.68 mm in diameter, respectively. Mice with MC38, 3LL, TS/A, and CT26 tumors were bled on day 25–26 when primary tumors for each group of wild-type and knockout mice with the same tumor were 13.29 ± 2.1, 8.2 ± 0.77, 12.4 ± 1.00, 13.55 ± 1.03 mm in diameter, respectively. RBCs were removed by lysis and blood leukocytes were stained with fluorescently labeled mAbs for CD11b and Gr1, or CD11b, Ly6C, and Ly6G. Gr1- and CD11b-labeled cells (top row dot plot of each tumor); CD11b-, Ly6G-, and Ly6C-labeled cells gated for CD11b$^+$ cells and analyzed for Ly6C and Ly6G expression (bottom row dot plot of each tumor). Right hand graphs show percentages of total MDSCs (Gr1$^+$CD11b$^+$ — top panel), and MO-MDSCs (CD11b$^+$Ly6G$^-$Ly6C^{hi}) and PMN-MDSCs (CD11b$^+$Ly6G$^+$Ly6C$^{low/-}$ — bottom panel). Each flow profile shows the results of individual mice and the bar graphs represent average + SD of three mice per group. There is no statistically significant difference between the levels of total MDSCs, MO-MDSCs, and PMN-MDSCs for wild-type and knockout mice with the same tumor (ANOVA single factor; $p > 0.05$ for all comparisons). Data are from one of three independent experiments.

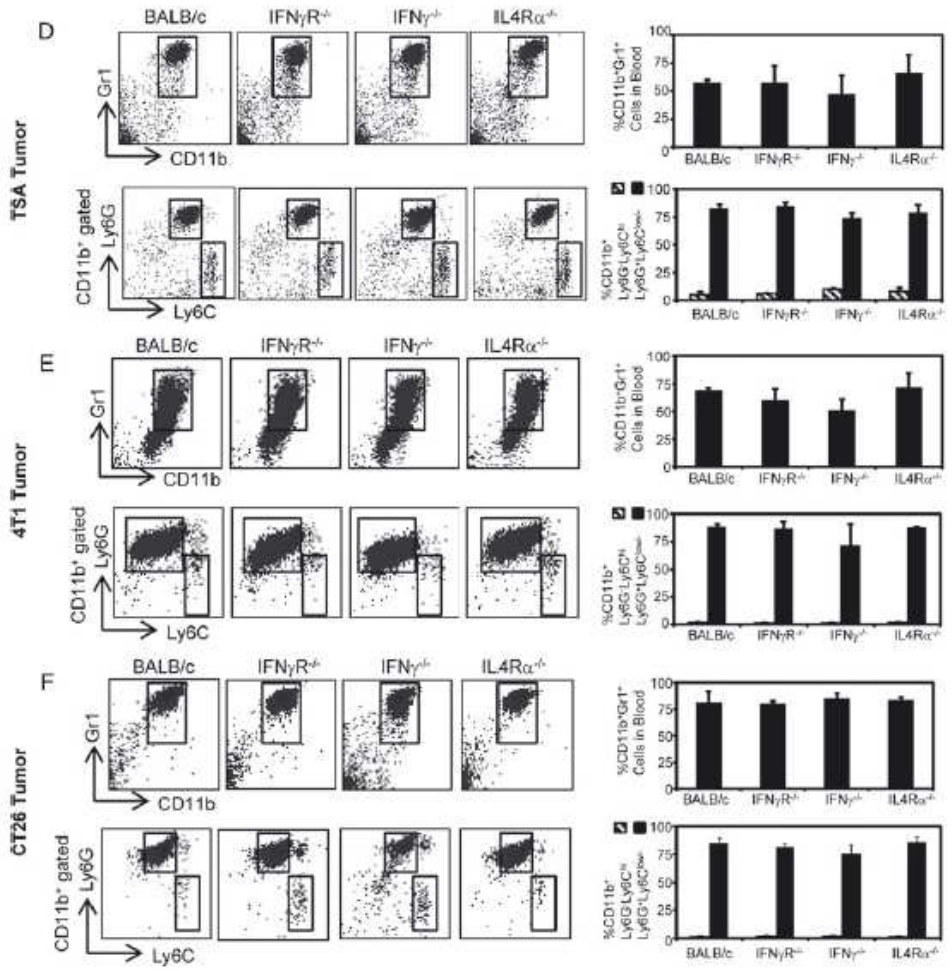

Figure 1. (Continued)

IFN-γ-treated MDSCs from wild-type and IFN-γ$^{-/-}$ mice, but not from control IFN-γR$^{-/-}$ mice, contained phosphorylated STAT1 (Fig. 3C) indicating that MDSCs have the potential to respond to IFN-γ.

Production of arginase has been attributed to IL-4 and IL-13 signaling through the common γ and IL-4Rα chains [9, 26]. Stimulation of MDSCs from wild type, but not from IL-4Rα$^{-/-}$ mice with IL-4, activated STAT6 (pSTAT6, where pSTAT6 is defined as phosphorylated STAT6) (Fig. 3C), demonstrating that MDSCs have the potential to respond to IL-4 through IL-4Rα.

Concluding remarks

These studies demonstrate that although MDSCs can respond to IFN-γ and IL-4, IFN-γ and IL-4Rα do not regulate MDSCs accumulation, phenotype, or suppression. Therefore, targeting IFN-γ and/or IL-4Rα will not reduce the quantity of MDSC, alter MDSC phenotype, or restore T-cell activation. MDSC production of IL-10 and macrophage-induced MDSC production of IL-10 are partially regulated by IFN-γ and IL-4Rα. However, targeting these molecules is unlikely to facilitate polarization toward a type 1

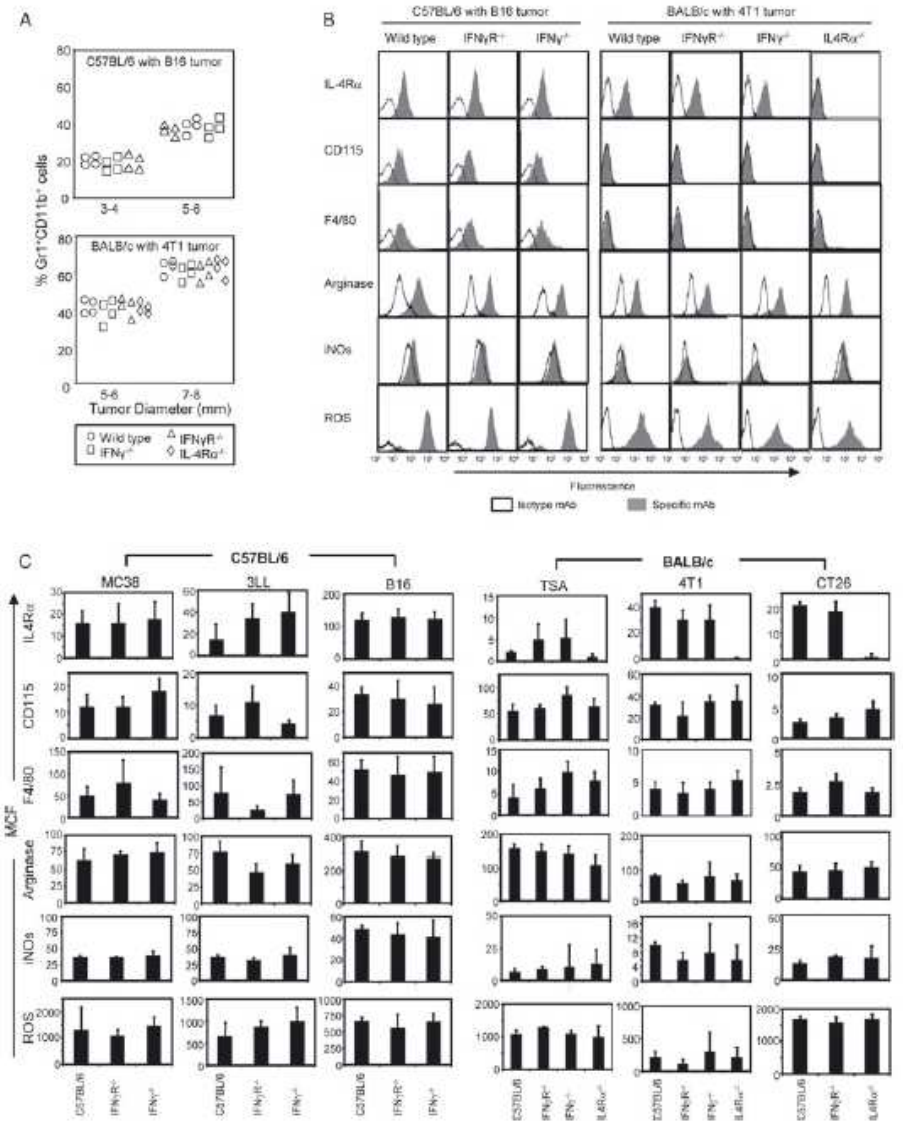

Figure 2. (A) BALB/c and C57BL/6 mice and their associated knockout strains with 4T1 or B16 tumors were bled when tumor diameters were at the indicated sizes and leukocytes stained as in figure 1 for CD11b and Gr1. Each symbol represents an individual mouse. Wild-type and knockout groups with the same tumor are not statistically different. $n = 4$ mice/group/strain/tumor diameter (ANOVA: single factor analysis $p > 0.05$). Data were pooled from four experiments. (B) C57BL/6 and BALB/c mice and their associated knockout strains with B16 or 4T1 tumors were bled and leukocytes stained as in figure 1 for CD11b and Gr1. Gated $CD11b^+$ $Gr1^+$cells were analyzed for IL-4Rα, CD115, F4/80, arginase, iNOS, and ROS. Data are from one of three independent experiments. (C) Gated $CD11b^+$ $Gr1^+$cells of figure 1 were analyzed for IL-4Rα, CD115, F4/80, arginase, iNOS, and ROS. Data shown are average + SD of mean channel fluorescence (MCF) (Experimental MCF — control MCF) of three mice per group. The levels of IL-4Rα, CD115, F4/80, arginase, iNOS, or ROS in wild-type and knockout groups with the same tumor are not statistically different (ANOVA single factor; $p > 0.05$ for all comparisons). Data are from one of two (MC38, 3LL, TSA, and CT26), three (B16), and four (4T1) independent experiments.

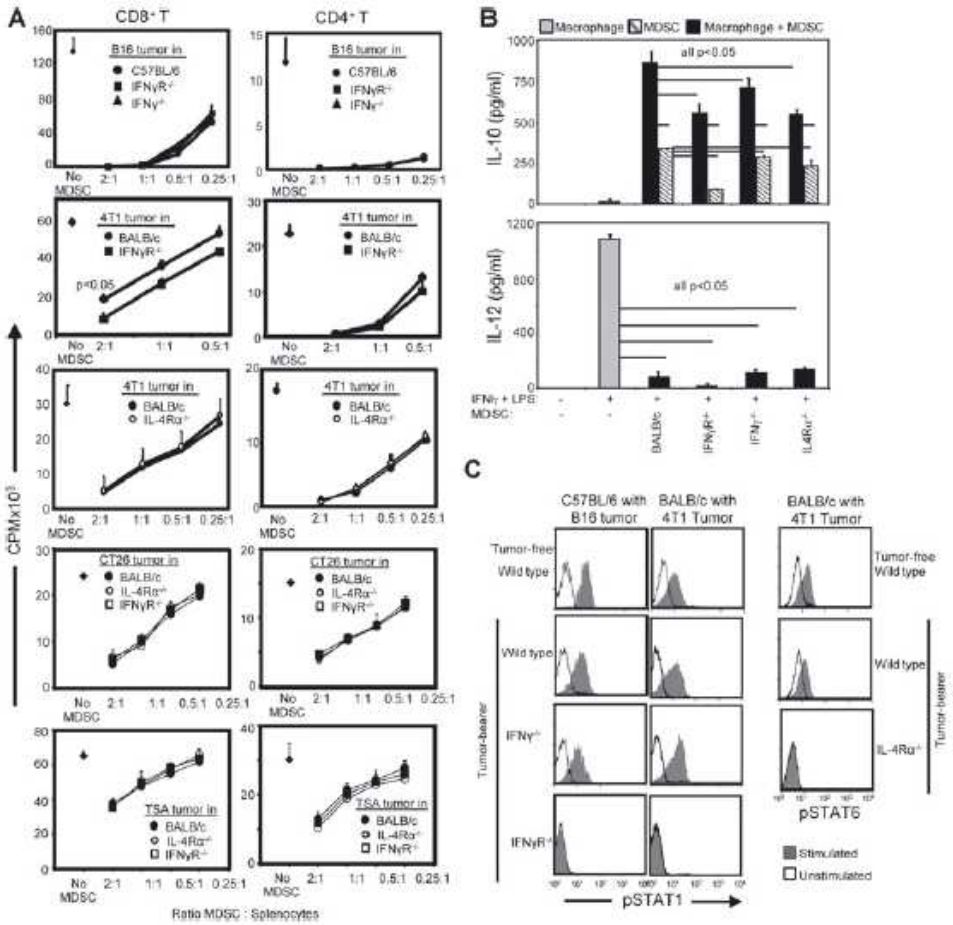

Figure 3. IFN-γ and IL-4Rα do not affect T-cell suppressive activity of MDSCs. MDSCs were generated in B16 tumor-bearing wild-type, IFN-$\gamma^{-/-}$, and IFN-$\gamma R^{-/-}$ C57BL/6 mice, and in 4T1, TS/A, and CT26 tumor-bearing wild-type, IFN-$\gamma R^{-/-}$, and IL-$4R\alpha^{-/-}$ BALB/c mice. Magnetic bead purified blood MDSCs were >90% $Gr1^+CD11b^+$ cells. (A) MDSCs were incubated at the indicated ratios with 1×10^5 splenocytes from OT-I (upper left-hand panel), Clone 4 (bottom four left panels), or DO11.10 (right panels) transgenic mice and cognate peptide [24]. T-cell activation was measured by incorporation of ^{3}H-thymidine. Data are the average of triplicate points + SD from one of two independent experiments with MDSCs pooled from three to four mice/group. There is no statistically significant difference between suppressive activity of MDSCs induced by the same tumor in wild-type vs. knockout mice (Student's two tailed t-test for paired two samples for means, $p > 0.05$), with the exception of 4T1 induced IFN-$\gamma R^{-/-}$ MDSCs that are more suppressive than BALB/c MDSCs for $CD8^+$ T cells ($p < 0.05$). (B) MDSC production of IL-10 and macrophage-induced MDSC production of IL-10 is modestly affected by IFN-γ and IL-4Rα; MDSC-mediated downregulation of macrophage-produced IL-12 is not affected by IFN-γ or IL-4Rα. Peritoneal macrophages (>90% $F4/80^+$) from wild-type BALB/c mice were untreated or activated with LPS and IFN-γ and cocultured overnight with MDSCs from 4T1 tumor-bearing wild-type, IFN-$\gamma^{-/-}$, IFN-$\gamma R^{-/-}$, or IL-$4R\alpha^{-/-}$ BALB/c mice at 0.75×10^6 macrophages/well. Culture supernatants were assayed by ELISA for IL-10 and IL-12 [24]. Data are the average + SD of quadruplicates from three mice/group and are representative of three independent experiments. (Student's two tailed t-test for paired two sample for means). Top panel: macrophages increase wild-type and knockout MDSC production of IL-10; knockout MDSCs produce less IL-10 than wild-type MDSCs. Bottom panel: wild-type and knockout MDSCs decrease macrophage production of IL-12 by >87%. (C) IFN-γ and IL-4 activate STAT1 and STAT6, respectively, in MDSCs. Left panel: blood MDSCs from tumor-free and tumor-bearing wild-type, IFN-$\gamma^{-/-}$, and IFN-$\gamma R^{-/-}$ C57BL/6 (B16) and BALB/c (4T1) mice were unstimulated or stimulated in vitro for 15 min with IFN-γ and then stained for Gr1, CD11b, and pSTAT1. Gated $Gr1^+CD11b^+$ cells were analyzed for phosphorylated STAT1 (pSTAT1). Right panel: MDSCs from tumor-free wild type, or tumor-bearing wild-type and IL-$4R\alpha^{-/-}$ mice were stimulated in vitro for 15 min with IL-4 and then stained for Gr1, CD11b, and pSTAT6. Gated $Gr1^+CD11b^+$ cells were analyzed for pSTAT6. Each panel depicts MDSCs pooled from three or more mice. Data are from one of three experiments.

response because the minimal reduction in MDSC production of IL-10 will not restore macrophage production of IL-12. Therefore, treatments that downregulate IFN-γ and/or IL-4Rα are unlikely to be therapeutically effective.

Materials and methods

Mice

Breeding stock for BALB/c, transgenic DO11.10 (TcR is I-A^d-restricted, ovalbumin (OVA) $peptide_{323-339}$-specific), transgenic OT-1 (TcR is H-$2K^b$-restricted, OVA peptide SINNFEKL-specific), IFN-γR-deficient C57BL/6, IFN-γ- deficient C57BL/6, IFN-γ-deficient, and IL-4Rα-deficient BALB/c, and BALB/c Clone 4 (H-$2K^d$-restricted, influenza hemagglutinin $peptides_{518-526}$-specific) mice were from The Jackson Laboratory (Bar Harbor, ME, USA) or maintained in the UMBC animal facility. IFN-γR-deficient BALB/c mice were generated from 129-IFN-$\gamma R^{-/-}$ mice (The Jackson Laboratory) by backcrossing to BALB/c for 12 generations. PCR screening was performed as described (http://jaxmice.jax.org/protocolsdb/f?p=116:2:144212 4967609278::NO:2:P2_MASTER_PROTOCOL_ID,P2_JRS_CODE: 7034,002702). Pups from the F12 generation were intercrossed and PCR screened to identify homozygous BALB/c IFN-$\gamma R^{-/-}$ mice. Mice were bred in the UMBC animal facility. All animal procedures were approved by the UMBC Institutional Animal Care and Use Committee.

Antibodies and flow cytometry

Fluorescently-coupled Gr1 (clone RB68C5), CD11b, Ly6C (clone AL-21), Ly6G (clone 1A8), IL-4Rα, IFN-γR, CD115, F4/80, CD3, CD4, CD8, DO11.10 TCR (clone KJ1-26), $V\beta_{8.1\&8.2}$ mAbs, mAbs to arginase I and iNOs, rat antimouse IgG1-FITC (A85-1), and isotype control mAbs were from BD Pharmingen (San Diego, CA, USA). Goat antimouse IgG2a-FITC was from Southern Biotech (Birmingham, AL, USA). Staining for flow cytometry was performed as described [25]. Samples were analyzed on a Beckman/Coulter XL or CyAn ADP flow cytometer and analyzed using FCS-Express or Summit software.

Tumor cells, tumor cell inoculation, and MDSC collection

4T1 cells were maintained as described [27]. B78H1-GM-CSF cells (B16 variant called B16 in the present study) [11], 3LL lung carcinoma, CT26 and MC38 colon carcinomas [5], and the TS/A mammary carcinoma [28] were maintained as described. Mice were inoculated in the abdominal mammary gland with 7000 4T1 or 1×10^6 TS/A cells, or in the abdominal flank with 1×10^6 B16, 3LL, MC38, or CT26 cells. Blood was collected from the tail, retro-orbital sinus, or submandibular vein into 500 μL of a 0.008% heparin solution and RBCs removed by lysis [14, 24, 25].

In vitro T-cell suppression and macrophage and MDSC coculture

Splenocytes from DO11.10, Clone 4, or OT-I mice were cocultured with cognate peptide and varying quantities of irradiated blood MDSCs (>90% $Gr1^+CD11b^+$ cells) isolated by magnetic bead sorting of $Gr1^+$ cells using Miltenyi Biotec magnetic beads as described [19]. Thioglycolate-induced peritoneal macrophages were generated and cocultured with blood-derived MDSCs as described [24].

IFN-γ and IL-4 stimulation

Blood leukocytes were either untreated or incubated for 15 min at 37°C with 2 ng/mL IFN-γ (Pierce Endogen, Rockford, IL, USA), or 10 ng/mL IL-4 and subsequently stained according to the manufacturer's protocol (BD Biosciences) with mAb to phosphor-STAT1 or phosphor-STAT6, respectively, and mAbs to CD11b and Gr1.

Statistical analysis

ANOVA and Student's *t*-test were performed using Microsoft Excel 2007. *p*-Values <0.05 were considered significant.

Acknowledgements: We thank Drs. Beth Pulaski and Samudra Dissanayake for their help in generating IFN-$\gamma R^{-/-}$ BALB/c mice, Drs. Dennis Klinman (NIH), Dmitry Gabrilovich (Moffit), and Hy Levitsky (Johns Hopkins) for providing CT26, MC38, and B16 cells, respectively, and Ms. Kimberley Daniels for initial studies with IFN-$\gamma^{-/-}$ and IFN-$\gamma R^{-/-}$ mice. This work was supported by NIH RO1CA84232, NIH RO1CA115880, NIH RO1GM021248 (SOR), and American Cancer Society IRG-97-153-07 (PS). KHP is supported by a predoctoral fellowship from the Graduate Assistance in Areas of National Need (GAANN) program of the U.S. Department of Education (P200A030235).

Conflict of interest: The authors declare no financial or commercial conflict of interest.

References

1 Rabinovich, G. A., Gabrilovich, D. and Sotomayor, E. M., Immunosuppressive strategies that are mediated by tumor cells. *Annu. Rev. Immunol.* 2007. 25: 267–296.

2 Gabrilovich, D. I., Ostrand-Rosenberg, S., and Bronte, V., Coordinated regulation of myeloid cells by tumors. *Nat. Rev. Immunol.* 2012. 12: 253–268.

3 Gabrilovich, D. I. and Nagaraj, S., Myeloid-derived suppressor cells as regulators of the immune system. *Nat. Rev. Immunol.* 2009. 9: 162–174.

4 Movahedi, K., Guilliams, M., Van den Bossche, J., Van den Bergh, R., Gysemans, C., Beschin, A., De Baetselier, P. et al., Identification of discrete tumor-induced myeloid-derived suppressor cell subpopulations with distinct T cell-suppressive activity. *Blood* 2008. 111: 4233–4244.

5 Youn, J. I., Nagaraj, S., Collazo, M. and Gabrilovich, D. I., Subsets of myeloid-derived suppressor cells in tumor-bearing mice. *J. Immunol.* 2008. 181: 5791–5802.

6 Dolcetti, L., Peranzoni, E., Ugel, S., Marigo, I., Fernandez Gomez, A., Mesa, C., Geilich, M. et al., Hierarchy of immunosuppressive strength among myeloid-derived suppressor cell subsets is determined by GM-CSF. *Eur. J. Immunol.* 2010. 40: 22–35.

7 Serafini, P., Borrello, I. and Bronte, V., Myeloid suppressor cells in cancer: recruitment, phenotype, properties, and mechanisms of immune suppression. *Semin. Cancer Biol.* 2006. 16: 53–65.

8 Gallina, G., Dolcetti, L., Serafini, P., De Santo, C., Marigo, I., Colombo, M. P., Basso, G. et al., Tumors induce a subset of inflammatory monocytes with immunosuppressive activity on CD8+ T cells. *J. Clin. Invest.* 2006. 116: 2777–2790.

9 Mandruzzato, S., Solito, S., Falisi, E., Francescato, S., Chiarion-Sileni, V., Mocellin, S., Zanon, A. et al., IL4Ralpha+myeloid-derived suppressor cell expansion in cancer patients. *J. Immunol.* 2009. 182: 6562–6568.

10 Huang, B., Pan, P. Y., Li, Q., Sato, A. I., Levy, D. E., Bromberg, J., Divino, C. M. et al., Gr-1+CD115+ immature myeloid suppressor cells mediate the development of tumor-induced T regulatory cells and T-cell anergy in tumor-bearing host. *Cancer Res.* 2006. 66: 1123–1131.

11 Serafini, P., Carbley, R., Noonan, K. A., Tan, G., Bronte, V. and Borrello, I., High-dose granulocyte-macrophage colony-stimulating factor-producing vaccines impair the immune response through the recruitment of myeloid suppressor cells. *Cancer Res.* 2004. 64: 6337–6343.

12 Morales, J. K., Kmieciak, M., Knutson, K. L., Bear, H. D. and Manjili, M. H., GM-CSF is one of the main breast tumor-derived soluble factors involved in the differentiation of CD11b-Gr1- bone marrow progenitor cells into myeloid-derived suppressor cells. *Breast Cancer Res. Treat.* 123: 39–49.

13 Filipazzi, P., Valenti, R., Huber, V., Pilla, L., Canese, P., Iero, M., Castelli, C. et al., Identification of a new subset of myeloid suppressor cells in peripheral blood of melanoma patients with modulation by a granulocyte-macrophage colony-stimulation factor-based antitumor vaccine. *J. Clin. Oncol.* 2007. 25: 2546–2553.

14 Bunt, S. K., Sinha, P., Clements, V. K., Leips, J. and Ostrand-Rosenberg, S., Inflammation induces myeloid-derived suppressor cells that facilitate tumor progression. *J. Immunol.* 2006. 176: 284–290.

15 Song, X., Krelin, Y., Dvorkin, T., Bjorkdahl, O., Segal, S., Dinarello, C. A., Voronov, E. et al., CD11b+/Gr-1 +immature myeloid cells mediate suppression of T cells in mice bearing tumors of IL-1beta-secreting cells. *J. Immunol.* 2005. 175: 8200–8208.

16 Marigo, I., Bosio, E., Solito, S., Mesa, C., Fernandez, A., Dolcetti, L., Ugel, S. et al., Tumor-induced tolerance and immune suppression depend on the C/EBPbeta transcription factor. *Immunity* 2010. 32: 790–802.

17 Sinha, P., Clements, V. K., Fulton, A. M. and Ostrand-Rosenberg, S., Prostaglandin E2 promotes tumor progression by inducing myeloid-derived suppressor cells. *Cancer Res.* 2007. 67: 4507–4513.

18 Rodriguez, P. C., Hernandez, C. P., Quiceno, D., Dubinett, S. M., Zabaleta, J., Ochoa, J. B., Gilbert, J. et al., Arginase I in myeloid suppressor cells is induced by COX-2 in lung carcinoma. *J. Exp. Med.* 2005. 202: 931–939.

19 Sinha, P., Okoro, C., Foell, D., Freeze, H. H., Ostrand-Rosenberg, S. and Srikrishna, G., Proinflammatory S100 proteins regulate the accumulation of myeloid-derived suppressor cells. *J. Immunol.* 2008. 181: 4666–4675.

20 Cheng, P., Corzo, C. A., Luetteke, N., Yu, B., Nagaraj, S., Bui, M. M., Ortiz, M. et al., Inhibition of dendritic cell differentiation and accumulation of myeloid-derived suppressor cells in cancer is regulated by S100A9 protein. *J. Exp. Med.* 2008. 205: 2235–2249.

21 Gabrilovich, D., Ishida, T., Oyama, T., Ran, S., Kravtsov, V., Nadaf, S. and Carbone, D. P., Vascular endothelial growth factor inhibits the development of dendritic cells and dramatically affects the differentiation of multiple hematopoietic lineages in vivo. *Blood* 1998. 92: 4150–4166.

22 Mazzoni, A., Bronte, V., Visintin, A., Spitzer, J. H., Apolloni, E., Serafini, P., Zanovello, P. et al., Myeloid suppressor lines inhibit T-cell responses by an NO-dependent mechanism. *J. Immunol.* 2002. 168: 689–695.

23 Apolloni, E., Bronte, V., Mazzoni, A., Serafini, P., Cabrelle, A., Segal, D. M., Young, H. A. et al., Immortalized myeloid suppressor cells trigger apoptosis in antigen-activated T lymphocytes. *J. Immunol.* 2000. 165: 6723–6730.

24 Sinha, P., Clements, V. K., Bunt, S. K., Albelda, S. M. and Ostrand-Rosenberg, S., Cross-talk between myeloid-derived suppressor cells and macrophages subverts tumor immunity toward a type 2 response. *J. Immunol.* 2007. 179: 977–983.

25 Sinha, P., Clements, V. K. and Ostrand-Rosenberg, S., Reduction of myeloid-derived suppressor cells and induction of M1 macrophages facilitate the rejection of established metastatic disease. *J. Immunol.* 2005. 174: 636–645.

26 Bronte, V., Serafini, P., Mazzoni, A., Segal, D. M. and Zanovello, P., L-arginine metabolism in myeloid cells controls T-lymphocyte functions. *Trends Immunol.* 2003. 24: 302–306.

27 Pulaski, B. A. and Ostrand-Rosenberg, S., Reduction of established spontaneous mammary carcinoma metastases following immunotherapy with major histocompatibility complex class II and B7.1 cell-based tumor vaccines. *Cancer Res.* 1998. 58: 1486–1493.

28 Nanni, P., de Giovanni, C., Lollini, P. L., Nicoletti, G. and Prodi, G., TS/A: a new metastasizing cell line from a BALB/c spontaneous mammary adenocarcinoma. *Clin. Exp. Metastasis* 1983. 1: 373–380.

Abbreviations: IFN-γR: interferon gamma receptor · IL-4Rα: IL-4 receptor alpha · MDSC: myeloid-derived suppressor cell · MO-MDSC: mononuclear MDSC · PMN-MDSC: polymorphonuclear MDSC

Full correspondence: Dr. Suzanne Ostrand-Rosenberg, Department of Biological Sciences, University of Maryland Baltimore County, 1000 Hilltop Circle, Baltimore, MD 21250, USA.
Fax: +1-410-455-3875
e-mail: srosenbe@umbc.edu

Received: 8/11/2011
Revised: 12/3/2012
Accepted: 23/4/2012
Accepted article online: 4/6/2012

Appendix 5: Myeloid-derived suppressor cells: critical cells driving immune suppression in the tumor microenvironment. Katherine Parker, Daniel Beury, Suzanne Ostrand-Rosenberg, Advances in Cancer Research, 2015.

ADVANCES IN
CANCER RESEARCH
VOLUME
128

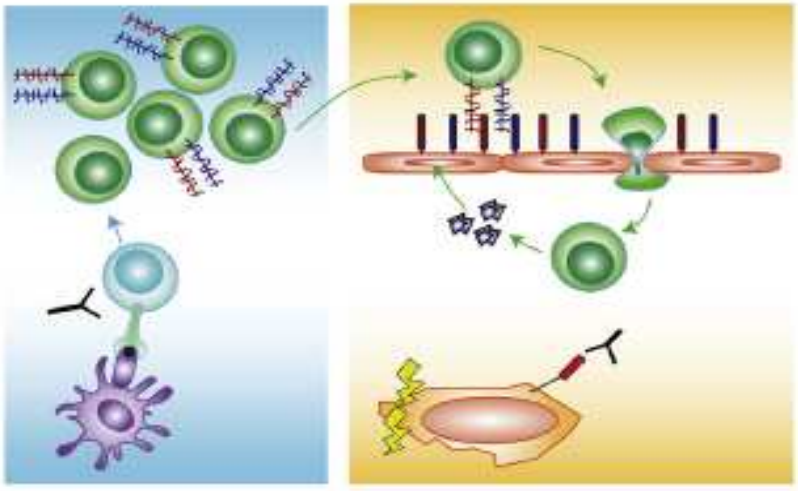

IMMUNOTHERAPY OF CANCER

Edited by
Xiang-Yang Wang
Paul B. Fisher

CHAPTER THREE

Myeloid-Derived Suppressor Cells: Critical Cells Driving Immune Suppression in the Tumor Microenvironment

Katherine H. Parker[1], **Daniel W. Beury**[1], **Suzanne Ostrand-Rosenberg**[2]
Department of Biological Sciences, University of Maryland Baltimore County, Baltimore, Maryland, USA
[2]Corresponding author: e-mail address: srosenbe@umbc.edu

Contents

[1] K.H.P. and D.W.B. are dual-first authors.

Advances in Cancer Research, Volume 128
ISSN 0065-230X
http://dx.doi.org/10.1016/bs.acr.2015.04.002

Abstract

Myeloid-derived suppressor cells (MDSCs) are a heterogeneous population of immature myeloid cells that suppress innate and adaptive immunity. MDSCs are present in many disease settings; however, in cancer, they are a major obstacle for both natural anti-tumor immunity and immunotherapy. Tumor and host cells in the tumor microenvironment (TME) produce a myriad of pro-inflammatory mediators that activate MDSCs and drive their accumulation and suppressive activity. MDSCs utilize a variety of mechanisms to suppress T cell activation, induce other immune-suppressive cell populations, regulate inflammation in the TME, and promote the switching of the immune system to one that tolerates and enhances tumor growth. Because MDSCs are present in most cancer patients and are potent immune-suppressive cells, MDSCs have been the focus of intense research in recent years. This review describes the history and identification of MDSCs, the role of inflammation and intracellular signaling events governing MDSC accumulation and suppressive activity, immune-suppressive mechanisms utilized by MDSCs, and recent therapeutics that target MDSCs to enhance antitumor immunity.

1. MYELOID-DERIVED SUPPRESSOR CELL HISTORY

Abnormal myelopoiesis and neutrophilia were observed in cancer patients for many years; however, the role of these pathologies was not appreciated until relatively recently, when myeloid-derived suppressor cells (MDSCs) were identified and associated with immune suppression. Studies from the early and middle 1980s in tumor-free mice identified a population of so-called natural suppressor cells that inhibited T cell proliferation and the generation of cytotoxic T lymphocytes in an antigen and MHC-independent manner (Strober, 1984). In the 1990s, studies of patients with head and neck cancer described $CD34^+$-suppressive myeloid cells that had

the capacity to differentiate into dendritic cells (DCs) (Garrity et al., 1997). Soon after their identification in head and neck cancer patients, similar cells were discovered in patients with various other forms of cancer. These cells prevented the *in vivo* and *in vitro* activation of T cells and were chemoattracted to the tumor microenvironment (TME) by tumor-produced vascular endothelial growth factor (VEGF) (Almand et al., 2001; Young et al., 2001). Mice with transplanted or spontaneous tumors also produced suppressive myeloid cells (Gabrilovich, Velders, Sotomayor, & Kast, 2001; Melani, Chiodoni, Forni, & Colombo, 2003), which expressed the granulocyte and macrophage markers Gr1 and CD11b/Mac1, respectively. Their accumulation correlated with tumor-produced granulocyte/monocyte-colony-stimulating factor (GM-CSF) (Bronte et al., 1999), and they inhibited antigen-specific $CD8^+$ T cell activation in a contact-dependent manner (Gabrilovich et al., 2001). Early studies used a variety of terms to identify the cells, including "immature myeloid cells (IMCs)," "immature macrophages (iMacs)," or "myeloid suppressor cells (MSCs)." In 2007, the terminology "myeloid-derived suppressor cells" (MDSCs) was adopted to reflect that the cells are the product of abnormal myelopoiesis (Gabrilovich et al., 2007).

MDSCs differentiate from a common myeloid progenitor cell that also gives rise to normal DCs, monocytes, macrophages, and granulocytes (Fig. 1). Unlike other fully differentiated myeloid cells that are relatively homogeneous, MDSCs are a heterogeneous population of cells since they represent varied stages in myelopoiesis. This heterogeneity is tumor dependent and is most likely spawned from the unique inflammatory milieu released by different tumors. These tumor-released factors, in turn, modulate the recruitment and suppressive potency of tumor-infiltrating MDSCs. The phenotype and functions of MDSCs may also vary with cancer progression since tumor cells evolve and change through immunoediting (Dunn, Bruce, Ikeda, Old, & Schreiber, 2002). Within this wide array of variation, human and mouse MDSCs have been separated into two major categories: monocytic (MO-MDSC) and granulocytic (PMN-MDSC).

1.1 Mouse MDSCs

MDSCs have been identified in the bone marrow, liver, blood, spleen, and tumor of tumor-bearing mice based on their expression of surface markers and their ability to prevent T cell activation. All murine MDSCs express the plasma membrane markers Gr1 and CD11b. The granulocyte marker Gr1

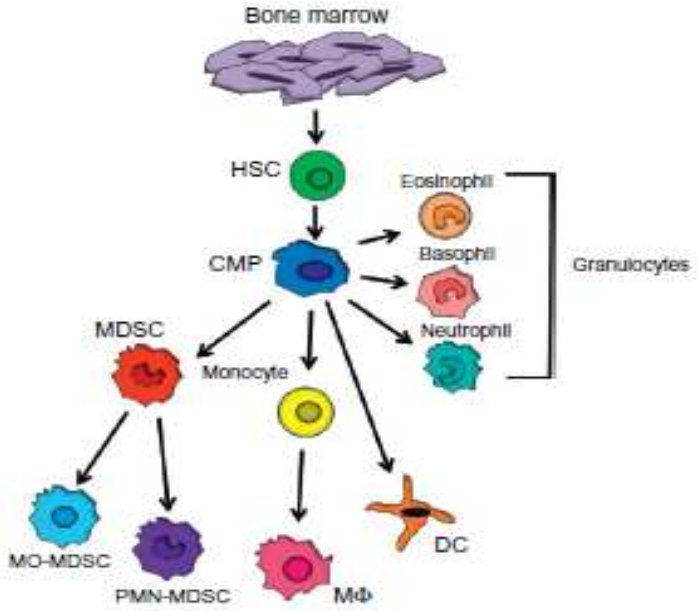

Figure 1 Myeloid cell differentiation under normal and tumor-induced conditions. Myeloid cells originate from bone marrow-derived hematopoietic stem cells (HSCs) that differentiate into common myeloid progenitors (CMPs). During normal myelopoiesis, CMPs differentiate into granulocytes including eosinophils, basophils, and neutrophils, as well as monocytes, macrophages, and dendritic cells. MDSCs also differentiate from CMPs and are categorized as MO-MDSCs or PMN-MDSCs. HSC, hematopoietic stem cell; CMP, common myeloid progenitor; DC, dendritic cell; MΦ, macrophage; MO-MDSCs, monocytic myeloid-derived suppressor cells; PMN-MDSCs, polymorphonuclear myeloid-derived suppressor cells.

includes the isoforms Ly6C and Ly6G. The differential expression of these molecules distinguishes MO-MDSCs from PMN-MDSCs. MO-MDSCs are $CD11b^{+}Ly6C^{+}Ly6G^{low/-}$; PMN-MDSCs are $CD11b^{+}Ly6C^{-}Ly6G^{+}$. MO-MDSCs are mononuclear and side $scatter^{low}$, while PMN-MDSCs are polymorphonuclear and side $scatter^{hi}$. The two subsets use different modes of suppression. PMN-MDSCs utilize reactive oxygen species (ROS) and the enzyme arginase 1 (ARG1), while MO-MDSCs use nitric oxide synthase 2 (NOS2) and ROS. These phenotypes apply to tumor-infiltrating MDSCs, as well as MDSCs residing in the spleen and blood of tumor-bearing mice. Tumor-infiltrating MDSCs are more suppressive than blood or splenic MDSCs on a per cell basis. Tumor-free mice contain cells with the same phenotype ($Gr1^{+}CD11b^{+}$) in the blood, spleen, and bone

marrow; however, they are present at much lower levels compared to tumor-bearing mice (Sinha et al., 2008, 2011).

The markers Gr1 and CD11b as well as the polymorphonuclear morphology of PMN-MDSCs are also characteristics of neutrophils, raising the question of whether MDSCs are different from neutrophils. MDSCs are not neutrophils; however, MDSCs can differentiate into neutrophils. Tumor-associated neutrophils have been categorized as N1, antitumorigenic, and as N2, protumorigenic, with their induction dependent on the presence of IFNβ or TGFβ, respectively (Fridlender et al., 2009; Jablonska, Leschner, Westphal, Lienenklaus, & Weiss, 2010). N1 neutrophils are characterized as $TNF\alpha^{hi}$, $CCL3^{hi}$, $ICAM\text{-}1^{hi}$, and $ARG1^{low}$, while N2 neutrophils are high in CCL2, 3, 4, 8, 12, and 17 as well as in CXCL1, 2, 6, and 16 (Sionov, Fridlender, & Granot, 2014). In contrast to MDSCs, neutrophils do not express CD244 (M-CSF receptor), are more phagocytic than MDSCs, produce lower levels of ROS, have enhanced chemokine secretion, express higher levels of TNFα, and most importantly cannot suppress T cell activation (Youn, Collazo, Shalova, Biswas, & Gabrilovich, 2012).

1.2 Human MDSCs

Human MDSCs have been isolated from patients with solid tumors who display elevated MDSC levels that directly correlate with clinical cancer stage and metastatic burden. MDSCs have been found in patients with breast cancer (Alizadeh et al., 2014; Diaz-Montero et al., 2009), head and neck squamous cell carcinoma (Brandau et al., 2011), nonsmall cell lung cancer (Huang et al., 2013; Srivastava et al., 2008), colon and colorectal cancer (OuYang et al., 2015), renal cell carcinoma (Rodriguez et al., 2009), bladder cancer (Eruslanov et al., 2012), gastrointestinal cancer (Wang et al., 2013), pancreatic adenocarcinoma (Porembka et al., 2012), esophageal cancer (Gabitass, Annels, Stocken, Pandha, & Middleton, 2011), prostate cancer (Vuk-Pavlović et al., 2010), urothelial tract cancer (Brandau et al., 2011), sarcoma, carcinoid, gall bladder, adrenocortical, thyroid, and hepatocellular carcinoma (Shen, Wang, He, Wang, & Zheng, 2014). Patients with multiple myeloma and non-Hodgkin's lymphoma also exhibit elevated levels of MDSCs in their blood (Brimnes et al., 2010; Lin et al., 2011).

Since humans lack an analog to Gr1, human MDSCs are characterized by the monocyte/macrophage marker CD11b, the monocyte differentiation antigen CD14, the mature monocyte marker CD15, the myeloid

lineage markers CD33, and the absence of HLA-DR, which is commonly expressed on myeloid cells (Dumitru, Moses, Trellakis, Lang, & Brandau, 2012). Similar to murine MDSCs, human MDSCs lack lineage markers characteristic of other hematopoietic-derived cells. Human PMN-MDSCs are $CD11b^{+}CD14^{-}CD15^{+}HLA\text{-}DR^{low/-}CD33^{+}$; MO-MDSCs are $CD11b^{+}CD14^{+}CD15^{-}IL4R\alpha^{+}HLA\text{-}DR^{low}CD33^{+}$ (Montero, Diaz-Montero, Kyriakopoulos, Bronte, & Mandruzzato, 2012). Since none of the individual markers are unique to MDSCs, definitive identification of MDSCs requires demonstration of immune-suppressive function.

2. MDSC DEVELOPMENT AND SUPPRESSIVE FUNCTIONS ARE INDUCED BY INFLAMMATION

Studies evaluating patients on long-term use of nonsteroidal anti-inflammatory drugs, epidemiological analyses, and trials involving blockade of inflammatory molecules have demonstrated that inflammation contributes to the onset of cancer (Balkwill & Mantovani, 2001). Four main sources of inflammation promote carcinogenesis: environmental inflammation, therapy-induced inflammation, tumor-associated inflammation, and chronic inflammation or infection.

Particulates from tobacco smoke are an example of an environmental source of inflammation. They cause chronic obstructive pulmonary disease which is associated with increased lung cancer (Punturieri, Szabo, Croxton, Shapiro, & Dubinett, 2009). Therapy-induced inflammation occurs following radiation and chemotherapy. It causes necrotic death of cancer cells and tumor stromal cells and initiates an inflammatory response similar to wound-healing (Zong & Thompson, 2006). Therapy-induced inflammation may enhance presentation of tumor antigens; however, it may also create tumor-promoting inflammation (Zitvogel, Apetoh, Ghiringhelli, & Kroemer, 2008). Many tumors are inherently inflammatory due to their production of inflammatory mediators such as IL-6 and prostaglandins. The resulting inflammation recruits immunosuppressive cells that also release cytokines and feed the inflammatory environment. As solid tumors outpace their blood supply and become deprived of nutrients and oxygen, necrosis sets in causing the chronic release of pro-inflammatory mediators such as IL-1 and high-mobility group box 1 (HMGB1), which in turn promote neoangiogenesis (Vakkila & Lotze, 2004). Long-term infection may also cause chronic inflammation and increased cancer risk. Examples include hepatocellular carcinoma in patients infected with hepatitis B or C viruses

(Karin, 2006), and bladder and colon cancer in individuals infected with Schistosoma or Bacteroides, respectively (Mostafa, Sheweita, & O'Connor, 1999; Wu et al., 2009).

Chronic inflammation promotes tumor development through various mechanisms including the production of proangiogenic factors, matrix metalloproteinases (MMPs), and damage-associated molecular pattern molecules (DAMPs), all of which drive MDSC accumulation and MDSC suppressive functions. Proangiogenic factors such as VEGF stimulate tumor neovascularization, while MMPs facilitate invasion and metastasis (Shacter & Weitzman, 2002). DAMPs such as S100A8/A9 chemoattract leukocytes and promote the expansion of MDSCs leading to an influx of inflammatory molecules within the TME (Cheng et al., 2008; Sinha et al., 2008).

The TME is a complex network that includes both tumor cells and host cells. MDSCs in this environment are therefore subjected to diverse pro-inflammatory factors. Since the TME varies between tumor types and individuals with cancer, as well as with stage of tumor progression, it is not surprising that MDSCs are a heterogeneous population that may vary from individual to individual.

Almost a decade ago, the connection between MDSCs and inflammation was established with the findings that the pro-inflammatory cytokines IL-1β, IL-6, and PGE_2 promote MDSC accumulation and suppressive function (Bunt, Sinha, Clements, Leips, & Ostrand-Rosenberg, 2006; Bunt et al., 2007; Ezernitchi et al., 2006; Sinha, Clements, Fulton, & Ostrand-Rosenberg, 2007; Song et al., 2005). Other studies demonstrated that additional cytokines, transcription factors, and DAMPs, including, but not limited to, C5a, PGE_2, COX_2, VEGF, GM-CSF, G-CSF, IL-17, IDO, HMGB1, and S100A8/A9, C/EBPβ, and chop, also drive MDSCs. The effects of these factors are discussed in the following section and are illustrated in Fig. 2.

2.1 Vascular Endothelial Growth Factor

VEGF is a pro-inflammatory growth factor that stimulates angiogenesis, and tumors producing high levels of VEGF have a poor prognosis. VEGF inhibits nuclear factor kappa-light-chain-enhancer (NF-κB) activation which blocks DC development while simultaneously driving MDSC accumulation (Gabrilovich et al., 1998). MDSCs express the VEGF receptor enabling VEGF to function as a chemoattractant for MDSCs. ROS

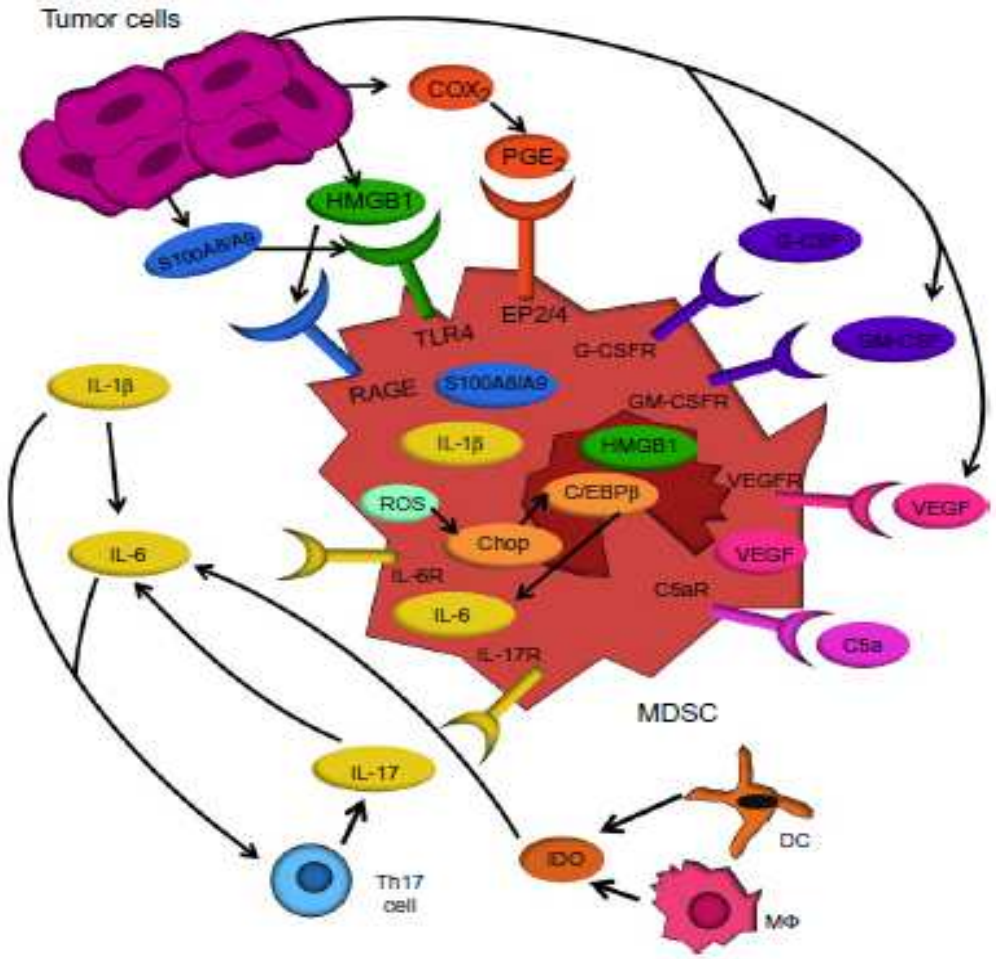

Figure 2 Inflammation drives MDSC development and function. Chronic inflammation induces the production of HMGB1, S100A8/A9, IL-1β, IL-6, C5a, and IL-17, all of which induce the accumulation of MDSC. Induction of MDSCs by IL-1β is mediated through IL-17 and IL-6. IL-1β induces Th17 cells to produce IL-17 which induces the production of IL-6. IL-6 production is also upregulated by IDO produced by DCs and macrophages (MΦ). C/EBPβ, which is activated by chop following MDSC production of ROS, also induces IL-6. MDSCs also produce VEGF, IL-6, IL-1β, HMGB1, and S100A8/A9, thereby perpetuating their accumulation. Tumor cells may produce COX_2, PGE_2, VEGF, IL-6, G-CSF, GM-CSF, S100A8/A9, and HMGB1 all of which induce the accumulation of MDSCs and may increase the suppressive potency of MDSCs.

production by MDSCs increases oxidative stress which upregulates MDSC expression of the VEGF receptor (Kusmartsev et al., 2008). Since other factors in solid tumors also contribute to oxidative stress, the TME is a critical factor in determining the responsiveness of MDSCs to VEGF.

In addition to tumor cells, MDSCs themselves produce VEGF, thereby creating an autocrine feedback loop that sustains MDSC accumulation (Kujawski et al., 2008). VEGF has been shown to be released from the extracellular matrix by MMP9, a matrix degrading enzyme (Bergers et al., 2000). Soluble MMP9 is produced by tumor cells and promotes MDSC accumulation and tumor angiogenesis (Melani, Sangaletti, Barazzetta, Werb, & Colombo, 2007). Therefore, MDSCs have multiple modes of generating VEGF.

2.2 Granulocyte-Macrophage Colony-Stimulating Factor and Granulocyte Colony-Stimulating Factor

GM-CSF is a growth factor for leukocytes. It is required for DC differentiation and is used to expand DC *ex vivo*. However, high levels of GM-CSF induce MDSC accumulation *in vivo* and *in vitro*, while *in vivo* knockdown of GM-CSF reduces MDSC expansion (Morales, Kmieciak, Knutson, Bear, & Manjili, 2010; Serafini et al., 2004). Inclusion of GM-CSF in cultures of bone marrow progenitor cells drives the differentiation of MDSCs, demonstrating that GM-CSF is a growth factor for MDSCs (Nefedova et al., 2004).

MDSC differentiation is also positively regulated by the growth factor granulocyte colony-stimulating factor (G-CSF). G-CSF plays a critical role in mobilizing bone marrow stem cells and is essential for differentiation of granulocytic lineages (Lieschke et al., 1994). Administration of G-CSF to tumor-bearing mice drives tumor growth and angiogenesis, while blockade of G-CSF reduces MDSC levels (Okazaki et al., 2006). G-CSF also preconditions metastatic sites by mobilizing MDSCs (Kowanetz et al., 2010). When G-CSF and VEGF are both inhibited, tumor growth is reduced (Okazaki et al., 2006). While the role of G-CSF in MDSC development is clear, the impact of G-CSF on MDSC function is more complicated. In mice bearing MCA203 sarcomas, G-CSF induced $Gr1^{hi}CD11b^{+}$ cells that were less suppressive than $Gr1^{int}CD11b^{+}$ cells, while in MMTV-PyMT transgenic mice with mammary carcinoma, G-CSF caused $CD11b^{+}Ly6G^{+}Ly6C^{+}$ cells to secret Bv8. Bv8 is an endocrine analog of VEGF and functions as a proangiogenic protein that promotes hematopoiesis (Dolcetti et al., 2010; Kowanetz et al., 2010). Therefore, G-CSF differentially affects MDSC function depending on the type of tumor.

2.3 Prostaglandin E2 and Cyclooxygenase 2

Prostaglandin E2 (PGE_2) is a potent inflammatory mediator that is generated by cyclooxygenase 2 (COX_2) conversion of arachidonic acid. PGE_2 supports tumor growth by promoting angiogenesis, stimulating tumor-cell proliferation, and protecting tumor cells from apoptosis. Many human and mouse tumors as well as tumor-infiltrating cells produce COX_2 and PGE_2. PGE_2 promotes MDSC differentiation at the expense of DC, while inhibition of COX_2 or PGE_2 in tumor-bearing mice blocks MDSC differentiation and delays tumor progression (Eruslanov, Daurkin, Ortiz, Vieweg, & Kusmartsev, 2010; Sinha, Clements, Fulton, et al., 2007). In the TME, PGE_2 mediates its effects through four integral membrane G-protein-coupled prostanoid receptors: EP1, EP2, EP3, and EP4. Mice deficient in EP2 display delayed tumor progression and reduced MDSC levels (Sinha, Clements, Fulton, et al., 2007). Blockade of PGE_2 or EP4 in tumor-bearing mice reduces MDSC production of ARG1 (Rodriguez et al., 2005). PGE_2 promotes the differentiation of progenitor cells in human blood to MDSCs ($CD11b^+CD33^+$ cells) from human blood progenitor cells that have elevated levels of NOS2, ARG1, IL-10, and IL-4Rα (Obermajer, Muthuswamy, Lesnock, Edwards, & Kalinski, 2011). Therefore, for mouse and human MDSCs, PGE_2 not only regulates the differentiation of MDSCs, but several suppressive mechanisms as well.

2.4 CCAAT/Enhancer Binding Protein β and C/EBP Homologous Protein

C/EBP proteins are a family of leucine zipper transcription factors that regulate inflammation and myeloid cell differentiation. While there are various isoforms of C/EBP proteins, CCAAT/enhancer binding protein β (C/EBPβ) acts during stress/inflammation-induced myelopoiesis. C/EBPβ has three isoforms: LAP* and LAP (liver-enriched activator proteins), and LIP (liver-enriched inhibitory protein). LAP* and LIP are transcriptional activators that drive inflammatory myelopoiesis by inducing IL-6 and ARG1. In contrast, LIP inhibits LAP signaling promoting an anti-inflammatory response. In inflammatory settings such as the TME, LAP* and LAP are active and drive inflammation-induced myelopoiesis. C/EBPβ is also required for the *ex vivo* generation of immunosuppressive MDSCs from bone marrow progenitor cells, via IL-6 and GM-CSF (Marigo et al., 2010).

2.5 Complement Component C5a

C5a (also known as anaphylatoxin) is a pro-inflammatory member of the complement and lectin pathway. When the complement pathway is activated, C5a in the blood becomes fixed in tissues. C5a triggers degranulation of mast cells (MCs), aids in vascular permeability, and stimulates smooth muscle contraction. In a tumor setting, C5a increases MDSC-mediated immune suppression by chemoattracting C5a receptor^{+} MDSCs to tumor vasculature and by increasing MDSC production of ROS and ARG1 (Markiewski et al., 2008).

2.6 S100A8/A9

S100A8/A9 proteins are pro-inflammatory danger signals. They are calcium binding proteins that are localized in the cytoplasm or nucleus of myeloid cells, and are released in response to cell damage, infection, or inflammation. Mice deficient in S100A9 reject transplanted tumors, while elevated expression of S100A8/A9 in solid tumors perpetuates inflammation by chemoattracting leukocytes that produce additional inflammatory molecules (Cheng et al., 2008; Sinha et al., 2008). MDSCs are one of the leukocyte populations that are chemoattracted by S100A8/A9, and chemoattraction is dependent on signaling through receptor for advanced glycation end-products (RAGE) (Sinha et al., 2008). Heterodimeric S100A8/A9 mediates it's pro-inflammatory effects by binding to the plasma membrane receptors TLR4, carboxylated N-glycans, RAGE, or heparin sulfate (Bresnick, Weber, & Zimmer, 2015). MDSCs amplify their own accumulation by secreting S100A8/A9, thus creating a self-sustained feedback loop (Sinha et al., 2008).

2.7 High-Mobility Group Box 1

HMGB1 is the second most abundant protein within a cell and is released from myeloid cells as a danger response to sepsis, infection, or arthritis. HMGB1 can signal through a number of receptors including thrombospondin, CD24, TLR2, 4, 7, and 9, as well as RAGE. HMGB1 consists of two functional domains, the A and B boxes, and an acidic tail. The A box is a RAGE antagonist and prevents HMGB1-mediated release of IL-1β and TNFα. The B box and part of the linker before the acidic tail is a RAGE agonist with pro-inflammatory properties (Bianchi & Manfredi, 2007). The B box signals via TLR4 on macrophages which initiate the release of

IL-1β, IL-6, TNFα, MIP-2, and IL-10. The A box is anti-inflammatory as it prevents HMGB1-mediated release of IL-1β and TNFα. Whether HMGB1 functions in a pro-inflammatory or anti-inflammatory manner is determined by its redox state. In the normal extracellular environment, the disulfide bridge between residues Cys_{23} and Cys_{45} maintains the A box in a dysfunctional conformation, so the B box is exclusively active. With inflammation, the microenvironment becomes oxidatively stressed and ROS is produced. ROS terminally oxidizes Cys_{23} and Cys_{45}, thereby breaking the disulfide bridge and allowing A box to resolve the inflammation (Venereau et al., 2012).

Elevated levels of HMGB1 are associated with numerous cancers and are known to directly promote tumor growth. However, HMGB1 also drives tumor progression by modulating MDSCs. Inhibition of HMGB1 prevents the expansion of MDSCs from bone marrow progenitor cells *in vitro*, demonstrating that HMGB1 is required for the differentiation of MDSCs. *In vivo* inhibition of HMGB1 in tumor-bearing mice reduces MDSC levels in the tumor, spleen, and blood, confirming HMGB1 as a driver of MDSCs. MDSC-mediated downregulation of T cell L-selectin (CD62L) is also HMGB1 dependent, since HMGB1 increases MDSC extracellular expression of A disintegrin and metalloproteinase 17 (ADAM17), a protease that cleaves L-selectin. Secretion of the protumor cytokines IL-10 and IL-1β by MDSCs is also increased by HMGB1 (Parker, Sinha, Horn, Clements, & Ostrand-Rosenberg, 2014), and HMGB1-driven MDSC accumulation facilitates metastasis (Li et al., 2013). Preliminary studies indicate that HMGB1 mediates its effects on MDSCs through RAGE and/or TLR4 (K.H. Parker & S. Ostrand-Rosenberg, unpublished). HMGB1 also binds to other receptors, but it is unknown if MDSCs are activated through additional receptors.

2.8 IL-1β, IL-6, and Indoleamine 2,3-Dioxygenase

The causative relationship between inflammation, cancer, and immune suppression was first proposed following the finding that IL-1β was a potent inducer of MDSC accumulation and suppressive activity (Ostrand-Rosenberg & Sinha, 2009). Mice bearing 4T1 tumor cells that were transfected to constitutively express high levels of IL-1β exhibit increased MDSC accumulation and more suppressive MDSCs compared to mice bearing parental 4T1 tumors. 4T1 tumor-bearing mice that lack the IL-1 receptor

antagonist, an inhibitor for IL-1β, also develop elevated levels of MDSCs that are more suppressive. Similarly, mice deficient for the IL-1R display slower tumor growth and their MDSCs are less suppressive (Bunt et al., 2006, 2007; Elkabets et al., 2010; Song et al., 2005). Since IL-1β induces the production of other mediators, including VEGF, IL-6, PGE_2, and GM-CSF, some of the effects of IL-1β on MDSCs may be indirect. 4T1 tumor cells transfected to constitutively express IL-6 induce elevated levels of MDSCs and restore MDSC levels in tumor-bearing IL-1 receptor knockout mice, indicating that IL-6 effects on MDSCs are either downstream of IL-1β, or have an overlapping mechanism of action with IL-1β (Bunt et al., 2007). Since MDSCs produce IL-6 and IL-1β, these studies also raise the question of whether MDSC production of IL-6 is regulated by IL-1β, and if MDSC production of IL-1β enhances MDSC production of IL-6. Indole amine 2,3 dioxygenase (IDO), which is utilized by MDSCs as an immune-suppressive mechanism, also regulates IL-6, and tumor-bearing IDO1-deficient mice have less suppressive MDSCs, reduced levels of IL-6, and delayed primary tumor growth and metastatic disease (Smith et al., 2012). Provision of IL-6 to tumor-bearing indoleamine 2,3-dioxygenase (IDO) knockout mice restores MDSC levels and suppressive potency (Smith et al., 2012).

2.9 IL-17

IL-17 is a pro-inflammatory cytokine secreted by CD4 Th17 and CD8 Tc17 cells. Tumor growth is suppressed and MDSC levels are decreased in IL-17-deficient mice, while administration of IL-17 raises MDSC levels (He et al., 2010; Wang et al., 2009). Patients with gastrointestinal cancers show a strong positive correlation between serum IL-17 and MDSC levels, further supporting a role for IL-17 as an inducer of MDSCs (Yazawa et al., 2013). The effects of IL-17 may be either direct or indirect. Most cells have IL-17 receptors so MDSCs may be directly impacted. However, IL-17 triggers the production of IL-6 which in turn activates STAT3, so many effects on MDSCs may be directly mediated by IL-6 and indirectly by IL-17 (Chatterjee et al., 2013; Wang et al., 2009).

3. MDSC ARE REGULATED BY MULTIPLE MOLECULAR MECHANISMS

Multiple signal transduction pathways, transcription factors, and microRNAs (miRNAs) regulate MDSC accumulation and function (Fig. 3).

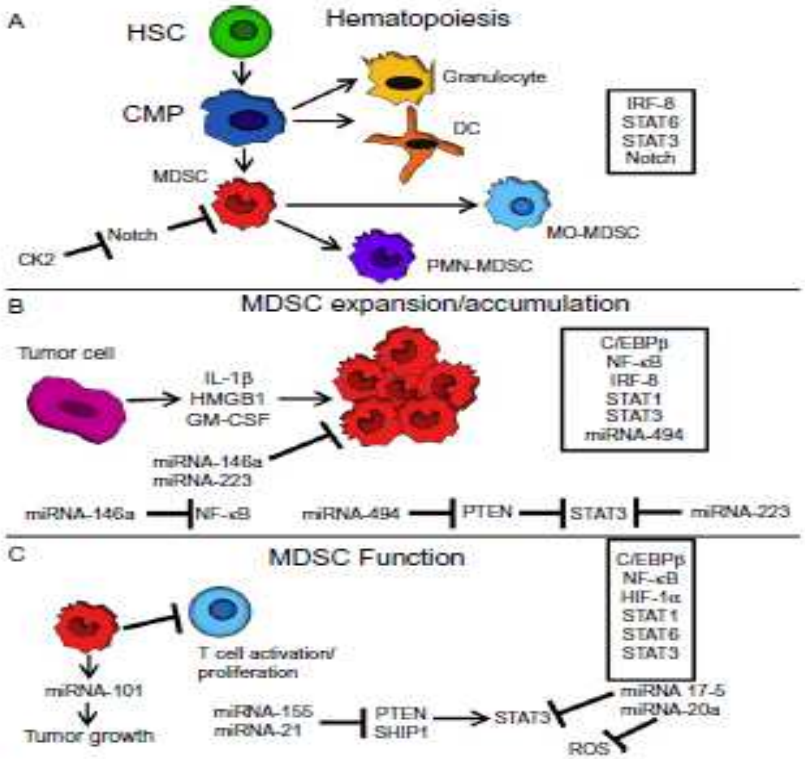

Figure 3 Multiple signal transduction pathways, transcription factors, and microRNAs regulate MDSC accumulation and function. (A) The differentiation of MDSCs from HSC and CMP is regulated by the transcription factors IRF-8, Notch, STAT6, and STAT3. IRF-8 and STAT6 regulate normal myelopoiesis and the differentiation of CMP to mature granulocytes and DCs. During abnormal myelopoiesis, which occurs in individuals with cancer, immature myeloid cells fail to terminally differentiate giving rise to elevated levels of MDSCs. Notch inhibits the differentiation of MDSCs, while CK2 blocks Notch and thereby increases MDSCs. STAT3 promotes MDSC development and suppressive potency. (B) Tumor and host cells produce multiple inflammatory molecules that perturb myelopoiesis and induce the expansion of MDSCs by activating or inactivating transcription factors. Pro-inflammatory mediators in the tumor microenvironment, such as IL-1β, HMGB1, and GM-CSF, drive the expansion of MDSCs by activating C/EBPβ, NF-κB, STAT1, STAT3, and miRNA-494 and downregulating IRF-8. Induction of miRNAs 146a and 223 prevents the expansion of MDSC. miRNA-494 promotes the expression of MMPs and inhibits PTEN function resulting in STAT3 induction. miRNA-146a inhibits NF-κB signaling, while miRNA-223 blocks C/EBPβ from binding to the c-myc promoter which downregulates STAT3 expression. (C) MDSC function is positively regulated by C/EBPβ, NF-κB, HIF-1α, STAT1, STAT6, and STAT3. The miRNAs 155 and 21 inhibit PTEN and SHIP1, negative regulators of STAT3, resulting in the activation of STAT3 and increased MDSC function. miRNAs 17-5 and 20a have the opposite effect by blocking STAT3 and ROS which negatively regulates MDSC function. MDSCs themselves also promote tumor growth by activating miRNA-101 in cancer cells.

3.1 Signal Transducer and Activator of Transcription 1

MDSC function is positively regulated by STAT1. STAT1 is activated by IFNγ or IL-1β and regulates the induction of NOS2 and ARG1 (Kusmartsev & Gabrilovich, 2005). MDSC accumulation is also dependent on STAT1 as tumor-bearing mice deficient in STAT1 exhibit reduced MDSC levels (Hix et al., 2013). Whether IFNγ is the ligand that activates MO-MDSCs is unclear. Early studies indicated that IFNγ was essential for the development of MO-MDSCs (Movahedi et al., 2008); however, subsequent experiments demonstrated that MDSC function, accumulation, and phenotype are independent of IFNγ as tumor-bearing $IFN\gamma^{+/+}$, $IFN\gamma^{-/-}$, $IFN\gamma R^{+/+}$, and $IFN\gamma R^{-/-}$ mice with equal-sized tumors contained equal numbers of equivalently suppressive MDSCs (Sinha, Parker, Horn, & Ostrand-Rosenberg, 2012).

3.2 Signal Transducer and Activator of Transcription 3 and 6

MDSC accumulation and function are enhanced by activation of both STAT3 and STAT6. Activation of STAT6 occurs from the binding of IL-4 or IL-13 to IL-4Rα resulting in the upregulation of ARG1 and TGFβ (Bronte et al., 2003; Sinha, Clements, & Ostrand-Rosenberg, 2005a; Terabe et al., 2003). In STAT6-deficient mice, signaling through IL-4Rα does not occur, MDSCs are less suppressive and accumulate more slowly, and spontaneous metastatic disease is delayed (Sinha, Clements, & Ostrand-Rosenberg, 2005b). STAT3 activation increases the half-life and proliferation of both human and mouse MDSCs by driving the expression of the antiapoptotic genes Bcl-xL, c-myc, and the proliferation gene cyclin D1 (Nefedova et al., 2005; Xin et al., 2009). STAT3 also increases the differentiation of MDSCs by inducing the pro-inflammatory mediators S100A8/A9 (Cheng et al., 2008) and by downregulating the transcription factor PKCβ II in hematopoietic progenitor cells (Farren, Carlson, & Lee, 2010). Since MDSCs and DCs are derived from a common progenitor cell, the increase in MDSC differentiation is accompanied by a decrease in DC expansion. In addition to regulating MDSC expansion, STAT3 also enhances MDSC suppressive activity (Kujawski et al., 2008). Tumor-derived exosomes containing heat-shock protein 72 on their membranes induce MDSC production of IL-6 which subsequently activates STAT3 and increases MDSC-mediated T cell suppression (Chalmin et al., 2010).

C/EBPβ is another transcription factor activated by STAT3. Activated C/EBPβ binds to the c-myc promoter and induces c-myc expression which

stimulates cell proliferation. C/EBPβ is a key molecule for induction of MDSCs since multiple factors (GM-CSF, G-CSF, and IL-6) activate MDSCs via C/EBPβ, (Marigo et al., 2010). C/EBPβ regulation of MDSCs is associated with chop. ROS produced by tumors upregulates MDSC expression of chop (Thevenot et al., 2014). Chop expression in MDSCs activates C/EBPβ and induces STAT3 signaling. MDSCs from chop-deficient mice have decreased ability to inhibit T cell proliferation and accumulate to lower levels. This reduced accumulation and decreased potency of MDSCs is attributed to lower levels of IL-6 and reduced phosphorylation of STAT3. Overexpression of IL-6 in chop-deficient mice rescues MDSC suppressive activity (Thevenot et al., 2014).

MDSC production of ROS is also regulated by STAT3. ROS are generated intracellularly by the NAD(P)H oxidase enzyme complex (NOX), which consists of membrane-bound gp91 and p22, and cytosolic p40, p47, and p67. This complex catalyzes the production of superoxide through the reduction of oxygen, with NAD(P)H serving as the one electron donor. Activation of STAT3 increases ROS levels through upregulation of p47 and gp91 (Corzo et al., 2009); however, it is not known which of the several activators of STAT3 upregulate p47 and gp91. Solid tumors contain oxidatively stressed hypoxic regions, and cells within these regions contain activated hypoxia-inducible factor-1 alpha (HIF-1α). Activated HIF-1α induces STAT3 signaling. Therefore, STAT3 induction of ROS may be regulated by HIF-1α.

3.3 Nuclear Factor Kappa-Light-Chain-Enhancer

Activation of NF-κB also promotes MDSC accumulation and function and occurs following ligation of MyD88-dependent TLRs. Exposure to a variety of pro-inflammatory mediators including S100A8/A9, HMGB1, and IL-1β activates the NF-κB pathway in MDSCs (Parker et al., 2014; Sinha et al., 2008; Tu et al., 2008).

3.4 Interferon Regulatory Factor-8

Interferon regulatory factor 8 (IRF-8) is a transcription factor that is essential for the normal development of granulocyte/monocyte lineage cells. IRF-8-deficient mice have myeloproliferative disorders and accumulate high levels of MDSCs. Expression of IRF-8 is downregulated by G-CSF and GM-CSF, so treating mice with these cytokines blocks IRF-8 activation and drives the accumulation of MDSCs (Stewart, Liewehr, Steinberg, Greeneltch, &

Abrams, 2009; Waight et al., 2013). IRF-8 may also negatively regulate MDSC survival as IRF-8 downregulates antiapoptotic genes Bcl-2 and Bcl-xL and upregulates the proapoptotic gene caspase-3 (Burchert et al., 2004; Gabriele et al., 1999). Inhibition of Bcl-2 and Bcl-xL enhances MDSC susceptibility to Fas-mediated apoptosis (Hu et al., 2013).

3.5 Notch

Another transcription factor implicated in the development of MDSCs from hematopoietic progenitor cells is Notch. Notch signaling permits the differentiation of MDSCs into DCs. Inhibition of notch signaling by casein kinase 2 (CK2) drives abnormal myeloid cell differentiation (Cheng et al., 2014).

3.6 Hypoxia-Inducible Factor-1 Alpha

The HIF complex consists of the subunits HIF-1α and HIF-1β, both of which are constitutively expressed. Hypoxia stabilizes HIF-1α and allows it to translocate from the cytoplasm into the nucleus where it dimerizes with HIF-1β. The HIF complex upregulates multiple target genes (e.g., VEGF, NOS2, and MMPs) by associating with their hypoxia response elements. HIF-1α is overexpressed in various cancers, where it increases MDSC expression of ARG1 and NOS2, rendering MDSCs more immune suppressive and facilitating their conversion to tumor-associated macrophages (TAMs) (Corzo et al., 2010). The capacity of HIF-1α to modulate the function of MDSCs highlights the plasticity of MDSCs and further demonstrates that MDSC function is governed by their environment.

3.7 MicroRNAs

miRNAs are noncoding single-stranded RNAs approximately 22 nucleotides long that regulate gene expression. miRNAs in the RNA-induced silencing complex bind to complementary target mRNAs causing target mRNA degradation. The generation of miRNAs is regulated by cell- and tissue-specific transcription factors as well as proteins involved in the processing of miRNA, both of which can be influenced by chronic inflammation (El Gazzar & McCall, 2012).

miRNAs enhance and inhibit MDSC accumulation and suppressive potency. For example, miRNAs 146a and 223 prevent MDSC accumulation (Boldin et al., 2011; Liu et al., 2011). miRNA-146a blocks inflammation, while miRNA-223 is needed for the development of granulocytes. In contrast, miRNAs 494, 155, and 21 facilitate the accumulation of MDSCs.

miRNA-494 induces MMPs 2, 13, and 14 which drive MDSC growth and survival signals, and by inhibiting phosphatase and tensin homolog (PTEN) which promotes STAT3 activation (Liu et al., 2012). miRNAs 155 and 21 promote MDSC accumulation by activating STAT3, which, as previously discussed, drives both MDSC accumulation and suppressive potency (Li et al., 2014). miRNAs also negatively regulate MDSC suppressive function. These include miRNAs 17-5 and 20a which silence STAT3, thereby reducing MDSC production of ROS and hydrogen peroxide (H_2O_2) (Zhang et al., 2011).

MDSCs also use miRNAs to modulate cancer cell growth. An example is the MDSC-mediated activation of miRNA-101 in ovarian cancer cells (Cui et al., 2013). miRNA-101 increases cancer cell stemness as well as metastatic and tumorigenic potential (Cui et al., 2013).

3.8 MDSC Turnover

MDSC turnover *in vitro* and *in vivo* varies with tumor type, with half-life ranging for only a few days. T cells may contribute to this rapid turnover since when activated, T cells express FasL and cause apoptosis of Fas^+ MDSCs. Inflammation counteracts the T cell effect by increasing MDSC resistance to Fas-mediated lysis (Chornoguz et al., 2011; Sinha et al., 2011).

4. MDSCs UTILIZE A NETWORK OF EFFECTOR AND SIGNALING MOLECULES TO MODULATE THE INFLAMMATORY MILIEU AND DECREASE IMMUNE SURVEILLANCE

MDSCs utilize multiple suppressive mechanisms to induce a tolerogenic, tumor-promoting environment. MDSCs directly suppress T cells by starving them of amino acids, inducing apoptosis, reducing homing to lymph nodes, or inhibiting their intracellular signaling pathways required for activation. MDSCs also indirectly suppress T cells by altering the ability of antigen-presenting cells (APCs) to activate T cells and by inducing immunosuppressive T regulatory cells (Tregs). In addition, MDSCs impact other cells involved in an antitumor response because they alter the inflammatory milieu in the TME by cross talk with macrophages, tumor cells, and MCs. These mechanisms are described below and are illustrated in Fig. 4.

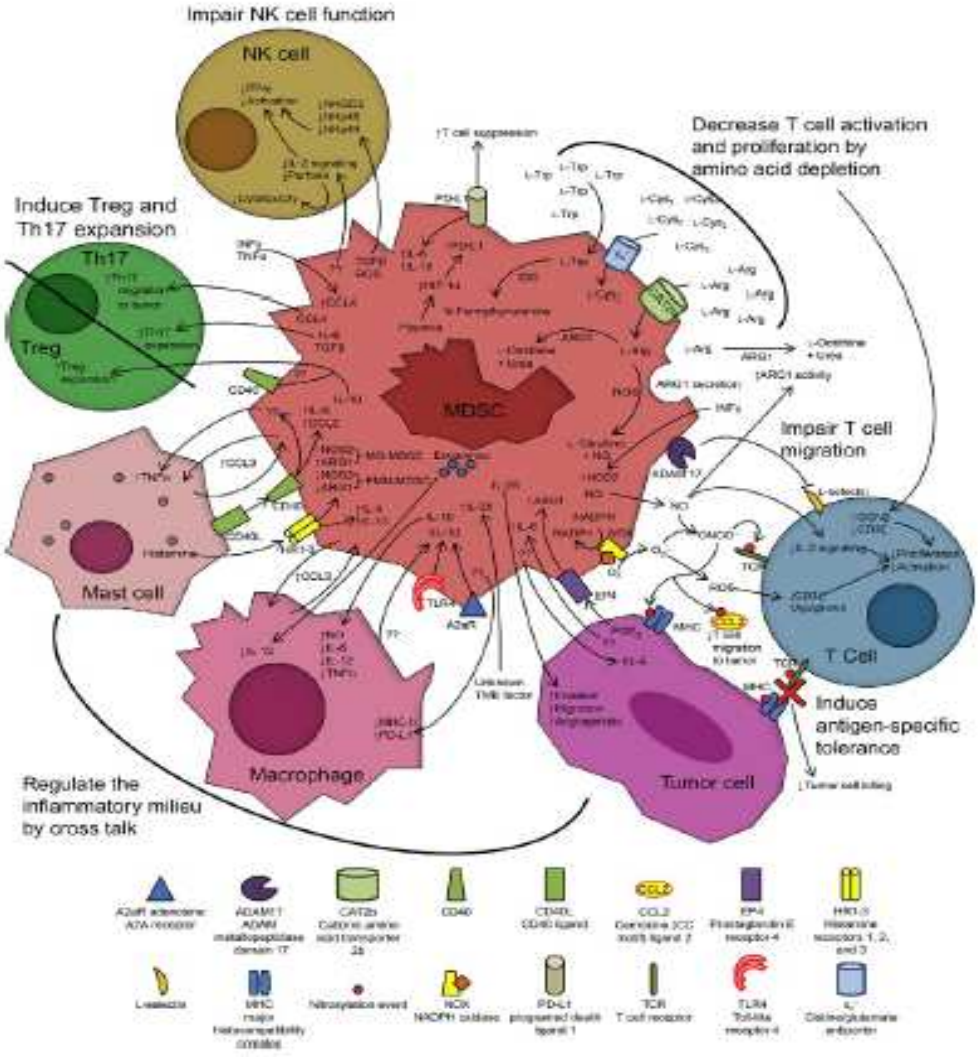

Figure 4 MDSCs suppress T cells and regulate the inflammatory milieu by multiple mechanisms. MDSCs regulate antitumor immunity by (i) secretion of IL-10, which induces Tregs; (ii) secretion of IL-6 and TGFβ, which induces Th17 cells; (iii) production of ROS and TGFβ, which inhibits NK cell function; (iv) degradation of amino acids essential for T cell activation and proliferation; (v) production of NO and O_2^-, which induces apoptosis and inhibits the activation and proliferation of T cells, and generates PNT that nitrates/nitrosylates MHC and TCR; and (vi) participation in cross talk with macrophages, tumor cells, and mast cells to generate a protumor environment. Question marks denote an unknown mechanism or signaling molecule.

4.1 MDSC Depletion of Amino Acids

Following initial contact with antigen, T cells undergo metabolic changes that are essential for their activation and clonal expansion. MDSCs limit several amino acids necessary for these processes and thereby inhibit T cell activation. An early event of amino-acid starvation is the accumulation of empty aminoacyl tRNAs, which activate serine–threonine kinase GCN2. GCN2 phosphorylates eIF2α, which binds eIF2B and suppresses the translation initiation complex from binding charged aminoacyl tRNA, thereby causing a global decrease in protein translation. Simultaneously, GCN2 enhances the translation of GCN4, which results in the transcription of genes required for the synthesis of amino acids (Wang & Green, 2012). MDSCs deplete the local environment of L-arginine (L-Arg), L-tryptophan (L-Trp), and L-cysteine (L-Cys) through different mechanisms.

One of the first suppressive mechanisms attributed to MDSCs was the inhibition of T cell activation and proliferation by the depletion of L-Arg. L-Arg is a nonessential amino acid and is a substrate for several enzymes: (i) NOS 1, 2, and 3 which metabolize L-Arg into L-citrulline and nitric oxide (NO); (ii) ARG 1 and 2 which convert L-Arg to L-ornithine and urea; (iii) arginine:glycine amidinotransferase which transfers the amidino group from L-Arg to L-glycine, yielding L-ornithine and glycocyamine; and (iv) arginine decarboxylase, which catalyzes the reaction of L-Arg to agmatine and CO_2 (Bronte & Zanovello, 2005).

In the absence of L-Arg, T cells decrease their expression of CD3ζ, which is required for signal transduction through the antigen-specific T cell receptor (TCR) (Rodriguez et al., 2002; Zea et al., 2004). L-Arg-depleted T cells are arrested in G_0–G_1 due to the failure to upregulate cyclin D3 and cyclin-dependent kinase 4 (cdk4). Cyclin D3 and cdk4 are not upregulated due to decreased mRNA stability and lower translation rates (Rodriguez et al., 2010). Despite their inability to proliferate, L-Arg-starved T cells express early activation markers and secrete IL-2, indicating that the early events of T cell activation are not L-Arg dependent (Fletcher et al., 2015). *In vivo* studies confirmed the critical role of MDSCs in L-Arg depletion since renal cell carcinoma patients and mice with chronic inflammation have elevated levels of MDSCs and low levels of serum L-Arg, which is correlated with decreased T cell activation (Ezernitchi et al., 2006; Zea et al., 2005). Depletion of L-Arg is mediated by ARG1, and MDSC synthesis of ARG1 is regulated by PGE_2 (Rodriguez et al., 2005). Tumor-derived MDSCs deplete their local environment of L-Arg by internalizing L-Arg

through the cationic amino-acid transporter 2B (Rodriguez et al., 2004) and by secreting ARG1 (Rodriguez et al., 2009).

L-Trp metabolism by MDSCs also facilitates T cell suppression. MDSCs express IDO, which degrades the essential amino-acid L-Trp into *N*-formylkynurenine. IDO causes T cell suppression by enhancing GCN2 kinase in a similar manner as L-Arg starvation (Munn et al., 2005). Expression of IDO in MDSCs is regulated by STAT3 (Yu et al., 2013). However, not all MDSCs express IDO (Smith et al., 2012), indicating that IDO is not a universal mechanism utilized by MDSCs to suppress T cell activation.

MDSCs also prevent T cell activation by sequestering L-Cys. In the extracellular oxidizing environment, L-Cys exists as the dipeptide cystine (L-Cys_2). Naïve T cells must acquire L-Cys from APCs because they lack the cystine transporter x_c^- and therefore cannot import L-Cys_2, and cannot *de novo* synthesize L-Cys because they lack cystathionase, the enzyme that converts methionine to L-Cys. MDSCs also lack cystathionase and therefore must scavenge L-Cys_2. Since MDSCs do not export L-Cys due to their lack of the neutral amino-acid alanine-serine-cysteine transporter 1 (ASC), high levels of MDSCs quickly deplete their local environment of L-Cys_2, thereby limiting the ability of APCs to provide T cells with L-Cys. The role of MDSCs and their biological relevance in L-Cys depletion is supported by the correlation between high levels of MDSCs and reduced serum L-Cys_2 in tumor-bearing mice (Srivastava, Sinha, Clements, Rodriguez, & Ostrand-Rosenberg, 2010). Since activated T cells express x_c^-, theoretically they should be resistant to this suppressive mechanism (Levring et al., 2012). However, since ARG1 production by MDSCs suppresses T cell activation, it is unclear if T cell upregulation of x_c^- is functionally relevant.

4.2 MDSC Production of NO

NOS also catabolizes L-Arg and contributes to MDSC-mediated immune suppression (Bronte & Zanovello, 2005; Raber et al., 2014). MDSCs produce NO by the action of NOS2 and NOS3. PMN-MDSCs are $NOS2^{low}NOS3^{hi}$, while MO-MDSCs are $NOS2^{hi}NOS3^{low}$ (Raber et al., 2014). NOS2 generates more NO than NOS3 and is induced by pro-inflammatory cytokines, endotoxin, hypoxia, and oxidative stress, while NOS3 is constitutively expressed (Fukumura, Kashiwagi, & Jain, 2006).

NO is labile and reacts with multiple compounds to produce many toxic and regulatory factors. For example, NO reacts with (i) cysteine thiol groups on proteins and peptides, which form S-nitrosothiols, thereby altering a protein's tertiary structure; (ii) superoxide anions (O_2^-), which form peroxynitrite (PNT, $ONOO^-$), a molecule that alters protein structure; (iii) divalent cations (e.g., Fe^{2+} and Zn^{2+}), which regulate the function of various transcription factors and enzymes; (iv) nucleic acids, which cause mutagenesis; and (v) unsaturated lipids, which lead to the formation of nitrolipids that can have pro- or anti-inflammatory activity (Bogdan, 2015). Since NO influences many biological processes, it is not surprising that NO is capable of pro- and antitumor activity. NO can induce tumor-cell apoptosis and inhibit metastasis, or enhance tumor-cell invasion, proliferation, and angiogenesis (Fukumura et al., 2006). However, MDSC-produced NO negatively impacts T cells. NO inhibits JAK3, STAT5, ERK, and AKT, which prevents IL-2 signaling, thereby impairing the generation of effector and memory T cells (Mazzoni et al., 2002). NO directly inhibits these signaling proteins by S-nitrosothiolation, or indirectly by activating guanylate cyclase and cyclic-GMP-dependent kinases (Serafini, 2013). S-nitrosothiolation of ARG1 enhances ARG1 affinity for L-Arg which subsequently increases ARG1 activity, thereby establishing a synergistic relationship between ARG1- and NO-mediated immune suppression (Santhanam et al., 2007).

4.3 MDSC Production of ROS

NOX is a membrane-bound enzyme complex that is utilized by MDSCs to suppress T cell activation. MDSCs from tumor-bearing mice have enhanced expression of the NOX subunits gp91, p22, and p47 and produce more ROS than MDSCs from tumor-free mice (Corzo et al., 2009). NOX generates superoxide which spontaneously reacts with many molecules to produce a variety of ROS including H_2O_2, hydroxyl radical, and hypochlorous acid. These ROS damage proteins, lipids, and nucleic acids, thereby enhancing inflammation and promoting apoptosis. For example, H_2O_2 production in cancer patients reduces T cell production of cytokines and expression of CD3ζ (Schmielau & Finn, 2001). Superoxide also reacts with NO to form PNT, which is produced by PMN-MDSCs through the action of gp91 and NOS3 (Raber et al., 2014). PNT nitrates/nitrosylates the TCR and MHC (Lu & Gabrilovich, 2012), thereby disrupting TCR-MHC I/peptide

binding and rendering tumor cells resistant to CTL-mediated apoptosis (Lu et al., 2011). Due to the short half-life of PNT, these reactions are limited to short distances and require close cell-to-cell contact. PNT also reacts with the chemoattractant CCL2, thereby inhibiting T cell infiltration into tumors (Molon et al., 2011).

4.4 MDSCs Inhibit T Cell Migration by Downregulating L- and E-Selectins

Activation of tumor-reactive T cells requires entry of naïve T cells into tumor-draining lymph nodes or migration to the TME. L-selectin mediates the first step in extravasation by facilitating T cell adhesion to high endothelial venules (HEVs). Naïve T cells with low expression of L-selectin do not adhere efficiently to HEVs and fail to enter lymph nodes (J. Mihich, S. Evans, S. Abrams, & S. Ostrand-Rosenberg, unpublished data). In tumor-bearing mice, MDSCs prevent T cell entry into lymph nodes by downregulating L-selection through their extracellular expression of ADAM17, the enzyme that cleaves L-selectin on naïve T cells (Hanson, Clements, Sinha, Ilkovitch, & Ostrand-Rosenberg, 2009; Parker et al., 2014).

In squamous cell carcinoma patients, MDSCs also prevent the homing of T cells to tumor sites by downregulating E-selectin on tumor vessels. In order for T cells to adhere to tumor vessels and subsequently enter the tumor mass, they must first bind to E-selectin. However, NO produced by MDSCs decreases E-selectin levels, thereby limiting T cell access to tumor (Gehad et al., 2012).

4.5 MDSCs Express Programmed Death-Ligand 1

Tumor cells escape antitumor immunity through their expression of programmed death-ligand 1 (PD-L1). When PD-L1 binds to its receptor PD-1 on T cells, it induces T cell exhaustion/apoptosis. MDSCs from some tumor-bearing mice and patients express PD-L1 (Youn, Nagaraj, Collazo, & Gabrilovich, 2008; Zhang, Wang, et al., 2013). Some tumor-infiltrating MDSCs have elevated expression of PD-L1 due to hypoxia-induced upregulation of HIF-1α (Noman et al., 2014). However, MDSCs do not universally express PD-L1, and PD-L1 blockade does not always decrease MDSC suppressive activity (Youn et al., 2008).

4.6 MDSCs Induce Tregs and Th17 Cells

Tregs play an important role in the control of immune reactivity against self- and non-self-antigens, and in some animal models, they protect tumors from antitumor immunity. Tregs are characterized as $CD4^+FoxP3^+$ cells. MDSCs induce/expand Tregs *in vitro* and *in vivo* in multiple tumor models (Adeegbe et al., 2011; Huang et al., 2006; MacDonald et al., 2005; Zoso et al., 2014). MDSCs induce Tregs by secreting IL-10 and TGFβ (Hoechst et al., 2008; Huang et al., 2006) and activate Tregs by presenting tumor-specific antigens in an ARG-dependent and TGFβ-independent manner (Serafini, Mgebroff, Noonan, & Borrello, 2008). MDSC expression of CD40 is required for MDSC-mediated Treg induction, since CD40-deficient MDSCs do not drive Treg expansion (Pan et al., 2010). Given the link between MDSCs and Tregs, therapies targeting MDSCs may also reduce Treg populations.

Th17 cells are a pro-inflammatory $CD4^+$ T cell subset ($CD4^+RORγt^+IL\text{-}17^+$). Since they have both pro- and antitumor effects, their role in antitumor immunity is controversial (Ye, Livergood, & Peng, 2013). MDSCs induce Th17 cells by producing IL-6 and TGFβ (Chatterjee et al., 2013). IFNγ- or TNFα-activated MDSCs also recruit Th17 cells through their production of CCL4, which is a Th17 chemoattractant (Ortiz et al., 2015). As previously mentioned, IL-17 drives the accumulation of MDSCs. Therefore, MDSCs and Th17 cells may induce each other.

4.7 MDSCs Impair NK Cell-Mediated Cytotoxicity

MDSCs impair NK function via contact-dependent mechanisms. MDSCs produce TGFβ and H_2O_2 which decrease NK cell expression of the activating receptors NKG2D, NKp46, and NKp44, thereby making NK cells more difficult to activate (Elkabets et al., 2010; Mao et al., 2014). MDSCs also decrease the ability of NK cells to induce apoptosis by downregulating NK cell production of perforin which is essential for NK-mediated target cell lysis. In addition, MDSCs suppress NK cells by limiting their response to IL-2, a growth factor that enhances NK cell proliferation and cytolytic activity (Liu et al., 2007).

4.8 Cross Talk Between MDSCs, Macrophages, Tumor Cells, and MCs Enhances Inflammation and Promotes MDSC Suppressive Activity

Solid tumors are a complex and frequently inflamed microenvironment. Both tumor and host (macrophages, DCs, MCs, MDSCs, and fibroblasts) cells

within solid tumors participate in cross talk that regulates the release of pro- and anti-inflammatory cytokines and drive the accumulation and suppressive function of immune-suppressive cells such as Tregs, TAMs, and MDSCs.

Macrophages can be either tumoricidal (M1-like) or tumor-promoting (M2-like) (Sica & Mantovani, 2012). MDSCs subvert macrophages toward an M2 phenotype through their production of IL-10 which downregulates macrophage production of IL-12 and TNFα, while simultaneously enhancing macrophage production of NO (Beury et al., 2014; Sinha, Clements, Bunt, Albelda, & Ostrand-Rosenberg, 2007). IL-12 downregulation is mediated by both intact MDSCs and MDSC-derived exosomes (Burke, Choksawangkarn, Edwards, Ostrand-Rosenberg, & Fenselau, 2014). MDSC production of IL-10 involves TLR4 signaling and is increased by inflammation and direct cell-to-cell contact with macrophages (Bunt, Clements, Hanson, Sinha, & Ostrand-Rosenberg, 2009; Sinha, Clements, Bunt, et al., 2007), and via the adenosine A2A receptor (Cekic, Day, Sag, & Linden, 2014). MDSCs also decrease macrophage expression of MHC II through both IL-10-dependent and -independent mechanisms (P. Sinha, D. Beury, V. Clements, & S. Ostrand-Rosenberg, unpublished) and upregulate PD-L1 on macrophages in the liver (Ilkovitch & Lopez, 2009).

MDSCs and tumor cells also participate in cross talk. Tumor cells increase MDSC production of IL-6, and in turn, MDSCs enhance tumor-cell production of IL-6. IL-6 also increases MDSC suppressive activity, but inhibits MDSC production of IL-10 (Beury et al., 2014). In addition, tumor cells enhance MDSC production of IL-28, which facilitates tumor-cell invasion, migration, and angiogenesis (Mucha, Majchrzak, Taciak, Hellmen, & Krol, 2014).

MCs and MDSCs also interact. MDSC and MC cross talk drives inflammation by increasing production of TNFα, CCL3, IL-4, IL-13, IL-6, and CCL2 (Danelli et al., 2015; Martin et al., 2014; Saleem et al., 2012). The latter two molecules are regulated by ligation of MC CD40L to CD40 on MDSCs. Activated MCs release histamine which signals through histamine receptors 1, 2, and 3 on MDSCs and enhances MDSC expression of IL-4 and IL-13. Histamine upregulates ARG1 and NOS2 in MO-MDSCs and decreases ARG1 and NOS2 in PMN-MDSCs (Martin et al., 2014). Since histamine increases MO-MDSC production of NO and downregulates immune-suppressive mediators of PMN-MDSC, the net effect of histamine is to increase MO-MDSC suppressive activity (Danelli et al., 2015).

5. MDSCs IN NONCANCER SETTINGS

MDSCs are also elevated in noncancer settings, where they can be either detrimental or beneficial. For example, elevated levels of MDSC decrease immune responsiveness in patients with toxoplasmosis (Voisin, Buzoni-Gatel, Bout, & Velge-Roussel, 2004) and trypanosomiasis (Goñi, Alcaide, & Fresno, 2002). MDSCs are also elevated in mice with antigen-induced autoimmune enterocolitis, where adoptive transfer of additional MDSCs reduces disease symptoms, suggesting a protective role for MDSCs (Haile et al., 2008). Likewise, mice with experimental autoimmune encephalomyelitis have elevated levels of immune-suppressive MDSCs in their spleens and blood, which are likely to be beneficial in limiting autoreactivity (Zhu et al., 2007). Elevated levels of MDSCs are also found in the serum of patients with sepsis where they polarize immunity toward an antibody-promoting Type 2 response (Delano et al., 2007). Whether the MDSCs are beneficial or detrimental in sepsis is unclear.

Both stress and aging are also associated with increased MDSC levels. For example, postsurgery traumatic stress in mice is accompanied by increased levels of splenic MDSCs that suppress T cell proliferation by an ARG1-dependent mechanism (Makarenkova, Bansal, Matta, Perez, & Ochoa, 2006). Psychological stress in breast cancer patients further elevates circulating MDSCs (Mundy-Bosse, Thornton, Yang, Andersen, & Carson, 2011). MDSCs also increase with aging as shown in a study of adults ages 19–59, 61–76 (seniors), and 67–99 (elderly). The elderly cohort had the highest levels of MDSCs as well as increased serum levels of IL-6 and IL-1β (Verschoor et al., 2013). Studies in aging mice similarly show increases in MDSCs (Grizzle et al., 2007; Hanson et al., 2009).

MDSCs have also been implicated in driving asthma, an allergy caused by a hyper Th2 response that disrupts the normal Th1/Th2 balance. Children with asthma have elevated serum levels of MDSCs and IL-10, and reduced levels of IL-12 (Zhang, Luan, et al., 2013). Since MDSCs produce IL-10 which decreases macrophage production of IL-12 (Sinha, Clements, Bunt, et al., 2007), MDSCs are likely increasing the severity of disease by exacerbating polarization toward a type 2 response. In contrast, in a mouse asthma model, MDSCs appear to reduce disease because injection of tumor-derived MDSCs

restored the Th1/Th2 balance by reducing the type 2 cytokine IL-4 and increasing the type 1 cytokine IFN-γ (Song et al., 2014).

MDSCs may play a beneficial role in obesity, which is considered a chronic low-grade inflammatory disease. Obese individuals have elevated levels of MDSCs in their peripheral tissues. These MDSCs counterbalance some of the detrimental effects of obesity by promoting insulin sensitivity and reducing inflammation. This latter effect occurs because MDSCs in adipose tissue skew macrophages toward an anti-inflammatory M2 phenotype (Xia et al., 2011), possibly by their production of IL-10. However, MDSCs may be detrimental in obese individuals undergoing vaccination, since mice with diet-induced obesity and elevated levels of MDSC displayed decreased antigen-specific T cell responses following vaccination (Chen et al., 2015).

Because of their immunosuppressive potency, MDSCs have been tested as therapeutic agents for autoimmune diseases or when tolerance is required. For example, adoptive transfer of bone marrow-generated MDSCs has been used to combat graft-versus-host disease (Highfill et al., 2010), ameliorate experimental autoimmune encephalomyelitis (Ioannou et al., 2012), aid in the retention of allogeneic islet grafts (Chou et al., 2012), and induce Tregs to protect against type1 diabetes (Yin et al., 2010). MDSCs may also be needed in mice to maintain maternal–fetal tolerance during the development of allogeneic fetuses (P. Sinha & S. Ostrand-Rosenberg, unpublished). The presence of elevated levels of immune-suppressive MDSCs in both mice and women pregnant with allogeneic embryos further supports the concept that MDSCs contribute to maternal–fetal tolerance and suggests that reduced levels of MDSCs in pregnant women could lead to miscarriage (Köstlin et al., 2014).

6. THERAPEUTIC TARGETING OF MDSCs

Because of their central role in immune suppression, many investigators have focused on neutralizing MDSCs in individuals with cancer. Strategies include targeting MDSC suppressive mechanisms, inducing MDSCs to differentiate into nonsuppressive mature APCs, blocking development of MDSCs, and killing of MDSCs. Table 1 lists recent approaches. Older therapies are reviewed in Wesolowski, Markowitz, and Carson (2013). It should be noted that none of these approaches universally neutralize MDSCs.

Table 1 Recently Reported Experimental Therapies Targeting MDSC Development, Viability, or Function

Therapy	Mechanism	Model	Effect
[a]2aG4 (phosphatidyl-serine antibody)	Reverses immunosuppressive effects by phosphatidyl-serine	LNCaP and PC3 prostate cancers (SCID mice)	Induces MDSC differentiation into M1 macrophages and DC; reduces MDSC numbers in tumor
[b]5-AZA (5-azacytidine)	Inhibits DNA methyltransferase	TRAMP-C2 prostate adenoma and TC-1/A9 pancreatic adenoma (C57BL/6 mice)	Reduces MDSC ARG1 expression, VEGF production, and suppressive activity; reduces MDSC accumulation.
[c]5-AZA + ENT (entinostat)	ENT is a class I HDAC inhibitor	CT26 colon carcinoma and 4T1 mammary carcinoma (BALB/c mice)	ENT causes apoptosis of PMN-MSDC *in vitro*, while 5-AZA has no effect on MDSCs; causes rejection of tumor when 5-AZA + ENT is used in combination with αPD-1 + αCTLA-4 immunotherapy
[d]ABT-737	Inhibitor of Bcl-2, Bcl-xL, and Bcl-w	CT26 colon carcinoma and 4T1 mammary carcinoma (BALB/c mice)	Increases MDSC susceptibility to FASL-mediated apoptosis; increases apoptosis of MDSC *in vivo*, not *in vitro*; decreases MDSC accumulation
[e]Antaxinib	VEGFR antagonist	RENCA renal cell carcinoma (BALB/c mice)	Inhibits STAT3 in MDSC; decreases MDSC ROS and ARG1; increases MDSC apoptosis
[f]ATRA (all-*trans* retinoic acid)	Agonist for retinoic acid receptor	SCLC patients	Causes apoptosis of PMN-MDSCs; differentiates MO-MDSCs to macrophages and DCs; reduces MDSCs in SCLC patients; enhanced the number of responders to p53 vaccine
[g]CD16XCD33 BiKE	Targets NK cells to $CD33^+$ cells	Myelodysplastic syndrome (MDS) patients	Induces NK cell-mediated killing of MDSCs
[h]Corosolic acid (Triterpenoid from apple pomace)	Blocks activation of STAT3 and NF-κB; inhibits polarization of macrophages to M2 phenotype	LM85 osteosarcoma (C3H mice)	Reduces MDSC suppressive activity
[i]Dopamine	Signals through D1-like DA receptors which inhibited MO-MDSC decreasing NO	LLC and B16 melanoma (C57BL/6 mice)	Reduces MDSC suppressive activity
[j]Gemcitabine + Capecitabine	Gemcitabine is a nucleoside analog. Capecitabine is a prodrug that is enzymatically converted to fluorouracil	Pancreatic cancer patients	No direct effect on MDSCs alone, but reduces MDSCs in patients receiving GM-CSF as an adjuvant for GV1001 (GV1001 is a telomerase vaccine)
[k]Gemcitabine + Rosiglitazone	Rosiglitazone activates PPARγ, thereby acting as an anti-inflammatory agent	Panc02 pancreatic carcinoma (C57BL/6 mice)	Rosiglitazone reduces early MDSC accumulation; combination therapy reduces late-stage MDSC accumulation
[l]J32	PI3K inhibitor	4T1 mammary carcinoma (BALB/c mice)	Causes PMN-MDSC apoptosis; no effect on tumor growth alone; causes tumor rejection in mice when used in combination with αPD-1 + αCTLA-4 immunotherapy
[l]Lenalidomide (thalidomide derivative)	Inhibits NF-κB, COX-2 activity, and angiogenesis; has immunomodulatory effects	A20 lymphoma (BALB/c mice)	Reduces MDSCs *in vivo*, but does not alter MDSC levels in naïve mice

Continued

Table 1 Recently Reported Experimental Therapies Targeting MDSC Development, Viability, or Function—cont'd

Therapy	Mechanism	Model	Effect
[m]MI-319	HDM2 inhibitor	Human renal cell carcinoma (nude mice)	Reverses sunitinib-induced MDSC infiltration into tumor (sunitinib is a RTK inhibitor and reduces angiogenesis)
[n]Polyphenon E (green tea extract)	Unknown mechanism	Neuroblastoma mouse models: TH-MYCN transgenic mice, human SHSY5Y (NOD/SCID mice), Neuro 2A (A/J mice)	Differentiates MO-MDSCs into PMN-MDSCs; reduces suppressive activity of MO-MDSCs; decreases ARG1 in MDSCs
[o]SAR131675	Inhibits VEGFR-3 tyrosine kinase	4T1 mammary carcinoma (BALB/c mice)	Reduces the number of MDSCs in tumor; promotes M1 macrophages
[p]Silibinin	Anti-inflammatory flavonoid	4T1 mammary carcinoma (BALB/c mice)	Reduces tumor volume, increases survival of tumor-bearing mice; decreases total number of MDSCs
[q]Tadalafil	PDE5 inhibitor	Human HNSCC patients	Lowers MDSCs and Treg numbers; increases tumor-specific $CD8^+$ T cells in a dose-dependent manner
[r]TCBA (tetrabromocinnamic acid)	Restores Notch signaling	EL4 lymphoma (C57BL/6 mice), CT26 colon carcinoma and MethA sarcoma (BALB/c mice)	Induces differentiation of MDSCs to DCs
[s]Vemurafenib	Inhibitor of B-RAF^{V600E}, a mutation leading to constitutive activation of MAP kinase pathway	Cutaneous melanoma patients	Inhibits the release of soluble factors from melanoma cells involved in the generation of MO-MDSC *in vitro*; decreases MO-MDSC *in vivo*
[t]Withaferin A (extract from ashwagandha plant)	Antioxidant with antitumor effects; inhibits Notch signaling and NF-κB activation	4T1 mammary carcinoma (BALB/c mice)	Decreases MDSC production of ROS and IL-10; decreases MDSC suppressive activity; reduces MDSC accumulation

[a]Yin, Huang, Lynn, and Thorpe (2013).
[b]Mikyskova et al. (2014).
[c]Kim et al. (2014).
[d]Hu et al. (2013).
[e]Yuan et al. (2014).
[f]Iclozan, Antonia, Chiappori, Chen, and Gabrilovich (2013).
[g]Gleason et al. (2014).
[h]Horlad et al. (2013).
[i]Wu et al. (2015).
[j]Annels et al. (2014).
[k]Bunt, Mohr, Bailey, Grandgenett, and Hollingsworth (2013).
[l]Sakamaki et al. (2014).
[m]Panka, Liu, Geissler, and Mier (2013).
[n]Santilli et al. (2013).
[o]Espagnolle et al. (2014).
[p]Forghani, Khorramizadeh, and Waller (2014).
[q]Weed et al. (2015).
[r]Cheng et al. (2014).
[s]Schilling et al. (2013).
[t]Sinha and Ostrand-Rosenberg (2013).

7. CONCLUSIONS

MDSCs encompass a range of immature immune-suppressive myeloid cells. Their suppressive activity and accumulation are induced by many inflammatory mediators with unique and redundant signaling pathways. MDSCs inhibit antitumor immunity through several mechanisms including (i) depletion of the local environment of the amino acids L-Arg, L-Trp, and L-Cys, which inhibits T cell activation and/or proliferation; (ii) secretion of NO, PNT, and ROS, which causes T cell apoptosis, inhibits peptide recognition by T cells, and inhibits T cell activation; (iii) induction of immunosuppressive Tregs; and (iv) impairment of T cell trafficking to lymph nodes. MDSCs also alter the inflammatory milieu by inducing inflammatory Th17 cells, participating in cross talk with macrophages, tumor cells, and MCs which promotes a protumor environment that enhances tumor-cell growth, invasion, and metastasis. Therefore, neutralizing MDSCs is an obvious strategy to enhance natural antitumor immunity and boost the efficacy of immunotherapies.

The concept of activating a patient's immune system to destroy their endogenous cancer cells has been a goal of immunotherapy for many years. Unfortunately, many cancer immunotherapy clinical trials have failed to show therapeutic efficacy. MDSCs may be responsible for at least some of these failures since they are present in many cancer patients, and have the ability to prevent T cell activation. Analysis of blood samples from non-responder patients indicated a correlation between lack of response and MDSC levels (Kimura et al., 2013). Regardless of the outcome of such studies, it is likely that cancer immunotherapies involving *in vivo* activation or proliferation of tumor-reactive T cells will require adjunctive treatment that neutralizes MDSCs.

Accumulation and suppressive potency of MDSCs are regulated by a complex milieu of inflammatory mediators. Environmental conditions such as hypoxia and inflammation act through similar signaling networks. These networks converge on common transcription factors such as STAT3 and NF-κB and regulate additional transcription factors, miRNAs, and proteins that mediate MDSC accumulation and suppression. Since multiple ligands initiate signaling through these pathways, MDSC regulation is highly redundant. This redundancy allows for the development of MDSCs under a broad range of conditions and may explain why MDSCs are so widespread in cancer patients. The redundancy also complicates therapeutic approaches for neutralizing MDSCs, since different inducers compensate for each other.

The past decade has seen remarkable progress in recognizing MDSCs as key players that inhibit antitumor immunity and facilitate tumor progression. Advances in understanding the mechanisms that drive MDSC accumulation and function have also been extensive. Hopefully, these studies will lead to the development of therapeutic strategies that are universally effective in neutralizing or eliminating MDSCs in cancer patients.

REFERENCES

Adeegbe, D., Serafini, P., Bronte, V., Zoso, A., Ricordi, C., & Inverardi, L. (2011). In vivo induction of myeloid suppressor cells and CD4(+)Foxp3(+) T regulatory cells prolongs skin allograft survival in mice. *Cell Transplantation, 20*, 941–954.

Alizadeh, D., Trad, M., Hanke, N. T., Larmonier, C. B., Janikashvili, N., Bonnotte, B., et al. (2014). Doxorubicin eliminates myeloid-derived suppressor cells and enhances the efficacy of adoptive T-cell transfer in breast cancer. *Cancer Research, 74*, 104–118.

Almand, B., Clark, J. I., Nikitina, E., van Beynen, J., English, N. R., Knight, S. C., et al. (2001). Increased production of immature myeloid cells in cancer patients: A mechanism of immunosuppression in cancer. *Journal of Immunology, 166*, 678–689.

Annels, N. E., Shaw, V. E., Gabitass, R. F., Billingham, L., Corrie, P., Eatock, M., et al. (2014). The effects of gemcitabine and capecitabine combination chemotherapy and of low-dose adjuvant GM-CSF on the levels of myeloid-derived suppressor cells in patients with advanced pancreatic cancer. *Cancer Immunology, Immunotherapy, 63*, 175–183.

Balkwill, F., & Mantovani, A. (2001). Inflammation and cancer: Back to Virchow? *Lancet, 357*, 539–545.

Bergers, G., Brekken, R., McMahon, G., Vu, T. H., Itoh, T., Tamaki, K., et al. (2000). Matrix metalloproteinase-9 triggers the angiogenic switch during carcinogenesis. *Nature Cell Biology, 2*, 737–744.

Beury, D. W., Parker, K. H., Nyandjo, M., Sinha, P., Carter, K. A., & Ostrand-Rosenberg, S. (2014). Cross-talk among myeloid-derived suppressor cells, macrophages, and tumor cells impacts the inflammatory milieu of solid tumors. *Journal of Leukocyte Biology, 96*, 1109–1118.

Bianchi, M. E., & Manfredi, A. A. (2007). High-mobility group box 1 (HMGB1) protein at the crossroads between innate and adaptive immunity. *Immunological Reviews, 220*, 35–46.

Bogdan, C. (2015). Nitric oxide synthase in innate and adaptive immunity: An update. *Trends in Immunology, 36*, 161–178.

Boldin, M. P., Taganov, K. D., Rao, D. S., Yang, L., Zhao, J. L., Kalwani, M., et al. (2011). miR-146a is a significant brake on autoimmunity, myeloproliferation, and cancer in mice. *The Journal of Experimental Medicine, 208*, 1189–1201.

Brandau, S., Trellakis, S., Bruderek, K., Schmaltz, D., Steller, G., Elian, M., et al. (2011). Myeloid-derived suppressor cells in the peripheral blood of cancer patients contain a subset of immature neutrophils with impaired migratory properties. *Journal of Leukocyte Biology, 89*, 311–317.

Bresnick, A. R., Weber, D. J., & Zimmer, D. B. (2015). S100 proteins in cancer. *Nature Reviews. Cancer, 15*, 96–109.

Brimnes, M. K., Vangsted, A. J., Knudsen, L. M., Gimsing, P., Gang, A. O., Johnsen, H. E., et al. (2010). Increased level of both CD4+FOXP3+ regulatory T cells and CD14+HLA-DR^{-}/low myeloid-derived suppressor cells and decreased level of dendritic cells in patients with multiple myeloma. *Scandinavian Journal of Immunology, 72*, 540–547.

Bronte, V., Chappell, D. B., Apolloni, E., Cabrelle, A., Wang, M., Hwu, P., et al. (1999). Unopposed production of granulocyte-macrophage colony-stimulating factor by tumors inhibits CD8+ T cell responses by dysregulating antigen-presenting cell maturation. *Journal of Immunology, 162*, 5728–5737.

Bronte, V., Serafini, P., De Santo, C., Marigo, I., Tosello, V., Mazzoni, A., et al. (2003). IL-4-induced arginase 1 suppresses alloreactive T cells in tumor-bearing mice. *Journal of Immunology, 170*, 270–278.

Bronte, V., & Zanovello, P. (2005). Regulation of immune responses by L-arginine metabolism. *Nature Reviews. Immunology, 5*, 641–654.

Bunt, S. K., Clements, V. K., Hanson, E. M., Sinha, P., & Ostrand-Rosenberg, S. (2009). Inflammation enhances myeloid-derived suppressor cell cross-talk by signaling through Toll-like receptor 4. *Journal of Leukocyte Biology, 85*, 996–1004.

Bunt, S. K., Mohr, A. M., Bailey, J. M., Grandgenett, P. M., & Hollingsworth, M. A. (2013). Rosiglitazone and Gemcitabine in combination reduces immune suppression and modulates T cell populations in pancreatic cancer. *Cancer Immunology, Immunotherapy, 62*, 225–236.

Bunt, S. K., Sinha, P., Clements, V. K., Leips, J., & Ostrand-Rosenberg, S. (2006). Inflammation induces myeloid-derived suppressor cells that facilitate tumor progression. *Journal of Immunology, 176*, 284–290.

Bunt, S. K., Yang, L., Sinha, P., Clements, V. K., Leips, J., & Ostrand-Rosenberg, S. (2007). Reduced inflammation in the tumor microenvironment delays the accumulation of myeloid-derived suppressor cells and limits tumor progression. *Cancer Research, 67*, 10019–10026.

Burchert, A., Cai, D., Hofbauer, L. C., Samuelsson, M. K., Slater, E. P., Duyster, J., et al. (2004). Interferon consensus sequence binding protein (ICSBP; IRF-8) antagonizes BCR/ABL and down-regulates bcl-2. *Blood, 103*, 3480–3489.

Burke, M., Choksawangkarn, W., Edwards, N., Ostrand-Rosenberg, S., & Fenselau, C. (2014). Exosomes from myeloid-derived suppressor cells carry biologically active proteins. *Journal of Proteome Research, 13*, 836–843.

Cekic, C., Day, Y. J., Sag, D., & Linden, J. (2014). Myeloid expression of adenosine A2A receptor suppresses T and NK cell responses in the solid tumor microenvironment. *Cancer Research, 74*, 7250–7259.

Chalmin, F., Ladoire, S., Mignot, G., Vincent, J., Bruchard, M., Remy-Martin, J. P., et al. (2010). Membrane-associated Hsp72 from tumor-derived exosomes mediates STAT3-dependent immunosuppressive function of mouse and human myeloid-derived suppressor cells. *The Journal of Clinical Investigation, 120*, 457–471.

Chatterjee, S., Das, S., Chakraborty, P., Manna, A., Chatterjee, M., & Choudhuri, S. K. (2013). Myeloid derived suppressor cells (MDSCs) can induce the generation of Th17 response from naive CD4+ T cells. *Immunobiology, 218*, 718–724.

Chen, S., Akbar, S. M., Miyake, T., Abe, M., Al-Mahtab, M., Furukawa, S., et al. (2015). Diminished immune response to vaccinations in obesity: Role of myeloid-derived suppressor and other myeloid cells. *Obesity Research & Clinical Practice, 9*, 35–44.

Cheng, P., Corzo, C. A., Luetteke, N., Yu, B., Nagaraj, S., Bui, M. M., et al. (2008). Inhibition of dendritic cell differentiation and accumulation of myeloid-derived suppressor cells in cancer is regulated by S100A9 protein. *The Journal of Experimental Medicine, 205*, 2235–2249.

Cheng, P., Kumar, V., Liu, H., Youn, J. I., Fishman, M., Sherman, S., et al. (2014). Effects of notch signaling on regulation of myeloid cell differentiation in cancer. *Cancer Research, 74*, 141–152.

Chomoguz, O., Grmai, L., Sinha, P., Artemenko, K. A., Zubarev, R. A., & Ostrand-Rosenberg, S. (2011). Proteomic pathway analysis reveals inflammation increases myeloid-derived suppressor cell resistance to apoptosis. *Molecular & Cellular Proteomics, 10*, M110.002980.

Chou, H. S., Hsieh, C. C., Charles, R., Wang, L., Wagner, T., Fung, J. J., et al. (2012). Myeloid-derived suppressor cells protect islet transplants by B7-H1 mediated enhancement of T regulatory cells. *Transplantation, 93,* 272–282.

Corzo, C. A., Condamine, T., Lu, L., Cotter, M. J., Youn, J. I., Cheng, P., et al. (2010). HIF-1α regulates function and differentiation of myeloid-derived suppressor cells in the tumor microenvironment. *The Journal of Experimental Medicine, 207,* 2439–2453.

Corzo, C. A., Cotter, M. J., Cheng, P., Cheng, F., Kusmartsev, S., Sotomayor, E., et al. (2009). Mechanism regulating reactive oxygen species in tumor-induced myeloid-derived suppressor cells. *Journal of Immunology, 182,* 5693–5701.

Cui, T. X., Kryczek, I., Zhao, L., Zhao, E., Kuick, R., Roh, M. H., et al. (2013). Myeloid-derived suppressor cells enhance stemness of cancer cells by inducing microRNA101 and suppressing the corepressor CtBP2. *Immunity, 39,* 611–621.

Danelli, L., Frossi, B., Gri, G., Mion, F., Guarnotta, C., Bongiovanni, L., et al. (2015). Mast cells boost myeloid-derived suppressor cell activity and contribute to the development of tumor-favoring microenvironment. *Cancer Immunology Research, 3,* 85–95.

Delano, M. J., Scumpia, P. O., Weinstein, J. S., Coco, D., Nagaraj, S., Kelly-Scumpia, K. M., et al. (2007). MyD88-dependent expansion of an immature GR-1(+)CD11b(+) population induces T cell suppression and Th2 polarization in sepsis. *The Journal of Experimental Medicine, 204,* 1463–1474.

Diaz-Montero, C. M., Salem, M. L., Nishimura, M. I., Garrett-Mayer, E., Cole, D. J., & Montero, A. J. (2009). Increased circulating myeloid-derived suppressor cells correlate with clinical cancer stage, metastatic tumor burden, and doxorubicin-cyclophosphamide chemotherapy. *Cancer Immunology, Immunotherapy, 58,* 49–59.

Dolcetti, L., Peranzoni, E., Ugel, S., Marigo, I., Fernandez Gomez, A., Mesa, C., et al. (2010). Hierarchy of immunosuppressive strength among myeloid-derived suppressor cell subsets is determined by GM-CSF. *European Journal of Immunology, 40,* 22–35.

Dumitru, C. A., Moses, K., Trellakis, S., Lang, S., & Brandau, S. (2012). Neutrophils and granulocytic myeloid-derived suppressor cells: Immunophenotyping, cell biology and clinical relevance in human oncology. *Cancer Immunology, Immunotherapy, 61,* 1155–1167.

Dunn, G. P., Bruce, A. T., Ikeda, H., Old, L. J., & Schreiber, R. D. (2002). Cancer immunoediting: From immunosurveillance to tumor escape. *Nature Immunology, 3,* 991–998.

El Gazzar, M., & McCall, C. E. (2012). MicroRNAs regulatory networks in myeloid lineage development and differentiation: Regulators of the regulators. *Immunology and Cell Biology, 90,* 587–593.

Elkabets, M., Ribeiro, V. S., Dinarello, C. A., Ostrand-Rosenberg, S., Di Santo, J. P., Apte, R. N., et al. (2010). IL-1beta regulates a novel myeloid-derived suppressor cell subset that impairs NK cell development and function. *European Journal of Immunology, 40,* 3347–3357.

Eruslanov, E., Daurkin, I., Ortiz, J., Vieweg, J., & Kusmartsev, S. (2010). Pivotal advance: Tumor-mediated induction of myeloid-derived suppressor cells and M2-polarized macrophages by altering intracellular PGE_2 catabolism in myeloid cells. *Journal of Leukocyte Biology, 88,* 839–848.

Eruslanov, E., Neuberger, M., Daurkin, I., Perrin, G. Q., Algood, C., Dahm, P., et al. (2012). Circulating and tumor-infiltrating myeloid cell subsets in patients with bladder cancer. *International Journal of Cancer, 130,* 1109–1119.

Espagnolle, N., Barron, P., Mandron, M., Blanc, I., Bonnin, J., Agnel, M., et al. (2014). Specific inhibition of the VEGFR-3 tyrosine kinase by SAR131675 reduces peripheral and tumor associated immunosuppressive myeloid cells. *Cancers, 6,* 472–490.

Ezernitchi, A. V., Vaknin, I., Cohen-Daniel, L., Levy, O., Manaster, E., Halabi, A., et al. (2006). TCR zeta down-regulation under chronic inflammation is mediated by myeloid

suppressor cells differentially distributed between various lymphatic organs. *Journal of Immunology*, *177*, 4763–4772.
Farren, M. R., Carlson, L. M., & Lee, K. P. (2010). Tumor-mediated inhibition of dendritic cell differentiation is mediated by down regulation of protein kinase C beta II expression. *Immunologic Research*, *46*, 165–176.
Fletcher, M., Ramirez, M. E., Sierra, R. A., Raber, P., Thevenot, P., Al-Khami, A. A., et al. (2015). L-Arginine depletion blunts antitumor T-cell responses by inducing myeloid-derived suppressor cells. *Cancer Research*, *75*, 275–283.
Forghani, P., Khorramizadeh, M. R., & Waller, E. K. (2014). Silibinin inhibits accumulation of myeloid-derived suppressor cells and tumor growth of murine breast cancer. *Cancer Medicine*, *3*, 215–224.
Fridlender, Z. G., Sun, J., Kim, S., Kapoor, V., Cheng, G., Ling, L., et al. (2009). Polarization of tumor-associated neutrophil phenotype by TGF-beta: "N1" versus "N2" TAN. *Cancer Cell*, *16*, 183–194.
Fukumura, D., Kashiwagi, S., & Jain, R. K. (2006). The role of nitric oxide in tumour progression. *Nature Reviews. Cancer*, *6*, 521–534.
Gabitass, R. F., Annels, N. E., Stocken, D. D., Pandha, H. A., & Middleton, G. W. (2011). Elevated myeloid-derived suppressor cells in pancreatic, esophageal and gastric cancer are an independent prognostic factor and are associated with significant elevation of the Th2 cytokine interleukin-13. *Cancer Immunology, Immunotherapy*, *60*, 1419–1430.
Gabriele, L., Phung, J., Fukumoto, J., Segal, D., Wang, I. M., Giannakakou, P., et al. (1999). Regulation of apoptosis in myeloid cells by interferon consensus sequence-binding protein. *The Journal of Experimental Medicine*, *190*, 411–421.
Gabrilovich, D. I., Bronte, V., Chen, S. H., Colombo, M. P., Ochoa, A., Ostrand-Rosenberg, S., et al. (2007). The terminology issue for myeloid-derived suppressor cells. *Cancer Research*, *67*, 425, author reply 426.
Gabrilovich, D., Ishida, T., Oyama, T., Ran, S., Kravtsov, V., Nadaf, S., et al. (1998). Vascular endothelial growth factor inhibits the development of dendritic cells and dramatically affects the differentiation of multiple hematopoietic lineages in vivo. *Blood*, *92*, 4150–4166.
Gabrilovich, D. I., Velders, M. P., Sotomayor, E. M., & Kast, W. M. (2001). Mechanism of immune dysfunction in cancer mediated by immature Gr-1+ myeloid cells. *Journal of Immunology*, *166*, 5398–5406.
Garrity, T., Pandit, R., Wright, M. A., Benefield, J., Keni, S., & Young, M. R. (1997). Increased presence of CD34+ cells in the peripheral blood of head and neck cancer patients and their differentiation into dendritic cells. *International Journal of Cancer*, *73*, 663–669.
Gehad, A. E., Lichtman, M. K., Schmults, C. D., Teague, J. E., Calarese, A. W., Jiang, Y., et al. (2012). Nitric oxide-producing myeloid-derived suppressor cells inhibit vascular E-selectin expression in human squamous cell carcinomas. *The Journal of Investigative Dermatology*, *132*, 2642–2651.
Gleason, M. K., Ross, J. A., Warlick, E. D., Lund, T. C., Verneris, M. R., Wiernik, A., et al. (2014). CD16xCD33 bispecific killer cell engager (BiKE) activates NK cells against primary MDS and MDSC CD33+ targets. *Blood*, *123*, 3016–3026.
Goñi, O., Alcaide, P., & Fresno, M. (2002). Immunosuppression during acute Trypanosoma cruzi infection: Involvement of Ly6G (Gr1(+))CD11b(+)immature myeloid suppressor cells. *International Immunology*, *14*, 1125–1134.
Grizzle, W. E., Xu, X., Zhang, S., Stockard, C. R., Liu, C., Yu, S., et al. (2007). Age-related increase of tumor susceptibility is associated with myeloid-derived suppressor cell mediated suppression of T cell cytotoxicity in recombinant inbred BXD12 mice. *Mechanisms of Ageing and Development*, *128*, 672–680.

Hailé, L. A., von Wasielewski, R., Gamrekelashvili, J., Krüger, C., Bachmann, O., Westendorf, A. M., et al. (2008). Myeloid-derived suppressor cells in inflammatory bowel disease: A new immunoregulatory pathway. *Gastroenterology, 135,* 871–881, 881.e1–5.

Hanson, E. M., Clements, V. K., Sinha, P., Ilkovitch, D., & Ostrand-Rosenberg, S. (2009). Myeloid-derived suppressor cells down-regulate L-selectin expression on CD4+ and CD8+ T cells. *Journal of Immunology, 183,* 937–944.

He, D., Li, H., Yusuf, N., Elmets, C. A., Li, J., Mountz, J. D., et al. (2010). IL-17 promotes tumor development through the induction of tumor promoting microenvironments at tumor sites and myeloid-derived suppressor cells. *Journal of Immunology, 184,* 2281–2288.

Highfill, S. L., Rodriguez, P. C., Zhou, Q., Goetz, C. A., Koehn, B. H., Veenstra, R., et al. (2010). Bone marrow myeloid-derived suppressor cells (MDSCs) inhibit graft-versus-host disease (GVHD) via an arginase-1-dependent mechanism that is up-regulated by interleukin-13. *Blood, 116,* 5738–5747.

Hix, L. M., Karavitis, J., Khan, M. W., Shi, Y. H., Khazaie, K., & Zhang, M. (2013). Tumor STAT1 transcription factor activity enhances breast tumor growth and immune suppression mediated by myeloid-derived suppressor cells. *The Journal of Biological Chemistry, 288,* 11676–11688.

Hoechst, B., Ormandy, L. A., Ballmaier, M., Lehner, F., Krueger, C., Manns, M. P., et al. (2008). A new population of myeloid-derived suppressor cells in hepatocellular carcinoma patients induces CD4(+)CD25(+)Foxp3(+) T cells. *Gastroenterology, 135,* 234–243.

Horlad, H., Fujiwara, Y., Takemura, K., Ohnishi, K., Ikeda, T., Tsukamoto, H., et al. (2013). Corosolic acid impairs tumor development and lung metastasis by inhibiting the immunosuppressive activity of myeloid-derived suppressor cells. *Molecular Nutrition & Food Research, 57,* 1046–1054.

Hu, X., Bardhan, K., Paschall, A. V., Yang, D., Waller, J. L., Park, M. A., et al. (2013). Deregulation of apoptotic factors Bcl-xL and Bax confers apoptotic resistance to myeloid-derived suppressor cells and contributes to their persistence in cancer. *The Journal of Biological Chemistry, 288,* 19103–19115.

Huang, B., Pan, P. Y., Li, Q., Sato, A. I., Levy, D. E., Bromberg, J., et al. (2006). Gr-1+CD115+ immature myeloid suppressor cells mediate the development of tumor-induced T regulatory cells and T-cell anergy in tumor-bearing host. *Cancer Research, 66,* 1123–1131.

Huang, A., Zhang, B., Wang, B., Zhang, F., Fan, K. X., & Guo, Y. J. (2013). Increased CD14(+)HLA-DR (-/low) myeloid-derived suppressor cells correlate with extrathoracic metastasis and poor response to chemotherapy in non-small cell lung cancer patients. *Cancer Immunology, Immunotherapy, 62,* 1439–1451.

Iclozan, C., Antonia, S., Chiappori, A., Chen, D. T., & Gabrilovich, D. (2013). Therapeutic regulation of myeloid-derived suppressor cells and immune response to cancer vaccine in patients with extensive stage small cell lung cancer. *Cancer Immunology, Immunotherapy, 62,* 909–918.

Ilkovitch, D., & Lopez, D. M. (2009). The liver is a site for tumor-induced myeloid-derived suppressor cell accumulation and immunosuppression. *Cancer Research, 69,* 5514–5521.

Ioannou, M., Alissafi, T., Lazaridis, I., Deraos, G., Matsoukas, J., Gravanis, A., et al. (2012). Crucial role of granulocytic myeloid-derived suppressor cells in the regulation of central nervous system autoimmune disease. *Journal of Immunology, 188,* 1136–1146.

Jablonska, J., Leschner, S., Westphal, K., Lienenklaus, S., & Weiss, S. (2010). Neutrophils responsive to endogenous IFN-beta regulate tumor angiogenesis and growth in a mouse tumor model. *The Journal of Clinical Investigation, 120,* 1151–1164.

Karin, M. (2006). Nuclear factor-kappaB in cancer development and progression. *Nature, 441,* 431–436.

Kim, K., Skora, A. D., Li, Z., Liu, Q., Tam, A. J., Blosser, R. L., et al. (2014). Eradication of metastatic mouse cancers resistant to immune checkpoint blockade by suppression of myeloid-derived cells. *Proceedings of the National Academy of Sciences of the United States of America, 111*, 11774–11779.

Kimura, T., McKolanis, J. R., Dzubinski, L. A., Islam, K., Potter, D. M., Salazar, A. M., et al. (2013). MUC1 vaccine for individuals with advanced adenoma of the colon: A cancer immunoprevention feasibility study. *Cancer Prevention Research (Philadelphia, PA), 6*, 18–26.

Köstlin, N., Kugel, H., Spring, B., Leiber, A., Marmé, A., Henes, M., et al. (2014). Granulocytic myeloid derived suppressor cells expand in human pregnancy and modulate T-cell responses. *European Journal of Immunology, 44*, 2582–2591.

Kowanetz, M., Wu, X., Lee, J., Tan, M., Hagenbeek, T., Qu, X., et al. (2010). Granulocyte-colony stimulating factor promotes lung metastasis through mobilization of Ly6G+Ly6C+ granulocytes. *Proceedings of the National Academy of Sciences of the United States of America, 107*, 21248–21255.

Kujawski, M., Kortylewski, M., Lee, H., Herrmann, A., Kay, H., & Yu, H. (2008). Stat3 mediates myeloid cell-dependent tumor angiogenesis in mice. *The Journal of Clinical Investigation, 118*, 3367–3377.

Kusmartsev, S., Eruslanov, E., Kübler, H., Tseng, T., Sakai, Y., Su, Z., et al. (2008). Oxidative stress regulates expression of VEGFR1 in myeloid cells: Link to tumor-induced immune suppression in renal cell carcinoma. *Journal of Immunology, 181*, 346–353.

Kusmartsev, S., & Gabrilovich, D. I. (2005). STAT1 signaling regulates tumor-associated macrophage-mediated T cell deletion. *Journal of Immunology, 174*, 4880–4891.

Levring, T. B., Hansen, A. K., Nielsen, B. L., Kongsbak, M., von Essen, M. R., Woetmann, A., et al. (2012). Activated human CD4+ T cells express transporters for both cysteine and cystine. *Scientific Reports, 2*, 266.

Li, W., Wu, K., Zhao, E., Shi, L., Li, R., Zhang, P., et al. (2013). HMGB1 recruits myeloid derived suppressor cells to promote peritoneal dissemination of colon cancer after resection. *Biochemical and Biophysical Research Communications, 436*, 156–161.

Li, L., Zhang, J., Diao, W., Wang, D., Wei, Y., Zhang, C. Y., et al. (2014). MicroRNA-155 and MicroRNA-21 promote the expansion of functional myeloid-derived suppressor cells. *Journal of Immunology, 192*, 1034–1043.

Lieschke, G. J., Grail, D., Hodgson, G., Metcalf, D., Stanley, E., Cheers, C., et al. (1994). Mice lacking granulocyte colony-stimulating factor have chronic neutropenia, granulocyte and macrophage progenitor cell deficiency, and impaired neutrophil mobilization. *Blood, 84*, 1737–1746.

Lin, Y., Gustafson, M. P., Bulur, P. A., Gastineau, D. A., Witzig, T. E., & Dietz, A. B. (2011). Immunosuppressive CD14+HLA-DR(low)/− monocytes in B-cell non-Hodgkin lymphoma. *Blood, 117*, 872–881.

Liu, Y., Lai, L., Chen, Q., Song, Y., Xu, S., Ma, F., et al. (2012). MicroRNA-494 is required for the accumulation and functions of tumor-expanded myeloid-derived suppressor cells via targeting of PTEN. *Journal of Immunology, 188*, 5500–5510.

Liu, C., Yu, S., Kappes, J., Wang, J., Grizzle, W. E., Zinn, K. R., et al. (2007). Expansion of spleen myeloid suppressor cells represses NK cell cytotoxicity in tumor-bearing host. *Blood, 109*, 4336–4342.

Liu, Q., Zhang, M., Jiang, X., Zhang, Z., Dai, L., Min, S., et al. (2011). miR-223 suppresses differentiation of tumor-induced $CD11b^{+}$ $Gr1^{+}$ myeloid-derived suppressor cells from bone marrow cells. *International Journal of Cancer, 129*, 2662–2673.

Lu, T., & Gabrilovich, D. I. (2012). Molecular pathways: Tumor-infiltrating myeloid cells and reactive oxygen species in regulation of tumor microenvironment. *Clinical Cancer Research, 18*, 4877–4882.

Lu, T., Ramakrishnan, R., Altiok, S., Youn, J. I., Cheng, P., Celis, E., et al. (2011). Tumor-infiltrating myeloid cells induce tumor cell resistance to cytotoxic T cells in mice. *The Journal of Clinical Investigation, 121,* 4015–4029.

MacDonald, K. P., Rowe, V., Clouston, A. D., Welply, J. K., Kuns, R. D., Ferrara, J. L., et al. (2005). Cytokine expanded myeloid precursors function as regulatory antigen-presenting cells and promote tolerance through IL-10-producing regulatory T cells. *Journal of Immunology, 174,* 1841–1850.

Makarenkova, V. P., Bansal, V., Matta, B. M., Perez, L. A., & Ochoa, J. B. (2006). CD11b+/Gr-1+ myeloid suppressor cells cause T cell dysfunction after traumatic stress. *Journal of Immunology, 176,* 2085–2094.

Mao, Y., Sarhan, D., Steven, A., Seliger, B., Kiessling, R., & Lundqvist, A. (2014). Inhibition of tumor-derived prostaglandin-e2 blocks the induction of myeloid-derived suppressor cells and recovers natural killer cell activity. *Clinical Cancer Research, 20,* 4096–4106.

Marigo, I., Bosio, E., Solito, S., Mesa, C., Fernandez, A., Dolcetti, L., et al. (2010). Tumor-induced tolerance and immune suppression depend on the C/EBPbeta transcription factor. *Immunity, 32,* 790–802.

Markiewski, M. M., DeAngelis, R. A., Benencia, F., Ricklin-Lichtsteiner, S. K., Koutoulaki, A., Gerard, C., et al. (2008). Modulation of the antitumor immune response by complement. *Nature Immunology, 9,* 1225–1235.

Martin, R. K., Saleem, S. J., Folgosa, L., Zellner, H. B., Damle, S. R., Nguyen, G. K., et al. (2014). Mast cell histamine promotes the immunoregulatory activity of myeloid-derived suppressor cells. *Journal of Leukocyte Biology, 96,* 151–159.

Marzoni, A., Bronte, V., Visintin, A., Spitzer, J. H., Apolloni, E., Serafini, P., et al. (2002). Myeloid suppressor lines inhibit T cell responses by an NO-dependent mechanism. *Journal of Immunology, 168,* 689–695.

Melani, C., Chiodoni, C., Forni, G., & Colombo, M. P. (2003). Myeloid cell expansion elicited by the progression of spontaneous mammary carcinomas in c-erbB-2 transgenic BALB/c mice suppresses immune reactivity. *Blood, 102,* 2138–2145.

Melani, C., Sangaletti, S., Barazzetta, F. M., Werb, Z., & Colombo, M. P. (2007). Amino-biphosphonate-mediated MMP-9 inhibition breaks the tumor-bone marrow axis responsible for myeloid-derived suppressor cell expansion and macrophage infiltration in tumor stroma. *Cancer Research, 67,* 11438–11446.

Mikyskova, R., Indrova, M., Vlkova, V., Bieblova, J., Simova, J., Parackova, Z., et al. (2014). DNA demethylating agent 5-azacytidine inhibits myeloid-derived suppressor cells induced by tumor growth and cyclophosphamide treatment. *Journal of Leukocyte Biology, 95,* 743–753.

Molon, B., Ugel, S., Del Pozzo, F., Soldani, C., Zilio, S., Avella, D., et al. (2011). Chemokine nitration prevents intratumoral infiltration of antigen-specific T cells. *The Journal of Experimental Medicine, 208,* 1949–1962.

Montero, A. J., Diaz-Montero, C. M., Kyriakopoulos, C. E., Bronte, V., & Mandruzzato, S. (2012). Myeloid-derived suppressor cells in cancer patients: a clinical perspective. *Journal of Immunotherapy, 35,* 107–115.

Morales, J. K., Kmieciak, M., Knutson, K. L., Bear, H. D., & Manjili, M. H. (2010). GM-CSF is one of the main breast tumor-derived soluble factors involved in the differentiation of CD11b-Gr1- bone marrow progenitor cells into myeloid-derived suppressor cells. *Breast Cancer Research and Treatment, 123,* 39–49.

Mostafa, M. H., Sheweita, S. A., & O'Connor, P. J. (1999). Relationship between schistosomiasis and bladder cancer. *Clinical Microbiology Reviews, 12,* 97–111.

Movahedi, K., Guilliams, M., Van den Bossche, J., Van den Bergh, R., Gysemans, C., Beschin, A., et al. (2008). Identification of discrete tumor-induced myeloid-derived suppressor cell subpopulations with distinct T cell-suppressive activity. *Blood, 111,* 4233–4244.

Mucha, J., Majchrzak, K., Taciak, B., Hellmen, E., & Krol, M. (2014). MDSCs mediate angiogenesis and predispose canine mammary tumor cells for metastasis via IL-28/IL-28RA (IFN-lambda) signaling. *PLoS One, 9*, e103249.

Mundy-Bosse, B. L., Thornton, L. M., Yang, H. C., Andersen, B. L., & Carson, W. E. (2011). Psychological stress is associated with altered levels of myeloid-derived suppressor cells in breast cancer patients. *Cellular Immunology, 270*, 80–87.

Munn, D. H., Sharma, M. D., Baban, B., Harding, H. P., Zhang, Y., Ron, D., et al. (2005). GCN2 kinase in T cells mediates proliferative arrest and anergy induction in response to indoleamine 2,3-dioxygenase. *Immunity, 22*, 633–642.

Nefedova, Y., Cheng, P., Gilkes, D., Blaskovich, M., Beg, A. A., Sebti, S. M., et al. (2005). Activation of dendritic cells via inhibition of Jak2/STAT3 signaling. *Journal of Immunology, 175*, 4338–4346.

Nefedova, Y., Huang, M., Kusmartsev, S., Bhattacharya, R., Cheng, P., Salup, R., et al. (2004). Hyperactivation of STAT3 is involved in abnormal differentiation of dendritic cells in cancer. *Journal of Immunology, 172*, 464–474.

Noman, M. Z., Desantis, G., Janji, B., Hasmim, M., Karray, S., Dessen, P., et al. (2014). PD-L1 is a novel direct target of HIF-1alpha, and its blockade under hypoxia enhanced MDSC-mediated T cell activation. *The Journal of Experimental Medicine, 211*, 781–790.

Obermajer, N., Muthuswamy, R., Lesnock, J., Edwards, R. P., & Kalinski, P. (2011). Positive feedback between PGE2 and COX2 redirects the differentiation of human dendritic cells toward stable myeloid-derived suppressor cells. *Blood, 118*, 5498–5505.

Okazaki, T., Ebihara, S., Asada, M., Kanda, A., Sasaki, H., & Yamaya, M. (2006). Granulocyte colony-stimulating factor promotes tumor angiogenesis via increasing circulating endothelial progenitor cells and Gr1+CD11b+ cells in cancer animal models. *International Immunology, 18*, 1–9.

Ortiz, M. L., Kumar, V., Martner, A., Mony, S., Donthireddy, L., Condamine, T., et al. (2015). Immature myeloid cells directly contribute to skin tumor development by recruiting IL-17-producing CD4+ T cells. *The Journal of Experimental Medicine, 212*, 351–367.

Ostrand-Rosenberg, S., & Sinha, P. (2009). Myeloid-derived suppressor cells: Linking inflammation and cancer. *Journal of Immunology, 182*, 4499–4506.

OuYang, L. Y., Wu, X. J., Ye, S. B., Zhang, R. X., Li, Z. L., Liao, W., et al. (2015). Tumor-induced myeloid-derived suppressor cells promote tumor progression through oxidative metabolism in human colorectal cancer. *Journal of Translational Medicine, 13*, 47.

Pan, P. Y., Ma, G., Weber, K. J., Ozao-Choy, J., Wang, G., Yin, B., et al. (2010). Immune stimulatory receptor CD40 is required for T-cell suppression and T regulatory cell activation mediated by myeloid-derived suppressor cells in cancer. *Cancer Research, 70*, 99–108.

Panka, D. J., Liu, Q., Geissler, A. K., & Mier, J. W. (2013). Effects of HDM2 antagonism on sunitinib resistance, p53 activation, SDF-1 induction, and tumor infiltration by CD11b+/Gr-1+ myeloid derived suppressor cells. *Molecular Cancer, 12*, 17.

Parker, K., Sinha, P., Horn, L., Clements, V., & Ostrand-Rosenberg, S. (2014). HMGB1 enhances immune suppression by facilitating the differentiation and suppressive activity of myeloid-derived suppressor cells. *Cancer Research, 74*, 5723–5733.

Porembka, M. R., Mitchem, J. B., Belt, B. A., Hsieh, C. S., Lee, H. M., Herndon, J., et al. (2012). Pancreatic adenocarcinoma induces bone marrow mobilization of myeloid-derived suppressor cells which promote primary tumor growth. *Cancer Immunology, Immunotherapy, 61*, 1373–1385.

Punturieri, A., Szabo, E., Croxton, T. L., Shapiro, S. D., & Dubinett, S. M. (2009). Lung cancer and chronic obstructive pulmonary disease: Needs and opportunities for integrated research. *Journal of the National Cancer Institute, 101*, 554–559.

Raber, P. L., Thevenot, P., Sierra, R., Wyczechowska, D., Halle, D., Ramirez, M. E., et al. (2014). Subpopulations of myeloid-derived suppressor cells impair T cell responses through independent nitric oxide-related pathways. *International Journal of Cancer, 134*, 2853–2864.

Rodriguez, P. C., Ernstoff, M. S., Hernandez, C., Atkins, M., Zabaleta, J., Sierra, R., et al. (2009). Arginase I-producing myeloid-derived suppressor cells in renal cell carcinoma are a subpopulation of activated granulocytes. *Cancer Research, 69*, 1553–1560.

Rodriguez, P. C., Hernandez, C. P., Morrow, K., Sierra, R., Zabaleta, J., Wyczechowska, D. D., et al. (2010). L-Arginine deprivation regulates cyclin D3 mRNA stability in human T cells by controlling HuR expression. *Journal of Immunology, 185*, 5198–5204.

Rodriguez, P. C., Hernandez, C. P., Quiceno, D., Dubinett, S. M., Zabaleta, J., Ochoa, J. B., et al. (2005). Arginase I in myeloid suppressor cells is induced by COX-2 in lung carcinoma. *The Journal of Experimental Medicine, 202*, 931–939.

Rodriguez, P. C., Quiceno, D. G., Zabaleta, J., Ortiz, B., Zea, A. H., Piazuelo, M. B., et al. (2004). Arginase I production in the tumor microenvironment by mature myeloid cells inhibits T-cell receptor expression and antigen-specific T-cell responses. *Cancer Research, 64*, 5839–5849.

Rodriguez, P. C., Zea, A. H., Culotta, K. S., Zabaleta, J., Ochoa, J. B., & Ochoa, A. C. (2002). Regulation of T cell receptor CD3zeta chain expression by L-arginine. *The Journal of Biological Chemistry, 277*, 21123–21129.

Sakamaki, I., Kwak, L. W., Cha, S. C., Yi, Q., Lerman, B., Chen, J., et al. (2014). Lenalidomide enhances the protective effect of a therapeutic vaccine and reverses immune suppression in mice bearing established lymphomas. *Leukemia, 28*, 329–337.

Saleem, S. J., Martin, R. K., Morales, J. K., Sturgill, J. L., Gibb, D. R., Graham, L., et al. (2012). Cutting edge: Mast cells critically augment myeloid-derived suppressor cell activity. *Journal of Immunology, 189*, 511–515.

Santhanam, L., Lim, H. K., Miriel, V., Brown, T., Patel, M., Balanson, S., et al. (2007). Inducible NO synthase dependent S-nitrosylation and activation of arginase1 contribute to age-related endothelial dysfunction. *Circulation Research, 101*, 692–702.

Santilli, G., Piotrowska, I., Cantilena, S., Chayka, O., D'Alicarnasso, M., Morgenstern, D. A., et al. (2013). Polyphenon [corrected] E enhances the antitumor immune response in neuroblastoma by inactivating myeloid suppressor cells. *Clinical Cancer Research, 19*, 1116–1125.

Schilling, B., Sucker, A., Griewank, K., Zhao, F., Weide, B., Gorgens, A., et al. (2013). Vemurafenib reverses immunosuppression by myeloid derived suppressor cells. *International Journal of Cancer, 133*, 1653–1663.

Schmielau, J., & Finn, O. J. (2001). Activated granulocytes and granulocyte-derived hydrogen peroxide are the underlying mechanism of suppression of t-cell function in advanced cancer patients. *Cancer Research, 61*, 4756–4760.

Serafini, P. (2013). Myeloid derived suppressor cells in physiological and pathological conditions: The good, the bad, and the ugly. *Immunologic Research, 57*, 172–184.

Serafini, P., Carbley, R., Noonan, K. A., Tan, G., Bronte, V., & Borrello, I. (2004). High-dose granulocyte-macrophage colony-stimulating factor-producing vaccines impair the immune response through the recruitment of myeloid suppressor cells. *Cancer Research, 64*, 6337–6343.

Serafini, P., Mgebroff, S., Noonan, K., & Borrello, I. (2008). Myeloid-derived suppressor cells promote cross-tolerance in B-cell lymphoma by expanding regulatory T cells. *Cancer Research, 68*, 5439–5449.

Shacter, E., & Weitzman, S. A. (2002). Chronic inflammation and cancer. *Oncology (Williston Park), 16*, 217–226, 229; discussion 230–232.

Shen, P., Wang, A., He, M., Wang, Q., & Zheng, S. (2014). Increased circulating Lin(-/low) CD33(+) HLA-DR(-) myeloid-derived suppressor cells in hepatocellular carcinoma patients. *Hepatology Research*, *44*, 639–650.

Sica, A., & Mantovani, A. (2012). Macrophage plasticity and polarization: In vivo veritas. *The Journal of Clinical Investigation*, *122*, 787–795.

Sinha, P., Chornoguz, O., Clements, V. K., Artemenko, K. A., Zubarev, R. A., & Ostrand-Rosenberg, S. (2011). Myeloid-derived suppressor cells express the death receptor Fas and apoptose in response to T cell-expressed FasL. *Blood*, *117*, 5381–5390.

Sinha, P., Clements, V. K., Bunt, S. K., Albelda, S. M., & Ostrand-Rosenberg, S. (2007). Cross-talk between myeloid-derived suppressor cells and macrophages subverts tumor immunity toward a type 2 response. *Journal of Immunology*, *179*, 977–983.

Sinha, P., Clements, V. K., Fulton, A. M., & Ostrand-Rosenberg, S. (2007). Prostaglandin E2 promotes tumor progression by inducing myeloid-derived suppressor cells. *Cancer Research*, *67*, 4507–4513.

Sinha, P., Clements, V. K., & Ostrand-Rosenberg, S. (2005a). Interleukin-13-regulated M2 macrophages in combination with myeloid suppressor cells block immune surveillance against metastasis. *Cancer Research*, *65*, 11743–11751.

Sinha, P., Clements, V. K., & Ostrand-Rosenberg, S. (2005b). Reduction of myeloid-derived suppressor cells and induction of M1 macrophages facilitate the rejection of established metastatic disease. *Journal of Immunology*, *174*, 636–645.

Sinha, P., Okoro, C., Foell, D., Freeze, H. H., Ostrand-Rosenberg, S., & Srikrishna, G. (2008). Proinflammatory S100 proteins regulate the accumulation of myeloid-derived suppressor cells. *Journal of Immunology*, *181*, 4666–4675.

Sinha, P., & Ostrand-Rosenberg, S. (2013). Myeloid-derived suppressor cell function is reduced by Withaferin A, a potent and abundant component of Withania somnifera root extract. *Cancer Immunology, Immunotherapy*, *62*, 1663–1673.

Sinha, P., Parker, K. H., Horn, L., & Ostrand-Rosenberg, S. (2012). Tumor-induced myeloid-derived suppressor cell function is independent of IFN-γ and IL-4Rα. *European Journal of Immunology*, *42*, 2052–2059.

Sionov, R. V., Fridlender, Z. G., & Granot, Z. (2014). The multifaceted roles neutrophils play in the tumor microenvironment. *Cancer Microenvironment*.

Smith, C., Chang, M. Y., Parker, K. H., Beury, D. W., DuHadaway, J. B., Flick, H. E., et al. (2012). IDO is a nodal pathogenic driver of lung cancer and metastasis development. *Cancer Discovery*, *2*, 722–735.

Song, X., Krelin, Y., Dvorkin, T., Bjorkdahl, O., Segal, S., Dinarello, C. A., et al. (2005). CD11b+/Gr-1+ immature myeloid cells mediate suppression of T cells in mice bearing tumors of IL-1beta-secreting cells. *Journal of Immunology*, *175*, 8200–8208.

Song, C., Yuan, Y., Wang, X. M., Li, D., Zhang, G. M., Huang, B., et al. (2014). Passive transfer of tumour-derived MDSCs inhibits asthma-related airway inflammation. *Scandinavian Journal of Immunology*, *79*, 98–104.

Srivastava, M. K., Bosch, J. J., Thompson, J. A., Ksander, B. R., Edelman, M. J., & Ostrand-Rosenberg, S. (2008). Lung cancer patients' CD4(+) T cells are activated in vitro by MHC II cell-based vaccines despite the presence of myeloid-derived suppressor cells. *Cancer Immunology, Immunotherapy*, *57*, 1493–1504.

Srivastava, M. K., Sinha, P., Clements, V. K., Rodriguez, P., & Ostrand-Rosenberg, S. (2010). Myeloid-derived suppressor cells inhibit T-cell activation by depleting cystine and cysteine. *Cancer Research*, *70*, 68–77.

Stewart, T. J., Liewehr, D. J., Steinberg, S. M., Greeneltch, K. M., & Abrams, S. I. (2009). Modulating the expression of IFN regulatory factor 8 alters the protumorigenic behavior of CD11b+Gr-1+ myeloid cells. *Journal of Immunology*, *183*, 117–128.

Strober, S. (1984). Natural suppressor (NS) cells, neonatal tolerance, and total lymphoid irradiation: Exploring obscure relationships. *Annual Review of Immunology*, *2*, 219–237.

Terabe, M., Matsui, S., Park, J. M., Mamura, M., Noben-Trauth, N., Donaldson, D. D., et al. (2003). Transforming growth factor-beta production and myeloid cells are an effector mechanism through which CD1d-restricted T cells block cytotoxic T lymphocyte-mediated tumor immunosurveillance: Abrogation prevents tumor recurrence. *The Journal of Experimental Medicine, 198*, 1741–1752.

Thevenot, P. T., Sierra, R. A., Raber, P. L., Al-Khami, A. A., Trillo-Tinoco, J., Zarreii, P., et al. (2014). The stress-response sensor chop regulates the function and accumulation of myeloid-derived suppressor cells in tumors. *Immunity, 41*, 389–401.

Tu, S., Bhagat, G., Cui, G., Takaishi, S., Kurt-Jones, E. A., Rickman, B., et al. (2008). Over-expression of interleukin-1beta induces gastric inflammation and cancer and mobilizes myeloid-derived suppressor cells in mice. *Cancer Cell, 14*, 408–419.

Vakkila, J., & Lotze, M. T. (2004). Inflammation and necrosis promote tumour growth. *Nature Reviews. Immunology, 4*, 641–648.

Venereau, E., Casalgrandi, M., Schiraldi, M., Antoine, D. J., Cattaneo, A., De Marchis, F., et al. (2012). Mutually exclusive redox forms of HMGB1 promote cell recruitment or proinflammatory cytokine release. *The Journal of Experimental Medicine, 209*, 1519–1528.

Verschoor, C. P., Johnstone, J., Millar, J., Dorrington, M. G., Habibagahi, M., Lelic, A., et al. (2013). Blood CD33(+)HLA-DR(-) myeloid-derived suppressor cells are increased with age and a history of cancer. *Journal of Leukocyte Biology, 93*, 633–637.

Voisin, M. B., Buzoni-Gatel, D., Bout, D., & Velge-Roussel, F. (2004). Both expansion of regulatory GR1+ CD11b + myeloid cells and anergy of T lymphocytes participate in hyporesponsiveness of the lung-associated immune system during acute toxoplasmosis. *Infection and Immunity, 72*, 5487–5492.

Vuk-Pavlović, S., Bulur, P. A., Lin, Y., Qin, R., Szumlanski, C. L., Zhao, X., et al. (2010). Immunosuppressive CD14+HLA-DRlow/− monocytes in prostate cancer. *Prostate, 70*, 443–455.

Waight, J. D., Netherby, C., Hensen, M. L., Miller, A., Hu, Q., Liu, S., et al. (2013). Myeloid-derived suppressor cell development is regulated by a STAT/IRF-8 axis. *The Journal of Clinical Investigation, 123*, 4464–4478.

Wang, L., Chang, E. W., Wong, S. C., Ong, S. M., Chong, D. Q., & Ling, K. L. (2013). Increased myeloid-derived suppressor cells in gastric cancer correlate with cancer stage and plasma S100A8/A9 proinflammatory proteins. *Journal of Immunology, 190*, 794–804.

Wang, R., & Green, D. R. (2012). Metabolic checkpoints in activated T cells. *Nature Immunology, 13*, 907–915.

Wang, L., Yi, T., Kortylewski, M., Pardoll, D. M., Zeng, D., & Yu, H. (2009). IL-17 can promote tumor growth through an IL-6-Stat3 signaling pathway. *The Journal of Experimental Medicine, 206*, 1457–1464.

Weed, D. T., Vella, J. L., Reis, I. M., De la Fuente, A. C., Gomez, C., Sargi, Z., et al. (2015). Tadalafil reduces myeloid-derived suppressor cells and regulatory T cells and promotes tumor immunity in patients with head and neck squamous cell carcinoma. *Clinical Cancer Research, 21*, 39–48.

Wesolowski, R., Markowitz, J., & Carson, W. E., 3rd. (2013). Myeloid derived suppressor cells—A new therapeutic target in the treatment of cancer. *Journal for Immunotherapy of Cancer, 1*, 10.

Wu, S., Rhee, K. J., Albesiano, E., Rabizadeh, S., Wu, X., Yen, H. R., et al. (2009). A human colonic commensal promotes colon tumorigenesis via activation of T helper type 17 T cell responses. *Nature Medicine, 15*, 1016–1022.

Wu, J., Zhang, R., Tang, N., Gong, Z., Zhou, J., Chen, Y., et al. (2015). Dopamine inhibits the function of Gr-1+CD115 + myeloid-derived suppressor cells through D1-like receptors and enhances anti-tumor immunity. *Journal of Leukocyte Biology, 97*, 191–200.

Xia, S., Sha, H., Yang, L., Ji, Y., Ostrand-Rosenberg, S., & Qi, L. (2011). Gr-1+ CD11b+ myeloid-derived suppressor cells suppress inflammation and promote insulin sensitivity in obesity. *The Journal of Biological Chemistry, 286*, 23591–23599.

Xin, H., Zhang, C., Herrmann, A., Du, Y., Figlin, R., & Yu, H. (2009). Sunitinib inhibition of Stat3 induces renal cell carcinoma tumor cell apoptosis and reduces immunosuppressive cells. *Cancer Research, 69*, 2506–2513.

Yazawa, T., Shibata, M., Gonda, K., Machida, T., Suzuki, S., Kenjo, A., et al. (2013). Increased IL-17 production correlates with immunosuppression involving myeloid-derived suppressor cells and nutritional impairment in patients with various gastrointestinal cancers. *Molecular and Clinical Oncology, 1*, 675–679.

Ye, J., Livergood, R. S., & Peng, G. (2013). The role and regulation of human Th17 cells in tumor immunity. *The American Journal of Pathology, 182*, 10–20.

Yin, Y., Huang, X., Lynn, K. D., & Thorpe, P. E. (2013). Phosphatidylserine-targeting antibody induces M1 macrophage polarization and promotes myeloid-derived suppressor cell differentiation. *Cancer Immunology Research, 1*, 256–268.

Yin, B., Ma, G., Yen, C. Y., Zhou, Z., Wang, G. X., Divino, C. M., et al. (2010). Myeloid-derived suppressor cells prevent type 1 diabetes in murine models. *Journal of Immunology, 185*, 5828–5834.

Youn, J. I., Collazo, M., Shalova, I. N., Biswas, S. K., & Gabrilovich, D. I. (2012). Characterization of the nature of granulocytic myeloid-derived suppressor cells in tumor-bearing mice. *Journal of Leukocyte Biology, 91*, 167–181.

Youn, J. I., Nagaraj, S., Collazo, M., & Gabrilovich, D. I. (2008). Subsets of myeloid-derived suppressor cells in tumor-bearing mice. *Journal of Immunology, 181*, 5791–5802.

Young, M. R., Petruzzelli, G. J., Kolesiak, K., Achille, N., Lathers, D. M., & Gabrilovich, D. I. (2001). Human squamous cell carcinomas of the head and neck chemoattract immune suppressive CD34(+) progenitor cells. *Human Immunology, 62*, 332–341.

Yu, J., Du, W., Yan, F., Wang, Y., Li, H., Cao, S., et al. (2013). Myeloid-derived suppressor cells suppress antitumor immune responses through IDO expression and correlate with lymph node metastasis in patients with breast cancer. *Journal of Immunology, 190*, 3783–3797.

Yuan, H., Cai, P., Li, Q., Wang, W., Sun, Y., Xu, Q., et al. (2014). Axitinib augments antitumor activity in renal cell carcinoma via STAT3-dependent reversal of myeloid-derived suppressor cell accumulation. *Biomedicine & Pharmacotherapy, 68*, 751–756.

Zea, A. H., Rodriguez, P. C., Atkins, M. B., Hernandez, C., Signoretti, S., Zabaleta, J., et al. (2005). Arginase-producing myeloid suppressor cells in renal cell carcinoma patients: A mechanism of tumor evasion. *Cancer Research, 65*, 3044–3048.

Zea, A. H., Rodriguez, P. C., Culotta, K. S., Hernandez, C. P., DeSalvo, J., Ochoa, J. B., et al. (2004). L-Arginine modulates CD3zeta expression and T cell function in activated human T lymphocytes. *Cellular Immunology, 232*, 21–31.

Zhang, M., Liu, Q., Mi, S., Liang, X., Zhang, Z., Su, X., et al. (2011). Both miR-17-5p and miR-20a alleviate suppressive potential of myeloid-derived suppressor cells by modulating STAT3 expression. *Journal of Immunology, 186*, 4716–4724.

Zhang, Y. L., Luan, B., Wang, X. F., Qiao, J. Y., Song, L., Lei, R. R., et al. (2013). Peripheral blood MDSCs, IL-10 and IL-12 in children with asthma and their importance in asthma development. *PLoS One, 8*, e63775.

Zhang, B., Wang, Z., Wu, L., Zhang, M., Li, W., Ding, J., et al. (2013). Circulating and tumor-infiltrating myeloid-derived suppressor cells in patients with colorectal carcinoma. *PLoS One, 8*, e57114.

Zhu, B., Bando, Y., Xiao, S., Yang, K., Anderson, A. C., Kuchroo, V. K., et al. (2007). CD11b+Ly-6C(hi) suppressive monocytes in experimental autoimmune encephalomyelitis. *Journal of Immunology, 179*, 5228–5237.

Zitvogel, L., Apetoh, L., Ghiringhelli, F., & Kroemer, G. (2008). Immunological aspects of cancer chemotherapy. *Nature Reviews. Immunology, 8*, 59–73.
Zong, W. X., & Thompson, C. B. (2006). Necrotic death as a cell fate. *Genes & Development, 20*, 1–15.
Zoso, A., Mazza, E. M., Bicciato, S., Mandruzzato, S., Bronte, V., Serafini, P., et al. (2014). Human fibrocytic myeloid-derived suppressor cells express IDO and promote tolerance via Treg-cell expansion. *European Journal of Immunology, 44*, 3307–3319.

Glossary

ADAM17 – A disintegrin and metalloproteinase 17

ADCC – Antibody-dependent cell mediated cytotoxicity

ADP - Adenosine diphosphate

AMP - Adenosine monophosphate

APC- Antigen presenting cell

Arg 1 - Arginase

Atg- Autophagy related gene

ATP – Adenosine triphosphate

Bcl-2- B-cell CLL/Lymphoma 2

bFGF - Basic fibroblast growth factor

Breg- Regulatory B cell

CAF- Cancer associated fibroblast

CAR - Chimeric-antigen receptors

CD- Cluster of differentiation

c-FLIP- Cellular FLICE-inhibitory protein

CHOP- C/EBP homologous protein

COX_2 - Cyclooxygenase-2

CSF1 - Colony stimulating factor 1

CTL - Cytotoxic T lymphocytes

CTLA-4 – Cytotoxic T-lymphocyte-associated protein 4

CXCL12 – C-X-C motif chemokine 12 AKA stromal cell-deriver factor 1 (SDF-1)

CXCR4 – C-X-C chemokine receptor type 4

DAMP- Damage-associated molecular pattern molecule

DAPK - Death-associated protein kinase

EMT - epithelial-mesenchymal transition

ER- Endoplasmic reticulum

ERK - Extracellular signal-regulated kinase

FAP - Fibroblast activation protein

Fas – Fas cell surface death receptor

Fas-L – Fas ligand

FO - Follicular

FSP - Fibroblast specific protein

GM-CSF- Granulocyte macrophage colony-stimulating factor

Gr1- Granulocyte marker 1

HMGB1 - High Mobility Group Box protein 1

IDO - Indoleamine 2,3-dioxygenase

IFNs- Interferons

IL- Interleukin

iNOs - Inducible nitric oxide synthase

KIRs- Killer cell Ig-like receptors

LC3 – Microtubule-associated protein 1 light chain 3

MDSC- Myeloid-derived suppressor cells

MHC- Major histocompatibility complex

MMP - Matrix metallopeptidases

mTOR- Mechanistic target of Rapamycin

NAC - N-acetylcysteine

NK- Natural killer cells

NO - Nitric oxide

NOX2 - NADPH oxidase

P62- Phosphotyrosine independent ligand for the Lck SH2 Domain p62

PD-1- Programmed cell death 1

PDGF-Rβ - Platelet-derived growth factor receptor-β

PD-L1- Programed death-ligand 1

PE - Phosphatidylethanolamine

PGE_2 - Prostaglandin E2

PI3KC3- Phosphatidylinositol 3-kinase, catalytic subunit type 3

RAGE - Receptor for advanced glycation endproducts

ROS- Reactive oxygen species

SOD - Super oxide dismutase

STAT- Signal transducer and activator of transcription

T2-MZP - Sransitional 2-marginal zone precursor

TAM- Tumor associated macrophage

TCR - T cell receptor

TGF-β - Transforming growth factor beta

TIL - Tumor infiltrating lymphocytes

TIM-3 – T cell immunoglobulin and mucin domain 3

TLR - Toll-Like Receptors

TME - Tumor microenvironment

TNF-α - tumor necrosis factor alpha

TRAIL- TNF-related apoptosis-inducing ligand

Treg - Regulatory T cells

TSLP - Thymic stromal lmyphopoietin

ULK1- Unc-51 like autophagy activating kinase 1

VEGF- Vascular endothelia growth factor

α-SMA - Alpha- smooth muscle actin